AUTOSOMAL DOMINANT RETINITIS PIGMENTOSA: MUTATION SCREEN OF RHODOPSIN AND IDENTIFICATION OF A NEW GENETIC LOCUS

MAY AL-MAGHTHEH
BSc, MSc

A thesis submitted for the Degree of Doctor of Philosophy

Department of Molecular Genetics
Institute of Ophthalmology
University College London
Bath Street
London EC1V 9EL

Septemper 1995

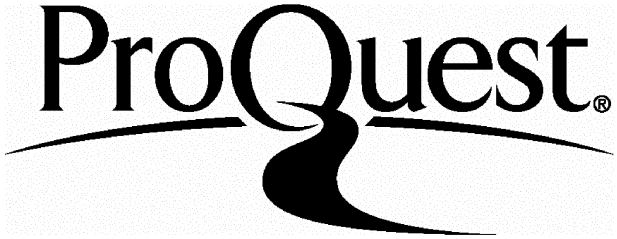

ABSTRACT:

Retinitis pigmentosa (RP) is an inherited group of retinal degenerations that are both clinically and genetically heterogeneous. adRP, the autosomal dominant form of RP, shows further heterogeneity. At the start of this project, adRP was known to result from mutations in two photoreceptor specific genes, namely rhodopsin and peripherin/RDS, and as yet an unidentified gene on chromosome 8. During the course of this thesis, four other loci on chromosomes 7p, 7q, 17p, and 17q were identified by linkage analysis. The aims of this thesis were to identify novel mutations in the rhodopsin gene and to identify new genetic loci implicated in adRP.

Identification of new mutations in rhodopsin should further elucidate its structural and functional properties. As part of this thesis, four new mutations were identified in this gene in addition to previously reported ones. These include a 42 bp deletion and 150 bp insertion in exon 5, and two point mutations at codons 40 and 216.

In the search for a new adRP locus, linkage analysis was performed in a large adRP family known as ADRP5. After exclusion of candidate genes, a total genome search for the disease gene was undertaken; more than 270 markers were genotyped in the family. The disease phenotype was eventually linked to a 22 cM region defined by markers D19S180 and D19S214 on chromosome 19q13.4. The new locus was given the symbol RP11. Linkage analysis in the same family with more markers refined the localization of RP11 to an 8 cM region between D19S180 and AFMb005wh1. To further refine this localization and in order to obtain an estimate of the frequency of RP caused by mutations at this locus, 20 more adRP families were genotyped for markers from the disease interval. Two new families, ADRP29 and RP1907 were found to be linked and haplotype analysis in ADRP29 further reduced the RP11 containing region to 5 cM between D19S180 and AFMc001yb1. Another family not included in this thesis has since been found to be linked to this locus. In a total of 27 families analysed by linkage analysis in this laboratory, four mapped to this locus giving an estimation of the frequency of RP11 as 15%. It therefore suggests that mutations at this locus may be the second most common cause of adRP after rhodopsin.

The gene for protein kinase C gamma isoenzyme (PRKCG), a member of a large family of serine/threonine protein kinases (PKC), is known to map in the RP11 interval. In *Drosophila* a mutation in an eye specific PKC gene was found to cause retinal degeneration and

photoreceptor deactivation. Therefore, for these and others reasons, PRKCG was suggested as a candidate for RP11. However, a preliminary mutation screen using primers derived from the cDNA sequence failed to detect any mutation in the 19q linked families. Future work will include characterization of the genomic structure of PRKCG and testing it thoroughly, further refinement of the disease locus if PRKCG is excluded, and establishing a YAC contig across the region as the first step towards positional cloning of this RP gene.

DECLARATION

I declare that:

This thesis submitted for the degree of Doctor of Philosophy is composed by myself, and the work herein is my own, or that the auther involved is clearly stated.

May Al-Maghtheh BSc, MSc

DEDICATION

This thesis is dedicated to:
my ***mother*** and ***father***,
Ghassan, and my little
baby...

Acknowledgments

First of all I would like to express my deepest thanks to my supervisor Professor Shomi Bhattacharya initially for giving me the opportunity to do this degree, and for his constant support and encouragement throughout, without which this thesis could have not come to existence. I particularly thank him for his personal friendship with both me and Ghassan.

I would also like to thank Professor Colin Green at the Surgical Research, Clinical Research Centre, Harrow, who, as a start, offered me, through the British Council and MAP, the opportunity to do a 4 months training course in haematology, which opened the way for me to do my MSc in Genetics, and gave me the opportunity to carry on with the PhD.

Many thanks also goes to Dr Chris Inglehearn for taking part in my supervision, and reading my thesis, with all the useful discussions that reflected on its formulation. I would also like to express my sincere gratitude to all members of the Department for ideas and useful discussions. Thanks also to Robin Howes for helping with photography.

I am particularly grateful to my parents and family and all friends in the UK and at home, whose encouragement had helped me a lot.

Finally, I would like to say that I am indebted to my husband Ghassan for whom all words will not be enough to express my deepest gratitude and thankfulness for his constant support and encouragement and his patience with me throughout the last three years, and particularly the last few months without which this work could have not been completed.

Publication list:

Al-Maghtheh M., Gregory C., Inglehearn C., Hardcastle A. & Bhattacharya S. (1993). Rhodopsin mutations in autosomal dominant retinitis pigmentosa. Hum. Mutation 2: 249-255.

Al-Maghtheh M., Kim R.Y., Hardcastle A., Inglehearn C. & Bhattacharya S.S. (1993). A 150bp insertion in the rhodopsin gene of an autosomal dominant retinitis pigmentosa family. Hum. Mol. Genet. 3: 205-206.

Al-Maghtheh M., Inglehearn C., Lunt P., Jay M., Bird A. & Bhattacharya S. (1994). Two new rhodopsin transversion mutations (L40R; M216K) in families with autosomal dominant retinitis pigmentosa. Hum. Mutation 3: 409-410.

Al-Maghtheh M., Inglehearn C.F., Keen T.J., Evans K., Moore A.T., Jay M., Bird A.C. & Bhattacharya S.S. (1994). Identification of a sixth locus for autosomal dominant retinitis pigmentosa on chromosome 19. Hum. Mol. Genet. 3: 351-354

Evans K., **Al-Maghtheh M.**, Fitzke F.W., Moore A.T., Jay M., Inglehearn C.F., Arden G.B. & Bird A.C. (1995). Bimodal expressivity in dominant retinitis pigmentosa genetically linked to chromosome 19q. Br. J. Ophthalmol. 79: 841-846.

Inglehearn C.F., Carter S.A., Keen T.J., Lindsay J. Stephenson A.M., Bashir R., **Al-Maghtheh M.**, Moore A.T., Jay M., Bird A.C. & Bhattacharya S.S. (1993). A new locus for autosomal dominant retinitis pigmentosa on chromosome 7p. Nature Genet. 4: 51-53.

Inglehearn C.F., Keen T.J., **Al-Maghtheh M.**& Bhattacharya S. (1994). Loci for autosomal dominant retinitis pigmentosa and dominant cystoid macular dystrophy on chromosome 7p are not allelic. Am. J. Hum. Genet. 55: 581-582.

Inglehearn C.F., Keen T.J., **Al-Maghtheh M.**, Gregory C.Y., Jay M.R., Moore A.T., Bird A.C. & Bhattacharya S.S. (1994). Further refinement of the location for autosomal dominant retinitis pigmentosa on chromosome 7p (RP9). Am. J. Hum. Genet. 54: 675-680.

Inglehearn C.F., Keen T.J., Tarttelin E.E., **Al-Maghtheh M.**, Evans K.E., Peacock R.E., Patel R.J., Jay M., Bird A.C. & Bhattacharya S.S. (1995). Genetic refinement and a YAC contig across the chromosome 7p autosomal dominant retinitis pigmentosa locus (RP9) and an estimation of the frequency of this and other forms of dominant RP in the UK. Invest. Ophthalmol. Vis. Sci. 36 (suppl.):1044 (abstract no. 4827).

Kim R.Y., **Al-Maghtheh M.**, Fitzke F.W., Arden G.B., Jay M., Bhattacharya S.S. & Bird A.C. (1993). Dominant retinitis pigmentosa associated with two rhodopsin gene mutations: Leu-40-Arg and an insertion disrupting the 5'-splice junction of exon 5. Arch. Ophthalmol. 111: 1518-1524.

Restango G., **Maghtheh M.**, Bhattacharya S., Ferrone M., Garnerone S., Samuelly R. & Carbonara A. (1993). A large deletion at the 3' end of the rhodopsin gene in an Italian family with a diffuse form of autosomal dominant retinitis pigmentosa. Hum. Mol. Genet. 2: 207-208.

CONTENTS IN BRIEF:

CONTENTS IN DETAIL:

List of figure presented in this thesis:

List of tables presented in this thesis:

ABBREVIATIONS

adRP	autosomal dominant retinitis pigmentosa
APS	Ammonium Per Sulphate
arRP	autosomal recessive retinitis pigmentosa
bp	base pair
cDNA	Complementary deoxyribonucleic acid
d.H2O	distilled water
dNTP	Deoxyribonucleotide
dsDNA	Double stranded DNA
DTT	Dithiothreitol
EDTA	Ethylenediaminetetra-acetic acid
kb	kilo base
kd	kilodalton
min	minute
mRNA	messenger ribonucleic acid
ng	nanogram
PCR	polymerase chain reaction
pmole	picomole
ROS	rod outer segment
RP	retinitis pigmentosa
RPE	retinal pigment epithelium
SSCP	Single Strand Conformation Polymorphism
SDS	Sodium Dodecylsulphate
ssDNA	Single stranded DNA
TBE	Tris-Borate-EDTA
TE	Tris-Cl-EDTA
TEMED	N,N,N',N'-tetramethylethylenediamine
UV	ultra violet light
X-GAL	5-Bromo-4-chloro-3-indolyl-β-galactoside
xlRP	X-linked retinitis pigmentosa

CHAPTER I

INTRODUCTION

1.1 INTRODUCTION:

Inherited eye diseases make up a substantial proportion of the classified genetic defects (McKusick, 1992). Amongst such diseases, retinal dystrophies constitute a major cause of blindness, and are responsible for considerable morbidity as they do not limit life expectancy. They comprise a clinically and genetically heterogeneous group, of which retinitis pigmentosa (RP), the subject of this research, is a subgroup. Before going into the detailed description of RP and in order to elucidate its pathogenesis, it is important to understand the normal structure and physiology of the retina and the photochemistry of visual transduction.

1.2 STRUCTURE OF THE RETINA:

The retina is the neural sensory stratum of the eye, which is situated at the interface between the optical imaging tissues of the eye and the neural processing and visual interpreting regions of the brain. It is one of the best characterized parts of the central nervous system. Structurally and functionally the retina consists of two distinct layers: (1) the non-neural retinal pigment epithelium (RPE), a single layer of hexagonally shaped cells resting on Bruch's membrane, and (2) the tightly opposed but non-anatomically joined neural retina (fig 1.1). During development, it is likely that each retinal cell type is specified through sequential restrictions by cell-cell interactions and microenvironmental cues. Cell lineage has been shown to play little or no role in determining cell fate (Wetts and Frazer, 1988; Turner *et al.*, 1990).

1.2.1 Neural retina:

A fully developed vertebrate retina has five major neuronal cell types which form a direct pathway from the retina to the brain. These are photoreceptors (rods and cones), horizontal, bipolar, amacrine and ganglion cells. Photoreceptor axons synapse with the bipolar and horizontal cells in the outer plexiform layer. The axons of the bipolar cells synapse with amacrine cells and with dendrites of the ganglion cells in the inner plexiform layer (fig 1.1).

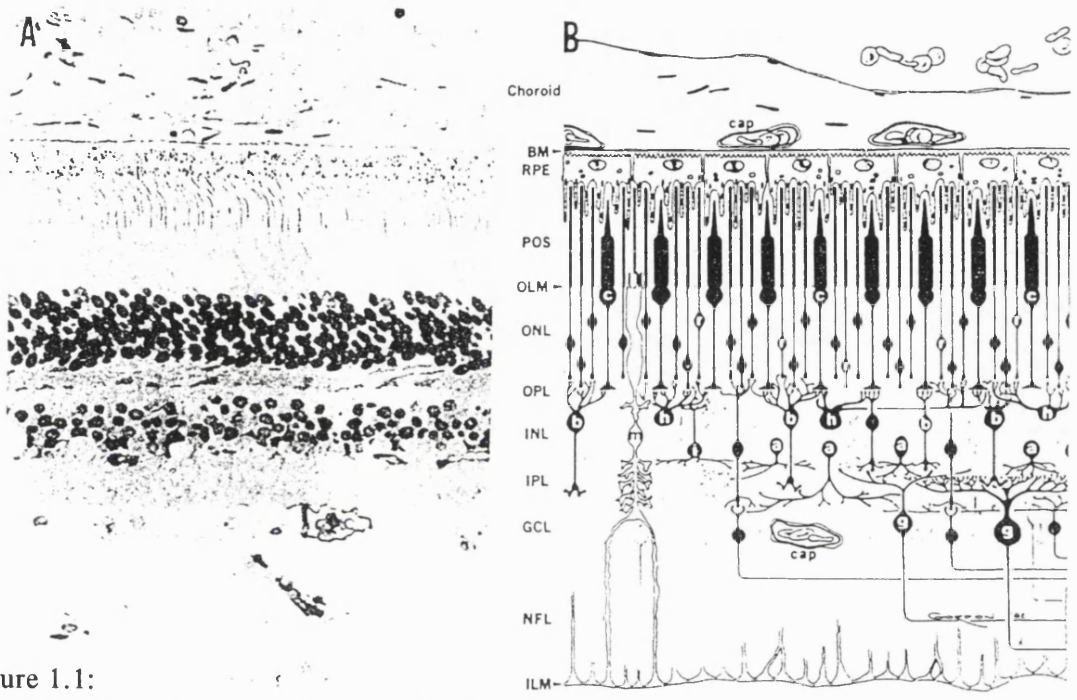

Figure 1.1:
(Figure and legend are from Berman, 1991)

Cellular organization of the vertebrate retina. (A) Histological cross-section of a human retina, and (B) a schematic diagram showing the spatial arrangement of the neuronal cell layers. Abbreviations used: a, amacrine cell; b, bipolar cell; c, cone; g, ganglion cell; h, horizontal cell; i, interplexiform cell; r, rod. The cell layers seen histologically consist of: RPE, retinal pigment epithelium; POS, photoreceptor outer segments; OLM, outer limiting "membrane" (a network of Müller cell apical processes in contact with photoreceptor inner segments); ONL, outer nuclear layer (the photoreceptor cell nuclei); OPL, outer plexiform layer (a region of synapses between photoreceptor, bipolar, and horizontal cells); INL, inner nuclear layer; IPL, interplexiform layer (another region of synapses between bipolar, amacrine, and ganglion cells); GCL, ganglion cell layer; NFL, nerve fiber layer (containing the axonal processes of the ganglion cells); ILM, inner limiting "membrane" (the Müller cell processes that terminate on the vitreal surface); M, Müller cell. (From Fliesler and Anderson, 1983.) (Reprinted with permission from *Prog. Lipid Res.* **22**, Steven J. Fliesler and Robert A. Anderson, "Chemistry and metabolism of lipids in the vertebrate retina," © 1983, Pergamon Press PLC.)

The horizontal and amacrine cells modify and control the impulses and form laterally directed pathways between the neurons. The axons of the ganglion cells join to form the optic nerve which is a natural blind spot near the centre of the retina. The optic nerve is directly connected to the visual cortex of the brain, where the signals transmitted from photoreceptors following a light exposure are processed and interpreted. The distribution of optic nerve fibres to receptors is not uniform. In the fovea centralis about 200,000 cones are connected to at least as many optic nerve axons. In the far periphery, however, 10,000 rods may be connected in clusters to a single nerve fibre, with considerable overlapping, so that a point of light may stimulate several clusters at once. The principal glial cell type of the vertebrate retina are Muller cells whose fibres extend from the vitreous surface or inner limiting 'membrane' of the retina to beyond the outer limiting 'membrane', spanning all retinal layers (fig 1.1). The outer limiting membrane consists of junctional complexes made between the Muller cell processes and the photoreceptor inner segments. Muller cells provide mechanical support for the retina. They also contribute to the generation of the b-wave in electroretinogram (Dowling, 1987; see section 1.7.1).

Functionally the neural retina is usually considered as two regions: The outer (light detecting) layer, containing rod and cone photoreceptor cells required for the reception and conversion of light energy into neural impulses, and the inner signal processing layers of retinal neurons which conduct these nerve impulses to the optic nerve. The photoreceptor cells are of particular interest in this respect since they are the cells that are commonly involved in retinal degenerations.

1.2.1.1 photoreceptor cells:

Vertebrates have two kinds of photoreceptor cells called rods and cones. They can be distinguished morphologically by the shape of their processes; thin cylindrical (rods) and conical (cones) (fig 1.2). Biophysically they can be distinguished by their absorbtion spectra. Cones function in bright light and are responsible for colour (photopic) vision, whereas rods function in dim light, and are responsible for night (scotopic) vision, but do not perceive colour. A human retina contains about six million cones and a hundred million rods.

Rods: As mentioned above, rods make up the majority of photoreceptor cells in the outer layer of the neural retina. Their concentration is higher in peripheral retina (ora serrata) where they reach their maximum concentration in the mid periphery of the retina. Concentration of rods drops suddenly as approaching the centre where they become completely absent in the fovea

centralis. Rods are slender elongated structures with a diameter of 1μm and a length of 40μm (Stryer, 1988). The major functions of a rod cell are highly compartmentalized (fig 1.2). The rod outer segment (ROS) is embedded in the microvilli of the RPE layer, and is specialized for photoreception. It contains a dense vertical stack of about 1000 discs which are closed, flattened sacs about 160A° thick (Stryer, 1988) formed by successive basal evagination of the outer segment plasma membrane (Steinberg *et al.*, 1980). As immature discs are displaced apically by newer ones, they grow to their final diameter and gradually lose attachment with the plasma membrane (Bok, 1985). The composition of the disc membrane has been well characterized. It consists of about 50% protein and 50% lipid with the visual pigment glycoprotein rhodopsin comprising 80-90% of the total protein present in the disc (Basinger *et al.*, 1976). The discs in the ROS are continually renewed throughout life by the "disc shedding" process in which the discs at the very apex of rods are removed in a light triggered rhythmic pattern and phagocytized by the RPE cells, maintaining the outer segments at a relatively uniform length (Young and Bok, 1969; Bok, 1985) (fig 1.3).

A slender immotile *cilium* joins the outer and inner segments. It functions in transmitting cellular components from the inner segment and cell nucleus to the discs and their plasma membrane. The inner segment is rich in mitochondria, which are grouped around the base of the cilium, and in free and membrane bound ribosomes, golgi complexes, and a variety of vesicles and vacuoles (fig 1.2). Therefore it generates ATP at a very rapid rate, and is highly active in synthesizing proteins, mainly for new outer segment discs. The outer fibre connects the inner segment to the cell body that contains the nucleus. The inner fibre terminates in special synaptic endings. Many synaptic vesicles are present in the synaptic body, which forms a synapse with a bipolar neuron.

Cones: The cones have a conical shaped outer segment with the apex pointing towards the RPE cell layer. Cone cells do not possess discs as found in rods, but instead contain a continuous serrated membrane containing the photopigment (fig 1.2). The majority of cones are concentrated in the fovea centralis in which visual resolution is the greatest, with a density of approximately 150,000 cones per mm^2, whereas this number reduces to 4500 cones per mm^2 towards the periphery. The cones are functional at medium and high levels of illumination (photopic vision) and are divided into three types according to the photopigment (opsin) they possess. These are the red, green, and blue opsins which, when attached to 11-*cis* retinal, have peak absorption (λ_{max}) at 560nm (long), 530nm (medium), and 420nm (short wave length)

Figure 1.2:

(Figure and legend are from Berman, 1991)

Schematic diagram of primate rod and cone cells and their relationship to the underlying pigment epithelial cell layer. The outer segments of the rod cell consist of parallel stacks of flattened disks; although usually considered to be free-floating, there may be weak attachments to each other and to the plasma membrane through thin spectrin-like filaments (see Section 7.2.1.1). In contrast, cone outer segments consist of continuous infoldings of the plasma membrane. The rod outer segments of most species are in close apposition to the apical surface of the pigment epithelium, surrounded in their distal portions by villous processes projecting from the surface of these cells. Cone outer segments are usually not in close apposition to the pigment epithelium but may have weak attachments through "cone matrix sheaths" (see Section 7.3.1). In both types of visual cell, the mitochondria are concentrated in the ellipsoid region of the inner segments; rough and smooth endoplasmic reticulum and the Golgi stacks are localized in the myoid region.

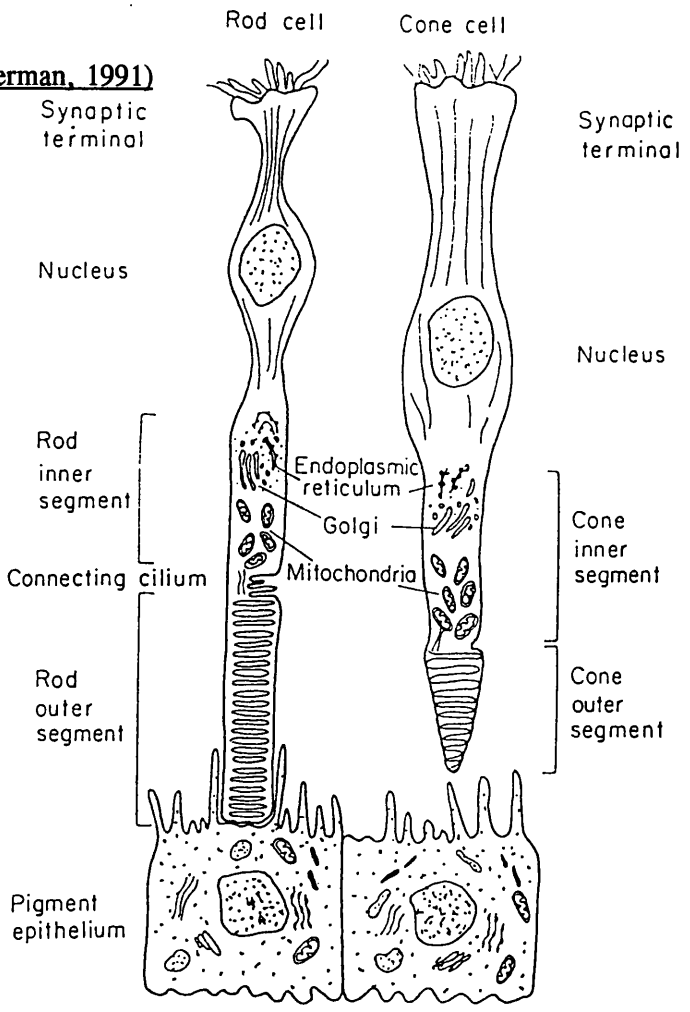

Figure 1.3:

(Figure and legend are from Berman, 1991)

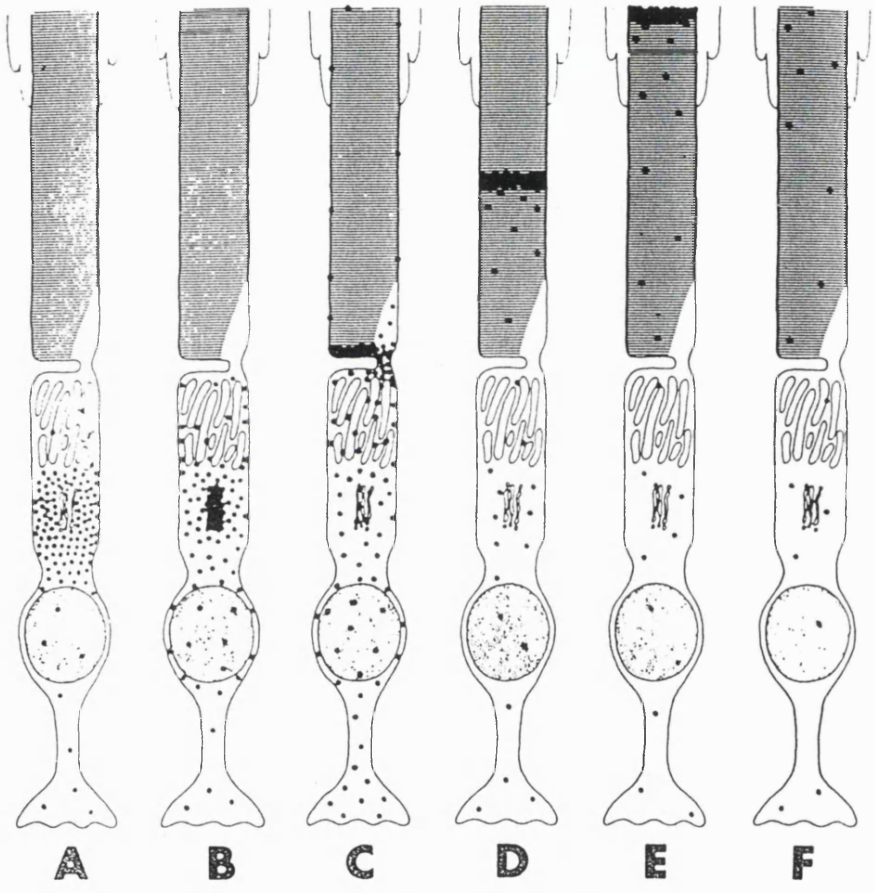

Diagram illustrating protein renewal in vertebrate rod outer segments. Autoradiographic studies show that newly synthesized protein is first concentrated in the rough endoplasmic reticulum and shortly afterward passes into the Golgi complex. After posttranslational glycosylation, the protein is transferred vectorially in vesicles through the inner segment to the connecting cilium, where it is incorporated into newly formed disk membranes. They are displaced distally, and, on reaching the distal tip, packets of outer segment disks are shed and phagocytized by the pigment epithelium. (From Young, 1976.)

respectively. These photopigments are responsible for colour vision in cones. Some animals do not have colour vision, since they have either a very low frequency or complete absence of cones.

Disc shedding also takes place in cone photoreceptor cells (Hogan *et al.*, 1974; Anderson and Fisher, 1976) in a process in which cone outer segments remodel themselves after each shedding event (since the most apical cone outer segment discs have a constant but smaller diameter than the basal ones in most species). Disc fluidity could be an important factor in this remodelling process, but cytoskeletal elements may play a role as well (Bok, 1985).

1.2.2 Retinal pigment epithelial layer:

The retinal pigment epithelium (RPE) is a single layer of cuboidal cells lying between Bruch's membrane and the photoreceptors. The apical RPE cell surface faces the photoreceptors and its villous processes interdigitate with their outer segments (fig 1.2). The basal surface with its numerous infoldings is functionally linked to the choroid via Bruch's membrane. RPE cells are joined to one another by tight junctions and constitute an important structural and functional part of the blood-retinal barrier. Together with the endothelium of choriocapillaries, it effectively excludes the exchange of potentially toxic substances between the choroidal circulation and the neural retina. Receptors for serum retinol-binding protein (RBP) are found on the basal and lateral plasma membranes of the RPE cells (Pfeffer *et al.*, 1986). The retinal pigment epithelium displays a wide variety of activities, including phagocytosis of photoreceptor outer segments (disc shedding), uptake and storage of retinoids, secretion of interphotoreceptor cell matrix (IPM) and basement membrane components, transport of substances between the photoreceptors and the choriocapillaries and maintenance of photoreceptor microenvironment. RPE also plays a role in the control of light scatter and absorption of light energy.

1.3 PHOTOTRANSDUCTION:

When electromagnetic radiation from the visible spectrum (400-700nm) is absorbed by the photopigment of rods or cones, a graded membrane hyperpolarization is initiated. This electrical signal is transmitted to the optic nerve which carries the coded message to the optic centre of the brain, where interpretation and perception occurs. The outer segments of rods and cones are the sites of visual transduction in vertebrate eyes. They represent up to 95% of photoreceptor mass in many vertebrate retinas and are well separated from the energy generating and protein

synthesizing material of the inner segments. This feature distinguishes the ROS as one of the few cellular fractions of the retina that can be isolated in essentially pure form, which makes it relatively easy to purify and study the proteins involved in phototransduction.

1.3.1 Rhodopsin activation:

Photoreceptor cells convert a single photon of light into atomic motion and then into a nerve impulse (Stryer, 1988). The primary event in the visual excitation is the light triggered isomerization of the 11-*cis*-retinal of rhodopsin (table 1.1; see also chapter III) to its all-*trans* isomer. This isomerization markedly alters the geometry of retinal and results in the release of all-trans from its membrane-bound protein cofactor into the disc membrane lipid (Wald, 1968). This results in the formation of a photoactivated rhodopsin (R^*) (fig 1.4) as a result of a conformational change in the opsin molecule.

1.3.2 Transducin activation:

Transducin is a peripheral membrane protein of the ROS which is a member of a large family of signal transducing guanosine nucleotide-binding proteins known as G proteins. The function of G proteins is to transmit signals between transmembrane receptors and cellular effectors. Transducin is composed of two functional subunits T_α and $T_{\beta\gamma}$ (T_β and T_γ) (Baehr *et al.*, 1982; Fung, 1987).

The T_α subunit is a member of a gene family that is relatively conserved among various members of the G-proteins, and is thought to confer the functional specificity to each G-protein (Simon *et al.*, 1991). Rod- and cone-specific T_α subunits in the outer segments of photoreceptors are examples of the diversity of this subunit (Yatsunami and Khorana, 1985). The β subunit is highly conserved and may even be identical to other G-protein β subunits (Fung, 1987 ; Simon *et al.*, 1991). The γ subunit does not share extensive homologies with γ subunits of other G-proteins (Hildebrandt *et al.*, 1985), so it seems likely that the γ subunit that confers specificity to the $\beta\gamma$ complex in its interaction with the α subunit (Fung, 1987).

In the visual transduction process, interaction of photoactivated rhodopsin (R^*) with transducin catalyses the exchange of guanosine diphosphate (GDP) bound to the T_α subunit for guanosine triphosphate (GTP) and the subsequent dissociation of the GTP-T_α complex from the $T_{\beta\gamma}$ heterodimer (fig 1.4). In retinal rods each photoactivated rhodopsin generates several hundred GTP-T_α molecules and each active GTP-T_α persists in the active state long enough to

find and activate cGMP-PDE molecules (see below).

1.3.3 cGMP-Phosphodiesterase:

Activated GTP-T_α interacts with inactive cGMP-phosphodiesterase (PDE). The $T_{\beta\gamma}$ subunit has been shown to have no effect on cGMP-PDE effector (Fung *et al.*, 1981). Rod cGMP-PDE is a heterotetrameric peripheral membrane protein composed of two catalytic α and β subunits and two smaller inhibitory γ subunits (table 1.1; Baehr *et al.*, 1979; Deterre *et al.*, 1988; Fung *et al.*, 1990). The binding of the GTP-T_α subunit to the PDE γ subunits relieves their inhibitory constraints, releasing the hydrolytic potential of the enzyme. Activated cGMP-PDE then hydrolyses 3',5'-cGMP to 5'-GMP at a high rate which is limited only by the availability of the substrate through diffusion. PDE remains active until the GTP which occupies T_α is hydrolysed by the intrinsic GTPase activity of this subunit (Bourne *et al.*, 1990). Upon GTP hydrolysis of T_α, the PDE γ subunits are released to form PDE complex and inhibit enzyme activity.

1.3.4 cGMP-gated cation channels:

The fall in cGMP that results from light triggered phosphodiesterase activation is detected by the cGMP-activated cation channel protein of the ROS plasma membrane (fig 1.4). This protein consists of a 63kd (Cook *et al.*, 1987) α subunit that is localized exclusively to the ROS plasma membrane and comprises 7% of its total protein (Cook *et al.*, 1989), and 240kDa (Molday *et al.*, 1990) tightly linked β (Chen *et al.*, 1993) and γ subunits (Illing *et al.*, 1994; table 1.1). The opening status of these light sensitive channels of the ROS membrane are controlled by cytosolic cGMP concentrations. The channels remain open when the cGMP concentrations are high.

1.3.5 Hyperpolarization of the ROS:

The hydrolysis of cGMP by PDE and the blockage of the cation channels results in a membrane hyperpolarization of photoreceptor cells (Fesenko *et al.*, 1985; Stryer, 1986; Yau and Baylor, 1989). This hyperpolarization is transmitted as an electrical signal through nerve cells within the retina and via the optic nerve to the optic sites of the brain.

1.4 REGULATION OF PHOTOTRANSDUCTION:

Two interesting aspects of photoreceptor biology are the sensitivity and adaptability these cells display in response to light stimuli. These cells are capable of responding to single photons

of light in the dark adapted state through amplification of signal (Stryer, 1988); this exquisite sensitivity is a key feature of this cascade. Such amplification is achieved because each rhodopsin is able to activate over 500 transducin molecule, and each molecule of PDE that is activated by transducin is capable of hydrolysing about 1000 cGMP molecules (Stryer, 1986). The visual systems of vertebrates and invertebrates are also able to modulate their sensitivity and respond to light stimuli that vary by more than six orders of magnitude in intensity without response saturation.

1.4.1 Calcium dependent regulation:

Calcium has been found to play a central role in photorecovery and adaptation in both rods and cones (Matthews *et al.*, 1988). In the dark, the entry of calcium ions through the cGMP-gated cation channels is balanced by efflux of calcium through the Ca^{2+}-Na^{+}-antiporter to give a Ca^{+2} concentration of 300nM (Koch and Stryer, 1988). Upon light exposure and closure of channels, the influx of calcium is blocked, but its efflux through the antiporter continues, which results in a drop of intracellular Ca^{+2} concentration ($[Ca_i^{2+}]$) to less than 70nM. Changes in $[Ca_i^{2+}]$ have been shown to modulate the synthesis and hydrolysis of cGMP by guanylate cyclase and phosphodiesterase respectively (Torre *et al.*, 1986). It is also evident that cGMP and $[Ca_i^{2+}]$ levels are reciprocally controlled by negative feedback (Stryer, 1986; Pugh and Cobbs, 1986) through guanylate cyclase as described below.

1.4.2 Guanylate cyclase:

Electrophysiological and biochemical experiments demonstrated that the main target of decreased calcium levels in photoreceptor cells is guanylate cyclase (GC) (table 1.1; Koch and Stryer, 1988). GC is a peripherally bound membrane protein that catalyses the resynthesis of cGMP from GTP. Its activity is regulated by a calcium switch, possibly another protein (see section 1.4.4), that senses changes in $[Ca_i^{2+}]$ concentration. This activation, which is controlled by a highly cooperative feedback mechanism, is a key event in restoring the dark current after visual excitation.

1.4.3 Recoverin:

Calcium dependent stimulation of GC was thought to be mediated by a ~26kd protein called recoverin (so called as it was thought to promote recovery of the dark state). Recoverin (table 1.1) is present in both rod and cone photoreceptor cells, and is thought to detect changes of cytosolic calcium in the physiological range of less than 300nM. Initially it was thought to

transmit the signal of decreased calcium levels after illumination to guanylate cyclase which is stimulated by the calcium free form of recoverin (Lambrecht and Koch, 1991 ; Dizhoor *et al.*, 1991). However, doubts about the role of recoverin were raised and the suggested role was excluded (Hurley *et al.*, 1993). A more recent study (Gray-Keller *et al.*, 1993) demonstrated that raising the concentration of recoverin within rod cell slows recovery from photoexcitation. The same results were also obtained with recoverin-like proteins, Visinin and S-modulin (Gray-Keller *et al.*, 1993), the 26kd Ca^{+2}-binding proteins of chicken cones and frog rods respectively (Yamagata *et al.*, 1990; Kawamura *et al.*, 1992). These proteins were found to play no significant role in Ca^{+2} regulation of guanylate cyclase. On the other hand, it has been found that when introduced intracellularly they prolong the rising phase of light response. It was suggested that these proteins interfere with the events that quench activated rhodopsin. Furthermore, recoverin is not only present in outer segments of photoreceptors but also more concentrated in inner segments and present in synaptic connections of rods and in the bipolar cells, which suggests a rather more general role in the cell physiology than was originally suggested.

Recently recoverin has been found to bind specifically to rhodopsin kinase (RK) (Chen and Hurley, 1994). A possible function for this Ca^{+2}-binding protein may involve interaction with RK and regulation of opsin phosphorylation. Moreover recoverin has been found to be the same protein previously known as CAR (cancer associated retinopathy) protein. It was found to map to the same mouse chromosomal region to which previously a mouse tumour supressor protein was mapped, and which is syntenic to human chromosome 17 (McGinnis *et al.*, 1993) where human recoverin has been previously mapped (Murakami *et al.*, 1992). Recoverin has also been found to be associated with some ocular cancers (McGinnis *et al.*, 1995).

1.4.4 Guanylate cyclase activating protein:

However, another protein, guanylate cyclase activating protein (GCAP), has been recently postulated to mediate Ca^{+2}-sensitive regulation of guanylyl cyclase, promoting recovery of the dark state of rod photoreceptors following light exposure (Gorczyca *et al.*, 1994). GCAP was cloned and the protein characterized from different vertebrate species (bovine, human, murine and frog). GCAP is expressed specifically in both rod and cone photoreceptor cells, and is believed to sublocalize to photoreceptor outer segments with a molar ratio to rhodopsin of 1:100. It is believed that GCAP is a novel photoreceptor-specific member of a large family of Ca^{+2}-binding proteins that participate in the Ca^{+2}-sensitive activation of GC. The consequent

formation of cGMP by guanylate cyclase restores the open state of the channels. The entry of calcium then leads to decreased activity of guanylate cyclase and the return to the dark state. This feed back loop involving calcium ions is likely to be a major contributor to the maintenance of a constant cGMP level in the dark and to recovery following illumination (Koch and Stryer, 1988).

1.4.5 Calmodulin:

This is a cytosolic calcium-binding protein which is expressed ubiquitously and has been found in the rod outer segment (Nagao *et al.*, 1987). In the dark, free cGMP levels in ROS maintain a small but significant number of channels in their open state, and also maintain the cGMP-gated channel (α subunit) in its low affinity state for cGMP through reversible Ca^{+2}-calmodulin binding to the 240 kd channel (β and γ subunits). Following illumination and when the channel is in its low affinity state, a small decrease in free cGMP concentration results in its closure. Consequently, as a result of decrease in $[Ca_i^{+2}]$, calmodulin will dissociate from the channel to switch to its high-affinity state for cGMP. This will allow the channel to reopen at lower cGMP levels, leading to recovery of the ROS to its dark level as cGMP synthesis proceeds. The opening of the channel will in turn restore the $[Ca_i^{+2}]$ to its dark level and the return of the channel to its low affinity state through Ca^{+2}-calmodulin rebinding (Hsu and Molday, 1993).

1.4.6 Rhodopsin kinase:

This is a cytosolic protein in the rod photoreceptors (table 1.1) that initiates the deactivation of the phototransduction cascade by phosphorylating photoactivated rhodopsin (R^*) (Sichi and Somers, 1978). It phosphorylates the threonine and serine residues located in the C-terminal domain of rhodopsin on the cytoplasmic surface of the disc membrane (Hargrave *et al.*, 1980). In addition to serine and threonine residues in the C-terminus, rhodopsin kinase also phosphorylates similar residues in the third cytoplasmic loop of rhodopsin (fig 3.3). Phosphorylated rhodopsin has a decreased ability to activate transducin and enhanced ability to bind 48kd protein, arrestin, the latter completing the deactivation of rhodopsin (fig 1.4 see below).

1.4.7 Arrestin:

Also known as 48kd protein or S-antigen, arrestin is a cytoplasmic protein which, under dark conditions, binds specifically to photoexcited-phosphorylated rhodopsin and quenches its

activation of transducin (Wilden *et al.*, 1986; fig 1.4).

1.4.8 GTPase activity of T_α subunit:

T_α subunit, like other G-proteins, is a GTPase that hydrolyzes bound GTP to GDP and inactivates itself (Bourne *et al.*, 1990). This results in the termination of the signal initiated by photoactivated rhodopsin. The GDP-T_α subunit then reassociates with the $T_{\beta\gamma}$ complex to reform the inactive transducin heterotrimer (Simon *et al.*, 1991; fig 1.4).

1.4.9 Phosducin:

This is a soluble 33kd phosphoprotein that is most abundantly expressed in retinal photoreceptors and the pinealocytes of the pineal gland (Lolley *et al.*, 1992), but also present in many other tissues where cell-specific isoforms of phosducin may participate in the modulation of signal transduction (Craft and Lolly, 1994). In its native conformation, phosducin exists as a 77kd heterotrimeric complex with the $\beta\gamma$-subunits of transducin ($T_{\beta\gamma}$) (Lee *et al.*, 1987). Phosducin/$T_{\beta\gamma}$ complex is present in the photoreceptor at a level similar to that of transducin. However, unlike transducin which is concentrated in the rod outer segments, phosducin/$T_{\beta\gamma}$ complex is dispersed through out the cytosol of photoreceptor cells (Lee *et al.*, 1990). Although phosducin binds to $T_{\beta\gamma}$, it does not have any homology with T_α; it may be involved in direct regulation of G protein function via inhibition of the GTPase activity of T_α chain (Bauer *et al.*, 1992).

1.5 SUMMARY OF PHOTOTRANSDUCTION PROCESS:

The primary event in the visual excitation process is the light isomerization of 11-*cis*-retinal to its all-*trans* isomer and the formation of photoactivated rhodopsin (R^*). Interaction of R^* with transducin catalyses the exchange of GDP bound to the T_α subunit for GTP and the subsequent dissociation of the GTP-T_α from the $T_{\beta\gamma}$ heterodimer. Activated GTP-T_α binds to the PDE γ subunits and relieves their inhibitory constraints, releasing the hydrolytic potential of PDE. Activated cGMP-PDE hydrolyses 3',5'-cGMP to 5'-GMP. The fall in cGMP is detected by the cGMP-activated cation channel protein, and results in closure of these channels. The closure of the cation channels results in a membrane hyperpolarization of photoreceptor cells which is transmitted as an electrical signal via the optic nerve to the optic centres of the brain for image processing.

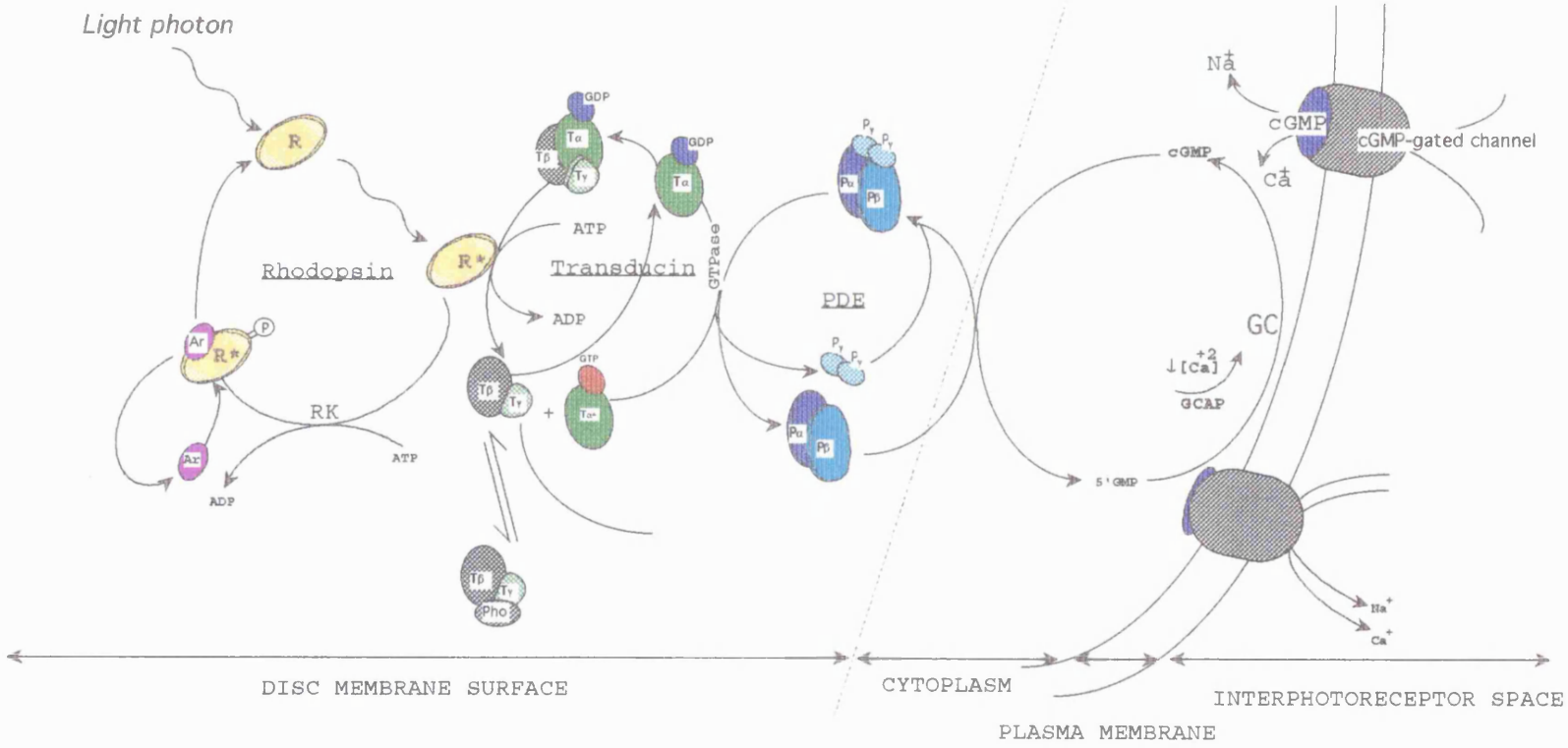

Figure 1.4:
Diagram of the biochemical events involved in the activation and inactivation of phototransduction. Ar: arrestin, Pho: phosducin, and other abbreviations are as described in text (figure modified from Farber, 1995).

Rhodopsin kinase initiates the deactivation of the phototransduction cascade by phosphorylating R^*. Phosphorylated rhodopsin has a decreased ability to activate transducin and enhanced ability to bind arrestin which quenches its activation of transducin. T_α subunit is a GTPase that hydrolyzes bound GTP to GDP and inactivates itself, which results in the termination of the signal initiated by R^*. The GDP-T_α subunit then reassociates with the $T_{\beta\gamma}$ complex to reform the inactive transducin heterotrimer. Phosducin, which exists in photoreceptor cells in the form of a phosducin/$T_{\beta\gamma}$ complex, may be involved in the direct regulation of transducin function via inhibition of the GTPase activity of T_α chain.

Light exposure and closure of channels results in a drop of $[Ca_i^{2+}]$. The main target of decreased calcium levels in photoreceptor cells is guanylate cyclase (GC) that catalyses the resynthesis of cGMP from GTP. Its activity is regulated by a calcium switch, possibly another protein, that senses changes in $[Ca_i^{2+}]$ concentration. GCAP has been recently postulated to mediate this Ca^{2+}-sensitive regulation of guanylate cyclase. The consequent formation of cGMP by guanylate cyclase restores the open state of the channels. The entry of calcium then leads to decreased activity of guanylate cyclase and the return to the dark state. In the dark, free cGMP levels in the ROS maintain a small but significant number of channels in their open state. It also maintains the cGMP-gated channel (α subunit) in its low affinity state for cGMP through reversible binding of Ca^{2+}-calmodulin to the 240kd channel protein (β and γ subunits). Following illumination and when the channel is in its low affinity state, a small decrease in free cGMP concentration results in its closure. Consequently, as a result of decrease in $[Ca_i^{2+}]$, calmodulin will dissociate from the channel, which will switch it to its high-affinity state for cGMP. This will allow the channel to reopen at lower cGMP levels, leading to recovery of the ROS to its dark level as cGMP resynthesis proceeds. The reopening of the channel will in turn restore the $[Ca_i^{2+}]$ to its dark level and the return of the channel to its low affinity state through Ca^{2+}-calmodulin rebinding.

1.6 OTHER RETINAL PROTEINS:

1.6.1 Peripherin/RDS:

Peripherin/RDS (retinal degeneration slow) is a photoreceptor specific transmembrane protein (table 1.1) expressed in the rim region of outer segment discs of both rods and cones (Connell and Molday, 1990; Travis *et al.*, 1991a). This protein, which has four membrane-spanning domains (fig 1.5a; Travis *et al.*, 1991a), could be involved in the photoreceptor

morphogenesis, possibly as an adhesion molecule for stabilization of the outer segment discs (Arikawa *et al.*, 1992). This function is probably mediated by the D2 loop, the larger of the two intradiscal loops, through homophilic interactions across the intradiscal space (Travis *et al.*, 1991a; fig 1.5b). The predicted amino acid sequence is highly conserved among mice (Travis *et al.*, 1989), cattle (Connell *et al.*, 1991), rats (Begy and Bridges, 1990) and humans (Travis *et al.*, 1991). However, missense mutations which give rise to amino acid polymorphisms in humans have been found in the carboxyl terminus of this protein (Jordan *et al.*, 1992a).

1.6.2 Rom1:

This is a 37kd rod photoreceptor membrane protein which is 35% identical and structurally similar to peripherin (Bascom *et al.*, 1992). Like peripherin, ROM-1 is a retina-specific integral membrane protein localized to rod photoreceptor disc rim. ROM-1 may play a critical role in the biogenesis of the discs in rod photoreceptors and in maintaining the structure of the mature ROS. Although both ROM-1 and peripherin form disulfide dimers, they do not form heterodimers with each other but appear to associate noncovalently. Thus ROM-1 and peripherin are functionally related members of a possibly new photoreceptor specific protein family (see section 1.7.1.4).

1.6.3 Retinoid binding proteins:

Retinoids are delivered to the RPE through both the basal and apical surfaces. To the former, *trans* retinol is delivered through the serum retinoid binding protein (RBP) which transports retinoids from the circulation to the RPE via receptors which are localized on the basolateral membrane of the RPE (Bok, 1985). To the latter, retinoids are delivered through the operation of the visual cycle. Cytosolic binding proteins play a major role in the transport and metabolism of retinoids in the RPE. These include cellular retinol-binding protein (CRBP) which carries all-*trans* retinol as an endogenous ligand. CRBP has also been detected in the nucleus of RPE cells in association with euchromatin, where it may be involved somehow in modification of gene expression (Bok, 1985). Cellular retinaldehyde-binding protein (CRALBP) is another cytosolic retinoid binding protein. It carries 11-*cis* retinal as an endogenous ligand from either unbleached rhodopsin in the RPE phagosomes, or produced in the RPE from *trans* retinol. Interstitial retinoid-binding protein (IRBP) serves for shuttling of retinoids in the subretinal space (Bok, 1985).

Figure 1.5:

(Figure and legend are from Travis et al., 1991a)

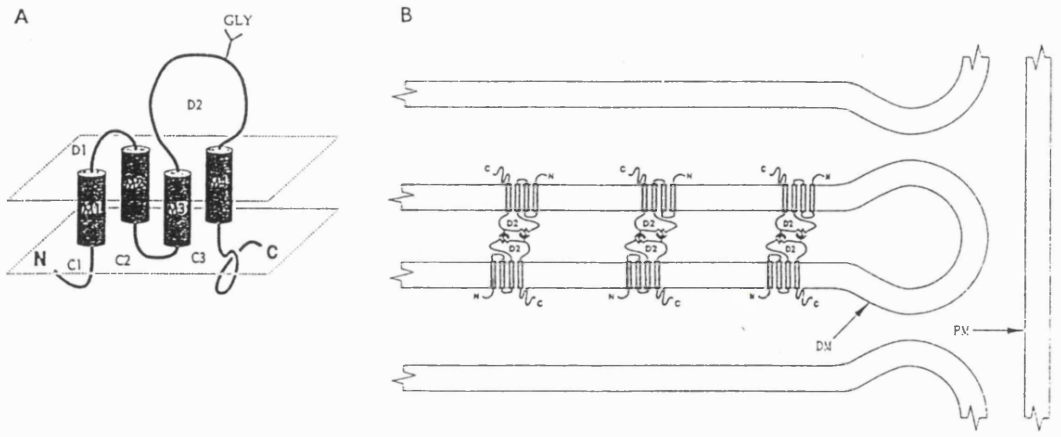

Structural Models for the *rds* Protein

(A) Model for the *rds* protein within the disc membrane. The four putative membrane-spanning domains are labeled M1–M4. This orientation places the amino- and carboxy-terminal domains within the cytoplasm and the two loops, one of which contains the conserved glycosylation site, within the extracellular (intradiscal) space.

(B) Functional model for the *rds* protein as an adhesion molecule responsible for stabilization of outer segment discs. The proposed function of the *rds* protein is to maintain opposing faces of the outer segment discs in close apposition through homophilic interactions of glycans across the disc space. These attractive interactions may also involve residues within the conserved D2 loops.

Table 1.1:

Chromosomal location of genes encoding proteins involved in the phototransduction pathway and other photoreceptor specific proteins. Diseases known to be caused by mutations in some of these genes are also listed.

protein	subunits/ isoenzymes	Chromosomal location	Disease caused by mutation in this gene
Rhodopsin	-	3q21-q24	adRP, arRP, CSNB
Red opsin	-	Xq28	colour blindness
Green opsin	-	Xq28	colour blindness
Blue opsin	-	7q22-qter	colour blindness
Transducin	α (rod)	3p21	-
	α (cone)	1p13	-
	β	1p31.2-pter	-
	γ	unknown	-
cGMP-PDE	α	5q31.2-q34	arRP
	β	4p16.3	arRP, CSNB
	γ	17q21.1	-
cGMP-gated cation channel	α (63 kd)	4p14-q13	arRP
	β (240 kd)	unknown	-
	γ (240 kd)	unknown	-
Guanylate cyclase	-	17p13.1	-
Recoverin	-	17p13.1	-
GCAP	-	6p21.1	-
Calmodulin	CAL2	1	-
	CAL3	19	-
Rhodopsin kinase	-	13q34	-
Arrestin	-	2q24-q37	Oguchi disease
Phosducin	-	1q25-32.1	-
Peripherin	-	6p12	adRP, macular dystrophies, digenic RP
ROM1	-	11q13	digenic RP
CRBP	-	3q21-q22	-
IRBP	-	10p11.2-q11.2	-
CRALBP	-	15q26	-

1.7 RETINAL DEGENERATIONS:

1.7.1 Retinitis pigmentosa:

Clinical description:

Retinitis pigmentosa (RP) is a collective term used to describe a group of inherited retinopathies characterized by night blindness (nyctalopia), and constricted visual fields, which often progress to complete blindness. This term was first used by Donders in 1855, to describe a group of retinal dystrophies with similar ophthalmoscopic appearances and symptomatology. RP is the most common amongst inherited eye disorders and it affects 1-2 in every 5,000 births in the western world (Bougman *et al.*, 1980; Bundy and Crews, 1984).

RP is progressive, although the mode and extent of this progression is variable. The variation in the age of onset of night blindness and the wide range of severity is a common feature in this group of retinal degenerations. However, a typical RP patient complains of night blindness from childhood years, with noticeable symptoms of visual field loss dating from late twenties. The patient will complain of severe visual disability with tunnel vision and night blindness in the forties and would have little or no functional vision by the age of sixty to seventy. In later stages, flashes or rolling waves of light are a common occurrence (Heckenlively, 1988).

The most characteristic ophthalmoscopic findings in RP are depigmentation or atrophy of the retinal pigment epithelial (RPE) layer, pigment deposition in the retina and attenuation of the retinal blood vessels. The pigmentary disturbance often takes the form of clumps and strands of black pigment, occurring most prominently in the periphery and often in a perivascular pattern due to pigment within vessel walls. Bone corpuscular-like (bone spicule) arrangements of pigment are common, but small irregular clumps and spots of pigment may be seen almost as often (fig 1.6). The RP pigmentary pattern can be regarded as a common feature of different acquired and hereditary retinal degenerations. Localized retinal pigment deposition is commonly seen in processes that injure or destroy the RPE layer. Some patients with pigmentary retinopathies as a consequence of vitamin A deficiency, previous inflammatory disease, ocular trauma, retinitis secondary to syphilis, rubella or drug toxicity, or systemic disorders such as abetalipoproteinemia syndrome are often misdiagnosed as having RP. These cases are referred to as "pseudo RP". Frequently it is difficult to distinguish pseudo RP patients from those who have inherited RP in a mendelian fashion. Despite the fact that the pigment deposition accounts for the disease name, it is still a secondary effect to the pathological process and whether it contributes to the

Figure 1.6:

Fundus photograph of the retina. Normal (top) and affected (bottom) retina showing the bone spicule appearance of pigmentary deposit seen in retinitis pigmentosa.

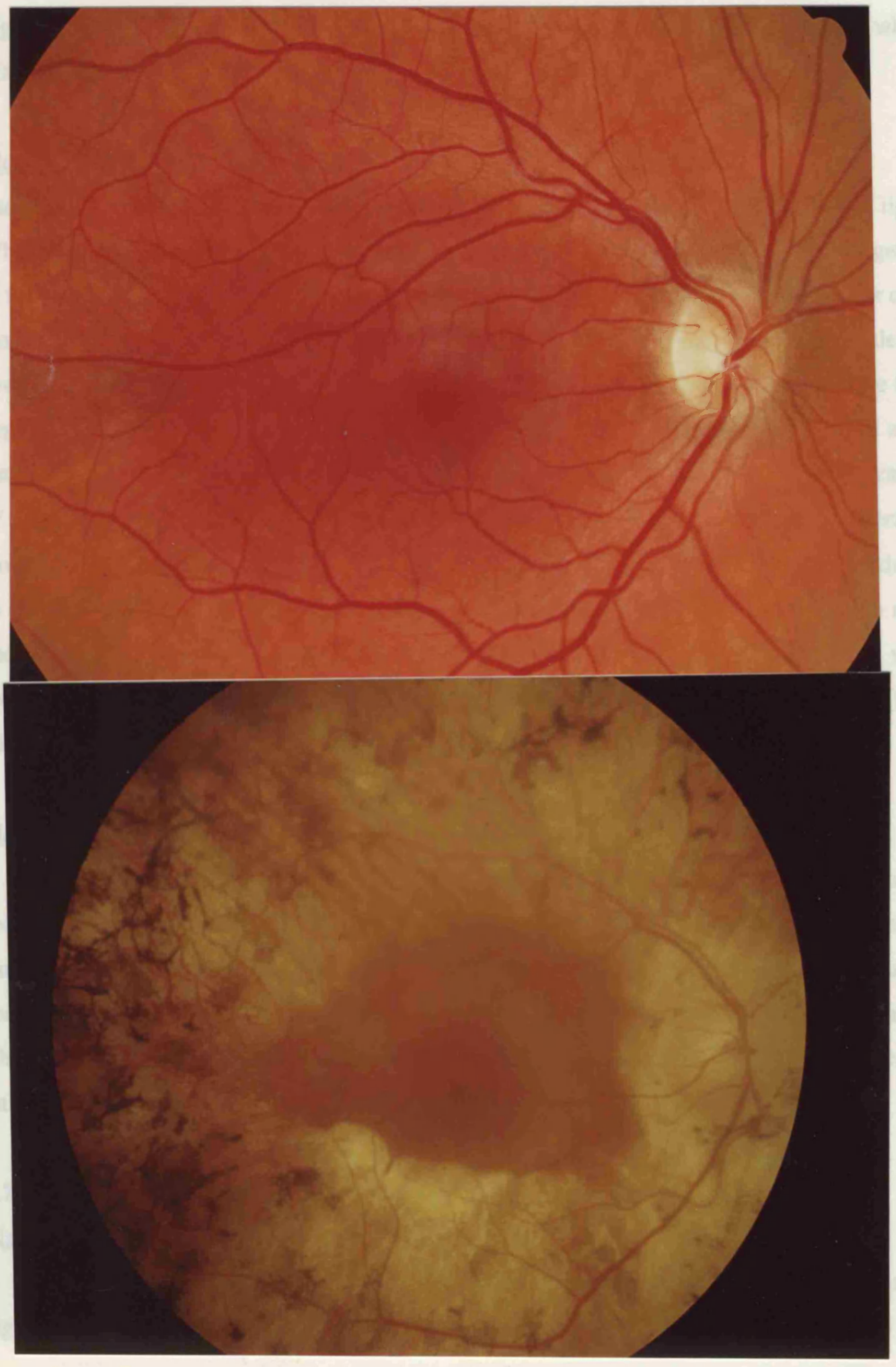

deterioration of the retinal function is not known. On the other hand, the term retinitis is a misnomer, since there is little evidence of inflammation on histopathology (Heckenlively, 1988). RP principally affects the photoreceptor cell layer (Heckenlively, 1988). It is the rod photoreceptors which are primarily affected and responsible for the classical early symptom of night blindness. This early loss of rods in the mid-periphery results in a ring scotoma which gradually encroaches centrally, eventually affecting central vision.

Electrophysiology:

The electroretinogram (ERG) is the electric response evoked from the retina by a flash of light. When a patch of the retina is illuminated the current generated by each cell type is mixed together in the extracellular space. Current generated from retinal bipolar, Muller, and photoreceptor cells tends to flow into the vitreous. This can be recorded as an electroretinogram (ERG) outside the eye at the cornea with a contact lens electrode. The standard ERG has a biphasic response. The first negative downward peak is called an 'a' wave, and the next positive upward peak is called a 'b' wave (fig 1.7). The a-wave represents the negative receptor potential mainly from repolarization of photoreceptors. The second positive wave (b-wave) is a combination of potential generated from both Muller and bipolar cells. Since the current generated by photoreceptors is considered as a prominant component of ERG, the latter is used to assess the relative normality of both rods and cones. ERG abnormalities in RP are usually recordable even in presymptomatic cases with reduced amplitude of rods; cones also may have reduced amplitude at an early stage (fig 1.7). In advanced cases of RP all responses are extinguished.

Mode of inheritance of RP:

About 50% of RP cases are inherited in either an autosomal dominant (adRP), autosomal recessive (arRP), or x-linked (xlRP) pattern. The genetic distribution of each form of RP varies in studies carried out in different populations (Boughman *et al.*, 1980; Bunker *et al.*, 1984; Bundy and Crews, 1984). Some of this variation may arise from difficulties in classifying sporadic cases, which may arise from new mutations, as a result of variable penetrance, or may be recessive, X-linked, or digenic cases where family history is not available.

1.7.1.1 Autosomal dominant RP (adRP):

Classification of adRP:

Autosomal dominant retinitis pigmentosa (adRP) accounts for about 25% of total retinitis pigmentosa (RP) cases (Jay 1982a; Bundy and Crews, 1984). adRP is both clinically and

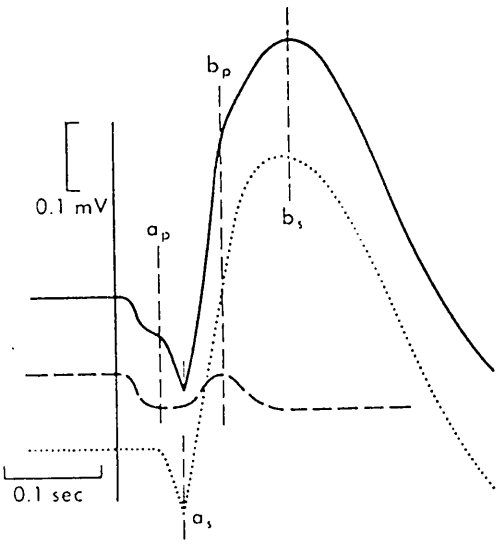

Figure 1.7:

(Figure and legend are from Berson, 1992)

Analysis of ERG in dark-adapted human eye as the resultant of photopic *(dashed line)* and scotopic *(dotted line)* components. The a-wave is composed of photopic (a_p) and scotopic (a_s) components, and the b-wave is similarly composed of photopic (b_p) and scotopic (b_s) components. (From Armington JC, Johnson EP, Riggs LA: J Physiol (Lond) 118:289, 1952.)

genetically heterogeneous. Before the identification of the underlying genetic defects, clinicians classified adRP into distinct subgroups. Massof and Finkelstein (1981) first proposed the distinction between severe diffuse rod disease (type 1) and regional photoreceptor disease (type 2). Another classification described by Lyness and coworkers (1985) was based on differences in the static perimetry of data obtained from large families rather than the observation of the fundus appearance. This divides adRP into two subgroups: D-type (for diffuse loss of rod function) where there is severe and diffuse loss of rod function which in some regions coexists with relatively normal cone function; and R type (for regional loss of rod function) where loss of rod function is regional and accompanied by loss of cone function.

Broadly speaking, D type patients of the second classification conform to the description of type 1 of the former and R type patients to type 2 (Lyness *et al.*, 1985). In type I/D adRP, night blindness usually occurs before 10 years, while pigmentary changes may not be evident until the second or third decade of life and visual difficulties are not identified until 10-20 years after onset of night blindness. In type II/R the onset of night blindness is much more variable. It could be before the age of 10, but there is a strong correspondence between R type disease and onset of night blindness after the age of 20 years. Field loss in day light in type II/R is usually apparent a short time after the onset of night blindness (Bird, 1988). Some of the type II/R adRP families show variable expressivity and occasionally appear to skip a generation, which in pedigree analysis terms is referred to as variable or incomplete penetrance (Boughman *et al.*, 1980; Kaplan *et al.*, 1990; Moore *et al.*, 1993).

Sector RP is a third subgroup proposed by some investigators (Fishman *et al.*, 1985; Heckenlively, 1988). It is characterized by retinal atrophy seen only in one part of the fundus, usually the lower nasal quadrant, and gross field loss confined to the area of visual field corresponding to the involved retina. In contrast to other forms of adRP, sector RP has a better visual prognosis.

Molecular genetics of adRP:

The molecular genetics of adRP has progressed remarkably in the last few years. Linkage to C17 (D3S47) on 3q21 in a large adRP family called TCDM1 (McWilliam *et al.*, 1989) was the first step towards the identification of the rhodopsin gene involvement in adRP. This was quickly followed by the finding of the first mutation in rhodopsin, pro 23-his (Dryja *et al.*, 1990a) which accounted for 12% of US adRP cases (see chapter 3). This RP locus was designated as

RP4. Peripherin/RDS, the human homologue of the gene found to be mutated in the *rds* mouse (see section 1.8.2) was mapped to 6p21.1-cen (Travis *et al.*, 1991b). Therefore this gene was selected by two groups as a candidate for human retinopathy. Both linkage analysis and mutation screening of this locus were performed on adRP families. As a result, an Irish adRP family was found to be linked to the same chromosomal region (Jordan *et al.*, 1992b). Meanwhile mutations were identified in this gene by two different laboratories (Farrar *et al*, 1991a; Kajiwara *et al.*, 1991). Several mutations were later identified in this gene, which accounts for around 5% of total adRP cases (Rosenfeld and Dryja, 1995). This locus was designated as RP7. At about the same time a third locus (RP1) was mapped to chromosome 8q11 (Blanton *et al.*, 1991) in a single adRP family. No other families have been found to be linked to this locus so far, and the gene has not been identified. At that time, many other families were excluded from these loci, indicating further genetic heterogeneity. Linkage analysis has since identified two further loci on 7p13-15 (RP9) (Inglehearn *et al.*, 1993) and 7q (RP10) (Jordan *et al.*, 1993), each assignment based on one adRP pedigree. Recently a sixth dominant locus has been mapped to 19q13.4 in a large adRP family called ADRP5 (Al-Maghtheh *et al.*, 1994; chapter 5 of this thesis). At least another two families have been mapped to this locus so far, which indicates that it is probably a commoner locus for adRP than the 7p, 7q, and 8cen loci. Finally, within the last year, two loci have been mapped to 17p13 (Greenberg *et al.*, 1994) and 17q24 (Bardien *et al.*, 1995) both in single families. However other families still exist from which all these loci have been excluded, indicating still further genetic heterogeneity (Inglehearn *et al.*, 1995).

1.7.1.2 Autosomal recessive RP (arRP):

Clinical description:

A typical case of arRP starts with white-greyish dots diffusely seen in the fundus with a thin retina, atrophic RPE, and attenuated blood vessels. Bone spicule-like pigment occurs late and increases much slower than in adRP. Loss of visual function is faster than in adRP, but slower relative to xlRP (Fishman, 1978; DeRouck *et al.*, 1986).

Molecular genetics of arRP:

Non syndromic forms of arRP can be caused by mutations in at least 6 different genes. Three of these genes have been identified by a candidate gene approach. A null mutation at codon 249 of the rhodopsin gene was the first to be identified in an arRP patient (Rosenfeld *et al.*, 1992; table 3.1). Another recessive rhodopsin mutation has been reported (Kumaramanickavel *et al.*, 1994). cGMP-PDEB is the second gene in which mutations were found to cause arRP (Mclaughlin

et al., 1993; McLaughlin *et al.*, 1994). This was a likely candidate for arRP since it encodes a rod specific component of the visual transduction cascade, and mutations in its murine and canine homologues have been found to cause retinal degeneration in *rd* mice and Irish setter dogs (see section 1.8.1). This is a classical example of recessive inheritance caused by mutations in a gene encoding an enzyme. Half the amount of the normal product is sufficient to prevent the disease in heterozygote individuals, whereas complete absence in homozygotes results in a severe disease. Mutations in cGMP-PDEB account for approximately 3-5% of arRP cases (Rosenfeld and Dryja, 1995). Recently mutations in two other genes, the gene encoding the cGMP-activated channel protein (McGee *et al.*, 1994) and the gene encoding the α subunit of rod cGMP phosphodiesterase (PDEA; Huang *et al.*, 1995), were found to cause arRP.

Linkage analysis implicated another two loci on 6p (Knowles *et al.*, 1994) and 1q31-32.1 (Soest *et al.*, 1994). The gene on 6p is approximately 20cM distal to the peripherin/RDS gene. On chromosome 1q there are two possible candidate genes for arRP, the choroideremia like gene (CHML) (Cremers *et al.*, 1992) and the phosducin gene which has been mapped to 1q25-31 (Sparkes *et al.*, 1993). The CHML gene is the autosomal homologue of the X-linked choroideremia gene, which is implicated in tapeto-choroidal and retinal dystrophies (Cremers *et al.*, 1990). The clinical similarities between choroideremia and RP and the colocalization of the two genes to 1q make CHML a possible candidate gene for arRP. Phosducin is considered to be a candidate gene in retinal dystrophies as it is widely expressed in the retina and may have a role in the regulation of phototransduction (Lee *et al.*, 1992; see section 1.4.9).

1.7.1.3 X-linked RP (xlRP):

Clinical description:

Relative to other types of RP, xlRP cases generally have the earliest age of onset, with symptoms appearing before ten years of age and with almost all patients showing cataracts by the age of 50 (Heckenlively, 1988). X-linked recessive inheritance of RP can often be determined from pedigree analysis. Only males are severely affected and there is no evidence of male to male transmission. Female carriers of xlRP may show signs of the disease as a result of non-random or biased lyonization (Lyon, 1988). As mentioned earlier, the frequency of xlRP varies in different parts of the world. The highest reported frequency is in the United Kingdom (Jay, 1982a; Bird, 1975). xlRP makes up more than 15% of total RP cases, and may be in excess of 25% if a proportion of simplex cases are included (Jay M., 1982b). Clinical heterogeneity exists among families with xlRP as is the case with other inherited forms of RP. This could be the result

of variable expressivity, allelic heterogeniety or different gene loci.

Molecular genetic studies in xlRP:

The inheritance pattern of X-linked disorders in general, and xlRP in particular, facilitates their molecular genetic studies as it immediately locates the disease gene to the X-chromosome. The first RP locus to be mapped more than 10 years ago was of the X-linked type. Bhattacharya and co-workers (1984) showed close genetic linkage between xlRP and DNA marker L1.28 (DXS7) mapping to Xp11.3 in five British families. However, genetic heterogeneity was evident since a patient known in literature as 'BB' was reported (Franke *et al.* 1985) to have RP resulting from a deletion in band Xp21. This patient suffered from a syndrome that included RP, Duchenne muscular dystrophy (DMD), chronic granulomatous disease, and McLeod syndrome. The presence of the deletion was detected by the absence of probe 754 (DXS84) in patient's DNA. This probe lies some considerable distance distal to DXS7. Thus a second xlRP locus was implicated close to the DMD locus. Wright and colleagues (1987) presented linkage data which placed the first xlRP locus between DXS7 and DXS14 and clearly distinguished it from the second locus. Genetic linkage to the second locus was also presented by Denton and co-workers (1988) in three Australian families. Thus it is clear that there are at least two xlRP loci on the X-chromosome short arm, RP2 localized within Xp11.3-p11.22, and RP3 localized to Xp21.1. RP6 is a putative third xlRP locus, which was suggested on the basis of linkage data from a single family, in the region Xp21.3-p21.2 (Ott *et al.*, 1990). However, further mapping data excluded the presence of this locus (Wright, 1990).

1.7.1.4 Digenic RP:

This name has been assigned to the mode of inheritance in some RP families in which the simultaneous segregation of heterozygous mutations at two unlinked genes give rise to RP. The presence of either mutation without the other is not pathogenic. There is only one confirmed case of this inheritance in the literature, namely Leu185-Pro of peripherin/RDS and a null allele of Rom1 (Kajiwara *et al.*, 1994). This could either be noncomplementation of two unlinked recessive alleles, or it could be that these mutations are in fact silent polymorphisms, so that homozygosity of either allele might result in no observable phenotype, and that only the combination of the two unlinked heterozygous mutations is pathogenic.

1.7.1.5 Syndromic forms of RP: Usher syndrome:

Usher syndrome is an autosomal recessive disorder which accounts for 15-20% of patients

with retinitis pigmentosa and 50% of patients with combined deafness and blindness (Rosenfeld and Dryja, 1995). It is both clinically and genetically heterogeneous. Based on clinical observations Usher has been classified into three subtypes known as types I, II and III. These types are distinguished on the basis of severity of hearing loss and the extent of vestibular involvement. Type I patients have retinitis pigmentosa and severe or profound congenital neurosensory deafness. Type II patients have retinitis pigmentosa and mild hearing impairment. The recently described type III is similar to type II with mild but progressive deafness (Sankila *et al.*, 1995). Vestibular function is a consistent discriminator between type I category and type II and III categories, since type I patients lack vestibular function while type II and III patients have normal vestibular function (Moller *et al.*, 1989; Sankila *et al.*, 1995). Within the type one and two categories there is further nonallelic genetic heterogeniety. At least five different genetic loci have been inferred from linkage studies. One form of Usher type I, designated USH1A, maps to chromosome 14q32.1-q32.3 in a number of French families (Kaplan *et al.*, 1992). Two additional loci, USH1B and USH1C, have been mapped to chromosome 11q13.5 in British pedigrees and 11p14-15.1 in Frenclı Acadian families, respectively (Kimberling *et al.*, 1992; Smith *et al.*, 1992). The gene for Usher IB has recently been identified as the '*shaker-1*' gene, a known deafness gene in mice (see section 1.8.3). Some, but not all, Usher type II families are linked to chromosome 1q42ter (USH2A) (Kimberling *et al.*, 1990; Pieke Dahl *et al.*, 1993). The choroideremia like gene (CHML) which maps to 1q42-qter is a good candidate for chromosome 1q Usher type II families, but no disease specific mutations have been found in this gene (Bokhoven *et al.*, 1994). Recently, the Usher syndrome type III (USH3) gene has been mapped to chromosome 3q (Sankila *et al.*, 1995).

1.7.2 Macular degenerations:

Macular degeneration is a general term that describes a variety of diseases characterized by progressive loss of central vision (in contrast to loss of peripheral vision in the case of RP), associated with degeneration of the retinal pigment epithelium underlying the retinal macula. These degenerations are both clinically and genetically heterogeneous. Clinically, the disorder ranges from a very common condition that affects older patients, known as age related macular degeneration (AMD), to a group of dystrophies that can be detected by ophthalmoscopy in the first decade of life (Heckenlively, 1988). The molecular mechanisms involved in the degeneration of the retinal pigment epithelium and the associated neovascularization of the retina are largely unknown. Genetically they can be inherited in an autosomal dominant, autosomal recessive, or X-linked fashion.

1.7.2.1 Age related macular degeneration (AMD):

AMD is the most common cause of legal blindness in older patients in the developed countries (Klein *et al.*, 1992). Linkage studies are difficult in families with AMD as in most cases the parents of affected patients are deceased and their children are too young to be affected. In contrast families affected with early-onset macular dystrophies (see below) can have many affected individuals in several generations and can serve as mendelian models for AMD. Once an early-onset dystrophy is linked to a particular locus, smaller families affected with AMD as well as other macular dystrophies can be typed for the same locus to test for possible linkage.

1.7.2.2 North Carolina macular dystrophy (MCD1):

This is an autosomal dominant retinal degeneration causing impaired central vision at an early age, is completely penetrant, and was initially clinically diagnosed in a single large family from North Carolina. The disease causing gene has been mapped to the long arm of chromosome 6 by linkage analysis (Small *et al.*, 1992). No obvious candidate genes are in that region, so a YAC contig map is being constructed to facilitate positional cloning of the disease gene (Small *et al.*, 1994).

1.7.2.3 Best's vitelliform macular dystrophy:

This is an autosomal dominant juvenile-onset macular degeneration first described by Best in 1905. It is characterized by an egg-yolk-like yellowish collection of lipofuscin beneath the retinal pigment epithelium of the macular area. The disease is slowly progressive and eventually results in atrophy of the retinal pigment epithelium and photoreceptor cells, thus severely impairing central vision. Linkage analysis has mapped the disease locus to chromosomal region 11q13 in some families (Stone *et al.*, 1992; Weber *et al.*, 1994a), but has excluded this locus in at least one family demonstrating locus heterogeneity (Mansergh *et al.*, 1994)

1.7.2.4 Cone-rod dystrophy (CRD):

CRD is a severe form of choroidoretinal dystrophy, characteristically leading to early blindness. Initially the disease is characterized by loss of colour vision and visual acuity followed by nyctalopia (night blindness) and peripheral visual field loss accompanied by widespread, advancing retinal pigmentation and chorioretinal atrophy of the central and peripheral retina. CRD is both clinically and genetically heterogeneous. It can be inherited as an autosomal dominant, autosomal recessive or X-linked disease. Clinical heterogeneity has been described with the association with non-ocular diseases. Deletion studies suggested a localization of a CRD locus to

18q21.1-q21.3 (Warburg *et al.*, 1991). Another locus has been suggested on 17q in association with neurofibromatosis type 1 (NF1) (Kylstra and Aylsworth, 1993). Recently Evans and coworkers (1994) have mapped a third locus to 19q13.3 in a large CRD family from the North West of England. No obvious candidate genes are in the disease interval and physical contiging of the region is being undertaken. This locus maps approximately 15cM proximal relative to the RP11 locus (the main subject of this thesis) on 19q13.4, and haplotype analysis clearly distinguishes the two loci (see chapter 5).

1.7.2.5 Sorsby's fundus dystrophy (SFD):

This is another autosomal dominant macular degeneration developing in the fifth decade of life. Patients lose central vision from subretinal neovascularization and atrophy of the choriocapillaries, pigment epithelium and the retina. The relatively late age of onset and clinical similarity makes it a suitable mendelian model for age related macular degeneration (AMD). The SFD phenotype has been found to be genetically linked to chromosome 22q13-qter (Weber *et al.*, 1994b). TIMP3, a new member of the "tissue inhibitor of metalloproteinases" (TIMP) gene family, has been recently localized to human chromosomal region 22q12.1-q13.2 (Apte *et al.*, 1994). TIMPs are a group of enzymes that are involved in the tight regulation of matrix metalloproteinases (MMPs). MMPs are necessary for continuous synthesis and degradation of normal extra cellular matrix (ECM). This is essential in the maintenance of integrity of ECM which is a component of the Bruch's membrane and is located between the choroid and the RPE layer of the retina. Disturbances in the regulation of metalloproteinases and in particular MMPs and their specific TIMPs have been implicated in several human degenerative diseases (Pelletier *et al.*, 1990; Milani *et al.*, 1994; Khokha and Denhardt, 1989). Recently, SFD has been found to be caused by a point mutation in TIMP3 (Weber *et al.*, 1994c).

1.7.2.6 Stargardt's disease (fundus flavimaculatus):

This disease, originally described in 1909, is an autosomal recessive condition of childhood characterized by bilateral loss of central vision over a period of several months (Stargardt, 1909). It is considered to be one of the most common inherited macular degenerations in childhood, with an age of onset of between 5-12 years. Stargardt's disease has been mapped to 1p21-p13 (Kaplan *et al.*, 1993). The cone α-subunit of transducin gene, which maps to chromosomal region 1p13 (Wilkie *et al.*, 1992), has been excluded as a candidate gene for this disease (Rozet *et al.*, 1995).

Stargardt's-like macular dystrophy is a dominant progressive form of macular degeneration

that is clinically similar to Stargardt's disease with the exception of its pattern of inheritance. Genetic linkage analysis has mapped this disease to chromosome 6q (Stone *et al.*, 1994) close to the locus for NCMD. However, this disease has been excluded from the interval containing the NCMD locus. Furthermore, the clearly progressive nature of the disease distinguishes it from NCMD. Recently a second locus for dominant Stargardt's has been mapped to chromosome 13q34 (Zhang *et al.*, 1994). The gene for rhodopsin kinase has been assigned to this region (Khani *et al.*, 1994). However, screening of this gene as a candidate for dominant Srargardt's failed to detect any causative mutation (Zhang *et al.*, 1995).

1.8 ANIMAL MODELS OF RETINAL DEGENERATIONS:

Vertebrate photoreceptors have a unique morphology which is designed for the trapping of light photons and transmission of signals to post synaptic neurons. This mechanism involves processes which were found to be highly conserved in evolution. This is of great value in the study of human ocular diseases. A genetic or acquired lesion which impairs photoreceptor function and initiates cell death in one species may have the same effect on another mammalian species. Therefore the search for animal models of human ocular diseases, and particularly retinitis pigmentosa, are of immense value. These animal models not only help in the identification of the genetic defect in man, but are also now available as an invaluable resource for further studies to establish the pathologic effects of such genetic defects *in vivo*. Furthermore these models are useful tools for therapeutic trials, particularly those for gene therapy. Animal models also facilitate, through comparative genetics and synteny groups, the study of complex genetic traits which could be difficult to perform on humans due to limitations on pedigree size and availability of appropriate family members for clinical and genetic studies. Non-vertebrate animal models such as drosophila are also of particular interest in studying conserved mechanisms and genetic disorders.

Described below are some of the best characterized animal models relevant to the study of retinal degenerations. In each case the disease gene has been fully characterized and its human homologue has been found to cause an equivalent human retinopathy.

1.8.1 *rd* Mouse:

The *rd*-mouse is an autosomal recessive animal model for retinal degeneration that has been extensively studied. In the rd mouse the photoreceptors develop normally up to the early part of the second week of life then photoreceptor cell degeneration starts. Degeneration is rapid by post

natal day 17 and virtually all the rod cells disappear by day 20. Although the cones survive at this stage, they later degenerate at a much slower rate than rods. Elevated levels of cGMP are detected in the rd retina before there are any signs of cell degeneration. This is followed by steep decline in cGMP levels until it is barely detected when visual cells have disappeared. The initial rise in cGMP correlates with a deficiency of rod-specific cGMP PDE activity, where the PDE of the rd mutant is scarcely activated by light compared to the normal enzyme. Linkage studies assigned the genetic locus for rd degeneration to mouse chromosome 5 (reviewed by Farber, 1995). An *rd* candidate cDNA, which was shown to encode the PDE β-subunit (Bowes *et al.*, 1990) was mapped to mouse chromosome 5 within 3.68 cM of the rd locus (Danciger *et al.*, 1990). Two mutations were later found in the β-PDE gene of the *rd* mouse. One, reported by Pittler and Baehr (1991), is a point mutation where a cytidine has been replaced by an adenine producing a stop codon (Tyr347X). The second reported by Farber and coworkers, is a viral insertion in the first intron of the β-PDE gene. Both mutations were found in every *rd* mouse strain, and were absent from normal mouse (Farber, 1995). These findings established the equivalence of the *rd* and *pdeb* loci (Bowes *et al.*, 1990). Similarly mutations in the homologous gene of rod cGMP-PDE β-subunit were found to cause arRP in humans (section 1.7.1.2) and the rod/cone dysplasia type 1 (rcd1) in Irish setter dogs (Suber *et al.*, 1993).

Furthermore rodless retina (*r*) in mice was discovered more than 70 years ago by Keeler (1924) as an autosomal recessive mutation leading to the absence of the rods. In a recent study by Baehr and coworkers (1994), PCR amplification and sequence analysis of DNA from 70 year old histological sections of this mouse, revealed the same nonsense mutation in *pdeb* as that found in the *rd* mouse. Therefore the '*r*' and *rd* mouse have an identical defect due to the same mutation(s) which arose more than 70 years ago.

1.8.2 *rds* Mouse:

The retinal degeneration slow (*rds*) mutation originally described by Van Nie and coworkers (1978) is characterized phenotypically by abnormal development of retinal photoreceptors followed by their slow degeneration. No other cell type in the retina or the central nervous system are affected. In *rds/rds* homozygotes the retina undergoes entirely normal development and differentiation of cells until the first postnatal week, the time at which photoreceptors normally appear. While other retinal cells continue their normal development, *rds/rds* photoreceptors fail to elaborate outer segments and rarely form outer segment discs (Sanyal, 1987). The photoreceptor inner segments, however, including the ciliary projections, are morphologically

normal (Cohen, 1983). The synaptic termini of photorecptors with second order retinal neurons also appear normal. The process of photoreceptor degeneration in *rds/rds* mice is first detectable histologically during the third postnatal week. The rate of loss of photoreceptors is greatest during the following few weeks and then becomes more gradual with significantly reduced thickness of the outer nuclear layer, and virtually all photoreceptors disappear by one year of age (Sanyal, 1987). Rods and cones are equally affected and the opsin destined for outer segment formation appears to be retained in the inner segment plasma membranes where it reaches its maximum and then declines to undetectable levels. Although the *rds* retina lacks outer segments, the components of phototransduction appear to be present, though at greatly reduced levels, and the visual transduction cascade is intact (Cohen, 1983; Reuter and Sanyal, 1984). The *rds* mutation was originally described as recessive, but *rds/+* heterozygotes are phenotypically mildly abnormal. In contrast to homozygotes, heterozygotes do form outer segments which are reduced in length and contain irregularly arranged discs that appear swollen and vacuolated with very slow degeneration (Sanyal, 1987).

The gene for *rds* has been cloned and its product was characterized as a transmembrane glycoprotein expressed specifically in the discs of photoreceptor outer segments (Travis *et al.*, 1989 ;Travis *et al.*, 1991a; see section 1.6.1). The *rds* mutation was found to be caused by a 10 kb insertion of exogenous DNA into a protein coding exon of the gene.

1.8.3 *Shaker-1* Mouse:

This is an autosomal recessive mouse model for deafness, which shows primary abnormalities of the sensory neuroepithelia of the inner ear. *Shaker-1* (*sh1*) homozygotes show vestibular dysfunction and typical neuroepithelial type cochlear defects involving dysfunction and progressive degeneration of the organ of Corti (Steel and Harvey, 1992). Recently the *sh1* gene has been found to encode an unconventional myosin. Mutations in this gene were found to be responsible for the *sh1* phenotype (Gibson *et al.*, 1995). The *sh1* gene maps to a mouse chromosomal region that is syntenic with human 11q13, and the Usher syndrome type 1B (USH1B) locus has been assigned to this region (Kimberling *et al.*, 1992) (see section 1.7.1.5). The identification of the molecular basis of the *sh-1* phenotype led to the screening of the human homologue of the *sh1* gene as a good candidate for USH1B (Weil *et al.*, 1995). Similarly this gene was found to be the human unconventional myosin VIIA, and several mutations were found in this gene in various unrelated USH1B patients. Mutations in this gene are likely to account for the cytoskeletal abnormalities seen in USH1 patients (Bonneau *et al.*, 1993). These findings

implicate the genes encoding other unconventional myosins and their interacting proteins as candidates for other genetic forms of Usher syndrome.

Although it has been concluded that the mouse *sh1* gene and human USH1B are homologous genes encoding myosin VIIA, the phenotype of the original *sh1* mutant is different from that of USH1 patients, since no sign of retinal degeneration has been reported in these mutants (Brown and Steel, 1994). Therefore another myosin could compensate for a defective myosin VIIA in the mouse retina, or the nature of the mutation itself might account for the phenotypic difference. However another form of human deafness without retinal involement has been mapped to the same chromosomal region as USH1B. The two phenotypes, USH1B and deafness, could be allelic mutations of the same gene, and the latter may represent the human equivalent of the *sh1* mutants.

1.9 AIMS OF THIS RESEARCH:

The basic protein defects of photoreceptor cell dysfunction and retinal degenerations are not fully understood. Without such knowledge, investigations into the biochemical or structural mechanisms involved in the disease process are difficult. The molecular and genetic approach as such will lead to the identification of loci involved in these degenerations. Subsequent cloning of the genes and identification of mutations that are involved in the malfunctioning of photoreceptors will lead to a better understanding of the physiology of the retina and the mechanisms that cause retinal degenerations.

In order to contribute to such understanding, this project was initiated to investigate the molecular and genetic basis of adRP, a subgroup of RP. Two approaches were undertaken. The first was to identify novel mutations in the rhodopsin gene (chapter 3). Involvement of this gene in RP had already been established, but the mechanisms by which defective rhodopsin leads to retinal degeneration remain largely unknown. Identification of new mutations in rhodopsin and correlation with phenotype helps further our understanding of the structure of this photoreceptor specific protein by establishing structure-function relationships.

The second approach was to use the method of linkage analysis to identify new adRP causing loci in the human genome. At the time when this project began, defective rhodopsin, peripherin/RDS, and the chromosome 8 adRP locus were known to underly about a third of all adRP cases. The biochemical and genetic basis for the rest remained unknown. ADRP5 is a large

family, for which DNAs are available in this laboratory and which had been excluded from the above 3 loci. Therefore, in addition to rhodopsin screening, the aims of this project were:

1- To undertake a total genome search using linkage analysis to identify the disease locus in ADRP5 (chapters 4).

2- To refine the disease gene containing interval by genotyping the family for all available markers in the region (chapter 5) and evaluating other families for linkage to the new locus (chapter 6).

3- To screen for mutations in any known candidate genes from the disease interval (chapter 7).

4- And, if no suitable candidate gene is found, to then undertake positional cloning by establishing a YAC contig across the disease interval, and to screen that interval for expressed sequences to identify new candidate genes.

CHAPTER II

MATERIALS AND METHODS

Note: A list of reagents and solutions used in this study is described at the end of this chapter (section 2.10).

2.1 DNA SAMPLES:

For mutation detection in the rhodopsin gene (chapter III) DNA samples from 120 unrelated autosomal dominant and sporadic RP patients from the genetic register of Moorfield Eye Hospital were extracted as described below. DNAs from another 50 normal individuals were used as controls. Some of the DNA samples from family ADRP5 (chapter 4), and other families (chapter 6) were available in the laboratory. Extractions were performed whenever additional blood samples were obtained from these families. DNA samples of the Italian families described in chapter 6 were sent to this laboratory from Italy.

2.1.1 DNA extraction:

Blood samples were collected in 10ml EDTA tubes then either extracted at the time of their arrival in the laboratory, or stored at -80°C until required. To extract the DNA from peripheral blood lymphocytes, reagent A (section 2.10) was added to 5-10 ml of EDTA-blood to a total volume of 50 ml in a falcon tube. After mixing, the tube was centrifuged at 4000 rpm for 5 min, supernatant discarded and 2 ml of reagent B (section 2.10) were added to the pellet. The mixture was then transferred to a 5 ml tube and 500 μl of 5M sodium perchlorate added, and mixed slowly for 15 min at room temperature, followed by 25 min at 65°C. Tubes were cooled on ice, then 2 ml of chloroform and 300 μl of silica suspension (Nucleon DNA extraction Kit from Scotlab) were added. Samples were mixed for 5 min and then centrifuged for 6 min at 1400g. The upper DNA-containing layer was transferred to a universal tube where two volumes of ethanol were added to precipitate DNA. After mixing, the DNA pellet was picked out and transferred to an eppendorf tube. It was then washed with 70% ethanol, allowed to dry, and resuspended in a suitable amount of sterile d.H2O or TE buffer (usually 300-400μl). These DNA samples were kept at 4°C for subsequent use, or at -20°C for long term storage. On

average the yield of DNA from 10 ml of whole blood was between 250-300 μg.

2.2 HETERODUPLEX ANALYSIS:

2.2.1 PCR amplification:

For the detection of mutations in the rhodopsin gene (chapter 3) intronic primers were synthesized flanking each of the five exons. For exons 1 and 4 another two pairs of exonic primers were synthesized to allow amplification of two overlapping fragments for each exon in order to give smaller fragment sizes for heteroduplex analysis. The following are the sequences of these primers (F=forward primer, R=reverse primer) ; and nucleotide positions (Nathans and Hogness , 1984; see addendum).

exon 1.1 (F)	TTCGCAGCATTCTTGGGTGG	(241-260)
exon 1.1 (R)	GCTAGGTTGAGCAGGATGTA	(533-514)
exon 1.2 (F)	CATGTTTCTGCTGATCGTGC	(423-442)
exon 1.2 (R)	ACTCTCCCAGACCCCTCCAT	(717-698)
exon 2 (F)	TTCCTAGCTACCCTCTCCCT	(2351-2370)
exon 2 (R)	GCTTCTTCCCTTCTGCTCAGTG	(2636-2615)
exon 3 (F)	TTGGCTGTTCCCAAGTCCCT	(3759-3778)
exon 3 (R)	TCCAGACCATGGCTCCTCCA	(4073-4054)
exon 4.1 (F)	TCACGGCTCTGAGGGTCCAG	(4003-4022)
exon 4.1 (R)	GAAGATGTAGAATGCCACGC	(4226-4207)
exon 4.2 (F)	ACGCCAGCGTGGCATTCTACAT	(4201-4222)
exon 4.2 (R)	GAGTAGCTTGTCCTTGGCAG	(4404-4385)
exon 5 (F)	AGTTCCAAGCACACTGTGGG	(5112-5131)
exon 5 (R)	GGATGGGAGACGCCTATAGT	(5322-5303)

Annealing was generally performed at 1 or 2 °C less than the lower melting temperature of either of the two primers. Melting temperature (Tm) was dependent on the nucleotide sequence of the primer and was calculated as described by the following equation:

$$Tm=4(A+T)+2(C+G)$$

However, for practical reasons, other annealing temperatures which were known to give satisfactory results, were sometimes used.

PCR amplifications were performed on 200 ng of patient DNA in 50 μl volumes of 1xTaq reaction buffer (10 mM Tris-HCl, 50 mM KCl, 1.5 mM MgCl2, and 0.1% non-ionic detergent), 0.2 mM of each dNTP, 25 pico moles of each primer, and 0.5 unit of Taq polymerase. The reaction mixtures were overlayed with one drop of mineral oil to prevent evaporation. Thirty cycles of PCR amplification at 94°C for 1 min (denaturation) and 63°C for 3 min (annealing and extension), was followed by denaturation for two minutes at 94°C.

Addendum to section 2.2.1:

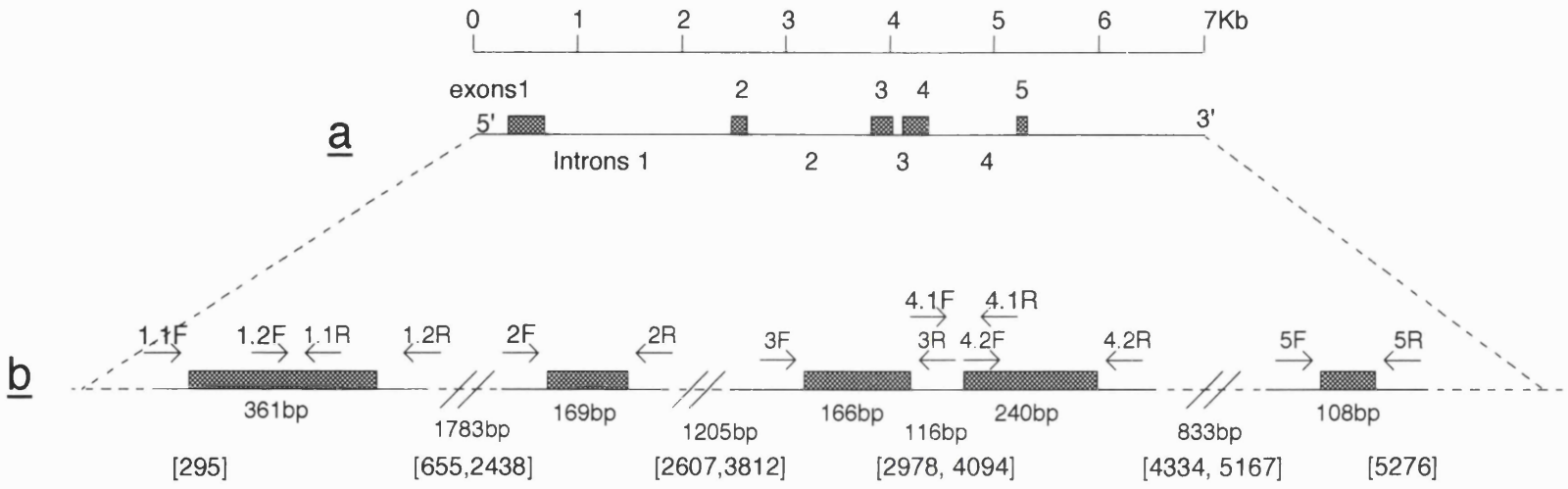

a: Diagram of the rhodopsin gene structure showing the relative size of each exon (shaded boxes 1-5), introns 1-4, and 3' UTR according to the sequence of roJHN clone (Nathans and Hogness, 1984).

b: Enlargement of exons shown in a. Numbered arrows refer to primers described in section 2.2.1. Sizes of exons and introns are shown beneath. Numbers in brackets show the nucleotide position of start codon, 5' and 3' splice sites of introns 1-4, and stop codon according to roJHN sequence (Nathans and Hogness, 1984).

Reactions were then left to reanneal at room temperature for 2-3 hours to allow heteroduplex formation. PCR reactions were performed on an Omnigene thermal cycler manufactured by Hybaid. 10μl of PCR product were mixed with 2-3 μl of 10x Ficoll-orange G loading buffer and electrophoresed on a 2.5% agarose-Nusieve (4:1) gel to check for proper amplification and to detect relatively large rearrangements (in the range of few hundreds bp of PCR amplifiable products). The above protocol was also used to amplify DNA fragments from the PRKCG gene (chapter 7) using primers designed from the cDNA sequence.

2.2.2 Hydrolink gel preparation:

Hydrolink gels were made from 35ml of Hydrolink solution, 4ml of 10x TBE buffer solution, 500μl of 10% (w/v) ammonium persulphate, and 35μl TEMED. After pouring, the gel was left to set for 1hr at room temperature. MDE (Mutation Detection Enhancement) is a modified form of Hydrolink gel matrix. An MDE gel is prepared and run in 0.6x TBE buffer, but is otherwise similar to Hydrolink.

2.2.3 Heteroduplex detection:

Around 0.5-1 μg (estimated relative to a known amount of λ DNA on the gel) of each PCR product was mixed with 0.1 volume of sucrose-orange G loading buffer, then loaded on a Hydrolink gel. The gels were run in 1x TBE buffer at 90 volts for 16-20hr at room temperature. After the run, gels were stained with ethidium bromide and photographed on a UV transilluminator (fig 3.5; 3.9b; 3.10a).

2.3 DNA SEQUENCING

Rhodopsin fragments from individuals showing a heteroduplex on Hydrolink gels were reamplified using external primers to the primers used for heteroduplex analysis and sequenced with the original (nested) PCR primers. PCR products were digested with proteinase K (1mg/ml) at 37°C for 30min, then phenol-chloroform extracted. 50μl of this DNA solution was purified through a CHROMA SPIN-30 COLUMN (from CLONTECH) to remove excess dNTPs and DNA oligos of less than 30bp. The dideoxy termination method (Sanger *et al.*, 1977) was used to direct sequence these PCR products using the SEQUENASE kit (from USB) as described below. The PCR fragments of the deletion and insertion alleles (see sections 3.4.1 and 3.4.2) were excised from 1% low melting point agarose (LMP) since they were different in size relative to the normal allele of the rhodopsin gene. DNA from these gel fragments was phenol-

chloroform extracted, 0.1 volume of 3M Na-acetate added, and the DNA precipitated using 2.5 volume of absolute ethanol. The subsequent steps for direct sequencing were the same as above. However, the result was not satisfactory for the insertion fragment. Hence the excised fragment was cloned using TA-cloning kit (see section 2.5) and subsequently sequenced.

For direct genomic sequencing, 20 pmoles of primer was end labelled (see section 2.4) with 20 μCi of γ-P^{32}-ATP (specific activity 3000 Ci/mmole). Two pmoles of the above end labelled primer were added to 9 μl of template DNA (~400 ng of the above purified PCR template, or 1-2 μg of cloned DNA; see section 2.5), denatured at 94°C for 3 min and kept on ice. 2μl of sequenase buffer (200 mM Tris.HCl, 100 mM MgCl2 and 250 mM NaCl), 1μl of DTT (Dithiothreitol) and 2μl of diluted sequenase enzyme (according to the manufacturer's protocol) were added while on ice. Meanwhile 3μl of each dideoxy termination mixture (d.dATP, d.dCTP, d.dGTP, d.dTTP) were warmed up to 37°C in four separate reaction tubes. To each of these, 3.5 μl of the above mixture was added, and tubes were incubated for 5min at 37°C for the extention-termination reaction to take place. 5μl of formamide loading buffer were then added to stop the reaction. The four reaction mixtures were then denatured, ice chilled, loaded on a 6% denaturing (using 5M urea) polyacrylamide gel, and electrophoresed in 1xTBE buffer at a constant power of 60 watts (for 20X60 cm sequencing gel apparatus from BioRad). After electrophoresing for the required length of time, gels were fixed in a 10% Methanol-10% acetic acid solution, vacuum dried, and autoradiographed overnight using Kodak or Fuji X-ray films. When required, gels were autoradiographed at -80°C with an intensifying screen toenhance the signal.

2.4 5'END LABELLING OF PRIMERS:

This reaction was performed in a 30 μl volume containing 10 mM Tris-acetate, 10 mM magnesium acetate, 50 mM potassium acetate (0.1 volume of One-Phor-All buffer *Plus* from Pharmacia), 9 units of poly-nucleotide kinase, 30μCi γ-P^{32}-ATP (specific activity 6000 Ci/mmole; from Amersham), and the required amount of primer. This was 20 pmole for the sequencing reaction, and 2 pmole/PCR reaction for microsatellite labelling. For multiplex PCR reactions 2 pmole of each primer were labelled in the same reaction. The reaction was then incubated at 37°C for 30 min.

2.5 CLONING OF PCR FRAGMENTS:

A TA Cloning kit (from Invitrogen) was used to clone the PCR product of exon 5 of the rhodopsin gene (see section 3.4.2). The TA Cloning System takes advantage of the non-template dependent activity of thermostable polymerase, used in PCR, that adds single deoxyadenosines to the 3'-end of all duplex molecules. Those A-overhangs are used to ligate the PCR product into a specifically designed plasmid vector (pCR™II) providing single 3'T-overhangs at the insertion site. Enough fresh PCR products to give a molar ratio from 1:1 to 1:3 of vector to PCR insert were used in the ligation reaction. The ligation mixture (including 1x ligation buffer, pCR vector, and T4 DNA ligase, all provided with the TA cloning kit, and PCR fragments to be cloned) was then used to transform competent *E.coli* cells. Transformed cells were then cultured on LB agar containing Kanamycin (50 μg/ml) and X-gal (25 μl of 40 mg/ml stock solution spread on each plate). White colonies, containing the PCR insert, were selected for plasmid mini preparations as described below.

2.5.1 Plasmid Mini preparations:

A single white colony is inoculated into 5ml of LB-broth and kanamycin (50 μg/ml) and grown overnight at 37°C in a shaking incubator (200 rpm). 1.5 ml of culture is then transferred to an eppendorf tube and spun in a microfuge at 13000 rpm for 3 min. The supernatant is discarded and the pellet is resuspended in 100 μl of lysozyme containing (4mg/ml) *Solution I* (50mM Glucose, 10mM EDTA, 25mM Tris-HCl, pH 8). The mixture is then left at room temperature for 5 min, and 200 μl of freshly made *Solution II* (0.2M NaOH, 1% SDS) are added. The tube is gently shaken (no vortexing) for 30 seconds, and then kept on ice for 30 min. Finally 150 μl of *Solution III* (3M Potassium acetate, 2M Acetic acid) were added, gently mixed in, and the tube kept on ice for at least another 5 min. The mixture was then spun in a microcentrifuge at 13000 rpm at room temperature for 5 min. The clear supernatant was transferred to another eppendorf, where 250 μl of phenol and 250 μl of chloroform were added. This was shaken vigorously for 2-3 min (no vortexing), and then spun in a microfuge at 13000 rpm for 5 min. The supernatant was then transferred to a clean eppendorf to which 0.1 volume of 3M Na-Acetate and 2.5 volume of cold absolute ethanol were added to precipitate DNA. The tube was placed at -20°C for at least 30 min (to ensure complete precipitation) and then spun (13000 rpm) in a microfuge at room temperature for 5 min. The pellet was then washed with 70% ethanol, and resuspended in 25 μl of TE buffer. DNA concentration was estimated using a spectrophotometer. 2μg DNA from this preparation were then sequenced using the Sequanase reaction kit as described above (section 2.3).

2.6 RESTRICTION ENZYME DIGESTS:

2.6.1 Genomic digests for Southern blots:

Approximately 6-10 μg of each DNA sample were digested in a total volume of 40 μl of 1x restriction enzyme buffer (as supplied by the manufacturer) and the required amount of the restriction enzyme (usually 4 units/μg genomic DNA). Complete digestion was confirmed by electrophoresis of 3μl of the digestion reaction on a 1% agarose gel.

2.6.2 PCR restriction digests:

Msp1 digests of exon 5 of the rhodopsin gene were performed in a 30 μl volume made up of 20 μl PCR product, 9μl d.H2O and 1μl (10 units) enzyme. Digests were left at 37°C overnight then electrophoresed on a 2.5% agarose-Nusieve (4:1) gel (fig 3.10b). Sau96.1 digests were similarly performed for exon 1 of the rhodopsin gene (fig 3.8b). Ideally, the DNA from the PCR reactions should be precipitated and reextracted before performing the specific restriction enzyme digests. However, since the above digests gave satisfactory results in the PCR buffer, this step was not necessary.

2.7 SOUTHERN BLOTS:

2.7.1 DNA transfer to nylon membranes:

Genomic digests were electrophoresed on 0.8% agarose gels at 40 volts overnight at room temperature. The gels were then placed in denaturing solution (section 2.10) for 30 min to denature DNA, then neutralizer for 60 min to restore a neutral pH. The DNA from gels were then transferred (Southern, 1975) to Hybond N^+ nylon membranes supplied by Amersham. DNA was fixed to the membrane by UV crosslinking.

2.7.2 Hybridisation:

The PCR product from the PRKCG cDNA probe (chapter 5) was purified from gel fragments as described for the deletion and insertion fragments of rhodopsin exon 5 (see section 2.3) and oligolabelled. Hybridization to Msp1 blots from the ADRP5 family was carried out overnight at 65°C in 5xDenhardts/5xSSC mixture using the labelled probe. Washes to remove non-specific hybridization were carried out to required stringency with decreasing concentrations of SSC and SDS solutions (starting with 1XSSC/0.1% SDS at room temperature as the lowest stringency, and progressing to 0.1XSSC/0.1%SDS at 65°C as the highest stringency). Membranes were autoradiographed overnight or as required, using Kodak or Fuji X-ray films.

This work was initially done using a bovine cDNA clone but did not give satisfactory results. The same work was repeated by another member of the laboratory (Dr Chris Inglehearn) using the human cDNA probe.

2.8 MICROSATELLITE ANALYSIS:

2.8.1 Radioisotopic detection method:

Microsatellite markers were selected from the various genome maps (Gyapay *et al.*, 1994; NIH/CEPH, 1992; Weber *et al.*, 1993) for linkage study in ADRP5 (chapters 4, 5, and 6), and primers were obtained from either the HGMP resource centre or Cruachem laboratories for these microsatellites. Forward primer for each marker was end labelled (see section 2.4) with 20 μCi of γ-P^{32}-ATP (specific activity 6000 Ci/mmole; Amersham), and PCR reactions were carried out using 96-well microtiter plates from Omnigene. Size-selected multiplexing of two microsatellites was routinely performed. PCR reactions were carried out in a total volume of 12.5 μl composed of 2 μl diluted genomic DNA ($\sim$ 100 ng), 1x PCR buffer, 0.2 mM dNTPs, 2 pmole of both forward and reverse primers, and 0.5 unit of Taq polymerase. Thirty cycles of PCR amplification were performed at 94°C for 1 min, 55°C for 1 min (unless specified otherwise) and 72°C for 1 min, using an Omnigene thermal cycler fitted with a microtiter block. After PCR amplification, 12.5 μl of formamide loading buffer was added to each reaction, denatured at 95°C for 4 min and chilled on ice. While on ice, 4 μl of each reaction was loaded on a 6% denaturing acrylamide gel. Gels were run at 120 watts (in a BioRad 48\60cm sequencing apparatus) for the required length of time to obtain the proper resolution of each system of the multiplexed microsatellites. Gels were processed and autoradiographed as described for sequencing gels (see section 2.3).

2.8.2 Fluorescence detection method:

Twenty five cycles of PCR reactions were performed in the same way as described above except that one of the amplification primers was fluorescently end labelled instead of P^{32}-labelled. 1μl of each reaction was diluted in 3 μl of loading buffer (deionized formamide with dextran blue) and 0.5 μl size standard (Rox 2500 standard from Applied Biosystems), denatured at 95°C for 2 min and kept on ice until loading on a 6% denaturing polyacrylamide gel. Electrophoresis was performed in 1xTBE buffer for the proper length of time using an Applied Biosystems 373 DNA sequencer. Genotype data were collected and analysed using Gene Scan 672 software supplied by Applied Biosystems. No further processing of the gels was required.

2.9 LINKAGE ANALYSIS:

Pedigree information, allele frequencies, and genotype data were processed using the Linksys programme (LS4 data management package; Attwood and Bryant, 1988). LS4 output files were used as input for the LINKAGE programme (Lathrop and Lalouel, 1984). Pairwise and multipoint analyses were performed using the MLINK and LINKMAP programmes of the LINKAGE package respectively. Maximum likelihood recombination fractions between pairs of markers were calculated using the ILINK programme (LINKAGE package). Multipoint analyses were performed on the HGMP resource center computing facility (Rysavy *et al.*, 1992) since they require more computing memory. The FASTMAP programme was also run at the HGMP resource centre.

2.10 REAGENTS AND BUFFERS USED IN THIS RESEARCH:

2.10.1 Reagents in general use:

2M Tris HCl (pH 7.5):
315.2 g Trizma Hydrochloride (Tris(hydroxymethyl)aminomethane hydrochloride)/litre, adjust pH to 7.5 with 5M NaOH. Autoclave before use.

0.5M EDTA (pH 8.0)
186.1 g EDTA (Ethylenediaminetetraacetic Acid) Disodium Dihydrate/litre, adjust pH to 8.0 by addition of 5M NaOH. Autoclave before use.

1M $MgCl_2$.6H2O:
203.3 g Magnesium chloride hexahydrate/litre, autoclave before use.

5M NaCl:
292.2 g Sodium chloride/litre.

5M NaOH:
200 g Sodium Hydroxide/litre

10% SDS:
100 g Sodium Dodecyl Sulphate/litre.

TE buffer:
0.5 ml Tris-HCl(2M)pH7.5 and 20 μl EDTA (0.5M) ph8.0 in 100 ml d.H2O, autoclave before use.

8M Urea:
320 g Urea/litre.

Ethidium bromide: (10mg/ml)
1g Ethidium bromide/100 ml d.H2O.

20xSSC:
175.3 g NaCl, 88.2 g tri-Na-citrate/litre

2.10.2 Electrophresis buffers:

TAE buffer (10X):
48.44 g Trisma Base, 20ml [0.5M] EDTA, 6ml Glacial Acetic Acid; dissolve in d.H2O to a total volume of 1 litre, and adjust pH to 8.2 using glacial acetic acid.

TBE buffer (10X):
121.1 g Tris (1M), 51.36 g Boric acid (0.83M), 3.72 g Na-EDTA.2H2O (10mM); dissolve in d.H2O to a total volume of 1 litre.

2.10.3 Gel loading buffers:

Ficoll-orange G (25%, 10X stock):
250 mg Orange G, 25 g Ficoll, 9.3 g EDTA; dissolve in d.H2O to a total volume of 100 ml.

Sucrose-Orange G (10X stock):
40 g Sucrose, 250 mg Orange-G, dissolve in d.H2O to a total volume of 100 ml.

Formamide (95%) (for loading radioactively labelled PCR products on denaturing polyacrylamide gels):
95 ml Formamide, 50 mg Bromophenol blue, 50 mg Xylene cyanol F.F., 4 ml EDTA (0.5M).

Formamide (for loading fluorescently labelled PCR products):
5:1 volume- deionized formamide : 50mM EDTA
0.75 g/100 ml Dextran Blue.

2.10.4 DNA extraction reagents:

Lysis buffer (Reagent A [5X])
547.7g sucrose, 25ml [2M] Tris-HCl PH 7.5, and 25ml [1M] $MgCl_2.6H_2O$, dissolve in d.H2O to a total volume of 950ml (At this point PH should be 7.5-8), then add 50ml Triton X-100.

Reagent B [1X]
200ml [2M] Tris-HCl PH 7.5, 30ml [5M] NaCl, 120ml[0.5M] EDTA (pH 8.0), dissolve in d.H2O to a total volume of 900ml, autoclave then add 100ml 10% (w/v) SDS.

Sodium Perchlorate 6M:
84.3g Sodium Perchlorate in 100ml d.H2O.

2.10.5 Southern blot reagents:

Denaturer:
20g NaOH, 87.6g NaCl, dissolve in 1 litre

Neutraliser:
60.5 g Trisma Base, 175 g NaCl, 88.3 g Tri Na-Citrate; dissolve in 1 litre, pH to 5.5 with HCl.

Depurinator:
0.25M HCl

Denhardt's (100x sol):
2g Ficoll, 2g PVP (Polyvinylpyrrolidone), and 2g BSA (Bovine Serum Albumin); dissolve in 100 ml 20xSSC.

CHAPTER III

IDENTIFICATION OF NOVEL RHODOPSIN GENE MUTATIONS

3.1 RHODOPSIN AS A CAUSE OF adRP:

In 1989, McWilliam and coworkers reported the first significant linkage to adRP. This was detected with the DNA marker C17 (D3S47) in an Irish pedigree called TCDM1. This marker maps to the long arm of chromosome 3 (Donis-Keller et al., 1987). Subsequently several adRP families were found to be linked to this locus (e.g. Lester et al., 1990). The gene for rhodopsin, the photopigment that initiates visual transduction, had been previously isolated (Nathans and Hogness, 1984) and mapped to this region (Nathans et al., 1986, Sparkes et al., 1986), so this gene was an appropriate candidate for the C17-linked adRP families. Later Dryja and coworkers (1990a) reported the first C→A mutation in codon 23 of the rhodopsin gene, which segregated with the disease phenotype in an adRP family. Since then more than 80 mutations in the rhodopsin gene (table 3.1) have been found to cause adRP. Rhodopsin mutations are now thought to account for approximately quarter of all dominant RP.

3.2 RHODOPSIN STRUCTURE AND FUNCTION:

Rhodopsin is a member of the guanine nucleotide binding protein (G protein) coupled receptor family, which are involved in signal transduction. It is available in greater quantities than any other receptor of this class and therefore has been studied biochemically and biophysically by methods difficult to apply to other receptors of the same family. It can be isolated from rod cells and studied in either pure form or in reconstituted systems.

3.2.1 Nucleic acid sequence of the rod opsin gene:

Using the bovine rod opsin gene as a hybridizing probe, genomic DNA clones of human rod opsin were isolated and the nucleic acid sequence obtained (Nathans and Hogness, 1984). It contains a 1044-bp highly conserved coding region that is interrupted by four introns. The rod opsin gene has two mRNA start sites at positions -95 and -93; taking the furthest upstream

of these two start points, the rhodopsin gene contains a 5'-untranslated region of 95 bp. The length of the 3'-untranslated region has not been defined. Two possible 3' cleavage polyadenylation signals, A-A-T-A-A-A and A-T-T-A-A-A are located at nucleotide positions 367 and 1423 bp respectively from the stop codon.

The polypeptide sequence of the rhodopsin gene is highly conserved in the opsin gene family and in all members of the G-protein super family. It is 89.7% homologous with the bovine opsin DNA sequence, and has 93.4% homology at the amino acid level. Furthermore introns of comparable lengths interrupt the coding regions of both genes at precisely analogous positions. The human rhodopsin gene also contains a 95 bp 5'-untranslated region which exhibits 77% sequence homology with the 96 bp 5'-untranslated region of bovine rhodopsin. In addition, the rhodopsin gene contains a 32 bp sequence, located 34 bp upstream from the A-A-T-A-A-A sequence, that is perfectly conserved in the human and bovine genes (Nathans and Hogness, 1984).

3.2.2 Rhodopsin synthesis in the rod inner segment:

Rhodopsin is composed of a 40 kd apoprotein, opsin, and the light sensitive ligand 11-*cis* retinal. Rod opsin is synthesized in the rough endoplasmic reticulum (RER) where it is inserted into the membrane and afterwards transferred to the Golgi apparatus for post translational modifications. Passage of opsin through the Golgi apparatus is an obligatory step for its incorporation into ROS disc membrane (Matheke et al., 1984). Newly synthesized opsin is transported vectorially in post-Golgi intra-cellular transport vesicles through the densely packed mitochondria in the ellipsoid region to the base of the connecting cilium where it fuses with the plasma membrane (Bok, 1985); figure 3.1).

3.2.2.1 N-terminal domain and N-linked glycosylation:

Rhodopsin polypeptide is modified by cotranslationally adding high-mannose core oligosaccharides to the N-glycosylation sites at Asn-2 and Asn-15 in the RER (Hargrave and McDowell, 1992). These oligosaccharides are further trimmed and elaborated in the Golgi apparatus (Kornfeld and Kornfeld, 1985). Proper glycosylation of rhodopsin is essential for protein insertion into the membrane and proper folding.

3.2.2.2 Rhodopsin is palmitoylated:

Acylation by palmitic acid of two cysteines at positions 322 and 323 is another covalent

Figure 3.1:

(Figure and legend are from Berman, 1991)

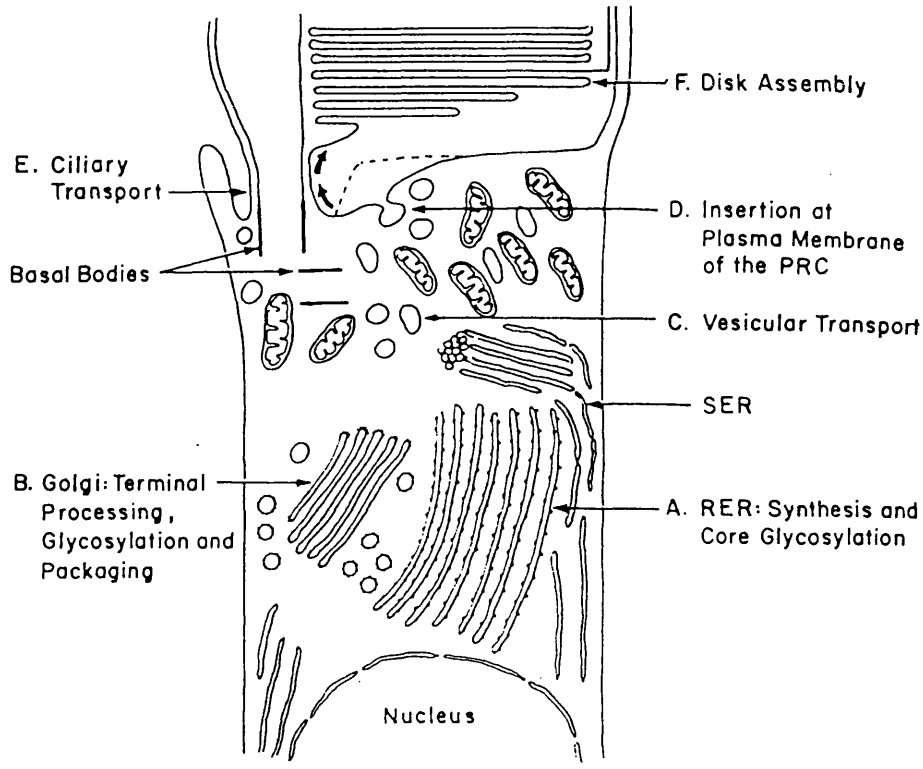

Biosynthesis and transport of opsin in *X. laevis* from its site of synthesis in the rough endoplasmic reticulum to the base of the outer segment. The diagram illustrates the vectorial transport of newly synthesized opsin in post-Golgi vesicles through the mitochondia-rich ellipsoid region; the vesicles apparently fuse with grooves of the periciliary ridge complex near the base of the connecting cilium. The opsin then travels along the ciliary plasma membrane and is then incorporated into newly forming disks. (From Papermaster *et al.*, 1985.)

a:

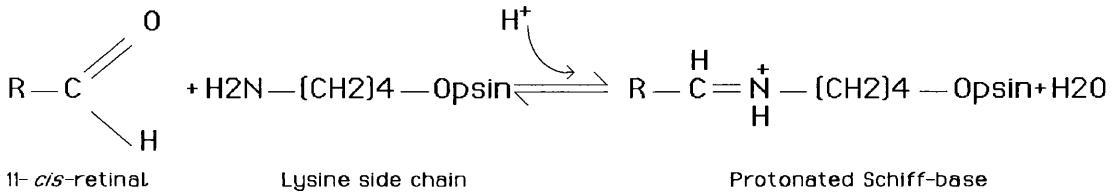

b:

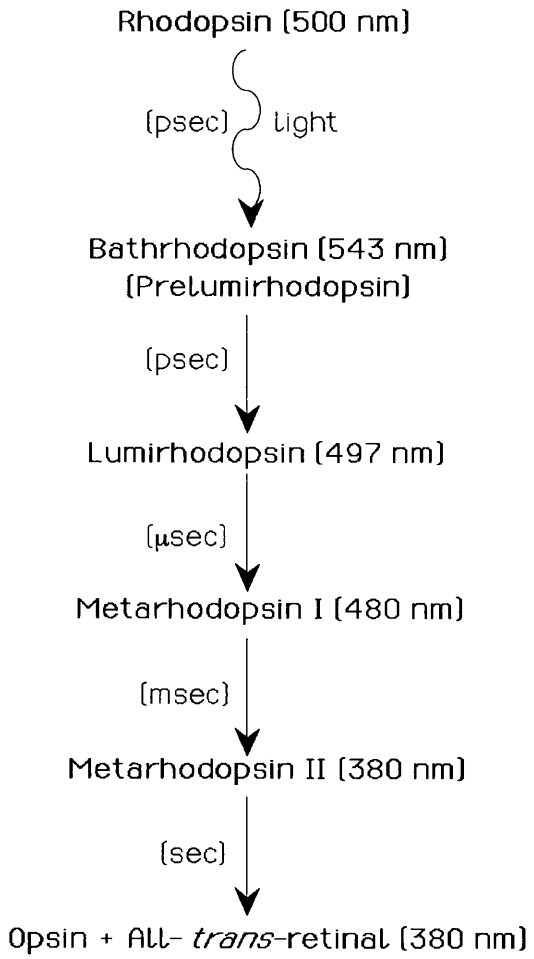

Figure 3.2:

a: Interaction between 11-*cis*-retinal and lysine 296 side chain (amino group) to form the protonated Schiff-base linkage. b: Intermediates in the photolysis of rhodopsin. The wavelength of the absorbtion maximum of each species and the time constant of each transition are given (figure reproduced from Stryer, 1988).

modification in the synthesis of opsin. Several studies show that the acylation events occur at two different intra-cellular sites (St.Jules and O'Brien, 1986). The first acylation takes place in the RER, which is the primary acylation site, prior to the transfer of nascent polypeptides of opsin to the Golgi apparatus; the secondary acylation occurs in the ROS. Intercalation of these palmitoyl groups into the lipid bilayer creates a fourth cytoplasmic loop for the rhodopsin molecule (see section 3.2.3).

3.2.2.3 Binding of 11-*cis* retinal:

11-*cis* retinal is a prosthetic group (chromophore) attached to the opsin molecule by a protonated Schiff base linkage (fig 3.2a). The precursor of 11-*cis*-retinal is all-*trans*-retinol (vitamin A) which cannot be synthesized *de novo* by mammals. A deficiency of vitamin A leads to night blindness and eventually to the deterioration of the outer segments of rods which is sometimes referred to as pseudo RP (see section 1.7.1). The site of addition of 11-cis retinal to the opsin apoprotein has been somewhat contoversial. The chromophore was thought to be added to opsin after its transport to the ROS. However there is strong evidence that in the rat 11-cis retinal is attached to opsin shortly after its translation in the RER and before it is transported to the ROS (St.Jules et al., 1989).

3.2.2.4 Prolyl Isomerase and rhodopsin folding:

A *cis-trans* prolyl isomerase may be required for some rhodopsins to fold properly (Shieh et al., 1989). This is one of a group of prolyl isomerases which are members of a class of well conserved proteins that have a wide phylogenetic distribution. These ubiquitous proteins may have a fundumental biochemical role, potentially in mediating protein folding. Cyclophilin, one of these prolyl isomerases, is present in photoreceptor cells and could be involved in folding of rhodopsin. A further clue for the role of such prolyl isomerases came from the genetic analysis of the Drosophila *nina A* mutants. These mutant flies are defective in visual transduction and have only 10% of the normal level of rhodopsin in their photoreceptor cells. However their rhodopsin gene is not defective, and they have normal levels of rhodopsin message. The defective gene in these mutants encodes the prolyl isomerase, cyclophilin (Shieh et al., 1989). Vertebrate retina contains a *nina A* related protein (Stamnes et al., 1991). Therefore it is possible that vertebrate rhodopsins may have a similar requirement for the presence of this enzyme to achieve proper folding in the membrane (Smith et al., 1991a).

3.2.3 Topography of rhodopsin:

The configuration of rhodopsin has been obtained from X-ray diffraction, electron diffraction, and other biophysical studies of the rhodopsin molecule together with a variety of observations from several other studies (Hargrave and McDowell, 1992). These topographical studies have shown rhodopsin as a transmembrane protein which traverses the lipid bilayer seven times. Its polypeptide chain consists of stretches of predominantly hydrophilic amino acids (inta- and extra-cellular domains) separated by seven stretches, 21-28 amino acids in length, of predominantly hydrophobic residues (transmembrane domains). These transmembrane domains are believed to be alpha helices, oriented roughly perpendicular to the plane of the membrane. Its carboxyl terminus faces the cytoplasmic side, and its amino terminus faces the extracellular or intradiscal side of the membrane (fig 3.3). About half of the rhodopsin mass is embedded in the hydrophobic portion of the lipid bilayer and the other half is divided approximately equally between the membrane aqueous surfaces (Dratz et al., 1979).

The seven transmembrane helices of rhodopsin are thought to form a bundle that serves as a binding pocket for 11-*cis* retinal, which binds to Lys-296 deep within the hydrophobic portion of the lipid bilayer (fig 3.4). The amino acid side chains from internal surfaces of the transmembrane helices are suggested to form a retinal binding environment, which specifies the absorption spectrum of the protein.

A disulfide bond that is conserved in the G protein-coupled receptors is present in rhodopsin between cysteines 110 and 187 (Karnik and Khorana, 1990). This disulfide bond seems to occur after the formation of a tertiary structure that involves the intradiscal domains, and could direct the correct alignment of the intradiscal domains. This in turn could lead to the correct alignment of the membrane embedded helices and the correct assembly of the functionally critical cytoplasmic domain (Doi et al., 1990).

Intercalation of the palmitoyl groups at positions cys322 and cys323 into the lipid bilayer provides an additional anchoring site for the long carboxyl tail of rhodopsin creating a fourth cytoplasmic loop (fig 3.3). The cytoplasmic domain represents the culmination of the signal transduction and is responsible for all the biochemical changes that are encountered consequently. All the protein-protein interactions and regulation of the sensory functions occur in this domain. The cytoplasmic face of rhodopsin includes several conserved sites close to the carboxyl terminus that are subject to light-dependent phosphorylation by rhodopsin kinase (Kuhn

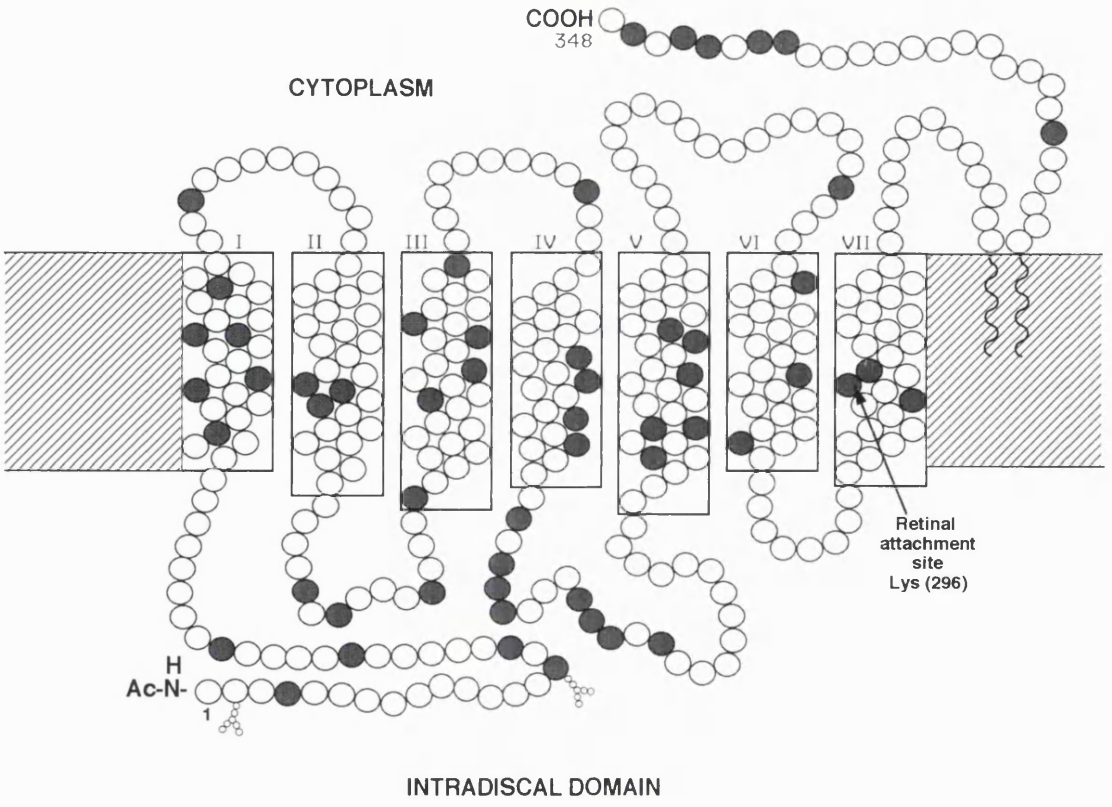

FIGURE 3.3:

Topographical model of human opsin in the lipid bilayer membrane of the rod outer segment disk. It shows the amino terminal at the intradiscal side of the membrane, and the carboxyl terminal at the cytoplasmic (intracellular) side of the membrane. Amino acids are numbered from the amino to the carboxy terminus. The 7 transmembrane helices are numbered from I-VII. The arrow points to the lysine 296 residue, the retinal attachment site. The figure also shows the two glycosylation sites at codons 2 and 15, and the intercalation of palmitoyl groups at cys322 and cys323 into the lipid bilayer forming a fourth cytoplasmic loop.

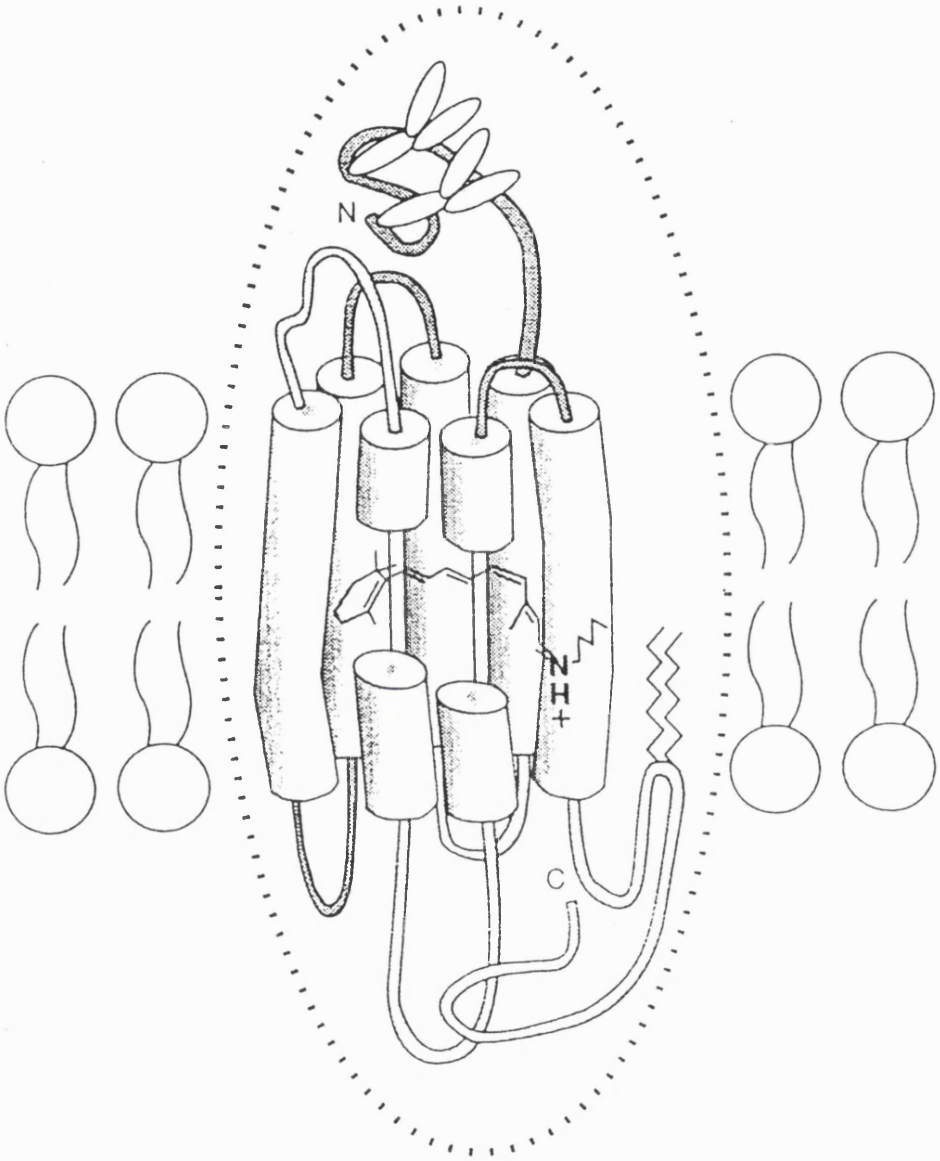

Figure 3.4:

Model for rhodopsin. The protein is presented as a bundle of seven helices that traverse the membrane and provide a binding pocket for retinal. The cutaway view through several helices shows the side chain of lysine 296 that is linked via a protonated Schiff-base to the 11-*cis* isomer of retinal (diagram taken from Hargrave and McDowell, 1992).

et al., 1974), and a catalytic site that is involved in transducin activation (Stryer, 1991).

3.2.4 Rhodopsin and photoreception:

Upon illumination, 11-*cis*-retinal of rhodopsin isomerizes to the all-*trans* form and drives the protein through a series of transient photointermediates (Wald et al., 1968; fig 3.2b). The intermediate, designated as metarhodopsin II (Meta II), also called photoexcited rhodopsin (R^*), binds to and activates the G protein transducin which initiates a cascade of biochemical reactions that culminate in the closure of the cGMP-gated channels in the plasma membrane (section 1.5). The Schiff-base linkage becomes deprotonated (fig 3.2a) in the transition from Meta I to Meta II which has an expanded more open structure. The unprotonated Schiff-base in Meta II is hydrolized to yield opsin and all-*trans* retinal which diffuses away from the protein because it does not fit into the binding site for the 11-*cis* isomer. In the dark, all-*trans* retinal is isomerized to 11-*cis* retinal, which reassociates with opsin to regenerate rhodopsin.

3.2.5 Cone opsins:

Cone visual pigments which mediate human colour vision resemble rhodopsin in consisting of an apoprotein opsin covalently linked to the same 11-*cis* retinal chromophore. Cone opsins have the same topography as rod opsin. However, the variation in absorption spectra observed among different visual pigments is believed to arise from differences in the primary structure of the opsin molecule (Stryer, 1988). The genes for the red and green visual pigments are located on Xq28. Individuals with normal colour vision have these opsin genes in a head-to-tail tandem repeat array consisting of a single red opsin gene upstream from one or more copies of the green opsin genes (Nathans et al., 1986a; Vollarth et al., 1988). The blue cone opsin is coded by a gene on chromosome 7 (Fitzgibbon et al., 1994). All the human cone pigments have approximately 40% amino acid identity to rhodopsin. The human red and green pigments have 96% amino acid identity to each other and 40% identity to the blue pigment (Nathans and Hogness, 1984; Nathans et al., 1986a). The head-to-tail arrangement of the red and green genes in which the transcription units and intergenic spacer DNA are 98% identical at the nucleotide level, predisposes these opsin genes to homologous but unequal recombination (Nathans, 1994). This process generates variant arrays in which entire repeat units are gained or lost, or contain hybrid genes. These rearrangements may lead to X-linked anomalous colour vision.

3.3 MUTATION DETECTION METHODS:

Genetic mutations range from cytogenetically visible chromosome rearrangements, micro deletions and insertions, to single base alterations. Some of these mutations can be detected by cytogenetic techniques (microscopic rearrangments), Southern blot hybridization using conventional or pulse field gels (alterations in fragment size usually in the kilobase to megabase range) or electrophoresis of PCR products on agarose or polyacrylamide gels (deletions and insertions in the range of few to hundreds of base pairs). These methods rely on size differences between mutated and normal alleles. Since the majority of human mutations are single base pair substitutions, which do not alter the size of a mutated allele, more sensitive methods are necessary for their detection. Restriction enzymes can be used to screen for base alterations that eliminate an existing enzyme site or create a new one. This method requires the use of a large number of restriction enzymes to increase the possibility of detecting a base alteration. Therefore this method is not particularly attractive to researchers since it is thought to have a relatively low detection rate and a high cost as a result of using large number of restiction enzymes. Genomic sequencing can detect all nucleic acid changes in a particular sequence. However, this is a lengthy and high cost method for identification of mutations in single patients. With the advent of the polymerase chain reaction several other methods which offer an alternative to genomic sequencing have evolved. These methods can be used to screen for known mutations (for diagnostic purposes) or unknown mutations in candidate genes. Optimization of these methods for the detection of known mutations is easily achievable, but most of them can not be optimised to detect all new mutations in a particular sequence. The use of a combination of two or more of such methods maximise the detection rate. Three of the commonly used methods are described below (Cotton, 1993; Grompe, 1993). These methods detect the presence of a sequence change in a fragment of a few hundred base pairs, and subsequent sequencing is needed to identify the exact nature and location of this change.

3.3.1 Heteroduplex analysis (HA):

This method detects differences in electrophoretic mobility between a homoduplex (formed by annealing of two perfectly matched complementary sequence strands) and heteroduplex that forms as a result of annealing of one DNA strand from the normal allele with the complementary strand from the mutated allele. Such annealing produces a mismatch in the double stranded DNA (dsDNA) sequence which results in altered electrophoretic mobility of the heteroduplex fragment on non-denaturing gels. The use of Hydrolink (Keen et al., 1991a) or MDE (Mutation Detection Enhancement; a new form of Hydrolink made by the same company)

gel matrices rather than polyacrylamide enhances the electrophoretic separation between the heteroduplex and homoduplex fragments. This method can only be applied to fragments hundreds of base pairs long (e.g. <300 bp; Keen et al., 1991a), while the mutation itself and its proximity from the primer sequence play an important role in its sensitivity. Therefore, a priori it is impossible to optimize detection conditions for unknown mutations and consequently the rate of mutation detection by this method is less than 100%. This method has been used for the identification of rhodopsin mutations in adRP patients presented in this thesis.

3.3.2 Single strand conformation polymorphism (SSCP):

In this method wild type and test DNA are amplified by PCR, denatured and electrophoresed through a nondenaturing acrylamide gel (Orita et al, 1989). Single-stranded DNA (ssDNA) molecules of denatured PCR product assume a sequence dependent three-dimensional conformation which varies between the normal and mutated sequences and can be detected as mobility shifts upon electrophoresis. These shifts depend on the percentage of acrylamide in the gel, whether or not glycerol is used, running temperature and a variety of other parameters. As is the case with HA, the mutation itself and its effect on the conformation of the flanking single stranded sequence together with the fragment size play an important role in the sensitivity of this method. Several studies have concluded that maximum detection can be obtained in fragment sizes less than 400bp.

3.3.3 Denaturing Gradient Gel Electrophoresis (DGGE):

Like HA and SSCP, DGGE relies on differential electrophoretic migration of wild-type and mutant DNA. dsDNA generated by PCR is electrophoresed through a gradient of increasing concentration of a denaturing agent such as urea or formamide. As the DNA migrates the strands progressively dissociate in discrete sequence-dependent domains of low melting temperature. This partial melting of the dsDNA leads to an abrupt decrease of mobility. DNA molecules differing in sequence by only a single base have been shown to exhibit differential mobility in such gels (Myers et al., 1987). Heteroduplex formation between wild-type and mutant DNA sequences greatly enhances the sensitivity of DGGE (Sheffield et al., 1989). Higher mutation detection rates are encountered when the sequence heterogeniety lies within a domain of relatively low melting temperature. The attachment of a (30-50 bp) high melting temperature GC-clamp (Sheffield et al., 1989) to one PCR primer is critical to ensure a relatively low dissociation temperature of the amplified sequence. Single base differences can be detected with high accuracy in PCR products of 600 bp in length (Grompe, 1993). Computer

programs are required to predict the theoretical melting profiles and design PCR primers to obtain domains of low melting temperatures (Lerman and Silverstein, 1987).

3.4 RESULTS:

The coding region of the rhodopsin gene from 80 unrelated adRP patients, 35 sporadic RP cases, and 5 arRP patients and their parents have been PCR amplified using intronic primers flanking the five exons (see section 2.2). PCR products, with sizes of 210-314 bp, were first run on 2.5% agarose-Nusieve (4:1) gels to check the quality of amplification and to test for possible insertion/deletion events. PCR products were then separated on Hydrolink gels to detect point mutations or small insertion/deletion events which could not have been detected on agarose gels. At later stages of the study MDE (Mutation Detection Enhancement) gel matrix was used instead of Hydrolink. To test the reliability of this gel matrix, several mutations previously detected on Hydrolink gels were used as positive controls (fig 3.5).

3.4.1 A deletion mutation in rhodopsin:

A deletion mutation in exon 5 of the rhodopsin gene was found to segregate with the adRP phenotype in a three generation Italian family. Upon PCR amplification and agarose gel electrophoresis of affected and normal individuals, two bands were detected only in the affecteds. The larger fragment was the same size as the normal allele, and therefore it was concluded that the smaller band must have resulted due to a deletion from the other allele of the gene (fig 3.6). Such a deletion was not seen on testing 50 normal controls. Sequence analysis revealed a 42 bp deletion with three possible breakpoints. The 5' breakpoint could be after codon 339 or after either the first or second nucleotide of codon 340. The 3' breakpoint should be 42bp from any of the above three 5' breakpoints. Any of these possible breakpoints would result in the deletion of the last nine codons and the termination codon of exon 5. The next possible stop codon ,TAA, is at nucleotide positions 5429-5431 (nucleotide numbers are according to the sequence of Nathans and Hogness, 1984). The resultant opsin molecule is expected to be 38 amino acids longer (386 instead of 348 amino acids). The family with this deletion has type I/D adRP with mild and slow progression of the disease (Restango et al., 1993).

3.4.2 An insertion mutation in rhodopsin:

This is the first report of an insertion mutation in the rhodopsin gene. The mutation was

detected in the exon 5 PCR product as an extra large band on a 2.5% agarose-Nusieve gel (fig 3.7a). Sequence analysis of the cloned PCR product of the mutated allele reveals an insertion of 150 bp (fig 3.7b) which replaces 30 bp of normal sequence from nucleotide 5145 in intron 4 to nucleotide 5174 at the 5'end of exon 5. The sense strand sequence of the insert is composed of AG rich repeated DNA which accounts for 88% of the residues. The sequence was analysed for homology using the FASTA algorithm (Pearson and Lipman, 1988) against standard databases. The highest homologies scored were 73% identity over 126bp with rat N-myc (GenBank), and 69% identity over 93bp with mouse T-cell receptor (GenBank). These homologies, along with others scored from different databases, were to GA-rich non-coding regions and appear to have no biological significance.

The deleted sequence of the rhodopsin gene includes the conserved 3' splice junction of intron 4 and the first 7 nucleotides of exon 5. It may be speculated that the resultant nuclear pre-mRNA would have any of three alternative splicing patterns. Firstly, a search for a consensus 3' splice junction (Cech, 1986) in the insertion sequence identified only one possible site after nucleotide position 17. Exon 5 of the resultant truncated protein would be replaced by four amino acids, namely Lys-Lys-Lys-Arg-Stop (the underlined DNA sequence in fig 3.7b). Secondly, if splicing were not to take place within the insert, the next AG sequence ends at position 5206 within exon 5. The sequence in that region is compatible with a potential splice site. The resultant truncated mRNA would be deleted for the first 13 codons of exon 5, but in-frame for the remainder of the exon. The third possibility is that neither of the two potential splicing events described above occur, resulting in the continuation of protein synthesis after exon 4 into the fourth intron up to position 4776, where a stop codon would terminate translation. The resultant protein would be 111 residues larger than the normal rhodopsin protein. It is therefore not possible to deduce exactly what would be the amino acid sequence of the protein encoded by the altered rhodopsin gene without carrying out *in vitro* expression studies.

Interestingly, the phenotype in this family is characterized by regional distribution of photoreceptor cell degeneration together with variation in the age of onset and severity of symptoms (Kim et al., 1993). This phenotype corresponds to type II/R by the clinical criteria of Lyness and coworkers (Lyness et al., 1985), which is unlike the previously described phenotype in most rhodopsin RP families (Al-Maghtheh et al., 1993). Patient II-3 (fig 3.7a) had first experienced mild difficulty seeing at night in her early teens. Subsequent ophthalmic

evaluation led to a diagnosis of retinitis pigmentosa (Kim et al., 1993). Neither her parents nor any of the relatives had a history of night blindness. Her twenty six year old daughter (III-2) was unaware of any symptoms at the time of examination. However, her twenty one year old daughter (III-3), in contrast, expressed difficulty seeing at night in her early teens, and more recently became aware of constriction in her visual field. No other unaffected family member for whom DNA was available has this insert (fig 3.7a) nor any one of the 50 normal controls. It is possible that I-1 had this mutation with a very mild or asymptomatic phenotype, assumed from the variation in severity seen in this family, and passed it to his daughter II-3. On the other hand, it is possible that this is a new mutation arising in II-3.

3.4.3 Point mutations in rhodopsin:

Electrophoresis of PCR products of the rhodopsin gene on Hydrolink gels shows a single band in all individuals corresponding to the homoduplexes of the wild type allele. In addition to the homoduplex band, heteroduplexes were observed in 6 adRP patients (out of 80) as extra bands with slight mobility retardation.

Direct sequencing of the PCR product of the first exon of rhodopsin from an adRP patient with a heteroduplex (fig 3.5, lane 1) revealed a T→G transversion at nucleotide position 413 (fig 3.8a) which results in a Leu→Arg amino acid substitution at codon 40 (L40R). This nucleotide alteration was found to create a new site for the restriction enzyme Sau 96.1. Cosegregation of the mutation with the disease phenotype in other family members was confirmed by digestion of the PCR products with Sau 96.1 in all available individuals (fig 3.8b).

In another adRP patient, direct sequencing of the exon 3 PCR product, which showed a heteroduplex, revealed a T→A transversion (fig 3.9a) at nucleotide position 3929. This results in a Met→Lys substitution at codon 216 (M216K) of the rhodopsin gene. Heteroduplexes were present in two affected members of the family and absent in a third member who was normal (fig 3.9b). This mutation disrupts a restriction site for the enzyme Nla III which could be used for diagnostic purposes. Both L40R and M216K were new mutations which have not been previously reported and were absent from the 50 normal controls.

In addition, sequence analysis of exon five revealed that three unrelated patients had heteroduplexes (Fig 3.10a) as a result of the relatively common C→T mutation at nucleotide position 5271 ~~(fig 3.10a)~~. This results in a Pro→Leu substitution at codon 347. This mutation was previously

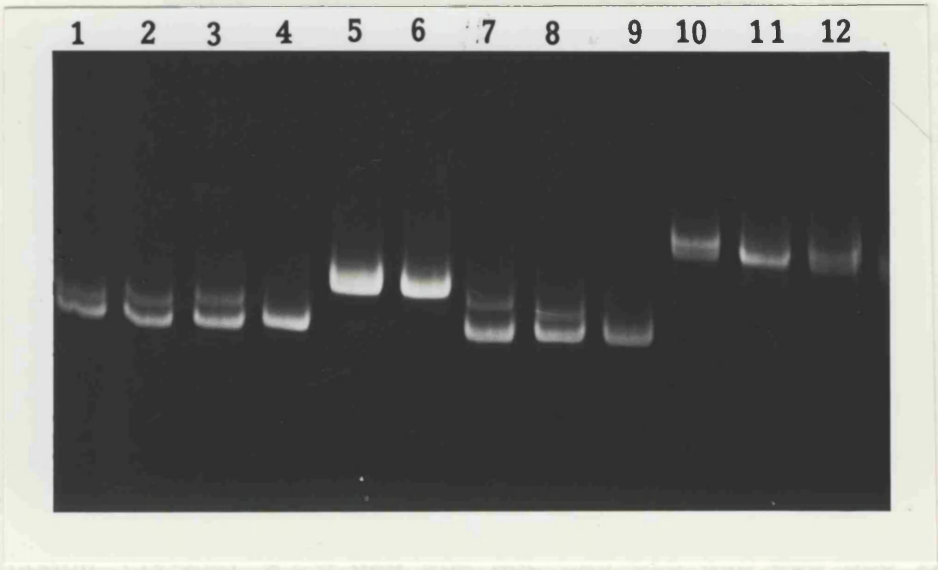

Figure 3.5:

MDE gel photograph of some rhodopsin mutations. Order of mutations from left to right (lanes 1-12) are: Leu40-Arg, Pro53-Arg, Thr58-Arg, normal control, Gly106-Arg, normal control, Leu125-Arg, Cys167-Arg, pro171-Leu, Met216-Lys, normal control, and Asp190-Asn.

Mutation Gly106-Arg, which shows a diffuse band (lane 5), was similarly detected on Hydrolink gel and was confirmed only by sequencing and segregation in the corresponding family. Mutation Pro171-Leu (lane 9) is not detected on both Hydrolink and MDE, as Heteroduplex method does not detect all base alterations in a particular sequence. Lanes 1-4, 5-6, 7-9, and 10-12 correspond to PCR products of exons 1.1, 1.2, 2, and 3 respectively.

a:

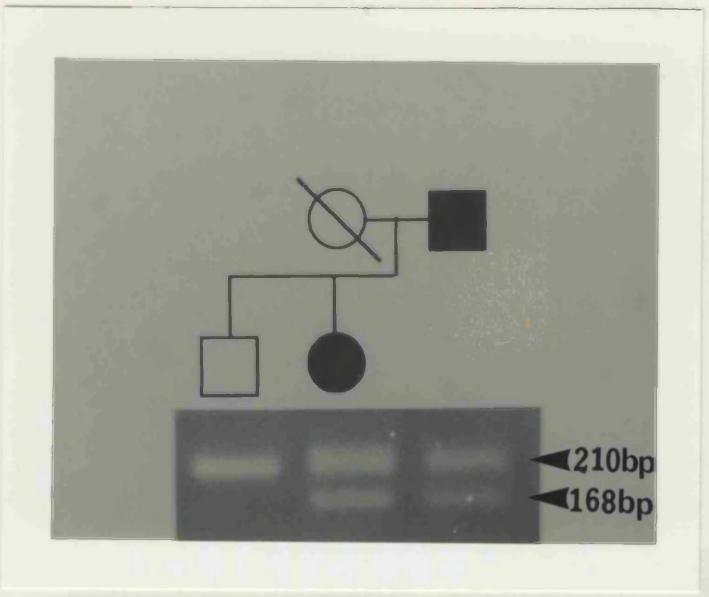

b:

Codon 339-AAG[1] **A[2]C[3]G GAG ACG AGC CAG GTG GCC CCG GCC TAA**
amino acid: Lys **Thr Glu Thr Ser Gln Val Ala Pro Ala stp**

GAC CTG CCT AGG[1] A[2]C[3]T CTG TGG CCG ACT ATA GGC GTC TCC CAT
Thr Leu Trp Pro Thr Ile Gly Val Ser His

CCC CTA CAC CTT CCC CCA GCC ACA GCC ATC CCA CCA GGA GCA GCG
Pro Leu His Leu Pro Pro Ala Thr Ala Ile Pro Pro Gly Ala Ala

CCT CTG CAG AAT GAA CGA AGT CAC ATA GGC TCC TTA ATT TTT TTT
Pro Leu Gln Asn Glu Arg Ser His Ile Gly Ser Leu Ile Phe Phe

TTT TTT TTT TTA AGA AAT AAT TAA
Phe Phe Phe Leu Arg Asn Asn stp.

Figure 3.6:

a: Pedigree and agarose gel photograph showing segregation of the rhodopsin exon 5 deletion allele (lower fragment, **168** bp) in affected individuals of an Italian adRP family (fragment size of the normal allele is 210 bp). b: Nucleic acid sequence of the deletion (underlined bold face) and the predicted amino acid sequence of the altered opsin molecule (double underlined). The three possible start and end points of the deletion are numbered on the sequence.

a:

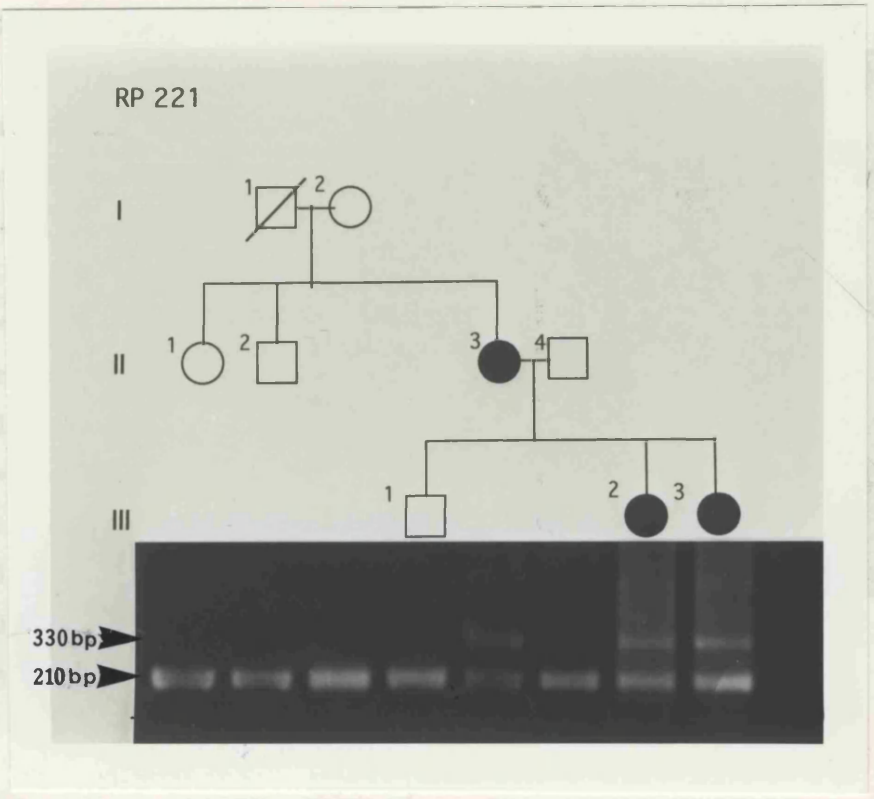

b:

```
     5144-t acatattaca ttataagaaa aaaaaaaggt agaggaaggg
          a tgtataatgt aatattcttt ttttttcca tctccttccc

 aggaagggaa ggggagggag gaagtggaga tgtggagacg cgagaggaag
 tccttccctt cccctccctc cttcacctct acacctctgc gctctccttc

 agagagaggc agagggagag ggaaaggtgg ggagagagga gggggcagag
 tctctctccg tctccctctc cctttcctcc cctctctcct cccccgtctc

 agagaggtgg A-5175
 tctctccacc T
```

Figure 3.7:

a: Pedigree and agarose gel photograph of rhodopsin exon 5 PCR products. It shows segregation of the insert with affected individuals of the family. Smaller fragment seen in all individuals correspond to the normal PCR product of exon 5. b: Insert sequence (150bp) including one normal flanking nucleotide from both sides of the insertion point, and its position within the normal genomic sequence of the rhodopsin gene. Donor splice site and stop codon are both double underlined, and in between sequence of exon 5 is underlined as described in the text.

Figure 3.8:

Left: Sequencing gel photograph of rhodopsin exon 1 A→C substitution (codon 40) on the reverse strand, which corresponds to T→G on the forward strand. Bottom: pedigree and agarose gel photograph of rhodopsin exon 1 Sau96.1 restriction digest in the family with codon 40 T→G mutation. All individuals have the 193bp fragment of the normal allele, while affected individuals have extra two bands (121, 72bp)as the T→G mutation creates a new Sau96.1 site within the 193 bp fragment. Lane 1: undigested normal control of exon 1 PCR; lane 2: digested normal control, it shows that the upper band seen in all digested DNAs is a digestion artifact.

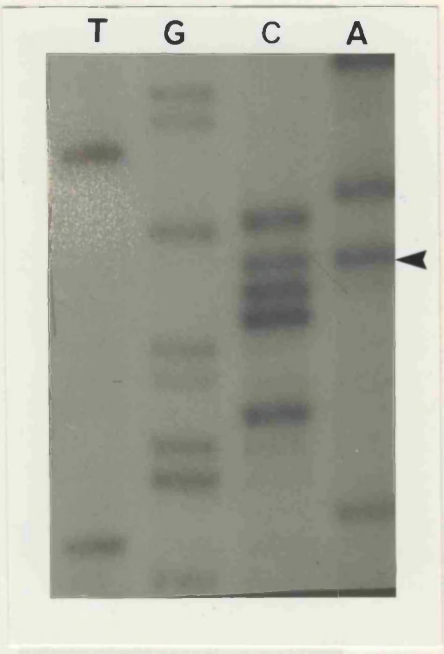

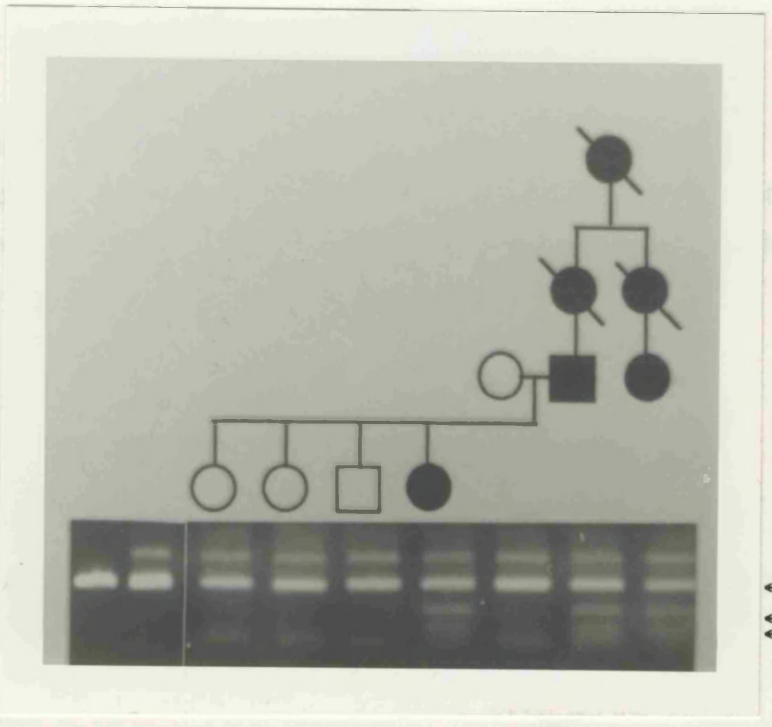

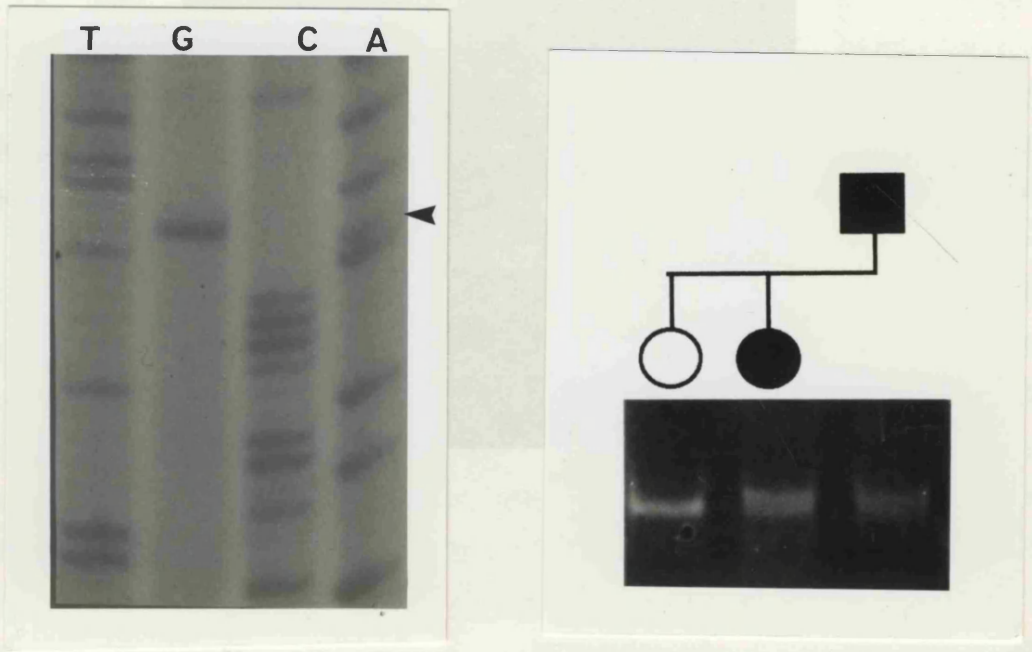

Figure 3.9:

Left: Sequencing gel photograph of rhodopsin codon 216 (exon 3) T→A substitution (see arrow).

Right: Pedigree and hydrolink gel photograph showing segregation of heteroduplex band in 2 affected members of the family (PCR fragment size is 310 bp).

Reverse strand sequencing also confirmed the presence of this mutation.

a:

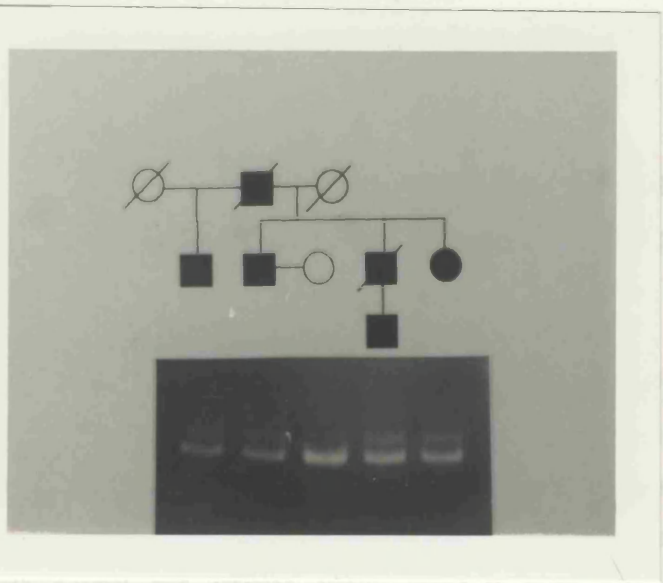

b:

Figure 3.10:

a: Pedigree and Hydrolink gel photograph which shows segregation of heteroduplex band as a result of Pro347→Lys mutation in affected family members. b: Msp1 digest of rhodopsin exon 5 PCR from adRP patients (lanes 1 and 2) with Pro347→Lys mutation and normal controls (lanes 3 and 4). Undigested band (fragment 211 bp) in adRP patients resulted from disruption of Msp1 site as a result of C→T substitution at codon 347.

shown to eliminate an Msp1 site (CCGG→CTGG) (Fig 3.10b), which was used to show segregation of this mutation in affected members of the family of each patient.

3.4.4 Non disease causing polymorphisms:

One other C→T substitution was also detected at nucleotide position 654 in exon one. This third position change of codon 120 (GGC→GGT) does not alter an amino acid residue (glycine) and is considered as a neutral coding region polymorphism. This base change polymorphism has been previously reported by several studies (table 3.1c).

Another previously reported (Dryja et al., 1991) non-coding region polymorphism, C→T at nucleotide position 3982, in intron 3 has been detected. This polymorphism was found in members of the family with the codon 216 mutation. It was detected by sequencing of the PCR products of exon 3 in patients who were found to have the codon 216 mutation. Apparently, even though both normal and affected family members were heterozygous for this polymorphism, the detected heteroduplex was not due to this base substitution, since a heteroduplex was only seen in affected individuals. This is probably because of its proximity to the primer sequence.

3.5 DISCUSSION:

3.5.1 Heteroduplex analysis method:

Heteroduplex mobility shifts are sequence dependent and vary from easily detectable to very subtle shifts which in some cases may be completely undetectable. Such variations are caused by the nature of the base substitution, its position within the sequence, and the fragment size. An optimum fragment size of less than 300bp has been recommended for a higher detection rate. However no optimization can be made for unknown mutations. Consequently HA, like SSCP and DGGE, does not detect all base changes in a particular sequence. However if a particular mutation is not detected by one method, it may be detected by another. Comparative studies are needed to establish whether the differences in sensitivity and the detection rates of various methods are statistically significant. It is also recommended that for diagnostic purposes a combination of methods be used to maximize the chances of mutation detection.

Heteroduplexes can be detected simply by electrophoresis of PCR generated dsDNA on

Hydrolink or MDE gels followed by ethidium bromide staining, avoiding the use of radioactive isotopes or other chemical detection methods which need special handling protocols. This practical simplicity of the HA method made it the method of choice in many laboratories over SSCP or DGGE, despite the fact that these mutation detection methods may have a higher detection rate. Using HA in this laboratory, rhodopsin mutations were detected in 11 out of 12 rhodopsin linked adRP families (Inglehearn et al., 1992); this gives a detection rate of more than 90%. Similar sensitivity of 80-90% was obtained in other studies with fragments less than 300bp (Artlich et al., 1992).

3.5.2 Frequency of rhodopsin adRP:

Large scale screening of the rhodopsin gene in various adRP populations has been undertaken by several groups using a variety of mutation detection methods (table 3.2). The obtained frequencies of rhodopsin mutations varied between 18-29% of total adRP cases. Pooling data from these studies suggests that rhodopsin accounts for approximately a quarter of all adRP. However, in this study of 80 adRP patients, 7 were found to be caused by rhodopsin mutations (less than 10%). This may imply that mutations have been missed in this study. However, the patient sample used in this screen is unique, and therefore other hypotheses may explain this apparent disparity, as detailed below.

Most of the patients used in this study were referred to Moorfields Eye Hospital in London, and their adRP classification was based on family history reported by the patient at the time of interview; all of them belonged to small nuclear families. No further evidence or clinical data on other family members were presented to confirm family history. Therefore it is possible that some of these patients did not truly have an autosomal dominant form of RP. Furthermore, since most of the samples were collected at Moorfields Eye Hospital it is likely that a significant proportion came from a relatively small geographical area (south east of England). It is therefore possible that a proportion of them are distantly related, and have the same mutation by descent. If such patients have none rhodopsin RP or have a rhodopsin mutation which is undetectable by HA, it would significantly reduce the detected frequency of the rhodopsin adRP in this sample. A similar effect would be noticed if such an undetectable mutation is as common as, for example, Pro347→Leu which accounts for 20% of total rhodopsin adRP detected in this laboratory.

Moreover, previously in this laboratory, 20 of 52 (38%) large adRP families were found

to have rhodopsin mutations (Inglehearn et al., 1992; Inglehearn et al., in preparation; table 3.2). This is the highest reported frequency of rhodopsin RP among adRP patients and contrasts greatly with what has been found in small clinic based families used in this study. Small adRP families may have a common underlying mechanism. This could be high frequency of occurence of new severe mutations in a particular gene with high selection against continuation in future generations. Alternatively this might be due to incomplete penetrance, or multigenic inheritance, which cause the link between successive generations to be lost. Both of these phenomena (incomplete penetrance and multigenic inheritance) could result in small RP pedigrees. The former would be dominant pedigrees as parts of larger families, probably mapping to 7p, 19q, or other incompletely penetrant loci, and therefore not rhodopsin. The latter might appear dominant (or recessive) but in fact would be caused by mutations in several genes. Since rhodopsin mutations segregate perfectly from one generation to another with complete penetrance, they are more likely to be represented in large multigeneration families, and less likely to cause adRP in such small families. Therefore, the adRP sample used in this study could have been biased towards less rhodopsin families. Estimating the frequency of rhodopsin RP from both studies performed in this laboratory (study 5, table 3.2 and this study) concluded a similar frequency (20%) to that reported from other laboratories, and therefore suggests the possible bias encountered in both samples.

None of the 35 sporadic RP and 5 arRP cases included in this study were found to have rhodopsin mutations. So far mutations in the rhodopsin gene have been implicated in only a few arRP cases (table 3.1). Therefore, rhodopsin mutations are unlikely to be involved in the majority of sporadic and arRP cases.

3.5.3 Rhodopsin mutations and polymorphisms:

So far more than 87 disease causing rhodopsin gene mutations have been identified, the majority of them in adRP patients, and few in arRP patients and in patients with congenital stationary night blindness (CSNB) (table 3.1). These mutations are spread throughout the coding region of the rhodopsin gene and no single mutation has been found to account for the majority of the disease cases. This is perhaps due to stronger natural selection against mutations that result in expression of disease in heterozygous individuals (dominant diseases) as compared to normal disease gene carriers of recessive traits. These mutations included 76 single base-pair substitutions, one two base-pair substitution (table 3.1a), one insertion (150bp) and 7 deletions (1-42bp) (table 3.1b). Two splice site mutations which segregate with an adRP phenotype were

also reported (table 3.1b). DNA sequence variations which do not correlate with adRP (polymorphisms) have been reported in the coding and the noncoding regions of the rhodopsin gene (table 3.1c).

The Pro347→Leu mutation which is due to C→T transition in a CpG dinucleotide has been seen in at least 6 unrelated British families (20% of rhodopsin adRP detected in this laboratoty; Inglehearn et al. 1992, results presented in this thesis, and unpublished data from this laboratory) as well as German (Apfelstedt-Sylla et al. 1992), American (Dryja et al. 1990b) and Japanese families (Fujiki et al. 1992). The higher frequency of this particular mutation could result from the tendency of methylated cytidine in the dinucleotide CpG to mutate to thymine, making CpG a mutational hot spot (Vogel and Rathenberg 1975). However this can not be the only reason since other CpG dinucleotides exist in the rhodopsin gene and do not show the same high frequency of new mutations. In contrast, the Pro23→His mutation (C→A transversion) which has attained a frequency of 12% in American adRP patients (Dryja et al. 1990a, Sheffield et al. 1991, Sung et al. 1991a), has not been found elsewhere (Farrar et al., 1990, and this study). This mutation was found to be in linkage disequilibrium with a rare allele at the CA repeat polymorphism in intron one of the rhodopsin gene, which strongly supports the hypothesis of a founder effect (Dryja et al. 1991).

Interestingly rhodopsin has been found to be involved in arRP in at least one family with a null mutation at codon 249 (Rosenfield et al., 1992) and another with the missense mutation E150K (Kumaramanickavel et al., 1994). It was also involved in dominant CSNB due to mutations G90D (Sieving et al., 1992) and A292E (Dryja et al., 1993). So far no mutations in the promotor sequences or in the 5' or 3' non-coding regions have been reported. Southern blot analysis also failed to reveal any large rearrangement in the rhodopsin gene (Inglehearn et al., 1992).

3.5.4 Rhodopsin mutations: biological relevance:

Rhodopsin constitutes 70% of the structural proteins in the ROS (Hamm and Bownds, 1986) and functionally is considered to be a key component of the visual transduction pathway in rod cells. Therefore mutations in the gene encoding this protein might be expected to have structural and functional implications in the rod cell in particular and in the retina in general.

For example, mutation Thr17→Met, which destroys one of the two glycosylation consensus

sequences (Asn-2 and Asn-15), causes adRP in humans. These two sites of rhodopsin glycosylation are conserved in bovine and human rhodopsin sequences (Nathans and Hogness, 1984). This underlines the importance of glycosylation of the rhodopsin molecule, which could have a significant role in proper protein insertion into the membrane and/or folding. Similarly, mutations that reside near Cys-110 or Cys-187 (G106W, Y178C, D190G) may destabilize the protein by interfering with the disulfide bond formation.

Lysine 296, the retinal attachment site to the opsin apoprotein (Stryer, 1988) is highly conserved in both vertebrate and invertebrate opsins. Substitution of Lys296 with glutamic acid which lacks the amino group to which retinal normally binds, causes a severe form of adRP (Keen et al., 1991a). Electrostatic interaction between Lys296 and Glu113, the counterion to the protonated Schiff base, results in the formation of a salt bridge between the two residues (Sakmar et al., 1989; Nathans, 1990). This salt bridge contributes to keeping the opsin apoprotein in a constrained inactive conformation. Mutation of either residue breaks this salt bridge and promotes the transition to the active conformation. Mutation Lys296→Glu, results in constitutive activation of opsin *in vitro* where the mutants can activate transducin in the absence of both chromophore and light (Robinson et al., 1992). However, this activation was found to be shut off *in vivo* by photoreceptor inactivation mechanisms (phosphorylation and binding to arrestin) (Li et al., 1995). St Jules and colleagues (1986) have shown that in the absence of retinal newly synthesized opsin accumulates in the rough endoplasmic reticulum of the isolated rat retina. Accumulation of defective opsin is likely to interfere with the normal cellular processes in the rod photoreceptor cell.

Similarly Ala292→Glu (A292E) and Gly90→Asp (G90D) constitutively activate transducin *in vitro* and causes CSNB in humans (Dryja et al., 1993). Mutagenesis studies place Gly90 (helix II, fig 3.11) in a position oriented towards Lys296 (helix VII) and at the same level in the membrane, such that both helices are side by side in the three dimentional structure of rhodopsin (Rao et al., 1994). This arrangement of the helices agrees with a recent model for G protein-coupled receptors (Baldwin, 1993). Therefore both mutants disrupt the salt bridge and constitutively activate opsin by introducing a negative charge that can compete with Glu113 for the positively charged Lys296 (Rao et al., 1994).

CSNB (with severly impaired rod vision) and RP are two different phenotypes. The mutations associated with RP (K296E, K296M) are incapable of binding retinal chromophore

Figure 3.11:

(Figure and legend are from Rao et al., 1994)

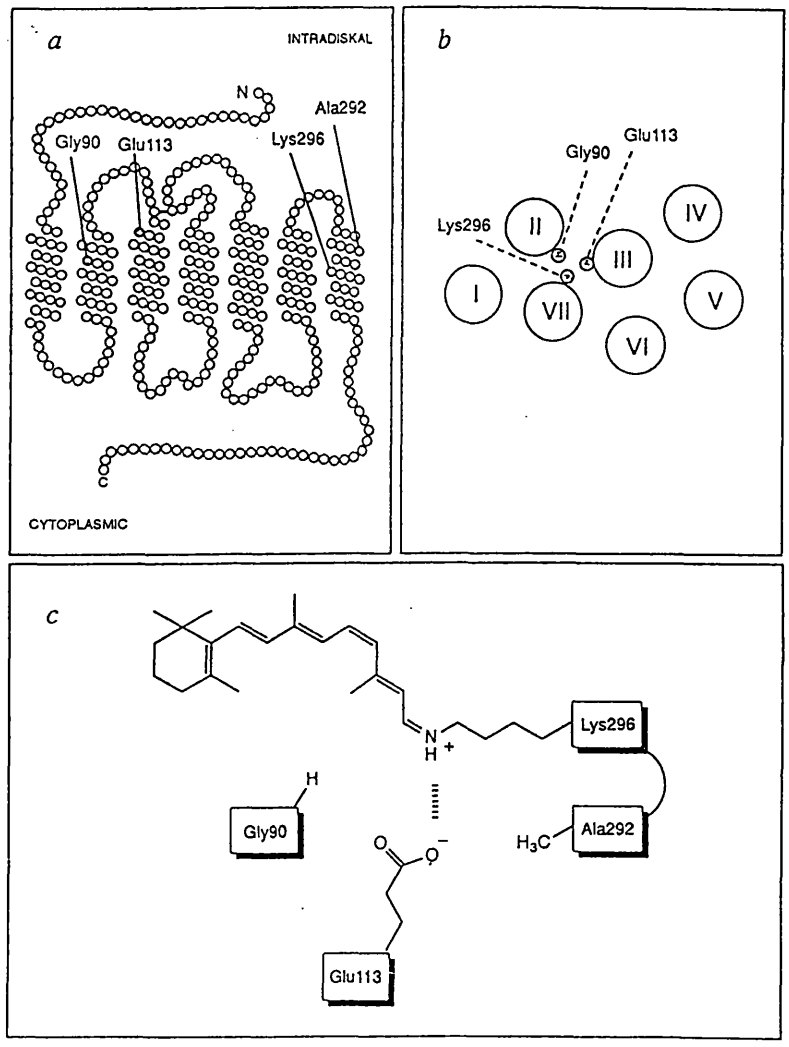

Structure of rhodopsin. *a*, Schematic diagram showing the seven transmembrane α-helical segments of rhodopsin. Shaded circles indicate the four amino acid residues that constitutively activate opsin when mutated. *b*, Cross-sectional view of rhodopsin. This view is rotated 90° relative to that in *a*, looking at the helical bundle parallel to the longitudinal axes of the helices. This diagram is based on a 9 Å projection map[18] obtained by cryoelectron microscopy of two-dimensional arrays of rhodopsin; and a model[19] for the structure of G-protein-linked receptors. Filled circles correspond to amino acids Gly 90, Glu 113 and Lys 296. *c*, Schematic diagram of chromophore-binding site.

(Zhukovsky et al., 1991) so that all the mutant protein is in the active opsin state. However mutations associated with stationary night blindness (A292E, G90D) can bind the chromophore and therefore are inactive in the dark due to retinal binding to rhodopsin. However, as the rod cell does not contain large excess of retinal, at any given moment there will be a number of opsin molecules (few hundreds) with vacant retinal binding site. This does not normally present the rod cell with any problem since the wild-type opsin is inactive, however, in the case of G90D and A292E mutants, the opsins are active and are present in sufficient amounts to severely desensitize the rod cell. Night blindness results as rod cells adapt to a dark signal coming from a relatively small number of constitutively active opsin molecules but enough to saturate the electrical response of rod cell (of the 10^8 rhodopsin molecules in the rod cell only ~200 need be activated to saturate the electrical response of the rod cell) (Rao et al., 1994). Therefore, CSNB and RP represent two retinal diseases with a quantitative difference of the same molecular defect.

3.5.4.1 Functional studies of RP causing rhodopsin mutations:

Mutant rhodopsin molecules were classified into two major classes (Sung et al., 1991). Class I (eg. F45L, Q344ter and P347L) resemble wild type in yield, electrophoretic pattern, regenerability with 11-*cis*-retinal and subcellular localization. On the other hand class II are expressed at significantly lower levels, appear predominantly as aggregates on immunoblots, regenerate with 11-cis-retinal to variable extents or not at all and were transported ineffeciently to the plasma membrane. Further subdivision was made within class II based on mutants that show predominantly intracellular localization (class IIa, eg. P23H) and those that also show significant cell surface localization (class IIb, eg. R135L).

Recently, in a series of studies of structure and function in rhodopsin, aiming at further understanding the *in vivo* assembly and folding of the nascent opsin polypeptide chain to the correct functional molecule, Khorana and co-workers (Kaushal and Khorana, 1994) performed a study of more than 30 adRP causing rhodopsin mutations. Focusing on the intradiscal domain, they confirmed that the formation of a precise tertiary structure comprising the N-terminal tail and all the loops in the intradiscal domain is an early requirement for rhodopsin assembly. The alignment of the seven transmembrane helices to form a cluster with specific interhelical interactions, and formation of a retinal binding pocket are a consequence of the above intradiscal structure. It was also inferred that the organisation of the cytoplasmic domain to a specific tertiary structure automatically follows assembly of the transmembrane domains. Thus the

correct assembly of the intradiscal domain is responsible for the formation of a fully functional rhodopsin molecule. Consistant with this conclusion, and in contrast with the critical folding requirement in the intradiscal domain, mutations in the cytoplasmic loops do not affect the folding of the receptor unless they affect the packing of the helices (Franke et al., 1992). Point mutations as compared with relatively larger deletions in the intradiscal domains (Doi et al., 1990), resulted in similar phenotypes which emphasize the stringent requirements for the tertiary structure in this domain.

adRP point mutations in the transmembrane domain provided important clues to the helix-helix interactions and orientation of different helices to form the retinal binding pocket. In all the amino acid replacements, the side chain of a particular residue and its actual location around the helix would be specifically important, and is clearly evident in replacements of counterion residues involved in salt bridge formation with the positively charged Schiff base (see above).

Similar studies are needed to classify the newly identified rhodopsin mutations presented in this thesis at codons 40, 216 and both the insertion and deletion mutations. However, based on the results obtained with various rhodopsin mutants (Kaushal and Khorana, 1994), it is possible to speculate on the genotype-phenotype and structure-function relationships of some of these newly identified mutations.

Codon 40 lies in the first (helix A) transmembrane domain of the opsin molecule (fig 3.11). Of the nonconservative mutants G51R, P53R, and T58R, (in helix A), T58R has class I characteristics, while G51R and P53R showed characteristics of class II. Mutation L40K represents a nonconservative replacement of nonpolar hydrophobic leucine with a positively charged arginine. Hence, it is not possible to predict the outcome of the L40K mutation without similar mutagenesis and expression studies. Nonconservative changes of codons 211 (H211P) and 222 (C222R) which flank codon 216 in helix E (figure 3.11), have characteristics of class II mutants (Kaushal and Khorana, 1994). Therefore, it is possible to speculate that the nonconservative substitution of the positively charged lysine residue for the nonpolar hydrophobic methionine (M216K) might result in a class II mutant phenotype.

Mutation P347L in the cytoplasmic domain has already been studied and found to represent a class I mutant. Both the insertion and deletion mutations affect the cytoplasmic domain and are expected to code for an opsin protein with an altered carboxyl terminus. Expression studies

should be performed in order to classify and fully characterize these mutant proteins.

3.5.5 Rhodopsin mutations: clinical relevance:

Most of the rhodopsin RP cases were found to be of the type I/D form (Lyness et al., 1985); however as more and more rhodopsin mutations are identified, it appears that in a proportion the phenotype coresponds to type II/R. In the more advanced cases it is difficult to distinguish between D and R types of adRP. Difference in severity of the disease has been demonstrated with many different rhodopsin mutations (Fitzke et al 1991). Phenotypic heterogeneity among adRP families with the same mutation have also been reported. For example, the codon 23 mutation in exon one described as causing sector RP (Heckenlively et al 1991) was also found to cause a wide range of variable phenotypes in another study by Berson et al (1991). Most of sector RP cases were associated with exon 1 mutations (codons 23, 58, and 106) (Inglehearn et al., 1992; Heckenlively et al., 1991) which may suggest that a particular subgroup of mutations in this region causes this characteristic phenotype. However some clinicians classify sector RP within the broader classification of type II/R phenotype (Berson et al., 1991; Stone et al., 1991). The wide range of phenotypic variation due to rhodopsin mutations is further extended by the finding of rhodopsin involvement in both arRP (Rosenfeld et al., 1992) and CSNB (Dryja et al., 1993).

3.5.6 Rhodopsin mutations: diagnostic relevance:

The relatively large number of rhodopsin mutations (table 3.1) and the substantial phenotypic overlap between these mutations, make predictive diagnosis difficult. The existence of phenotypic variation within family members carrying the same mutation further complicates this approach. Therefore identification of the precise mutation will have to be carried out in each adRP family. Once a particular mutation has been identified, methods for its detection can be optimised and can then serve as useful diagnostic tools for systematic large scale screening which will help overcome the laborious work of sequencing the whole gene for mutations in single patients. Moreover, some of the mutations either create or eliminate a restriction enzyme site, so that such enzymes can be used for quick diagnosis of these mutations in other family members as well as for large scale screening for that particular mutation in other adRP patients.

Table 3.1:
A list of the mutations and polymorphisms found in the rhodopsin gene.

a: RP and other disease causing point mutations:

Exon	Codon	Nucleotide change	Amino acid change	Clinical phenotype	Reference
1	4	ACA-AAA	Thr-Lys	adRP	Bunge et al., 1993
1	15	AAT-AGT	Asn-Ser	sector	Sullivan et al., 1993
1	17	ACG-ATG	Thr-Met	adRP	Sung et al., 1991a
1	23	CCC-CAC	Pro-His	adRP	Dryja et al., 1990a
1	23	CCC-CTC	Pro-Leu	sector	Dryja et al., 1991
1	28	CAG-CAC	Gln-His	adRP	Bunge et al., 1993
1	40	CTG-CGG	Leu-Arg	adRP	Al-Maghtheh et al., 1994
1	45	TTT-CTT	Phe-Leu	adRP	Sung et al., 1991a
1	46	CTG-CGG	Leu-Arg	adRP	Rodriguez et al., 1993a
1	51	GGC-GTC	Gly-Val	adRP	Dryja et al., 1991
1	51	GGC-CGC	Gly-Arg	adRP	Dryja et al., 1992
1	51	GGC-GCC	gly-Ala	adRP	Macke et al., 1993
1	53	CCC-CGC	Pro-Arg	sector	Inglehearn et al., 1992
1	58	ACG-AGG	Thr-Arg	adRP	Dryja et al., 1990b
1	64	CAG-TAG	Gln-stop	adRP	Macke et al., 1993
1	87	GTC-GAC	Val-Asp	adRP	Sung et al., 1991a
1	89	GGT-GAT	Gly-Asp	adRP	Sung et al., 1991a
1	90	GGC-GAC	Gly-Asp	CSNB	Sieving et al., 1992
1	106	GGG-TGG	Gly-Trp	adRP	Sung et al., 1991a
1	106	GGG-AGG	Gly-Arg	sector	Inglehearn et al., 1992
1	110	TGC-TAC	Cys-Tyr	adRP	Dryja et al., 1992
1	114	GGC-GAC	Gly-Asp	adRP	Vaithinathan et al., 1994
2	125	CTG-CGG	Leu-Arg	adRP	Dryja et al., 1991
2	127	TCC-TTC	Ser-Phe	adRP	Souied et al., 1994
2	131	CTG-CCG	Leu-Pro	adRP	Souied et al., 1994
2	135	CGG-CTT	Arg-Leu	adRP	Sung et al., 1991a
2	135	CGG-CCG	Arg-Pro	adRP	Rodriguez et al., 1993b
2	135	CGG-CTG	Arg-Leu	adRP	Andreasson et al., 1992
2	135	CGG-TGG	Arg-Trp	adRP	Sung et al., 1991a
2	135	CGG-GGG	Arg-Gly	adRP	Bunge et al., 1993
2	140	TGT-TCT	Cys-Ser	adRP	Macke et al., 1993
2	150	GAG-AAG	Glu-Lys	arRP	Kumaramanickavel et al., 1994
2	164	GCG-GAG	Ala-Glu	adRP	Vaithinathan et al., 1994
2	167	TGC-CGC	Cys-Arg	adRP	Dryja et al., 1991
2	171	CCA-CTA	Pro-Leu	adRP	Dryja et al., 1991
2	171	CCA-TCA	Pro-Ser	adRP	Vaithinathan et al., 1994
2	171	CCA-CAA	Pro-Gln	adRP	Antinolo et al, 1994
2	174	GGC-AGC	Gly-Ser	RP	Fujiki et al., 1995
3	178	TAC-TGC	Tyr-Cys	adRP	Sung et al., 1991a
3	178	TAC-AAC	Tyr-Asn	adRP	Souied et al., 1994
3	180	CCC-GCC	Pro-Ala	adRP	Rodriguez J.A., unpup.
3	181	GAG-AAG	Glu-Lys	adRP	Dryja et al., 1991
3	182	GGC-AGC	Gly-Ser	adRP	Sheffield et al., 1991
3	186	TCG-CCG	Ser-Pro	adRP	Dryja et al., 1991
3	187	TGT-TAT	Cys-Tyr	adRP	Scott et al., 1993

3	188	GGA-AGA	Gly-Arg	adRP	Dryja et al., 1991
3	188	GGA-GAA	Gly-Glu	adRP	Macke et al., 1993
3	190	GAC-GGC	Asp-Gly	adRP	Sung et al., 1991a
3	190	GAC-AAC	Asp-Asn	adRP	Keen et al., 1991a
3	190	GAC-TAC	Asp-Tyr	adRP	Fishman et al., 1992
3	207	ATG-AGG	Met-Arg	adRP	Farrar et al., 1992
3	209	GTG-ATG	Val-Met	adRP	Macke et al., 1993
3	211	CAC-CCC	His-Pro	adRP	Keen et al., 1991a
3	211	CAC-CGC	His-Arg	adRP	Macke et al., 1993
3	216	ATG-AAG	Met-Lys	adRP	Al-Maghtheh et al., 1994
3	220	TTT-TGT	Phe-Cys	adRP	Bunge et al., 1993
3	222	TGC-CGC	Cys-Arg	adRP	Bunge et al., 1993
4	249	GAG-TAG	Glu-stop	arRP	Rosenfeld et al., 1992
4	267	CCC-CTC	Pro-Leu	adRP	Sheffield et al., 1991
4	267	CCT-CGT	Pro-Arg	adRP	Souied et al., 1994
4	292	GCG-GAG	Ala-Glu	CSNB	Dryja et al., 1993
4	296	AAG-GAG	Lys-Glu	adRP	Keen et al., 1991a
4	296	AAG-ATG	Lys-Met	adRP	Sullivan et al., 1993b
4	297	AGC-AGA	Ser-Arg	adRP	Souied et al., 1994
5	328	CTG-CCG	Leu-Pro	adRP	Rodriguez et al., 1993b
5	341	GAG-AAG	Glu-Lys	adRP	Scott et al., 1993
5	342	ACG-ATG	Thr-Met	adRP	Stone et al., 1993
5	344	CAG-TAG	Gln-stop	adRP	Sung et al., 1991a
5	345	GTG-ATG	Val-Met	adRP	Dryja et al., 1991
5	345	GTG-CTG	Val-Leu	adRP	Vaithinathan et al., 1994
5	347	CCG-CTG	Pro-Leu	adRP	Dryja et al., 1990b
5	347	CCG-TCG	Pro-Ser	adRP	Dryja et al., 1990b
5	347	CCG-CGG	Pro-Arg	adRP	Gal et al., 1991
5	347	CCG-CAG	Pro-Gln	adRP	Vaithinathan et al., 1994
5	347	CCG-GCG	Pro-Ala	adRP	Stone et al., 1993
5	347	CCG-ACG	Pro-Thr	adRP	Rodriguez et al., 1993b

B: Disease-causing insertions, deletions, and splice site mutations:

exon	codon	mutation	phenotype	reference
1	68-71	del: 68-71	adRP	Keen et al., 1991a
4	255/256	del: Ile	adRP	Inglehearn et al., 1991
4	264	del: Cys	adRP	Vaithinathan et al., 1994
-	intron 4	del: 30bp/inst:150bp	adRP	Al-Maghtheh et al., 1994
-	intron4 doner splice	G→T	arRP	Rosenfeld et al., 1995
-	intron4 acceptor splice	G→A	adRP	Rodriguez et al., unpub.
5	332	GAG→G--	adRP	Rodriguez et al., 1993b
5	340	ACG→A-G	adRP	Horn et al., 1992
5	340-348	del: 42bp	adRP	Restango et al., 1993
5	341-343	del: 8bp	adRP	Bunge et al., 1993

C: Non-disease causing polymorphisms:

Position	Nucleotide & a.a. change		Type	Reference
5'noncoding	296A→G	-	normal variant	Sung et al., 1991a
Codon 104	GTC→ATC	Val-Ile	normal variant	Macke et al., 1993
Intron 1	(CA)n	-	microsatellite	Weber et al., 1989
Codon 120	GGC→GGT	Gly-Gly	silent substitution	Bunge et al., 1993
Codon 146	TTC→TTT	Phe-Phe	silent substitution	Macke et al., 1993
Codon 160	ACC→ACT	Thr-Thr	silent substitution	Sung et al., 1991a
Codon 160	ACC→ACA	Thr-Thr	silent substitution	Reig et al., 1994
Codon 173	GCC→GCT	Ala-Ala	silent substitution	Dryja et al., 1991
Codon 186	TCG→TCA	Ser-Ser	silent substitution	Rosenfeld et al., 1992
Codon 244	CAG→CAA	Gln-Gln	silent substitution	Rosenfeld et al., 1992
Codon 248	AAG→AAA	Lys-Lys	silent substitution	Sung et al., 1991a
Codon 297	AGC→AGT	Ser-Ser	silent substitution	Rosenfeld et al., 1992
Intron 4	G→A	-	normal variant	Sung et al., 1991a
3' noncoding	C→A	-	normal variant	Sung et al., 1991a

Table 3.2:

Summary of rhodopsin mutation screens performed in adRP patients. Addition of studies 5 and 6 shows that even though both samples studied in this laboratory show the highest (study 5) and the lowest (study 6) frequencies of rhodopsin adRP, the percentage of total rhodopsin adRP detected in this laboratory does not significantly vary from that of other laboratories.

study no	no. of unrelated adRP patients	no. of patients with rho. mutations	% of rho. adRP to total cases	Mutation detection method	Ref.
1	150	43	29%	SSCP	(1)
2	161	39	20%	DGGE	(2)
3	34	8	25%	DGGE	(3)
4	59	11	18%	SSCP&D.S.	(4)
total(1)	404	101	25%	-	-
5	52	20	38%	H A or D.S.	(5)
6	80	7	9%	HA	(6)
5+6	132	27	20%	-	-
total(2)	**536**	**128**	**24%**	-	-

D.S.= Direct sequencing.

(1) Dryja et al., 1991.

(2) Sung et al., 1991.

(3) Sheffield et al., 1991.

(4) Souied et al., 1994.

(5) Inglehearn et al., 1992; Inglehearn et al., in preparation.

(6) This study

Total (1)=studies from other laboratories.

Total (2)=studies from other laboratories and this laboratory.

CHAPTER IV

TOTAL GENOME SEARCH FOR A NEW AUTOSOMAL DOMINANT RETINITIS PIGMENTOSA LOCUS IN FAMILY ADRP5

4.1 INTRODUCTION:

Retinitis pigmentosa (RP) is a clinically and genetically heterogenous group of retinal degenerations as disscussed in chapters 1 and 3. Autosomal dominant retinitis pigmentosa (adRP), a sub-group of RP, is itself heterogeneous. Before the beginning of this study, five adRP loci had already been identified, and a sixth locus had been implied by exclusion of all known loci (Rhodopsin, peripherin/rds, 8cen, 7p, 7q) in an adRP family called ADRP5. All previously known adRP loci were mapped by linkage analysis. The aim of this study was to use the same method to map the adRP disease gene in family ADRP5.

4.2 LINKAGE ANALYSIS:

The genetic material of humans exists in linear arrays of thousands of genes along 23 pairs of homologous units known as chromosomes which are found in the nucleus of the cell. During meiotic cell division homologous chromosome pairs, each consisting of two chromatids, are aligned side by side in the centre of the cell. During this alignment DNA segments are exchanged between chromatids of homologous chromosomes. This process, which results in recombinant chromosomes, is known as crossing over. Only homologous regions of chromosomes are exchanged such that each chromosome has the same set of genetic loci. Though in a diploid cell each copy of the same chromosome come from a different parent, they are more than 99% identical in DNA sequence. Nevertheless, each copy contains many small variations the sum of which gives each individual a unique genetic makeup. Thus the formation in the germ line cells of a single chromosome derived from segments of each of the parental copies (as a result of the crossover events) passes on a unique assortment of genes to the next generation.

During this jumbling up process, crossover events, or recombinations, are more likely to occur between genes or loci which are far apart. Distant loci or loci on different chromosomes are considered to have 50% recombination rate as such loci tend to segregate independently. The closer two loci are on a particular chromosome the less the likelihood of a recombination event between them; for tightly linked loci the recombination fraction tends to minimize towards zero. Hence, the relative distances (known as genetic distances) between genes or loci can be assessed by determining the frequency of recombination events between them. These distances are measured in map units which are referred to as 'centi-Morgans' (cM), where 1 cM is equal to a 1% chance of recombination between two loci during a meiotic event; on average this distance is approximately 10^6 bp (Ott, 1991).

In order to detect these recombination events, loci which are polymorphic (i.e., commonest allele frequency is <99%) are necessary to score segregation of genetic material in families. Such analysis capitalizes on such loci, known as genetic markers (see section 4.3), to detect crossover events and so assess whether they segregate with less than 50% recombination. Such markers are then said to be genetically linked, hence the term "linkage analysis". Disease gene mapping by linkage analysis employs the use of a large number of polymorphic DNA markers of known localizations (see section 4.4) in a random search throughout the genome in a particular family that segregates the disease or trait of interest. The purpose of such a search is to detect linkage between the disease locus, represented by the disease phenotype, and a known marker in its vicinity; in other words, each of the affected individuals has to physically inherit a genomic region (piece of DNA) containing the defective gene from his or her affected parent. This region should also contain other markers which are physically and genetically linked to the disease gene. Establishing such segregation of a known marker locus with the disease phenotype will infer linkage between the two loci and therefore localizes the disease gene to the region where the marker maps.

Estimates of the likelihood of recombination between a disease locus and a random marker are used to infer linkage or non-linkage between two loci (Morton, 1955). The *odds ratio* is the ratio of the probability of observing a segregation pattern of two loci if they are linked at a given recombination value, called theta (Θ) where $\Theta<0.5$, versus the probability of such segregation if they are not linked ($\Theta=0.5$) (probability of linkage versus non-linkage); this ratio is calculated at a series of recombination values (from $\Theta=0$ to $\Theta=0.5$). The logarithm of the odds ratio, called log of the odds or *lod score* (Z), is used to report linkage results. These

calculations can be summarized in the following equation

$$Z(\Theta)=\log_{10}[L(\Theta)/L(0.5)]$$

where:

$L(\Theta)$= the likelihood that a certain set of observed family segregation data can be obtained if the two loci are linked at a Θ value.

$L(0.5)$= the likelihood of observing such data if the two loci are not linked.

The recombination value (Θ) that gives the maximum lod score ($\hat{Z}$) is the best estimate of the degree of linkage between the two loci. Positive lod scores suggest the presence of linkage, whereas negative lod scores indicate linkage is less likely. By convention a positive lod score ($\hat{Z}$) of 3 (equivalent to an odds ratio of 1000:1 of linkage versus nonlinkage) or higher is accepted as a proof of linkage. Similarly a negative lod score of -2 at a given Θ value is accepted as an evidence against linkage within an interval equal to Θ from both sides of the marker locus. Lod scores between -2 and 3 are considered as inconclusive linkage results. In this likelihood method of linkage analysis, a precise mode of inheritance has to be specified. Misrepresentation of the mode of inheritance may mask an existing linkage, or lead to spurious evidence for linkage.

4.2.1 Interference and Map functions:

Crossing over events between adjacent intervals on a chromosome do not occur independently, that is occurrence of a new crossover seems to be suppressed in the immediate vicinity of an existing crossover; this non-independence is called *interference*. *Map distance* is a term referred to genetic distance, which is proportional to the recombination frequency (Θ) between two loci, and need not correlate with physical distance. Map distance is not additive for substantial Θ values (greater than >0.10) as a result of the possibility of multiple crossovers between two loci. When the occurrence of multiple crossovers can be excluded then the map distance between two loci is simply equal to Θ. A function that relates recombination fraction Θ to map distance is called *mapping function*; several mapping functions were formulated which translate recombination frequency (in percent) into map distance (in cM). The Haldane map function (1919) takes into account the possibility of multiple crossovers between two loci assuming there is no interference. On the other hand, the Kosambi map function (1944), which makes a particular assumption on interference, has been widely used in human genetic calculations since it appears to produce more realistic map distance values than does Haldane's

formula. In addition to these two, many other map functions were derived to take into account various mechanisms of interference (Ott, 1991).

4.2.2 Penetrance:

Penetrance represents the probability that the phenotype is expressed for a given genotype. Both genetic and environmental factors are believed to contribute to incomplete penetrance of a particular trait. For some genetic traits, for example Huntington disease, penetrance is described as age dependent since such traits are not expressed at birth and develop only later in life. Another factor that may influence the penetrance of a trait is sex. Penetrance is also used to incorporate quantitative phenotypes, such as blood cholesterol levels or level of creatine kinase in DMD female carriers, into linkage analysis. The effect of such covariates is generally taken into account by forming covariate classes, and for each such class, defining an appropriate set of penetrances, for example, age classes or male-female classes. In simple cases penetrances are either 0 or 1; for many diseases, however, intermediate values of penetrance do occur. The adRP phenotype in family ADRP5 described in this thesis shows an example of such incomplete penetrance (see section 4.7.1).

4.2.3 Support interval:

In human linkage analysis the accuracy of the estimate of maximum likelihood Θ ($\hat{\Theta}$) is assessed by constructing a specific support interval. The *'1-unit-down'* method defines a support interval as Θ values of $\hat{Z}$-1 to $\hat{Z}$ (Conneally *et al.*, 1985). As recommended by the above method, the $\hat{Z}$-1 support interval is obtained by drawing a horizontal line at 1 unit of lod below $\hat{Z}$ provided that $\hat{Z} \geq 3$. The points of intersection of this line with the lod score curve when projected on the Θ axis, mark the end point Θ values of the support interval.

4.2.4 Exclusion maps:

All values of Θ at which $\hat{Z} < -2$ are said to be definitely excluded (Ott, 1991). This concept is used in defining regions of exclusions in the process of mapping a disease gene by testing it against various genetic markers, and accordingly defining exclusion intervals around each marker locus. The excluded regions relative to the total genome is known as the exclusion map (fig 4.3).

4.2.5 Multipoint analysis:

Multipoint linkage analysis generally refers to the simultaneous analysis of more than 2

genetic loci where the order of loci and the phenotype of each individual is not necessarily known for each locus. However, in conventional disease gene mapping, multipoint is particularly used to position an unknown disease locus in relation to several genetic markers, with known order and genetic distances. Multipoint analysis adds up the informativeness of various partially informative markers to obtain more significant lod score results from a particular set of segregation data (see section 4.6).

4.3 MARKERS USED IN LINKAGE ANALYSIS:

4.3.1 RFLP and minisatellite markers:

In the past linkage studies were performed using blood group and other biochemical (protein) polymorphisms. These polymorphisms are detected in the gene product rather than the gene itself, and cover a modest fraction of the genome. In 1980 restriction fragment length polymorphisms (RFLP) emerged as an abundant supply of polymorphic genetic markers at the DNA level (Botstein *et al.*, 1980). These are polymorphisms found in the human genome as a result of sequence variation between individuals that creates or eliminates a restriction enzyme site. Variable number of tandem repeat polymorphisms (VNTRs), also known as minisatellites, are another type of DNA polymorphisms which are due to variation in the number of head to tail repeats, usually > 10 bp, at a given locus (Jeffreys *et al.*, 1985). *Heterozygosity* is directly proportional to the number of alleles each marker exhibits and the frequency of each allele in the general population. It takes the value between 0 and 1, and reflects the degree of informativeness, and therefore the usefullness of a genetic marker for linkage studies. VNTRs have the advantage of being multiallelic, and therefore have higher heterozygosity values, compared to diallelic RFLPs. On the other hand, RFLPs are more evenly distributed than VNTRs which tend to aggregate towards telomeric regions of chromosomes. Both RFLPs and VNTRs are mainly detected by southern blotting and hybridization (Southern *et al.*, 1975).

4.3.2 Microsatellite markers:

Microsatellites are length polymorphisms of the human genome that are present in the form of a variable number of repeated blocks of a simple DNA motif at a given locus. Interspersed DNA elements of the form $(CA)_n.(GT)_n$ constitute one of the most abundant human repetitive DNA families (Weber and May; 1989; Litt and Luty, 1989). With the exception of $A_n.T_n$ multimers, $(CA)_n.(GT)_n$, or simply $(CA)_n$, repeats are the most frequent simple sequence repeats of the human genome; on average they occur every 30 kbp (Beckman and Weber, 1992) and

distributed equally in the 5'- and 3'-untranslated and intronic regions of genes. Microsatellites also include other simple repeat motifs such as AAAN, AAN and AG repeats, in decreasing order of abundance. These microsatellites, together with A_n and $(CA)_n$ repeats, constitute 76% of total repeats in the human genome (Beckmann and Weber, 1992). Other relatively abundant tri- and tetranucleotide repeats do exist in the human genome which also constitute an important class of human genetic markers (see section 8.1).

Compared to RFLPs and VNTRs, microsatellites and particularly $(CA)_n$ repeats, which have been used in this study, are far more abundant and evenly distributed throughout the genome. They can be simply detected by PCR analysis from few nanograms of DNA (compared to the microgram range required for Southern blot), and separation on an acrylamide gel, a quicker and simpler protocol than Southern blotting. Furthermore, microsatellites are multiallelic (e.g. in this study markers were found to have up to 12 alleles), therefore exhibit higher levels of heterozygosity.

4.4 GENETIC MAPS:

CEPH families:

The availability of a common reference pedigree collection from the Centre d'Etude du Polymorphisme Humain (CEPH) in Paris is considered to be an important aspect in the development of genetic maps. This centre provides DNA from a set of reference pedigrees to collaborating laboratories, maintains a genotype database, and sponsors the construction of consortium linkage maps (Dausset *et al.*, 1990).

4.4.1 NIH/CEPH map:

Total genome searches were greatly facilitated by the publication of a comprehensive genetic linkage map of the human genome by the NIH/CEPH collaborative linkage mapping group (1992) which contains 1676 polymorphic systems. In addition to newly identified, this map contains markers from several previous genome maps (for example, Donis-Keller *et al.*, 1987). Most of these markers are of the RFLP and VNTR types and a proportion (339) are PCRable markers.

4.4.2 Genethon map:

Shortly after the publication of the NIH/CEPH map, Genethon group published the second

generation linkage map of the human genome (Weissenbach *et al.*, 1992). The construction of this map was based on the segregation analysis of 814 newly characterized $(CA)_n$ microsatellite markers in the CEPH families; the mean heterozygosity of these markers was close to 0.75. The NIH/CEPH chromosome maps frequently extend slightly beyond the Genethon maps; the Genethon map is estimated to cover 90% of the NIH/CEPH map. This discrepancy between the two maps, which varies from chromosome to chromosome, might be attributable to the heterogeneous set of data used to construct the NIH/CEPH map compared to the homogeneous data set used to construct the Genethon map. More recently this map has been further expanded to contain an extra 1267 new $(CA)_n$ microsatellite markers (Gyapay *et al.*, 1994). The current Genethon human linkage map is therefore composed of more than 2066 $(CA)_n$ polymorphic loci, of which 60% have a heterozygosity of over 0.7.

4.5 AUTOMATED MICROSATELLITE DETECTION:

The use of microsatellite markers has been further simplified by fluorescent labelling and automated detection and sizing of PCR products (Ziegle *et al.*, 1992) using an ABI sequencer. Three distinct fluorescent dyes can be used to uniquely label PCR products that overlap in size. A fourth dye is used to label an internal lane size standard. This increases by three fold the number of markers that can be analyzed simultaneously. In other words, with the use of both size and dye multiplexing it is possible to run as many as 15 microsatellite markers in one lane (Ziegle *et al.*, 1992). Moreover, the use of the internal lane size standard helps overcoming the problem of lane to lane variation during gel running. Combinations of sets of markers that can be multiplexed simultaneously, and which cover most of the human genome, are now available from several resources (Human Genome Mapping Project resource centre (HGMP), UK; Levitt *et al.*, 1994). After the automated collection and analysis of genotype data, programs are available to prepare and process this data as input files for the linkage program. These advances in the methodology of microsatellite genotyping should provide speed and accuracy in mapping and analysing human disease genes.

4.6 LINKAGE ANALYSIS SOFTWARE:

LIPED (Ott, 1974) and LINKAGE (Lathrop and Lalouel., 1984) are the two most widely used programmes for disease gene mapping. As input, they take files from Linksys (Attwood and Bryant, 1988) or Preplink (family data and marker data), and calculate the likelihoods of

such data. The LIPED programme is designed for the analysis of two loci while the LINKAGE package is an integrated system of programmes designed to perform linkage analysis and genetic risk calculations for an arbitrary number of loci. LINKAGE programs include MLINK, which is used to calculate lod score tables and risk analysis, ILINK which is the iterative version of MLINK and finds maximum likelihood estimates of linkage between two loci, and LINKMAP which is used to perform multipoint analysis and calculation of location scores. LINKMAP assumes a fixed map of markers and calculates likelihoods for a new locus at various specified points in each interval along the known map. FASTMAP (Curtis and Gurling, 1993) is a programme which does multipoint simulation analysis using multiple two point lod scores. This programme is particularly useful for large linkage jobs where use of LINKMAP is not possible due to limitations on the number of markers and number of alleles for each marker. FASTMAP implements an algorithm to provide an approximate multipoint lod score for the disease against a number of markers. It takes as input two point lod scores from these markers and produces a graph of estimated multipoint lod scores. MAPFUN is a programme which calculates map distances from recombination fractions and vice versa using various map functions. CRI-MAP and MAPMAKER are widely used in construction of multilocus linkage maps. However these programs require simple three generation families as input data, and are therefore rarely used in disease gene mapping. In addition, a large collection of other programmes are available from the HGMP menu, which are designed to be used with varying sets of parameters and for more specific linkage requirements.

4.7 RESULTS:

4.7.1 Clinical assessment and DNA samples:

Members of ADRP5 (fig 4.1) who agreed to participate in the study were examined by clinicians at Moorfields Eye Hospital in London. Blood samples were collected from family members including affected individuals, their normal spouses and normal first degree relatives. DNA was extracted as described in Materials and Methods. All affected individuals were examined and their disease status was confirmed.

Autosomal dominant mode of inheritance was ascertained in ADRP5. Clinically, the phenotype in this family is of type II/R (Massof and Finkelstein, 1981; Lyness *et al.*, 1985). Another important characteristic of the adRP phenotype in this family is incomplete penetrance; asymptomatic obligate carriers, who are identified by having both affected parent and affected

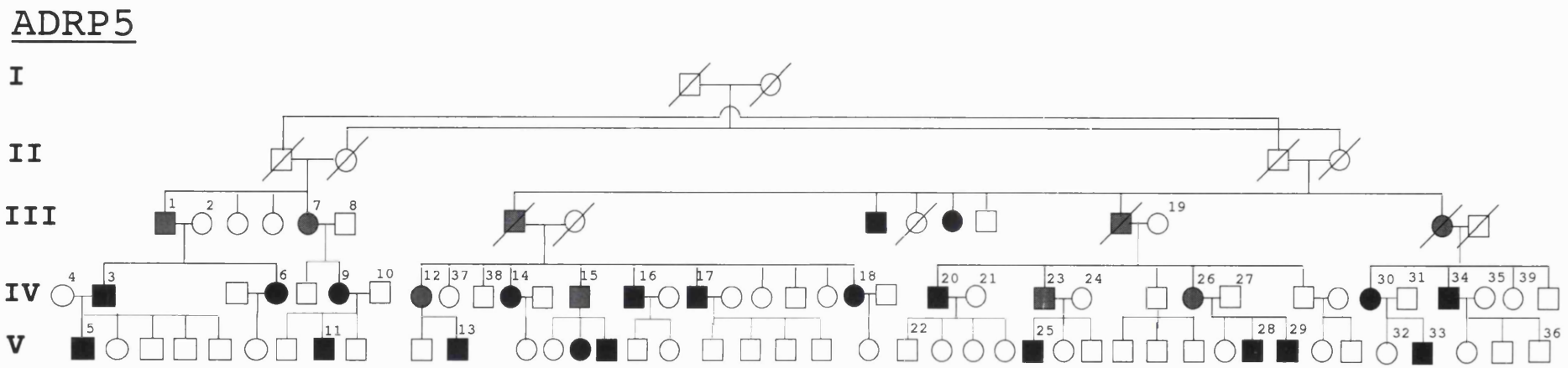

Figure 4.1:

Pedigree of ADRP5 family:

normal male and female symbols respectively.

affected members.

individuals who are known to be obligate disease gene carriers.

(Crossed symbols represent deceased family members).
Symbols numbered 1-39 represent family members
included in the total genome search, they also correspond to
lanes 1-39 in figure 5.1.

offspring, are almost indistinguishable from normal individuals and they remain asymptomatic for their entire lives. On the other hand, all symptomatic individuals had night blindness by their teens, and develop a severe form of the disease (Moore *et al.*, 1993; see section 6.3.3 for more clinical details).

Normal individuals were excluded from the linkage study to avoid misclassification of asymptomatic disease gene carriers who are either very young and have not yet developed the disease symptoms, or who are examples of incomplete penetrance which characterizes the phenotype in this family. As some of the affected individuals were not available for the study (fig 4.1: III-7, III-13, III-15) four of their normal children (fig 4.1: IV-9, IV-10, IV-26, IV-35) were included in the linkage panel to infer parental genotypes. However, the phenotypes of these normal individuals were not included in the linkage calculations.

4.7.2 Previous linkage studies of ADRP5:

ADRP5 and ADRP7 are two large families that both have type II/R phenotype with incomplete penetrance. A linkage study to map the adRP gene(s) in these families was started earlier in this laboratory. After exclusion of all adRP candidate loci (rhodopsin, peripherin/RDS, 8cen), a genome wide search was started. In this search 15 RFLP markers, 20 VNTRs, 15 blood group markers, and around 100 $(CA)_n$ and other microsatellite markers were genotyped in both families (data not shown). The above linkage study ended with mapping of the disease locus in ADRP7 to chromosome 7p13-15.1 (Inglehearn *et al.*, 1993) and exclusion of around 25% of the genome in ADRP5. Later, another adRP disease locus was mapped to chromosome 7q in a Spanish adRP family (Jordan *et al.*, 1993).

This study aimed to carry on the mapping of the disease gene in ADRP5 from the point where previous study ended. This work involved exclusion of the new 7p locus (the region of the new 7q locus was included in the 25% already excluded) followed by a total genome linkage search.

4.7.3 Selection of microsatellite markers:

Most of the markers used in the previous linkage study, which excluded ADRP5 disease locus from 25% of the genome, were present in the NIH/CEPH map. To continue the linkage search (after exclusion of the 7p locus) using the more informative Genethon markers, these exclusions had to be related to the Genethon map. Despite the use of anchor markers which

relate the two maps, construction of an exclusion map (fig 4.3) proved to be difficult. Previous exclusions were conservatively underestimated as some regions, particularly telomeric, were expanded on one map relative to the other. Based on this exclusion map, more than 150 $(CA)_n$ markers were selected to cover the unexcluded regions. These markers were selected at intervals of $\Theta=0.15$-0.25 between adjacent loci (fig 4.3). Where possible the markers were selected to have a heterozygosity value of 0.7 or more. However in some intervals such markers were not available, so markers with lower heterozygosity values were used. All markers were amplified using flanking primers in multiplex PCR reactions of two markers that could be size separated.

4.7.4 Reading of genotypes:

Genotypes were recorded independently from the family data, and transferred to the family pedigree where Mendelian segregation was confirmed. Genotyping inconsistencies were resolved by going back to the autoradiograph and rescoring the alleles. If such inconsistencies were not due to misscoring of alleles, these genotypes were not included in the linkage calculations, provided that such loci were likely to be excluded, otherwise the reaction was repeated. Misscoring of alleles where it occurs, is usually the result of spurious bands that are frequently seen accompanying $(CA)_n$ marker alleles. Each allele is represented by a ladder of bands (fig 5.1), which are believed to result from mechanisms such as strand slippage (Richards and Sutherland, 1994; Kunkel *et al.*, 1993) and the terminal transferase activity of Taq DNA polymerase (Clark, 1988). Although they normally have a unique pattern which can be easily distinguished, quite often these products could have an unusual pattern and cause scoring problems. Most often these problems were resolved by confirmation of Mendelian segregation in the family. Inconsistencies which were not due to misscoring were interpreted as new mutations. Both misscoring and new mutations were very rare. Similarly, misscoring of alleles or new mutations which were consistant with Mendelian segregation were thought to be very rare and should not significantly affect the data. Tube mix up or non-paternity were excluded from previous studies performed on the family.

4.7.5 Linkage analysis:

Pairwise linkage analysis was performed between disease phenotype in ADRP5 and various marker loci using the Linksys data management (Attwood and Bryant, 1988) and the two point analysis program MLINK from the LINKAGE package version 5.1 (Lathrop and Lalouel, 1984). Allele frequencies were estimated from 14 unrelated spouses within the family. This gives a more reliable value since it estimates frequencies in the gene pool from which the family

has come. Occasionally these frequencies were found to be significantly different from the published ones, but most of the time they were similar. Quite frequently new rarer unpublished alleles were seen in the family. Lod scores were calculated assuming an autosomal dominant mode of inheritance. Complete penetrance was also assumed since affected individuals only were used in the analysis.

4.7.6 Exclusion of the 7p locus:

The disease locus in ADRP7 (RP9) has been mapped to chromosome 7p13-15.1 (Inglehearn *et al.*, 1993). Linkage was established with $(CA)_n$ markers D7S460 and D7S435 (Hudson *et al.*, 1992; Mishra *et al.*, 1992). Since ADRP5 has a similar phenotype to ADRP7, 7p locus was a strong candidate and therefore should be excluded before starting a total genome search. Markers D7S435, D7S460, the original 7p linked markers were not fully informative in ADRP5. D7S460 gave an exclusion of 3 cM, while D7S435 gave inconclusive two point linkage results (table 4.1). With the use of more markers (Weissenbach *et al.*, 1992) in ADRP7, the locus was refined between markers D7S526 and D7S484 (Inglehearn *et al.*, 1994; fig 4.2). These markers were also not fully informative in ADRP5. D7S526 gave a poor exclusion of 1 cM while D7S484 gave a lod score of 1.1 ($\Theta=0.05$) (table 4.1). Another marker, D7S485 maps 8 cM centromeric to D7S484, and gave an exclusion of 10 cM. However, this alone is not sufficient to exclude the RP9 locus. Multipoint analysis of the disease phenotype with markers D7S435, D7S526, D7S484 and D7S460 was therefore carried out. This gave a lod score ($\hat{Z}$) of -6.7 in the RP9 interval. This clearly excludes the region from containing the disease locus for ADRP5 (fig 4.2).

4.7.7 Total genome search:

A total of 138 $(CA)_n$ markers (table 4.1) were genotyped in ADRP5. The majority of markers were moderately informative and gave exclusions, based on Θ values for which the lod score was <-2 (Ott, 1991), in the range of 5-15cM. Nineteen markers (14%) were informative enough to give exclusions of more than 15cM, on the other hand, 29 (21%) were poorly informative and gave exclusions of <5cM. In total, these markers excluded around 60% of the total genome (fig 4.3).

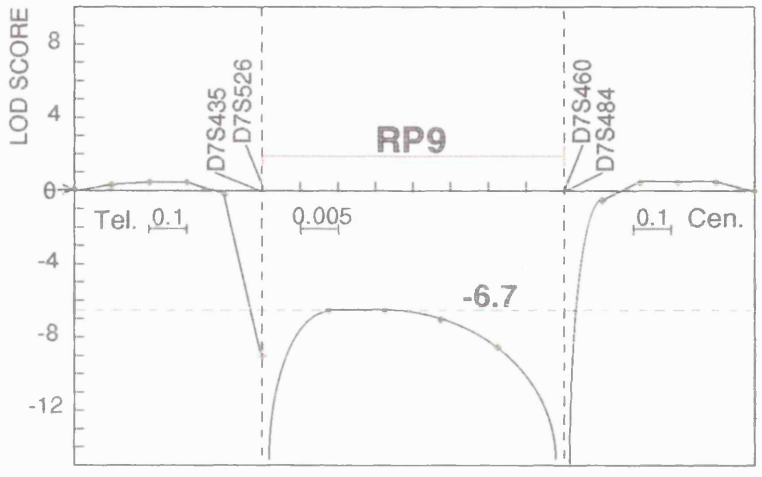

Figure 4.2

Multipoint linkage analysis of ADRP5 phenotype and markers flanking RP9 locus on chromosome 7p13. Maximum lod score of -6.7 indicates exclusion of ADRP5 locus from the RP9 interval (marked by red line).

4.8 DISCUSSION:

4.8.1 NIH/CEPH versus Genethon markers:

In total over 280 markers were genotyped in ADRP5 throughout the autosomal genome. These include around 150 markers previously genotyped and on a conservative estimate excluded less than 25% of the genome. On the other hand, 138 $(CA)_n$ markers (table 4.1) used in this study have excluded over 60% of the genome. This difference in the amount of exclusion between the two sets of markers reflects the degree of informativeness, or usefulness for linkage analysis, of each set. The first marker set used in the previous study included 15 RFLP markers, 20 VNTRs, 15 blood group markers, and around 100 $(CA)_n$ and other microsatellites; while the recent study used the newly identified Genethon $(CA)_n$ markers. As mentioned earlier (see section 4.3.2), RFLPs and VNTRs are less informative than microsatellite markers. Moreover, the microsatellite markers used in the previous study were the early markers isolated in the process of gene sequencing, and often they were uninformative compared to the Genethon markers which were specifically selectd for their high heterozygosities (most of them have heterozygosity values of 0.7 or more). The overall exclusion obtained by both sets of markers was in excess of 80% of the total genome with 5% overlapping exclusions. An exclusion map for ADRP5 (fig 4.3) was built according to the Genethon chromosomal linkage map; whenever a discrepancy arose in assigning previous exclusions to the map, due to expansion of one map relative to the other, exclusions were considered relative to the expanded map to avoid over estimation of excluded intervals.

4.8.2 Linkage analysis using affected pedigree members only:

In general linkage analysis can be hindered by uncertainty in some genetic parameters, such as expected age of onset, or penetrance. In ADRP5 the phenotype is characterized by incomplete penetrance (Moore *et al.*, 1993). To overcome this problem, individuals with definite disease were considered as affected and other individuals as phenotype unknown (except spouses). To do this the family size should be sufficiently large to allow exclusion of normal individuals from linkage calculations and still obtain significant lod scores. In ADRP5 using affected members only was sufficient to give significant exclusions with the majority of moderately informative genetic markers (table 4.1).

4.8.3 Assigning allele frequencies to markers:

Most current linkage searches make use of the highly polymorphic microsatellite markers. Assigning correct allele frequencies for those markers may be extremely difficult in a particular

study population. Designation of erroneous frequencies or assuming that frequencies of all alleles are equal may result in false evidence for linkage as well as in failure to detect true linkage (Knowls *et al.*, 1992; Ott, 1992). These effects are most pronounced in small pedigrees, and pedigrees with key individuals unavailable for genotyping, particularly in multigeneration families where genotypes of the top generations are to be inferred by the linkage program. This is exactly the case in ADRP5 where most of the individuals in the top three generations are not available, which creates relatively large strings of inferred genotypes. In this case, segregation of the disease phenotype with a common allele will greatly reduce the significance of linkage since the LINKAGE program will consider it more likely that this allele, instead of being the same allele in each branch, could have come to the family from the normal population pool through spouses of affected individuals. This will, therefore, reduce the significance of a true linkage, or even mask linkage if the family size is too small. On the other hand by falsely assuming lower frequency of a common allele that segregates with the disease, a false linkage will be concluded since the program will give very little significance to the fact that this allele could have come to affected individuals from their normal parent. To overcome this problem in ADRP5 allele frequencies were calculated from 28 chromosomes of spouses, who are assumed to be unrelated to the family, but are the best match to that particular population.

Table 4.1:
Lod score tables of markers genotyped in family ADRP5. Lod scores of $\Theta=0$ are not included in the table since the use of affected only individuals with complete penetrance will give a lod score of $-\infty$ at $\Theta=0$ once a cross over is seen in the family. Exclusions were based on lod scores <-2. Whenever $\Theta\leq 0.1$ exclusions (cM) were assumed to be equivalent to Θ. For $\Theta>0.1$ the Kosambi mapping function was used to estimate map distance or the exclusion interval from genetic distance (see section 4.2.1).

Θ	0.01	0.05	0.10	0.20	0.30	0.40	$\Theta_{[-2]}$	excl.$_{(cm)}$
Chromosome 1:								
D1S198	-9.59	-4.34	-2.33	-0.76	-0.19	-0.00	0.10	10
D1S208	-6.46	-3.12	-1.80	-0.71	-0.26	-0.06	0.08	8
D1S235	-9.91	-4.66	-2.67	-1.12	-0.53	-0.24	0.10	10
D1S236	-9.96	-4.94	-2.96	-1.38	-0.69	-0.26	0.13	13
D1S248	-6.55	-3.27	-2.02	-0.96	-0.43	-0.13	0.10	10
D1S252	-11.8	-6.60	-4.26	-1.91	-0.76	-0.19	0.18	19
D1S304	-7.60	-3.86	-2.38	-1.16	-0.62	-0.28	0.11	11
D1S305	-12.1	-6.06	-3.71	-1.69	-0.77	-0.31	0.15	15
Chromosome 2:								
D2S111	-12.1	-6.13	-3.67	-1.41	-0.40	0.00	0.12	12
D2S117	-4.12	-2.22	-1.54	-0.92	-0.53	-0.25	0.05	5
D2S119	-11.7	-5.13	-2.59	-0.57	0.12	0.23	0.12	12
D2S125	-10.2	-5.13	-2.86	-0.99	-0.26	-0.01	0.12	12
D2S126	-9.78	-6.02	-3.98	-1.94	-0.89	-0.30	0.19	20
D2S144	-16.0	-8.42	-5.70	-2.80	-1.33	-0.49	0.23	25
D2S150	-10.9	-5.17	-2.87	-1.00	-0.26	0.02	0.12	12
D2S162	-8.53	-3.60	-1.68	-0.27	0.09	0.05	0.08	8
D2S176	-1.80	-0.61	-0.24	-0.05	-0.01	0.01	0.00	0
D2S206	-3.53	-1.62	-0.78	-0.20	-0.06	-0.03	0.03	3
Chromosome 3:								
D3S1262	-1.72	-0.38	0.15	0.47	0.43	0.25	-	0
D3S1283	-7.49	-3.17	-1.45	-0.13	0.27	0.26	0.08	8
D3S1285	-2.01	-1.30	-0.98	-0.63	-0.40	-0.20	0.01	1
D3S1289	-12.5	-6.93	-4.30	-1.85	-0.75	-0.21	0.17	18
D3S1291	-8.79	-4.29	-2.39	-0.79	-0.17	-0.03	0.10	10
D3S1302	-5.07	-2.28	-0.85	0.26	0.50	0.36	0.05	5
D3S1304	-12.4	-6.25	-3.65	-1.44	-0.49	-0.07	0.16	17
Chromosome 4:								
D4S394	-8.12	-3.79	-2.05	-0.66	-0.13	0.06	0.10	10
D4S395	-6.99	-2.74	-1.10	0.06	0.32	0.24	0.06	6
D4S397	-4.62	-2.23	-1.38	-0.72	-0.26	-0.01	0.05	5
D4S407	-6.98	-3.32	-1.42	0.15	0.58	0.45	0.06	6
D4S408	-4.47	-2.17	-1.18	-0.31	0.05	0.12	0.05	5
D4S413	-6.93	-2.98	-1.27	0.08	0.45	0.37	0.06	6
D4S425	-5.81	-2.00	-0.68	0.12	0.18	0.07	0.05	5
D4S622	-4.23	-1.87	-0.96	-0.29	-0.08	0.00	0.04	4

Chromosome 5:								
D5S412	-12.2	-6.42	-4.07	-1.96	-0.95	-0.37	0.19	20
D5S414	-18.4	-9.86	-6.31	-3.11	-1.54	-0.61	0.25	27
D5S416	-7.66	-3.80	-2.34	-1.14	-0.63	-0.31	0.10	10
D5S421	-11.2	-5.84	-3.60	-1.60	-0.66	-0.19	0.14	14
D5S426	-11.1	-5.75	-3.44	-1.48	-0.63	-0.20	0.14	14
D5S431	-0.53	0.00	0.11	0.09	0.03	0.00	-	0
Chromosome 6:								
D6S264	-11.3	-6.03	-3.75	-1.69	-0.73	-0.23	0.15	15
D6S268	-5.11	-2.42	-1.26	-0.26	0.04	0.05	0.05	5
D6S282	-5.47	-2.23	-1.01	-0.09	0.19	0.18	0.05	5
D6S286	-9.65	-5.39	-3.45	-1.60	-0.68	-0.20	0.14	14
D6S290	-6.53	-3.21	-1.93	-0.86	-0.40	-0.17	0.09	9
D6S292	-10.0	-4.31	-2.04	-0.26	0.28	0.26	0.10	10
Chromosome 7:								
D7S483	-16.0	-8.51	-5.47	-2.74	-1.38	-0.56	0.22	24
D7S435*	-0.94	-0.37	-0.19	-0.10	-0.05	-0.02	-	0
D72526	-2.28	-0.48	0.07	0.30	0.23	0.09	0.01	1
D7S460*	-3.80	-1.35	-0.40	0.23	0.32	0.20	0.03	3
D7S484	0.66	1.10	1.09	0.83	0.52	0.24	-	0
D7S485	-7.06	-3.57	-2.11	-0.94	-0.48	-0.22	0.10	10
Chromosome 8:								
D8S256	-8.16	-3.50	-1.86	-0.30	0.24	0.29	0.08	8
D8S258	-11.5	-6.15	-3.97	-1.97	-0.96	-0.37	0.19	20
D8S260	-12.1	-6.14	-3.91	-1.88	-0.86	-0.30	0.17	18
D8S270	-4.53	-2.66	-1.80	-1.05	-0.63	-0.29	0.07	7
D8S277	-3.88	-1.71	-0.77	-0.08	0.10	0.10	0.04	4
Chromosome 9:								
D9S158	-6.97	-2.43	-0.79	0.33	0.46	0.17	0.05	5
D9S160	-11.6	-6.03	-3.73	-1.67	-0.67	-0.17	0.12	12
D9S162	-8.71	-4.11	-2.32	-0.86	-0.29	-0.07	0.10	10
D9S168	-2.49	-0.66	-0.08	0.20	0.17	0.08	0.01	1
D9S175	-5.44	-1.82	-0.46	0.41	0.49	0.28	0.03	3
D9S195	-8.71	-4.28	-2.53	-1.03	-0.33	-0.03	0.10	10
D9S196	-6.26	-2.79	-1.35	-0.24	0.10	0.14	0.06	6
Chromosome 10:								
D10S189	-6.81	-2.97	-1.61	-0.66	-0.36	-0.18	0.06	6
D10S191	-11.8	-6.45	-4.16	-2.08	-1.02	-0.41	0.20	21
D10S195	-5.06	-1.32	0.00	0.78	0.72	0.34	0.03	3
D10S196	-6.61	-2.73	-1.29	-0.26	-0.02	-0.02	0.06	6
D10S197	-5.59	-2.37	-1.19	-0.34	-0.09	-0.02	0.05	5
D10S209	-2.08	-0.87	-0.46	-0.18	-0.07	-0.02	0.01	1
D10S212	-6.78	-2.25	-0.62	0.48	0.62	0.36	0.05	5
D10S215	-4.88	-2.77	-1.55	-0.39	-0.01	0.07	0.06	6
D10S217	-7.16	-3.23	-1.75	-0.60	-0.21	-0.08	0.07	7
D10S222	-6.19	-2.94	-1.69	-0.70	-0.28	-0.07	0.06	6
D10S249	-7.73	-4.52	-2.79	-1.18	-0.51	-0.18	0.13	13

Chromosome 11:								
D11S901	-12.4	-5.99	-3.42	-1.30	-0.44	-0.08	0.15	15
D11S905	-10.6	-5.04	-2.52	-0.50	0.03	0.11	0.11	11
D11S907	-5.73	-2.31	-0.93	0.04	0.25	0.19	0.05	5
D11S925	-5.73	-2.31	-0.93	0.04	0.25	0.19	0.05	5
D11S928	-5.38	-2.54	-1.28	-0.26	0.01	-0.01	0.06	6
D11S932	-6.28	-2.95	-1.55	-0.45	-0.05	0.07	0.07	7
Chromosome 12:								
D12S76	-14.9	-8.18	-5.24	-2.53	-1.17	-0.40	0.21	22
D12S89	-7.64	-4.03	-2.56	-1.25	-0.67	-0.33	0.12	12
D12S92	-9.04	-4.06	-2.09	-0.53	0.03	0.16	0.10	10
D12S95	-7.25	-3.62	-2.15	-0.91	-0.36	-0.13	0.02	10
D12S99	-3.76	-1.19	-0.30	0.26	0.30	0.17	0.03	3
D12S103	-3.69	-1.50	-0.65	-0.07	0.06	0.06	0.02	2
Chromosome 13:								
D13S152	-3.81	-1.31	-0.47	0.04	0.14	0.10	0.02	2
D13S160	-5.26	-2.29	-1.10	-0.22	0.04	0.05	0.05	5
D13S171	-6.35	-3.08	-1.84	-0.82	-0.38	-0.14	0.07	7
D13S173	-8.59	-3.95	-2.14	-0.70	-0.17	0.00	0.10	10
D13S174	-4.47	-1.60	-0.46	0.29	0.38	0.21	0.02	2
D13S175	-4.00	-1.52	-0.66	-0.07	0.05	0.03	0.02	2
D13S217	-9.38	-4.58	-2.63	-1.03	-0.41	-0.14	0.11	11
D13S218	-7.85	-3.83	-2.25	-0.91	-0.35	0.10	0.10	10
Chromosome 14:								
D14S62	-7.83	-3.69	-2.03	-0.71	-0.19	0.00	0.10	10
D14S64	-13.0	-6.32	-3.67	-1.42	-0.50	-0.12	0.13	13
D14S66	-3.97	-2.03	-1.29	-0.66	-0.34	-0.13	0.05	5
D14S68	-10.4	-5.14	-3.03	-1.22	-0.45	-0.11	0.12	12
D14S70	-9.73	-4.47	-2.47	-0.87	-0.24	-0.01	0.10	10
D14S72	-13.0	-6.34	-3.71	-1.45	-0.47	-0.05	0.12	12
D14S77	-5.04	-1.86	-0.73	0.01	0.13	0.06	0.04	4
D14S78	-7.37	-3.96	-2.24	-0.76	-0.18	0.01	0.10	10
Chromosome 15:								
D15S117	-6.37	-3.47	-1.93	-0.62	-0.12	0.04	0.09	9
D15S118	-5.37	-1.59	-0.29	0.46	0.41	0.15	0.03	3
D15S120	-10.1	-5.60	-3.77	-2.15	-1.28	-0.60	0.20	21
D15S124	-3.45	-1.51	-0.80	-0.26	-0.08	-0.02	0.02	2
D15S127	-4.95	-1.90	-0.75	0.12	0.27	0.15	0.03	3
D15S130	-8.61	-3.99	-2.21	-0.78	-0.24	-0.04	0.10	10
D15S165	-7.13	-3.15	-1.60	-0.37	0.06	0.14	0.07	7
Chromosome 16:								
D16S408	-10.3	-4.83	-2.56	-0.70	0.00	0.17	0.12	12
D16S413	-10.9	-5.32	-2.99	-1.03	-0.22	0.07	0.14	14
D16S414	-9.02	-4.56	-2.77	-1.25	-0.56	-0.20	0.14	14
D16S422	-7.44	-3.52	-1.93	-0.56	-0.02	0.12	0.09	9
Chromosome 17:								
D17S784	-13.9	-7.12	-4.29	-1.86	-0.78	-0.23	0.17	18
D17S789	-5.53	-2.41	-1.14	-0.22	0.02	0.00	0.03	3
D17S790	-10.1	-5.22	-3.18	-1.42	-0.62	-0.21	0.13	13

D17S796	-12.5	-7.01	-4.38	-1.87	-0.73	-0.19	0.17	18
D17S849	-5.09	-1.94	-0.86	-0.20	-0.08	-0.05	0.04	4
Chromosome 18:								
D18S53	-9.21	-4.75	-3.05	-1.47	-0.62	-0.17	0.13	13
D18S54	-6.72	-2.86	-1.46	-0.45	-0.13	-0.02	0.07	7
D18S58	-7.80	-3.15	-1.28	0.07	0.04	0.32	0.07	7
D18S62	-5.48	-2.26	-1.09	-0.27	-0.04	-0.00	0.05	5
D18S64	-5.83	-2.57	-1.38	-0.49	-0.17	-0.02	0.06	6
D18S72	-1.66	-0.45	-0.05	0.18	0.18	0.11	-	0
Chromosome 19:								
D19S216	-10.8	-5.43	-3.30	-1.48	-0.67	-0.24	0.16	17
D19S225	-9.53	-4.72	-2.76	-1.04	-0.31	-0.04	0.13	13
D19S211	-5.81	-1.95	-0.57	0.32	0.39	0.13	0.04	4
D19S49*	-9.31	-4.73	-2.99	-1.42	-0.56	-0.13	0.13	13
D19S47*	-4.82	-2.50	-1.54	-0.68	-0.28	-0.09	0.07	7
Chromosome 20:								
D20S95	-15.1	-8.78	-5.82	-2.91	-1.43	-0.55	0.22	24
D20S100	-8.86	-4.26	-2.53	-1.12	-0.52	-0.19	0.12	12
D20S105	-10.2	-5.21	-3.90	-1.77	-0.74	-0.21	0.16	17
D20S110	-11.2	-6.17	-3.24	-1.65	-0.91	-0.39	0.15	15
Chromosome 21:								
D21S261	0.27	0.22	0.16	0.08	0.04	0.01	-	0
D21S265	-6.33	-3.13	-1.69	-0.52	-0.09	0.04	0.08	8
Chromosome 22:								
D22S278	-10.0	-5.46	-3.20	-1.25	-0.43	-0.08	0.14	14
D22S282	-12.9	-6.86	-4.39	-2.07	-0.92	-0.30	0.20	21
D22S315	-8.52	-3.91	-2.17	-0.79	-0.27	-0.06	0.10	10

*Not Genethon markers.

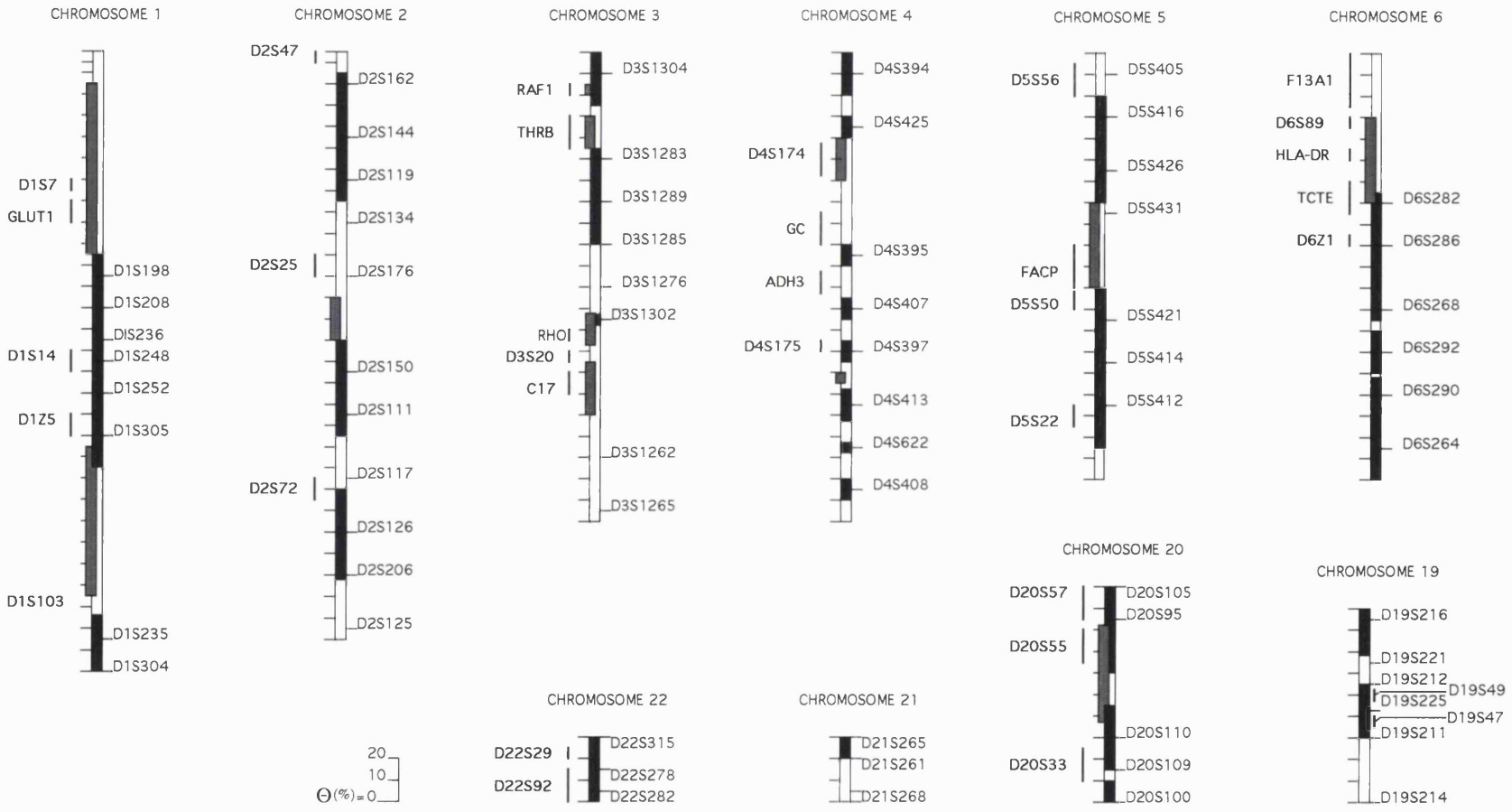

Figure 4.3

Diagramatic representation of the genomic regions that had been excluded in ADRP5 before mapping of the disease gene. Regions that had been previously excluded are reperesented by shaded blocks, while regions that have been excluded in this study (table 4.1) are represented by solid blocks. Anchor markers which were used to relate the two genome maps (NIH / CEPH, 1992; Weissenbach et al., 1992) are presented to the left of each chromosomal diagram.

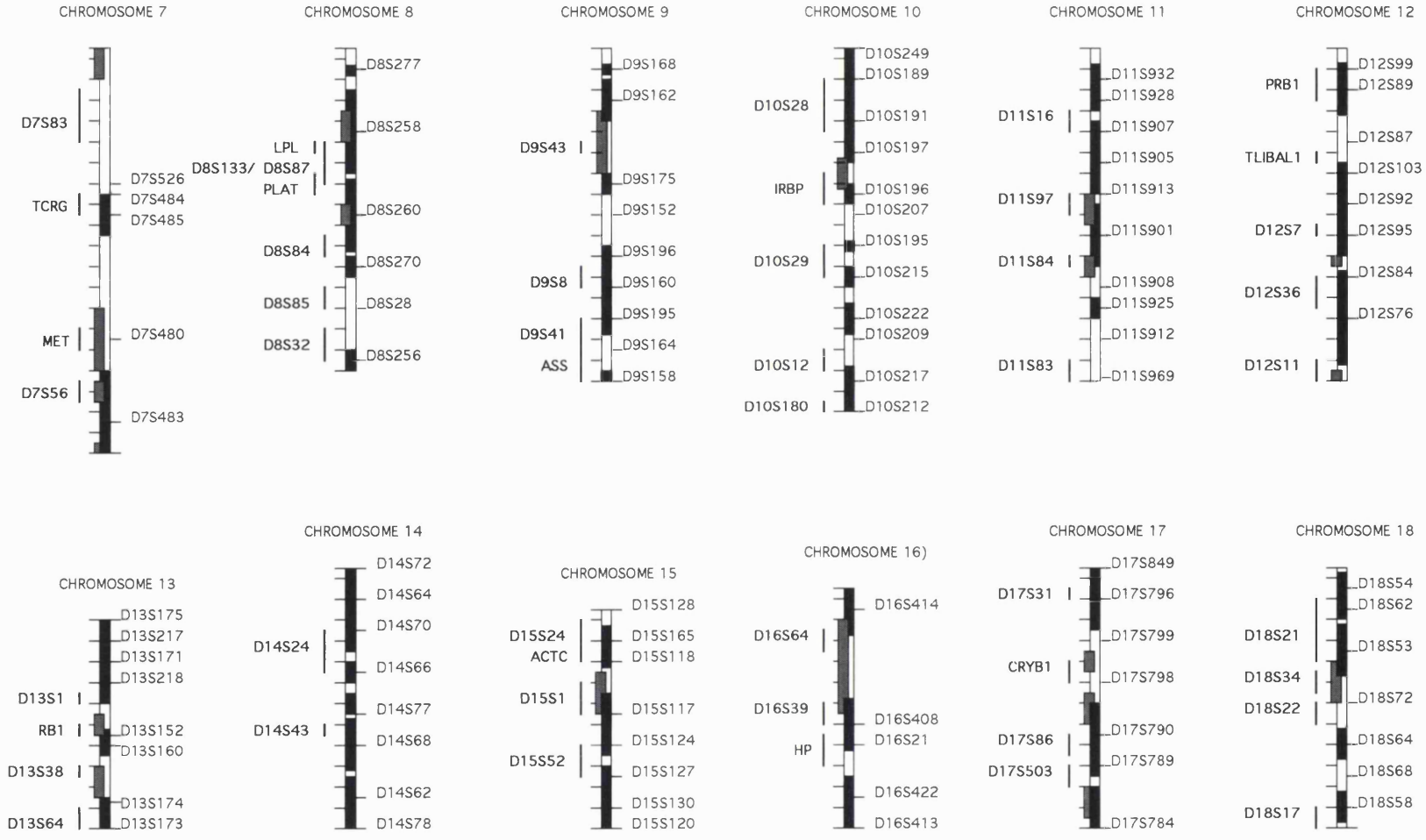
CHROMOSOME 7
D7S83
D7S526
D7S484
TCRG
D7S485
MET
D7S480
D7S56
D7S483
CHROMOSOME 8
D8S277
LPL
D8S133/ D8S87
PLAT
D8S258
D8S260
D8S84
D8S270
D8S85
D8S28
D8S32
D8S256
CHROMOSOME 9
D9S168
D9S162
D9S43
D9S175
D9S152
D9S196
D9S8
D9S160
D9S195
D9S41
D9S164
ASS
D9S158
CHROMOSOME 10
D10S249
D10S189
D10S28
D10S191
D10S197
IRBP
D10S196
D10S207
D10S195
D10S29
D10S215
D10S222
D10S209
D10S12
D10S217
D10S180
D10S212
CHROMOSOME 11
D11S932
D11S928
D11S16
D11S907
D11S905
D11S913
D11S97
D11S901
D11S84
D11S908
D11S925
D11S912
D11S83
D11S969
CHROMOSOME 12
D12S99
PRB1
D12S89
D12S87
TLIBAL1
D12S103
D12S92
D12S7
D12S95
D12S84
D12S36
D12S76
D12S11
CHROMOSOME 13
D13S175
D13S217
D13S171
D13S218
D13S1
RB1
D13S152
D13S160
D13S38
D13S174
D13S64
D13S173
CHROMOSOME 14
D14S72
D14S64
D14S70
D14S24
D14S66
D14S77
D14S43
D14S68
D14S62
D14S78
CHROMOSOME 15
D15S128
D15S24
D15S165
ACTC
D15S118
D15S1
D15S117
D15S124
D15S52
D15S127
D15S130
D15S120
CHROMOSOME 16)
D16S414
D16S64
D16S408
D16S39
D16S21
HP
D16S422
D16S413
CHROMOSOME 17
D17S849
D17S31
D17S796
D17S799
CRYB1
D17S798
D17S790
D17S86
D17S789
D17S503
D17S784
CHROMOSOME 18
D18S54
D18S62
D18S21
D18S53
D18S34
D18S72
D18S22
D18S64
D18S68
D18S58
D18S17

CHAPTER V

MAPPING OF ADRP5 PHENOTYPE TO CHROMOSOME 19q13.4

5.1 INTRODUCTION:

After exclusion of more than three quarters of the genome (chapter 4) the adRP locus in ADRP5 was mapped to the telomeric region of chromosome 19 long arm (19q13.4). Significant linkage was established between the disease phenotype and chromosome 19 markers D19S214 (Weissenbach *et al.*, 1992) and D19S180 (CEPH/NIH, 1992). Crossover analysis showed that the adRP locus maps in the estimated 22 cM interval between these two markers. This confirmed the existence of a new adRP locus which was inferred earlier by exclusion of another family from the five previously known adRP loci (Kumar-Singh *et al.*, 1993).

5.2 RESULTS:

5.2.1 Estimation of penetrance:

So far all linkage analyses (chapter IV) were performed in the family using affected individuals only. In an attempt to obtain more representative and significant linkage estimates, and after preliminary linkage was established, a few normal family members were incorporated into the analysis. To overcome the possibility of late onset of disease, only normal individuals who were over 40 years of age and have normal offspring (individuals III-3, III-4, IV-5, IV-9, IV-10, IV-20, IV-27, and IV-36 in figure 5.4) were incorporated in the linkage study. However, since normal obligate disease gene carriers remain asymptomatic for the rest of their lives (incomplete penetrance), a penetrance factor should be incorporated into the analysis.

Penetrance is simply defined as the proportion of affected individuals among susceptible disease gene carriers (see 4.2.2). In a rare dominant disease (such as adRP) only one parent is expected to carry the disease allele and that parent may or may not be affected. On average, half of the offspring will receive the disease allele, and of these a proportion f, depending on the degree of penetrance, will develop the disease. The proportion of affected offspring will be $P_A = 1/2\, f$, and so $f = 2P_A$ (Ott, 1991). Therefore penetrance (f) can be estimated by finding the proportion of affecteds among offspring of affected or obligate gene carrier parents. Penetrance

was estimated in ADRP5 as 0.7 by counting 12 affected family members among 35 offspring of both affected and obligate gene carriers. Younger family members (generation V in figure 5.4) were not incorporated in the calculation as they may develop the disease later. Therefore a penetrance value of 0.7 and normal individuals who are described above were used in all subsequent lod score calculations.

5.2.2 Linkage of ADRP5 to 19q13.4:

The disease phenotype in ADRP5 was mapped to chromosome 19q13.4 region. Particular alleles of markers D19S214 and D19S180 were found to segregate with the disease phenotype in the family (fig 5.1, 5.4). Two point analysis between D19S214 and the adRP phenotype gave a maximum lod score ($\hat{Z}$) of 4.92 at $\hat{\Theta}=0.06$ (*one-lod-down* support interval from $\Theta=0.01$ to 0.20). This marker was mapped to the telomeric region of chromosome 19 on the Genethon map (Weissenbach *et al.*, 1992). Similar analysis with D19S180, the most telomeric marker on the CEPH/NIH (1992), gave a $\hat{Z}$ of 4.35 at $\hat{\Theta}=0.04$ (*one-lod-down* support interval from $\Theta=0.01$ to 0.19) (table 5.1). Crossover analysis mapped the adRP locus between these two markers, a region estimated in ADRP5 and other families from this laboratory (since the two markers were from two different maps) to be 22 cM. This new adRP locus has been given the locus symbol RP11 (MIM 600138).

5.2.3 Exclusion of the CRD locus:

By the time linkage was found in ADRP5, another retinal degeneration locus for cone rod dystrophy (CRD) had been mapped to 19q13.3-13.4 (Evans *et al.*, 1993). This locus has since been refined to a 5 cM interval flanked by markers D19S219 and D19S246, both centromeric to D19S180. Thus by haplotype data alone it is clear that the two disease loci cannot be allelic. Two point analysis with D19S219 and D19S246 excluded the adRP locus from the immediate vicinity of each marker (table 5.1). Multipoint analysis of both CRD flanking markers and disease phenotype in ADRP5 clearly confirm the exclusion of the adRP locus ($\hat{Z}=-6.5$) from the whole CRD-containing interval (fig 5.2b). A pentrance value of 0.7 was again used in these analyses. This exclusion, together with haplotype analysis in both ADRP5 (see section 5.2.6) and the CRD family, confirm the localization of two retinal degeneration loci (CRD and adRP), separated by approximately 15 cM, to chromosome 19q13.3-13.4.

5.2.4 Genotyping more markers in the family:

Soon after mapping the RP11 locus to chromosome 19q13.4, more $(CA)_n$ markers which

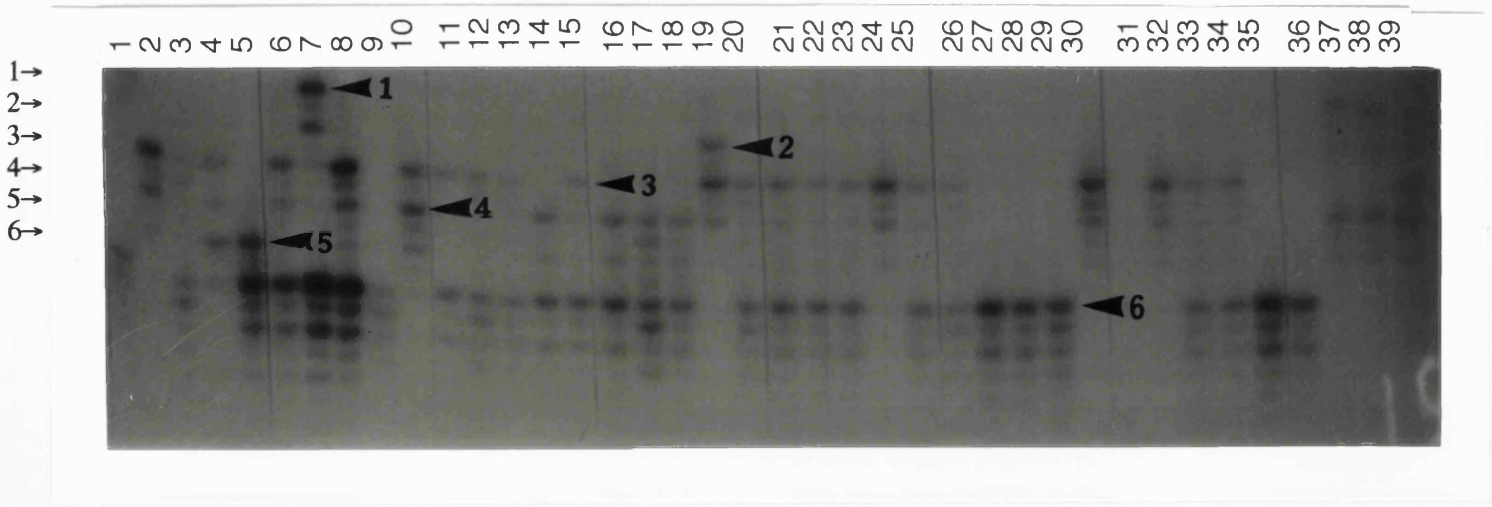

Figure 5.1:

Autoradiograph of marker D19S180 showing segregation of allele 6 of this marker with phenotype in affected members of ADRP5. Lanes 1-39 correspond to individuals numbered from 1-39 on top of each individual symbol in figure 4.1.

map to that interval, were isolated (Gyapay *et al.*, 1994 and personal commmunication). Lod scores of pairwise linkage analyses between the ADRP5 phenotype and these markers are shown in table 5.1. Four markers, D19S572, PRKCG, AFMc001yb1, and D19S418, showed very tight linkage to the disease locus, giving pairwise lod scores of 7.3, 5.7, 7.7, and 5.9 respectively, with no recombination indicating close linkage. The tetranucleotide microsatellite D19S254 (Weber *et al.*, 1993) was found to be genetically indistinguishable from D19S214 in ADRP5. In another study, this marker was also found to be very close genetically to the most distal markers found by Genethon including D19S210, D19S214 and D19S218 (Weber *et al.*, 1993; Weissenbach *et al.*, 1993). KLK and D19S180, the proximal flanking markers, and D19S254 were cytogentically mapped to 19q13.4 (Weber *et al.*, 1993), which indicate the cytogenetic localization of RP11 to 19q13.4 region.

5.2.5 Multipoint analysis:

LINKMAP:

Given the size and structure of the family, the number of markers, and the number of alleles per marker, true multipoint analysis with all marker systems was impossible with the available computing memory. Therefore, multiple three point analyses with two markers and the disease phenotype were performed (fig 5.2). Using the program LINKMAP from the computing package LINKAGE version 5.1 (Lathrop and Lalouel, 1984) this analysis was performed twice, once with markers D19S219, D19S571, D19S572, AFMc001yb1, D19S418, AFMb005wh1, and D19S214 (figure 5.2a) from the Genethon map using published recombination fractions (Gyapay *et al.*, 1994 and personal communication) (fig 5.2a), and a second time with markers D19S219, D19S246, KLK, D19S571, D19S180, D19S572, PRKCG, AFMc001yb1, and D19S254 (fig 5.2b) from various chromosome 19 maps (Gyapay *et al.*, 1994; NIH/CEPH, 1992; Weber *et al.*, 1993). Recombination fractions between markers in the second analysis were estimated using ILINK program from the LINKAGE package (fig 5.2b). Both sets of analyses confirm the initial localization of the disease between D19S180 and D19S214. Maximum lod scores of 9.1 and 9.3 were obtained, in the first (fig 5.2a) and second (fig 5.2b) analyses respectively, both with markers D19S572 and AFMc001yb1 at $\Theta=0$ from AFMc001yb1.

FASTMAP:

FASTMAP is a multipoint simulation programme which uses two point lod score data as its input (Curtis and Gurling, 1993; see 4.6). FASTMAP was used on ADRP5 two point lod

Table 5.1:

Two point lod scores between 19q13.4 markers (shown in order from proximal to distal) and disease phenotype in ADRP5. a: Lod scores were calculated at a disease penetrance of 0.7, assuming sex average recombination fractions. Maximum lod scores are highlighted (bold face). b: Lod scores calculated at a penetrance value of 0.6 and sex average.

a:

Marker	$\Theta=0$	0.01	0.05	0.1	0.2	0.3	0.4	Z_{max}	Θ_{max}
D19S219	-13.0	-4.40	-0.80	0.52	**1.32**	1.27	0.79	**1.32**	0.20
D19S246	-7.90	-3.50	-1.40	-0.43	0.23	**0.33**	0.20	**0.33**	0.30
KLK	-1.40	0.43	0.96	**1.05**	0.89	0.58	0.25	**1.05**	0.10
D19S571	3.06	4.98	5.16	4.81	3.82	2.72	1.43	**5.20**	0.03
D19S180	1.99	4.06	4.34	4.08	3.16	1.98	0.64	**4.35**	0.04
D19S572	**7.31**	7.19	6.71	6.07	4.67	3.09	1.37	**7.31**	0.00
PRKCG	**5.71**	5.62	5.23	4.72	3.62	2.41	1.12	**5.71**	0.00
AFMc001ybl	**7.67**	7.54	7.00	6.30	4.80	3.15	1.40	**7.67**	0.00
D19S418	**5.91**	5.81	5.40	4.86	3.72	2.46	1.08	**5.91**	0.00
AFMb005wh1	0.98	3.86	4.14	3.90	3.05	2.00	0.87	**4.15**	0.04
D19S404	-1.60	2.15	3.62	**3.86**	3.36	2.36	1.12	**3.86**	0.10
D19S210	-1.60	0.24	**0.79**	0.89	0.79	0.56	0.29	**0.79**	0.05
D19S214	-0.60	4.03	4.89	4.81	3.94	2.67	1.18	**4.92**	0.06
D19S254	-0.80	2.88	4.34	**4.55**	3.98	2.88	1.49	**4.55**	0.10
D19S218	-0.85	1.12	**1.66**	1.61	1.23	0.78	0.37	**1.66**	0.06

b:

Marker	$\Theta=0$	0.01	0.05	0.1	0.2	0.3	0.4	Z_{max}	Θ_{max}
D19S180	2.07	3.97	4.23	3.97	3.06	1.90	0.61	**4.24**	0.04
AFMb005wh1	1.04	3.64	3.93	3.71	2.90	1.89	0.82	**3.94**	0.04

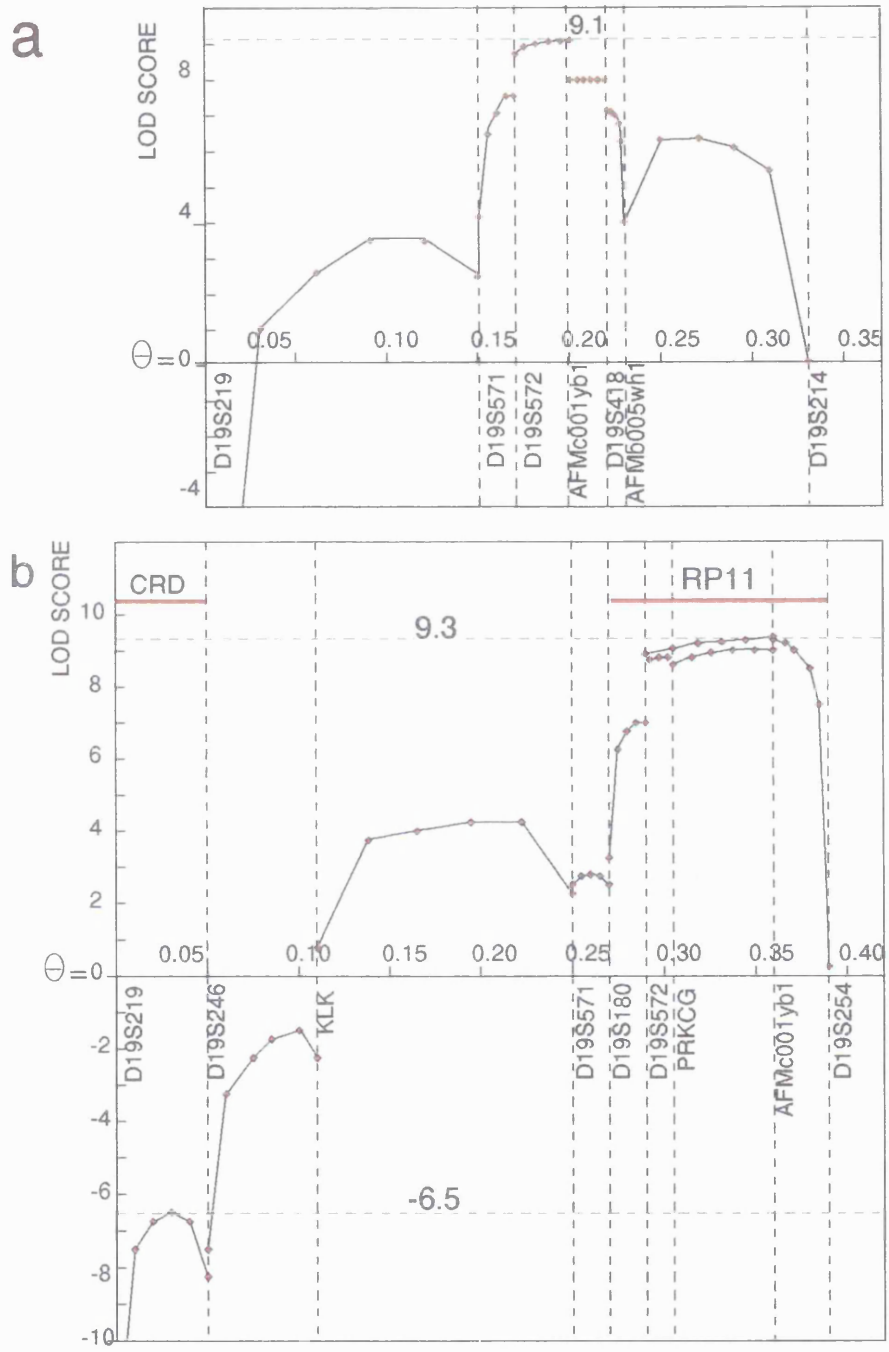

Figure 5.2

Multiple 3-point analysis between marker pairs and disease phenotype in ADRP5 using a: Genethon markers with published recombination fractions (Gyapay et al., 1994), and b: a set of markers from both genetic maps (Gyapay et al., 1994 & CEPH/NIH, 1992) with recombination fractions as calculated by the ILINK program from the LINKAGE package 5.1, assuming sex equal recombination. Figure also shows the exclusion of the RP11 locus from the CRD interval.

score data shown in table 5.1a. Using the Genethon markers (D19S219, D19S571, D19S572, AFMc001yb1, D19S418, AFMb005wh1, and D19S214) this analysis gave a lod score ($\hat{Z}$) of 10.6 (fig 5.3). The *one-lod-down* support interval showed a disease gene localization between D19S572 and AFMb005wh1.

5.2.6 Haplotype analysis:

All 15 markers (table 5.1) were haplotyped in ADRP5 (fig 5.4). The disease locus was flanked by two inferred recombination events between marker and phenotype which possibly took place in individuals III-15 and III-7 with markers D19S180 and AFMb005wh1 respectively (fig 5.4). The interval flanked by these two markers is estimated to be 8 cM according to the Genethon map. This haplotype analysis clearly exclude the RP11 locus from the CRD containing interval (between D19S219 and D19S246).

5.3 DISCUSSION:

5.3.1 Linkage and haplotype analyses in ADRP5, and exclusion of the CRD locus:

The two point lod scores obtained in ADRP5 (table 5.1) together with haplotype (crossover) analysis (fig 5.4), demonstrated the localization of the adRP gene to the interval between D19S180 and AFMb005wh1 (see fig 6.2). According to published data, this interval is estimated to be 8cM (Gyapay *et al*, 1994, and personal communication). Most of the markers within the disease interval (D19S572, PRKCG, AFMc001yb1, D19S418) were almost fully informative. The maximum lod scores obtained with these markers (table 5.1) do not necessarily indicate the disease gene localization within that interval since all these markers were not recombinant with the disease phenotype. Lod score variations within this interval simply reflect variation in the degree of informativeness of each marker in the family. Multipoint linkage should give a comprehensive and simultaneous analysis with data obtained from several marker systems, therefore, localizing the disease gene relative to an interval rather than to a series of single map points. However, a true multipoint was not possible with all the markers for reasons described earlier (section 5.2.5). In this particular case, multipoint linkage analysis was not crucial for the localization of the disease gene or to obtain any further statistical significance for the data. However, a series of multiple 3-point analyses were performed for successive combinations of two markers and disease in the region (fig 5.2). This analysis further supported the localization of the adRP gene to the same interval indicated by two point and haplotype analysis. FASTMAP analysis of the data in ADRP5 gave a maximum lod score within the same interval indicated by previous linkage and haplotype analysis, thus supporting the afore

Figure 5.3:

FASTMAP analysis of 19q13.4 markers in ADRP5. Recombination fractions between markers are as published (Gyapay et al., 1994).

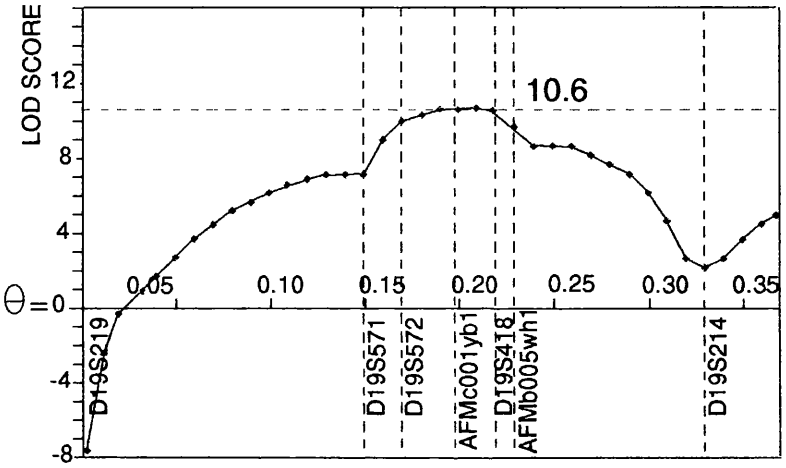

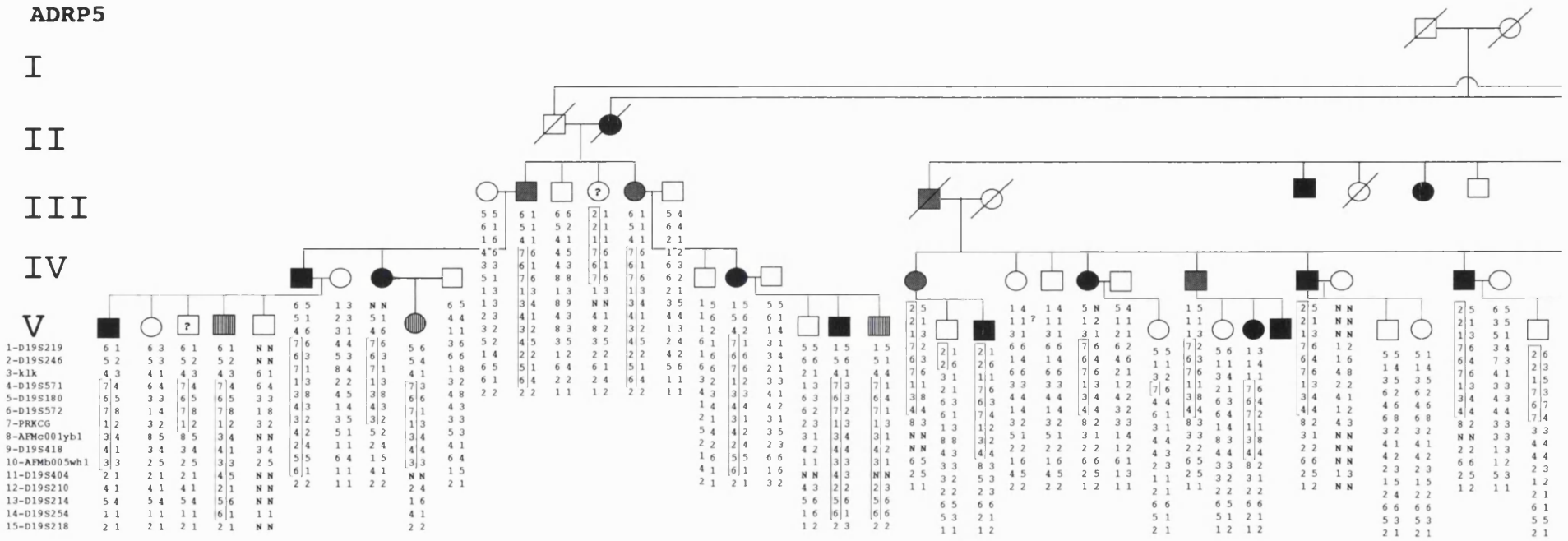

Figure 5.4:

Haplotype analysis of 15 markers from the 19q13.4 in ADRP5, the disease haplotype is boxed.

□ ○ normal male and female symbols respectively.

■ ● affected symbols.

▩ ◍ obligate disease gene carriers.

▨ ◍ disease haplotype carriers.

[?] (?) not known if normal or disease haplotype carriers since recombination break point took place within the RP11 interval.

N N Genotype not known.

(Crossed symbols represent deceased family members).

Fgure 5.4(contd)

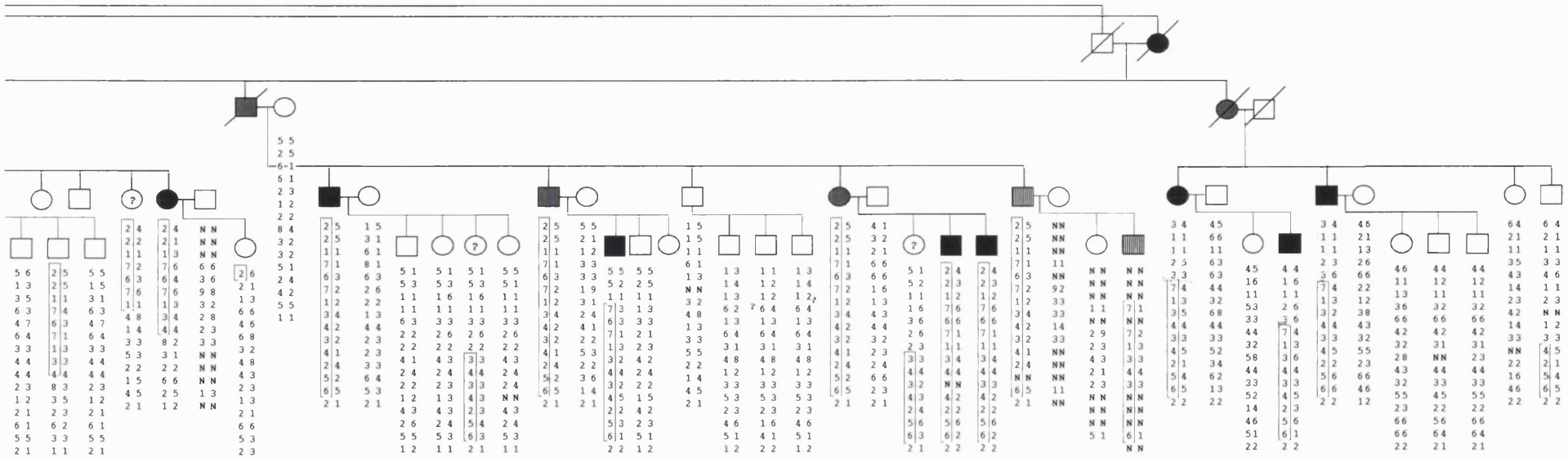

mentioned localization.

Genotyping of the 15 markers from 19q region in the whole family (fig 5.4) allowed the identification of the haplotype associated with the disease phenotype. Knowing the disease haplotype allowed identification of most of the disease gene carriers from younger generations of ADRP5 (fig 5.4). This resulted in a more accurate estimation of the disease penetrance (see section 5.2.1) and a better understanding of the clinical phenotype in the family. Thus informed genetic counselling is now available for most family members. Affected individuals can be given a clearer picture of the expected progression of the disease, while the risk of recurrence in their children can be accurately estimated as 30% (based on penetrance value, see section 5.3.2) rather than 50%. Similarly asymptomatic gene carriers over the age of 30 years will probably remain unaffected for the rest of their lives, though once again their children will be at a 30% risk of showing symptoms of RP.

Double recombinants within an estimated interval of 33cM between markers D19S219 and D19S218 were not detected in more than 90 meiosis in ADRP5, which indicates meiotic recombination interference within that region. These results support the findings of a previous study (Weber *et al.*, 1993) which demonstrated evidence of meiotic recombination interference (see section 4.2.1) through the construction of a short tandem repeat polymorphism linkage map of chromosome 19. In addition, their data showed regional differences between male and female recombination frequencies. Male recombination frequencies, indicated by map distance, were higher at the telomeric regions, while recombination in female meiosis was higher in centromeric regions (fig 5.5). In ADRP5 recombination fractions of 0.26 and 0.13 were found in males and females respectively between D19S180 (proximal) and D19S254 (distal). On the other hand, Θ values of 0.06 and 0.34 were estimated between D19S180 and D19S219 (a more proximal interval) for males and females respectively. This is in agreement with the above mentioned study and further demonstrated regional variation in the male and female recombination fractions. However this is not expected to affect the previous linkage conclusions obtained with ADRP5 assuming sex average recombination. To demonstrate this, various three point lod score analyses were repeated assuming sex specific recombination fractions as described in Weber *et al.*, 1993 (fig 5.5). These analyses did not show any significant difference between sex specific lod scores and lod scores calculated assuming sex average recombination. For example, 3-point analysis with markers D19S572 and AFMc001yb1 gave a maximum lod score of 9.1 compared to 9.3 obtained with sex average recombination (fig 5.2b).

Figure 5.5:

(Figure and legend are from Weber et al., 1993)

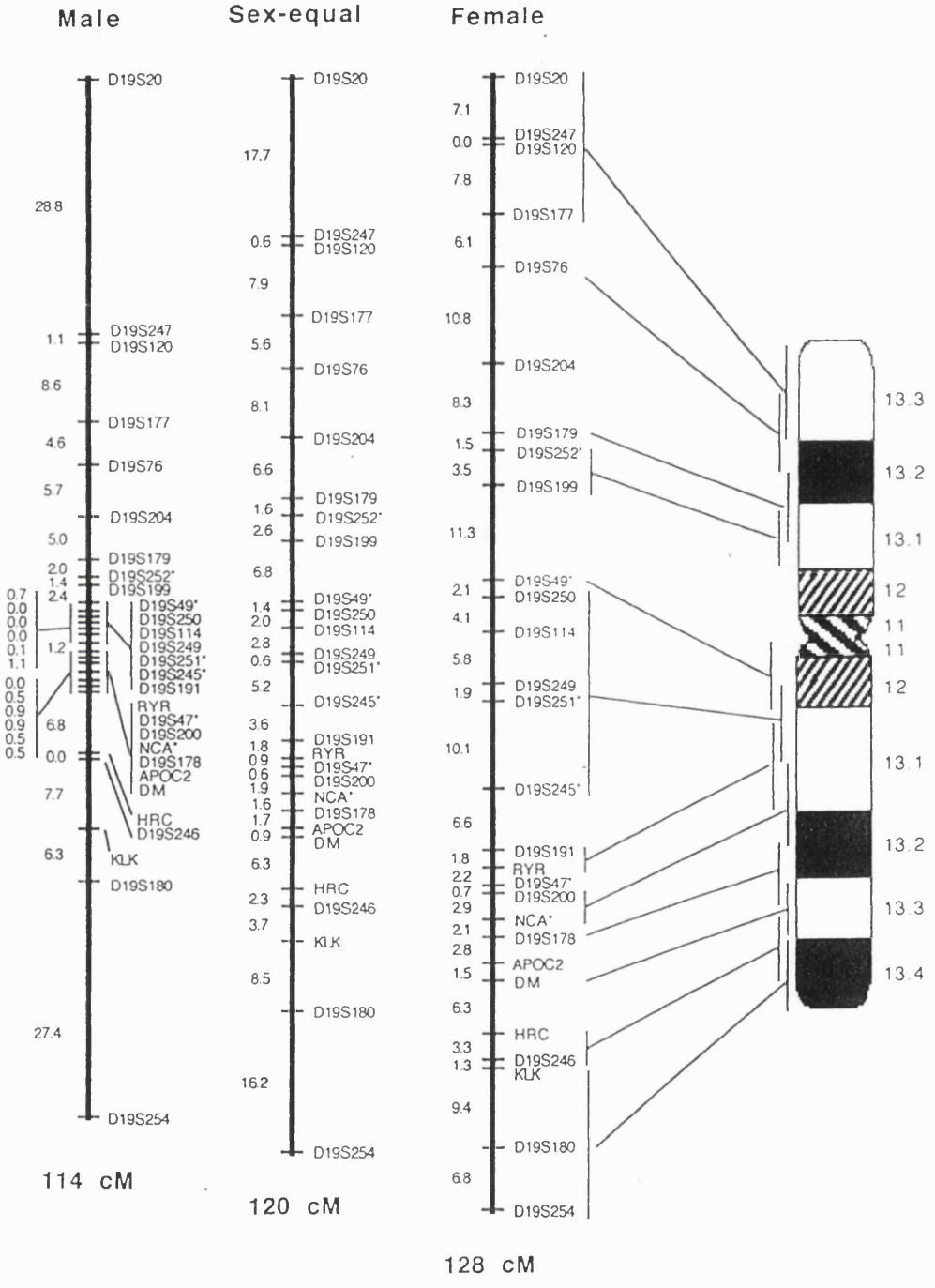

Linkage map for chromosome 19. Asterisks denote loci at which sets of two or three markers were not separated by recombinations and therefore could not be ordered by genetic means (see the Appendix). Odds against inversion of adjacent markers shown on the map were all >1,000:1, except for the 80:1 odds for D19S247–D19S120. The total lengths of the three maps are shown at the bottom. Cytogenetic positions for most of the loci, as determined by fluorescent in situ hybridization, are indicated on the right.

With the initial linkage of adRP and CRD to chromosome 19q, and before the genetic refinement of both loci, there was the possibility that these two phenotypes could be allelic variation at the same locus. However haplotype analysis in both families clearly excluded this possibility, and confirmed the existence of two retinal dystrophy genes on 19q13.3-13.4.

5.3.2 Penetrance:

Penetrance was initially estimated from affected offspring of affected patients and obligate gene carriers in generations III and IV as described in section 5.2.1. Younger individuals from generation V were not included in the penetrance calculation as they might be too young to develop the disease symptoms. Penetrance was estimated to be 0.7 (12 affecteds out of 34 offspring). However, a more thorough study of the clinical phenotype in the family (Evans *et al.*, 1995) was performed after linkage and disease haplotype had been established. All symptomatic individuals were consistantly found to have early age of onset, latest by their teens. Therefore all individuals who were over 20 years old (fig 5.4), were incorporated in the penetrance estimation which was found to be lower, 0.6, than the previously estimated 0.7. This is expected to have very little effect on the linkage calculations already performed in the family. The overall conclusion of the mapping and linkage data should not be affected. As an example, two point lod scores with flanking markers D19S180 and AFMc001yb1 were calculated using a penetrance value of 0.6 (table 5.1b). These lod scores did not significanltly differ from those calculated using 0.7 value.

5.3.3 Misclassification:

A discordance between the phenotype and the underlying genotype may be viewed as a misclassification. This could be due to a susceptible genotype having a normal phenotype (misdiagnosis, later onset of the disease, or non-penetrance), or, on the other hand, the nonsusceptible genotype having the disease phenotype (misdiagnosis, or phenocopies). Family size is an important factor in the effect of a misclassification on linkage data. With a relatively large family size such as ADRP5, one can afford to have one or two misdiagnoses or misclassifications without significantly affecting the linkage results. In this case it would be possible to detect two point linkage, but it would result in contradictory haplotyping and multipoint estimates. However, for many traits, the probability of such a misclassification is often compensated for by incomplete penetrance. For fully penetrant traits a penetrance value of 0.99, rather than 1 (complete penetrance), should always be used. Such missclassifications were encountered twice in ADRP5. Individuals V-23 and V-38 were thought to be affected.

Two point lod scores were still significantly over 3. However, haplotype analysis was confusing, since these two individuals inherited the normal haplotype from their affected parents. Initially the diagnosis in these individuals was verbally reported by family members, however, when examined by clinicians they were found to be normal.

5.3.4 Why did it take so long to map the adRP gene in ADRP5:

The linkage study in ADRP5 started five years ago before a complete genome map existed and when most of the available markers were based on RFLPs. Around 150 markers were genotyped in the family before the publication of Genethon map (Weissenbach *et al.*, 1992). Around 15 of these markers were of the RFLP type and 20 were VNTRs. Typing these markers in the family using the Southern blotting method takes a considerable length of time and uses large quantities of patient DNA (see also section 4.8.1). In addition to RFLPs and VNTRs, over one hundred CA and other repeat type microsatellites were tested. As described in section 4.8.1, most of these microsatellite markers were isolated incidentally in the process of gene identification and sequencing and were of widely ranging heterozygosities, while the Genethon markers were selected for high informativeness and clarity of interpreting alleles from the X-ray autoradiographs. These markers were also unevenly distributed throughout the genome; telomeric regions were particularly sparse of markers, and ADRP5 subsequently mapped to a telomeric region. Also such genome maps as existed at that time had very low resolution, and included large gaps, so that if a particular marker was not sufficient to exclude a particular region, or gave a weak hint of linkage, such results could not be further investigated because of the lack of nearby markers in that region. Subsequently, with new Genethon markers, a systematic linkage mapping study began. This study started from chromosome 1 forward. The fact that the disease locus was on chromosome 19 therefore contributed to some extent to this delay.

CHAPTER VI

SCREENING OF OTHER ADRP FAMILIES AND FURTHER REFINEMENT OF THE RP11 LOCUS

6.1 INTRODUCTION:

Autosomal dominant retinitis pigmentosa (adRP) is believed to account for about 25% of all RP cases (Jay, 1982b). Approximately a quarter of adRP is caused by mutations in the rhodopsin gene (chapter 3), and another 5% is believed to be caused by mutations in the peripherin/RDS gene (Rosenfeld and Dryja, 1995). With the exception of the 7q locus, each of the remaining adRP loci (8q, 7p, 17p and 17q) has, so far, been reported in a single family. The genetic loci which underlie the remaining adRP families are still to be identified. Initially, the chromosome 19q adRP locus was also mapped in a single large family (ADRP5), members of which have the type II/R form of RP with incomplete penetrance (chapter 5). In this chapter, results are presented of new adRP families screened for chromosome 19q (RP11) linkage in order to estimate the fraction of adRP that results from mutations at this locus, and to further refine the genetic location. Twenty unrelated adRP families, for which DNAs are available in this laboratory, were used in this screening. These families represented a mixture of both type I/D and type II/R adRP with or without incomplete penetrance, as well as some families unclassified by these criteria. Disease in some of these families had already been excluded from rhodopsin, peripherin/RDS, and loci at 8q, 7p, 7q, and 17p. Other families were new and were not excluded for any of the previously known loci. Therefore simultaneous screening of these families for other loci was performed by other members of this laboratory. All families were also screened for the newly identified 17q adRP locus. Two apparently unrelated adRP families, which have a phenotype similar to that of ADRP5 (type II/R with incomplete penetrance), were found to be linked to this locus. Another Japanese family has been reported to be linked to this locus by another group (Nakazawa *et al.*, 1995). With the exception of rhodopsin, it appears that the 19q locus may be a more common locus compared to other adRP loci.

6.2 RESULTS:

6.2.1 Ascertainment and diagnosis of adRP in these families:

Most of the pedigrees were ascertained by clinically testing the patients at Moorfields Eye Hospital. Some of the families came from different parts of England where patients were seen in the corresponding eye clinics. The mode of inheritance in each family was concluded from family history provided by the patient(s). In some instances, samples from other members who were unable to attend the clinical examination were collected through their GPs, and their disease status was only verbally established and not confirmed by clinical examination. Where families were classified as type I/D or type II/R, with or without incomplete penetrance, this information is shown in figure 6.1. Finally, all families were Caucasians of European origin.

6.2.2 Family linkage results:

Twenty pedigrees have been genotyped for various markers at the RP11 locus, in the region between D19S571 and D19S254. Pairwise linkage analyses were performed as described in the previous chapter (Lathrop and Lalouel, 1984). Normal individuals who where over thirty years of age were included in the analysis. However, lod scores were calculated using a penetrance value of 0.7 to account for possible disease gene carriers. Sex averaged recombination frequencies were used. Pedigrees and haplotype analysis are shown in figure 6.1, together with lod scores for the markers tested.

6.2.2.1 ADRP29: linkage to, and further refinement of the RP11 locus:

ADRP29 is a family from the south of Wales, members of which show an R-type form of retinal degeneration. Some individuals of the family appear to be normal (fig 6.1, pedigree 1: IV-3, IV-7) though they have affected parents and affected children, which confirms the incomplete penetrance in this family. This characteristic phenotype is similar to that seen in ADRP5. Furthermore, this family has been excluded from all previously known loci (these loci do not include newly identified 17p and 17q loci). Therefore this family was a likely candidate for the RP11 locus. A lod score of 2.1 was obtained with marker D19S572 with no recombination ($\Theta=0$). A lod score of 2 is accepted as sufficient evidence for the localization of a disease (with similar phenotype) gene to a previously known locus (Ott J., personal communication). Such understanding falls within the broader concept often referred to as 'posterior probability'. Incomplete penetrance was further confirmed in the family, where normal individuals were found to carry the disease haplotype (fig 6.1). Interestingly, haplotype analysis in this family demonstrated an inferred recombination event as seen in individuals V-3

and V-4 (fig 6.1). This recombination took place between AFMc001yb1 and D19S572, therefore refining the disease containing interval from 8 cM, as estimated in the original 19q linked family (ADRP5) to a 5 cM interval between D19S180 and AFMc001yb1 (fig 6.2).

6.2.2.2 RP1907 linkage to the RP11 locus:

Another family, RP1907 (fig 6.1, pedigree 2), members of which have a similar phenotype to both ADRP5 and ADRP29, also gave lod scores of 2.5, 2.1, and 2.0 with markers D19S572, AFMc001yb1, and D19S180 respectively at $\Theta=0$. Haplotype analysis did not help in further refinement of the disease locus, since no recombination was detected with the flanking markers for RP11.

6.2.2.3 The Japanese family:

This family was found to be linked to the RP11 locus by another group (Nakazawa *et al.*, 1995). DNA samples were obtained from this group, and new closely linked and more informative markers (AFMc001yb1, D19S572, and AFMb005wh1) were typed in the family. D19S180 was repeated since the published data does not show genotyping of this marker in the family. Haplotype analysis of these markers did not reveal any recombination events in order to refine the genetic localization of the disease gene (fig 6.1, pedigree 3). However, linkage analysis with the new markers further confirmed the presence of the adRP locus on chromosome 19q in this family.

6.2.2.4 ADRP24 and RP677:

Based on clinical information, these two smaller families (fig 6.1) were suggested as candidates for the RP11 locus. They did not show any significant linkage to the previously known loci. Haplotype analysis in ADRP24 with RP11 linked markers (fig 6.1) did not show any recombination events in affected family members. However recombinants were detected in clinically normal individuals in the family. Since non-penetrance is a feature of the RP11 phenotype,these individuals could be disease gene carriers, provided the family is linked. Lod score analysis in this family gave inconclusive results. Efforts are now being made to obtain DNA samples from other family members, which may clarify the linkage data. Therefore this family remains a candidate for this locus, and once the RP11 gene is found it should be screened for mutations in this gene. If the RP11 locus is excluded, it will be proof of further genetic hetrogeneity within families exhibiting this particular adRP phenotype (see section 6.3.3).

RP677 gave a lod score of 1.1 with marker D19S572. Once again, clinically the family appeared to be a good candidate for the RP11 locus. However haplotype analysis, with the available markers in the region (figure 6.1), suggests the segregation of two different haplotypes in the two branches of the family. This could be the result of multiple independent crossovers which took place in the top generations. Therefore, having more markers in the disease interval would help in finding the smallest region that did not recombine, which may help in narrowing the disease interval. On the other hand, segregation of different haplotypes in the two branches could have happened due to the rare possibility that individual I-2 was compound heterozygote for different mutations at the RP11 locus. Alternatively, these data could be interpreted as tentatively excluding the RP11 locus in this family. Nevertheless since the data is inconclusive, the family should also be tested for mutations once the RP11 gene has been cloned, to firmly test for its involvement in this family.

6.2.2.5 Exclusion of other families:

None of the other 16 families (families 6-20 in figure 6.1) showed linkage to RP11 locus. Due to family size, most of the families gave poor exclusions of the region containing the RP11 locus (the majority of markers tested gave lod scores of -2 at Θ values of 0.01 or less). However most of the families were excluded based on haplotype analysis, where at least one affected individual was recombinant for the entire RP11 region, and where double recombinations in such a small interval (5 cM) are highly unlikely. Moreover, families ADRP6, ADRP16, ADRP26, ADi-1, ADi-2, and RP2650 for which rhodopsin had not previously been screened, were found to have mutations in this gene. Additionally, families RP1729 and ADRP40 were found to be genetically linked to loci on chromosome 17p and 17q respectively.

6.3 DISSCUSSION:

6.3.1 Further refinement of the RP11 locus:

Further genetic refinement of the RP11 locus should facilitate a positional cloning approach and subsequent identification of the disease gene. This can be established by finding new affected individuals who are recombinant for markers in the RP11 region. These affected individuals can be either members of the ADRP5 family, or from families newly linked to this locus. Haplotype analysis in all available members of ADRP5 (see section 5.2.6) demonstrated the mapping of RP11 to the 8 cM interval between markers D19S180 and AFMb005wh1 (fig 6.2). Of the three newly mapped families (ADRP29, RP1907, and the Japanese family) only

ADRP29 showed a recombination event that refined the above localization further. Accordingly, the disease gene localization has been narrowed down from 8 cM to a 5 cM interval between D19S180 and AFMc001yb1 (figure 6.2).

6.3.2 Frequency of adRP mapping to the RP11 locus:

In a total of 27 European families studied by linkage analysis in this laboratory (including ADRP5 and several families more recently analysed and therefore not included in this thesis), 4 families (ADRP5, ADRP29, RP1907, and another family not included in this study) showed linkage to chromosome 19q13.4 region. Therefore, this locus probably accounts for about 14% of European RP families, or as much as 17% of British RP families (by excluding the 3 Italian families from the denominator). Haplotype analysis in the three British families showed no evidence of a founder effect (figure 6.1). The possibility that this locus is probably more common than other RP loci reported in single families, was further supported by the finding of a Japanese family linked to this locus (fig 6.1, pedigree 3). Of the remaining families 4 were excluded from some of the loci but were not informative for one or more of the remaining loci. These include ADRP24 and RP677, which gave insignificant exclusion results for the 19q13.4 (RP11) region. Therefore a fraction of these families could be caused by mutations in the RP11 gene, which would further increase the frequency of adRP families mapping to this locus. To conclude, these results suggest that of the 8 known adRP loci, RP11 is probably the second most common after rhodopsin. Screening more RP families for this locus should establish a more accurate figure for the proportion of RP cases caused by mutations at this locus.

6.3.3 Phenotype of chromosome 19 linked (RP11) families:

The phenotype in ADRP5 and ADRP29 has been thoroughly studied (Evans *et al.*, 1995). A clinical, psychophysical and electrophysiologic investigation was undertaken. Differences in clinical presentation were noticed between members of the same family, a phenomena known as variable expressivity. Autosomal dominant inheritance in these families is evident with affected individuals in each generation and male to male transmission. Haplotype data analysis shows that 50 (52%) of the 97 at risk individuals had inherited the disease locus (expected value 50%) but only 32% (31 individuals) were symptomatic; 38% (19 from 50 individuals) of disease haplotype carriers were asymptomatic (these estimates were based on generations III, IV, and V of pedigrees ADRP5 and ADRP29 shown in figures 5.4 and 6.1 respectively).

While all symptomatic individuals reported nyctalopia by their mid teens, no asymptomatic

obligate carriers or disease haplotype carriers reported any signs of night blindness. Clinical examinations showed that typical fundus features of extensive peripheral retinal degeneration were seen in even the youngest examined symptomatic patient (24 years) whereas in older patients macular atrophy, oedema and secondary cataract formation is also seen. Normal visual acuities and fundus examination were recorded for even the oldest asymptomatic obligate carrier (75 year) and disease haplotype carrier (55 year). Minor abnormalities in the scotopic vision and ERG in some asymptomatic disease gene carriers were suggested by some clinicians. However these changes are considered to fall at the edge of the normal range by other clinicians. Therefore these changes are still controversial and can not be considered as diagnostic.

A phenotype consisting of variable expression and an R type pattern has been described in the adRP family linked to the chromosome 7p locus (RP9) (Kim *et al.*, 1995). However in this family a graded disease severity has been reported with mild, moderate and severely affected individuals. Therefore its possible to speculate that the 19q adRP phenotype, type II/R functional deficit with "bimodal expressivity", may be unique. This phenotype suggests that another factor is involved in the causation of the disease. According to clinicians, this factor is unlikely to be environmental since the influence of such element would be expected to be dose-dependent, and should produce a graded rather than the "all or none" phenotype seen in 19q linked families. Furthermore, environmental factors have not been proved to have great influence on disease severity of RP (Heckenlively, 1988). Neither the position of an affected individual within the family (anticipation), nor the sex of the parent (imprinting) were found to be significant factors in determination of severity of the disease.

Digenic inheritance is a mode of inheritance referred to when simultaneous mutations of two genetic loci are involved in disease pathogenesis (section 1.7.1.4). This mode of inheritance has already been implicated in at least one example of RP, where heterozygous mutations (or polymorphism) at the peripherin/RDS and ROM1 genes, occuring together, are found to cause retinal degeneration (Kajiwara *et al.*, 1994). Similarly, digenic (or multigenic) inheritance could explain the bimodal expressivity of 19q locus. A second locus can not be allelic with the 19q mutation(s) segregating in RP11 families, since there are two examples in ADRP5 of two siblings (fig 5.4: IV-23 and IV-25, and V-1 and V-4) who appear to have inherited the same RP11 and normal haplotypes from both parents, yet one is affected and the other is asymptomatic. The second locus effect could result from a polymorphism at a different locus that segregates in the normal population such that inheritance of a particular allele with a 19q

mutation gives rise to the RP phenotype. The effect of such a locus could be either recessive or dominant. The two loci could functionally complement each other such that a mutation in one of them was not sufficient in effect to be pathogenic, or that a mutation in the second locus could result in a gain of function in the RP11 gene which gave rise to RP phenotype. Since the 19q mutation segregates in a dominant fashion and is clearly the major determinant of RP in this family, it was easy to pick up linkage to this locus, while it would be more difficult to identify the second locus by linkage analysis.

In view of the above speculations, the 19q locus together with another locus (or loci) could be responsible for a proportion of arRP families where either parent in these families could be an asymptomatic disease gene carrier of a chromosome 19q mutation. Identification of the disease gene on chromosome 19 and further understanding of the pathogenesis of such mutation could lead to the identification of the biological basis of incomplete penetrance characteristic of RP11.

Figure 6.1:

Pedigrees of the 20 adRP families screened for linkage to the RP11 locus, together with the haplotype (boxed) segregating with the RP phenotype. Order of markers in the haplotype is similar to their order in the lod score table of each family. Markers showing lod scores of more than 0.5 are underlined. The figure also shows the clinical classification if available (type I/D, or type II/R; IP= incomplete penetrance). For key to pedigree symbols see figure 5.4.

Order of Genethon markers is according to Gyapay et al., 1994. The order of D19S180 and D19S254 relative to the genethon markers have been established by haplotype analysis in ADRP5 and other families.

(1) ADRP-29

(Type II/R, IP)

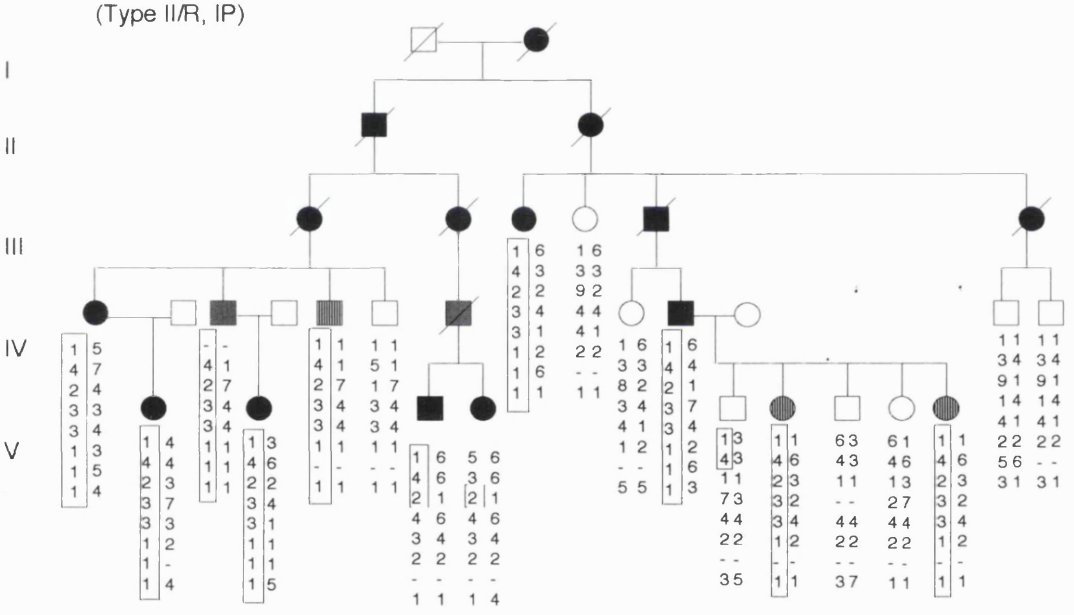

	0.0	0.01	0.05	0.10	0.20	0.30	0.40
D19S571	-6.81	-3.35	-1.71	-0.99	-0.40	-0.17	-0.07
D19S180	-0.83	0.84	1.33	1.36	1.09	0.67	0.26
D19S572	2.07	2.02	1.84	1.61	1.14	0.67	0.28
AFMc001yb1	-2.70	-0.60	-0.01	0.15	0.17	0.09	0.02
D19S418	2.26	2.21	2.00	1.73	1.18	0.65	0.23
AFMb005wh1	-2.67	-0.47	0.13	0.29	0.29	0.18	0.07
D19S214	--	--	--	--	--	--	--
D19S254	-0.44	-0.42	-0.35	-0.27	-0.14	-0.06	-0.01

(2) RP1907

(Type II/R, IP)

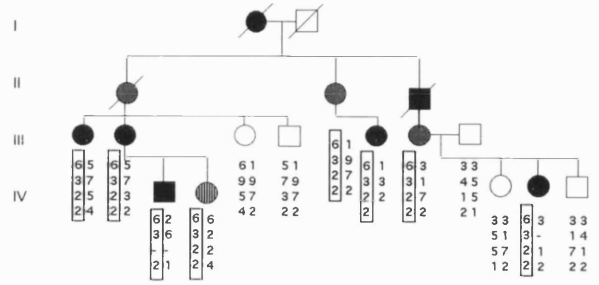

	0.0	0.01	0.05	0.10	0.20	0.30	0.40
D19S180	2.04	2.00	1.84	1.64	1.20	0.73	0.28
D19S572	2.49	2.45	2.28	2.05	1.53	0.96	0.39
AFMc001yb1	2.12	2.08	1.92	1.70	1.21	0.70	0.23
AFMb005wh1	0.26	0.25	0.21	0.17	0.10	0.04	0.01

(3) Japanese family

(Type II/R, IP).

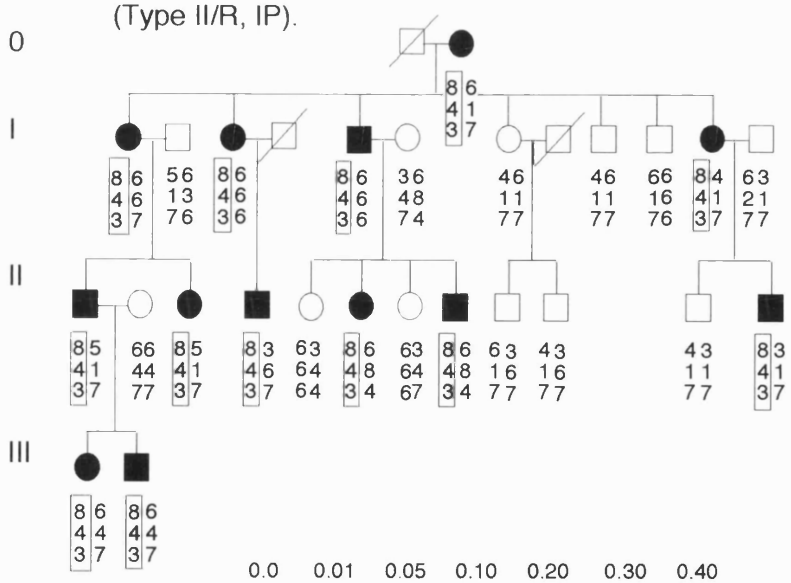

	0.0	0.01	0.05	0.10	0.20	0.30	0.40
D19S180	4.50	4.42	4.13	3.37	2.92	1.99	0.97
D19S572	3.56	3.50	3.29	2.99	2.34	1.60	0.76
AFMc001yb1	4.50	4.42	4.13	3.75	2.92	2.00	0.97

(4) ADRP24

(Type II/R, IP)

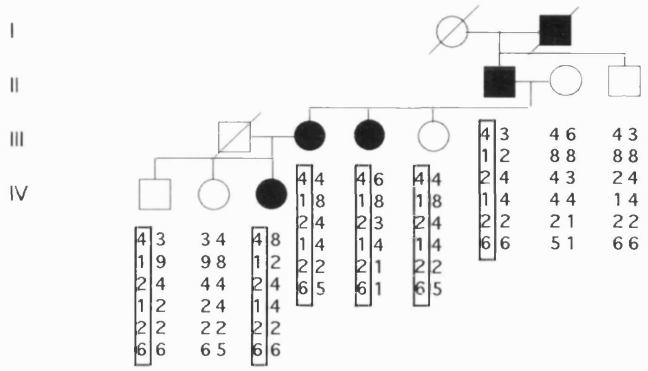

	0.0	0.01	0.05	0.10	0.20	0.30	0.40
D19S180	-0.23	-0.22	-0.18	-0.14	-0.07	-0.03	-0.01
D19S572	0.30	0.30	0.29	0.27	0.22	0.16	0.08
AFMc001yb1	-0.11	-0.09	-0.04	0.01	0.07	0.08	0.06
D19S418	-0.18	-0.16	-0.11	-0.05	0.03	0.05	0.04
AFMb005wh1	-0.17	-0.16	-0.13	-0.10	-0.05	-0.02	-0.01
D19S214	0.04	0.05	0.07	0.09	0.11	0.10	0.07

(5) RP677

(Type II/R, IP)

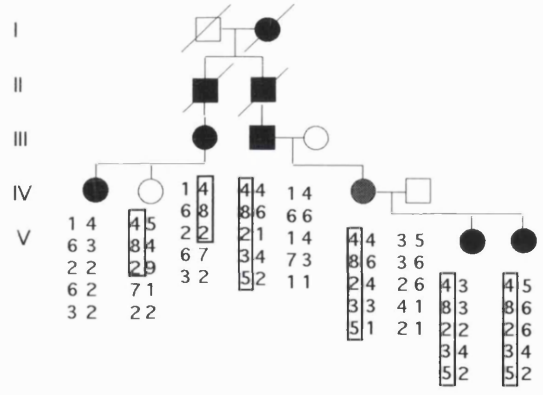

	0.0	0.01	0.05	0.10	0.20	0.30	0.4
D19S571	0.00	0.00	0.01	0.01	0.00	-0.01	-0.02
D19S180	-2.29	-0.48	0.12	0.29	0.34	0.25	0.13
D19S572	1.16	1.14	1.03	0.90	0.64	0.41	0.21
AFMc001yb1	-3.24	-1.10	-0.46	-0.23	-0.06	-0.01	0.00
AFMb005wh1	-2.86	-0.69	-0.07	0.14	0.24	0.21	0.12

(6) ADRP6

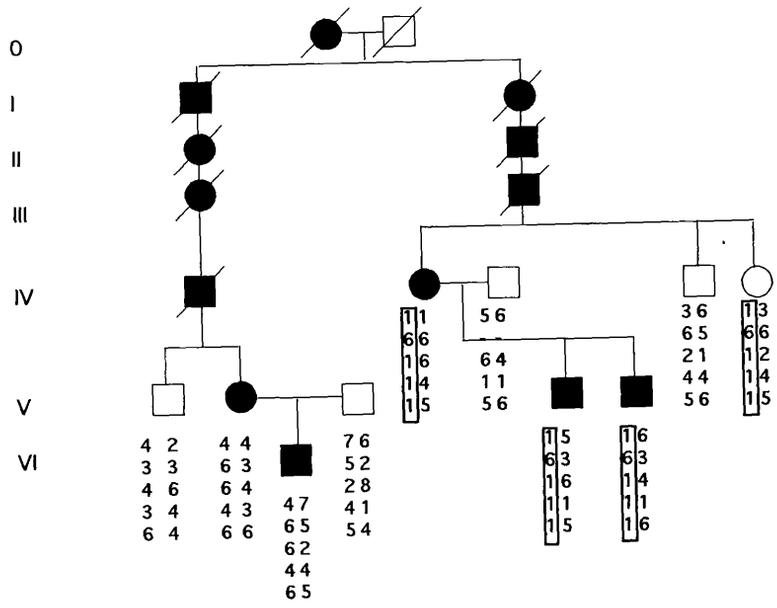

	0.0	0.01	0.05	0.10	0.20	0.30	0.40
D19S571	-3.28	-1.09	-0.46	-0.24	-0.08	-0.03	-0.01
D19S180	0.79	0.75	0.61	0.44	0.19	0.06	0.01
D19S572	-2.97	-0.98	-0.33	-0.11	0.03	0.04	0.01
D19S418	-2.92	-0.78	-0.19	-0.02	0.05	0.04	0.01
D19S214	-2.88	-0.68	-0.10	0.06	0.10	0.06	0.01

(7) ADRP8
(Type I/D)

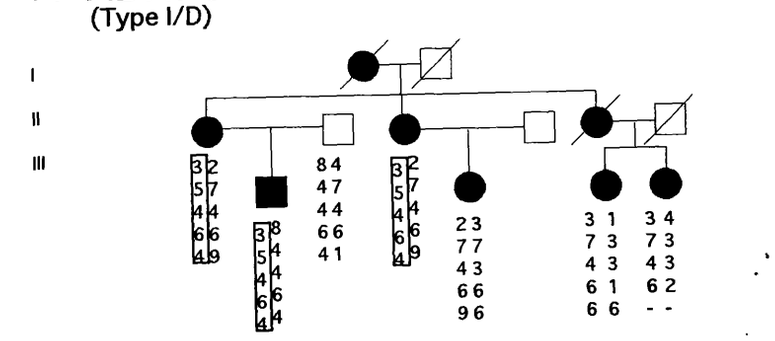

	0.0	0.01	0.05	0.10	0.20	0.30	0.40
D19S180	-2.78	-1.19	-0.56	-0.32	-0.14	-0.05	-0.01
AFMc001yb1	-2.51	-0.91	-0.30	-0.10	0.01	0.02	0.01
D19S418	0.12	0.12	0.11	0.09	0.06	0.03	0.01
D19S214	0.16	0.15	0.12	0.10	0.05	0.02	0.00
D19S254	-6.03	-2.64	-1.31	-0.78	-0.31	-0.11	-0.02

(8) ADRP16

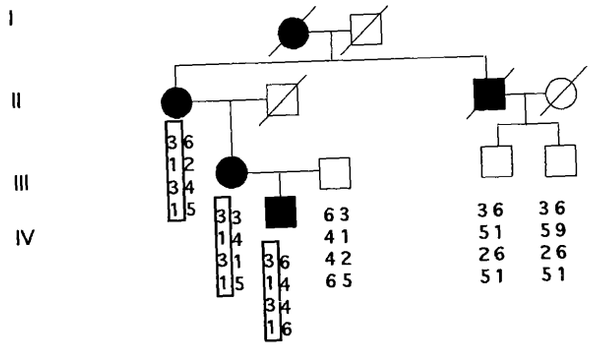

	0.0	0.01	0.05	0.10	0.20	0.30	0.40
D19S180	-0.54	-0.47	-0.30	-0.18	-0.07	-0.02	0.00
D19S572	-3.28	-0.42	0.13	0.26	0.27	0.21	0.12
D19S418	-3.21	-0.98	-0.34	-0.11	0.05	0.09	0.07
D19S214	-3.44	-1.07	-0.44	-0.21	-0.06	-0.01	0.00

(9) ADRP21

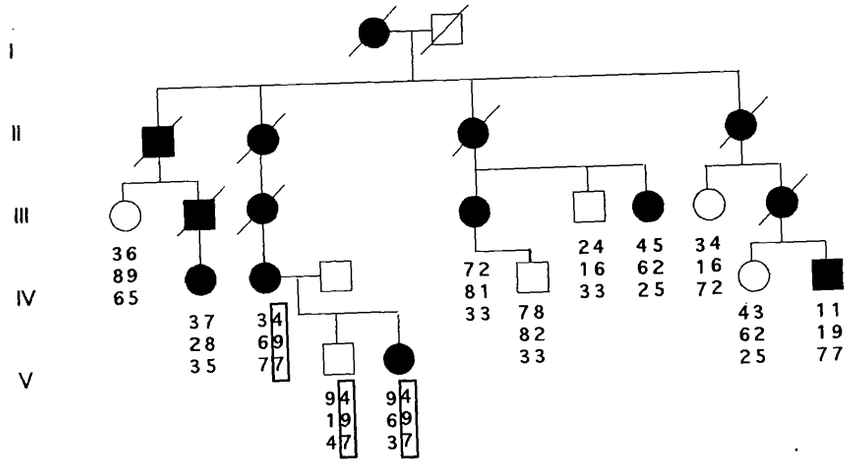

	0.0	0.01	0.05	0.10	0.20	0.30	0.40
D19S571	-6.53	-4.03	-2.13	-1.30	-0.59	-0.26	0.09
D19S572	-6.44	-4.03	-2.14	-1.13	-0.56	-0.23	-0.07
AFMc001yb1	-5.65	-3.62	-1.80	-1.04	-0.42	-0.17	-0.06

(10) ADRP26

(Type I/D)

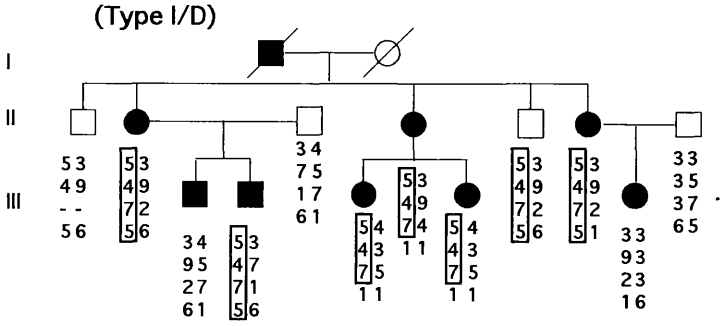

	0.0	0.01	0.05	0.10	0.20	0.30	0.40
D19S180	-3.31	-2.68	-1.43	-0.88	-0.38	-0.15	-0.03
A19S572	-3.29	-2.66	-1.42	-0.87	-0.38	-0.15	-0.03
AFMc001yb1	-3.33	-2.70	-1.46	-0.91	-0.42	-0.18	-0.05
D19S214	-6.94	-2.44	-1.14	-0.65	-0.26	-0.10	-0.03

(11) ADRP27

(Type II/R)

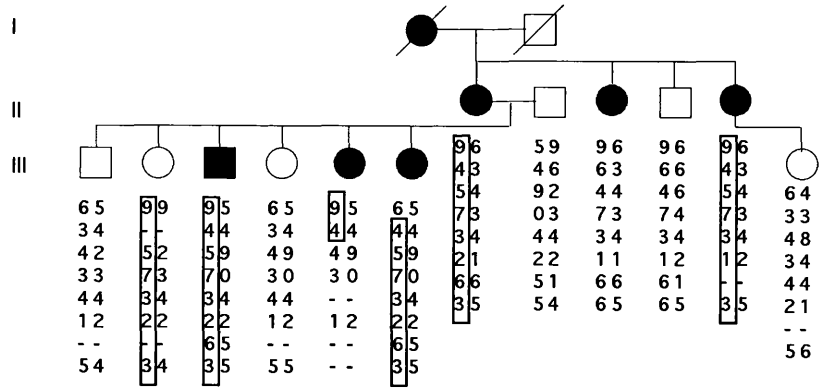

	0.0	0.01	0.05	0.10	0.20	0.30	0.40
D19S571	-2.86	-1.05	-0.40	-0.16	0.00	0.02	0.01
D19S180	-2.14	-0.40	0.20	0.37	0.40	0.27	0.10
D19S572	-3.75	-2.33	-1.03	-0.52	-0.12	0.01	0.02
AFMc001yb1	-2.73	-0.96	-0.31	-0.08	0.06	0.08	0.03
D19S418	0.63	0.62	0.58	0.52	0.36	0.20	0.06
AFMb005wh1	-4.44	-2.79	-1.42	-0.84	-0.33	-0.11	-0.02
D19S214	-3.10	-1.10	-0.46	-0.22	-0.04	0.00	0.01
D19S254	-2.42	-0.70	-0.08	0.12	0.20	0.14	0.05

(12) ADRP32

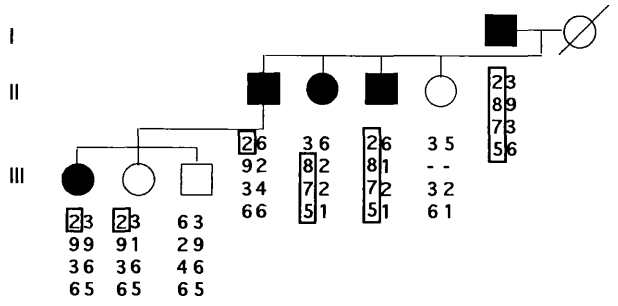

	0.00	0.01	0.05	0.10	0.20	0.30	0.40
D19S180	-2.85	-1.06	-0.40	-0.15	0.04	0.09	0.07
D19S572	-3.92	-1.25	-0.56	-0.28	-0.04	0.05	0.06
AFMc001yb1	-3.75	-1.07	-0.40	-0.15	0.04	0.09	0.07
D19S214	-3.58	-1.22	-0.56	-0.32	-0.12	-0.04	-0.01

(13) ADRP40

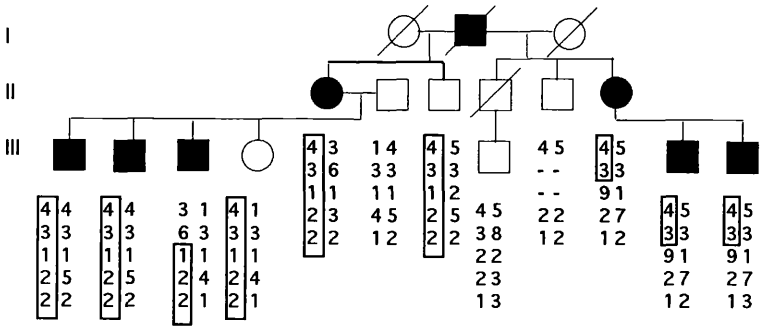

	0.00	0.01	0.05	0.10	0.20	0.30	0.40
D19S571	-4.75	-2.64	-1.30	-0.67	-0.15	0.02	0.06
D19S180	-2.77	-1.07	-0.04	-0.13	0.09	0.15	0.11
D19S572	-3.53	-1.67	-1.02	-0.77	-0.51	-0.32	-0.15
AFMc001yb1	0.39	0.39	0.39	0.39	0.35	0.28	0.16
AFMb005wh1	-4.21	-1.45	-0.76	-0.47	-0.21	-0.08	-0.02

(14) RP 1729

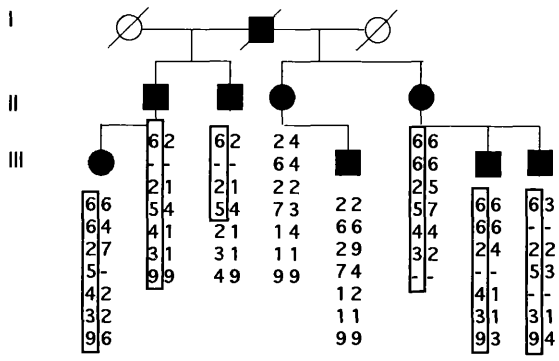

	0.00	0.01	0.05	0.10	0.20	0.30	0.40
D19S571	-3.07	-1.26	-0.57	-0.30	-0.07	0.01	0.02
D19S180	0.31	0.29	0.24	0.17	0.08	0.03	0.01
D19S572	0.58	0.57	0.52	0.46	0.33	0.21	0.10
AFMc001yb1	-2.92	-1.70	-0.93	-0.57	-0.24	-0.09	-0.02
D19S418	-3.36	-2.41	-1.14	-0.64	-0.22	-0.06	0.00
AFMb005wh1	-4.10	-2.31	-1.43	-0.97	-0.49	-0.24	-0.10
D19S254	-0.03	-0.03	-0.04	-0.06	-0.09	-0.08	-0.05

(15) RP2650

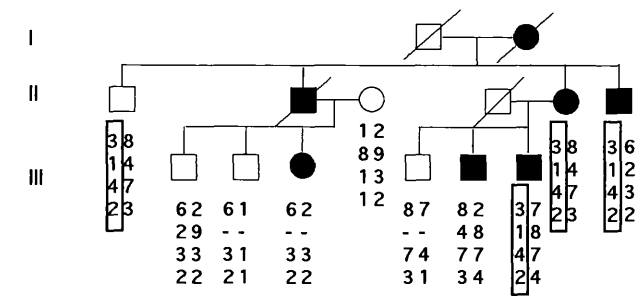

	0.00	0.01	0.05	0.10	0.20	0.30	0.40
D19S571	-4.78	-2.77	-1.47	-0.91	-0.40	-0.16	-0.04
D19S572	-2.46	-1.56	-0.88	-0.57	-0.26	-0.10	-0.02
AFMc001yb1	-4.27	-1.80	-1.03	-0.67	-0.31	-0.12	-0.03
AFMb005wh1	-2.06	-1.18	-0.58	-0.34	-0.15	-0.06	-0.02

(16) ADM

(IP)

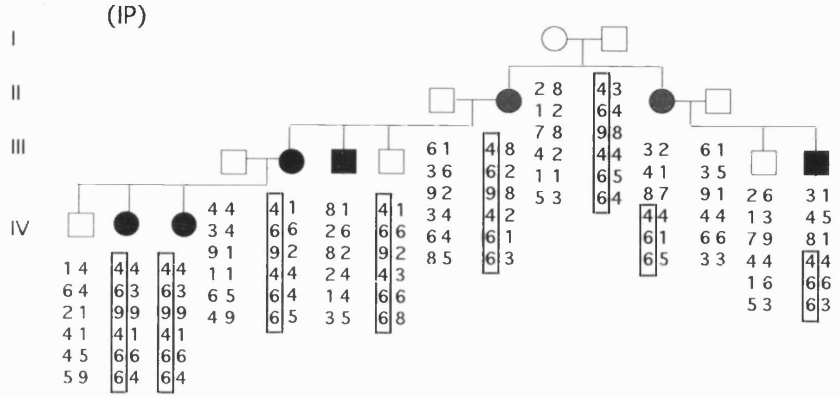

	0.00	0.01	0.05	0.10	0.20	0.30	0.40
D19S571	-6.01	-1.97	-0.66	-0.15	0.22	0.29	0.21
D19S180	-6.61	-2.75	-1.38	-0.82	-0.31	-0.09	0.00
D19S572	-6.01	-1.97	-0.66	-0.15	0.22	0.29	0.21
D19S418	-3.49	-1.82	-1.06	-0.70	-0.34	-0.15	-0.05
D19S214	-2.04	-0.28	0.32	0.50	0.54	0.42	0.24
D19S254	-2.01	-0.28	0.32	0.49	0.53	0.42	0.24

(17) ADi-1

(Type I/D)

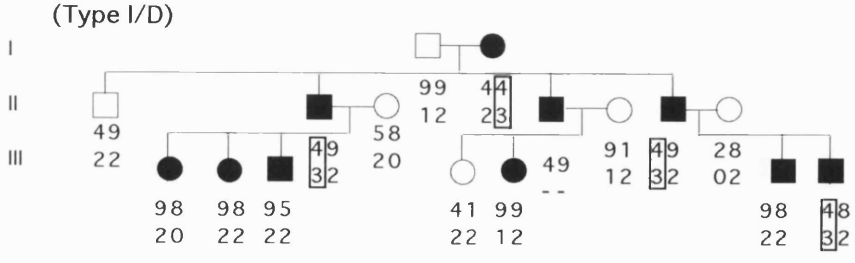

	0.00	0.01	0.05	0.10	0.20	0.30	0.40
D19S572	-2.86	-2.86	-2.87	-2.78	-1.90	-1.06	-0.45
AFMb005wh1	-2.84	-2.84	-2.82	-2.49	-1.42	-0.74	-0.31

(18) ADi-2

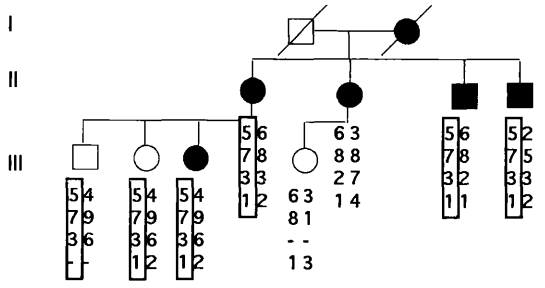

	0.00	0.01	0.05	0.10	0.20	0.30	0.40
D19S180	-2.39	-1.60	-0.87	-0.52	-0.20	-0.07	-0.01
D19S572	-3.39	-1.63	-0.89	-0.53	-0.20	-0.07	-0.01
AFMc001yb1	-2.01	-1.31	-0.70	-0.44	-0.19	-0.07	-0.02
AFMb005wh1	-2.11	-1.24	-0.63	-0.38	-0.17	-0.07	-0.02

(19) ADi-3

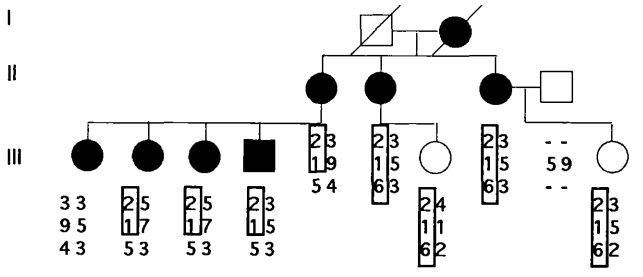

	0.00	0.01	0.05	0.10	0.20	0.30	0.40
D19S180	-1.95	-1.08	-0.47	-0.23	-0.05	-0.01	0.00
D19S572	-2.24	-1.36	-0.70	-0.41	-0.17	-0.07	-0.02
AFMc001yb1	-4.93	-2.34	-1.08	-0.59	-0.21	-0.07	-0.01

(20) ZMK-92

(RP with deafness)

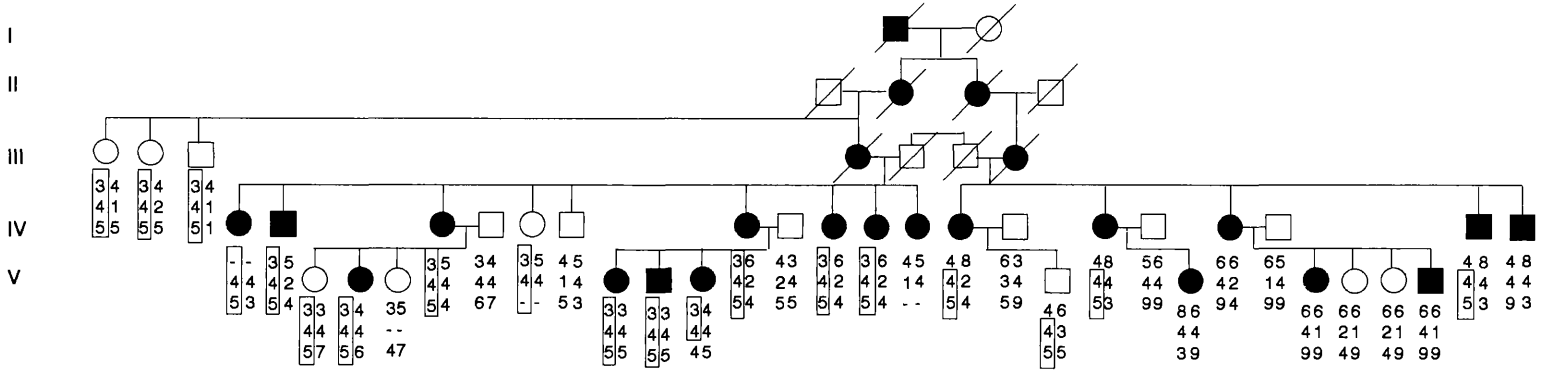

	0.00	0.01	0.05	0.10	0.20	0.30	0.40
D19S180	-2.53	-0.63	-0.03	0.15	0.20	0.13	0.04
D19S418	0.56	0.54	0.49	0.42	0.27	0.12	0.03
D19S254	-5.50	-3.49	-2.07	-1.28	-0.55	-0.21	-0.05

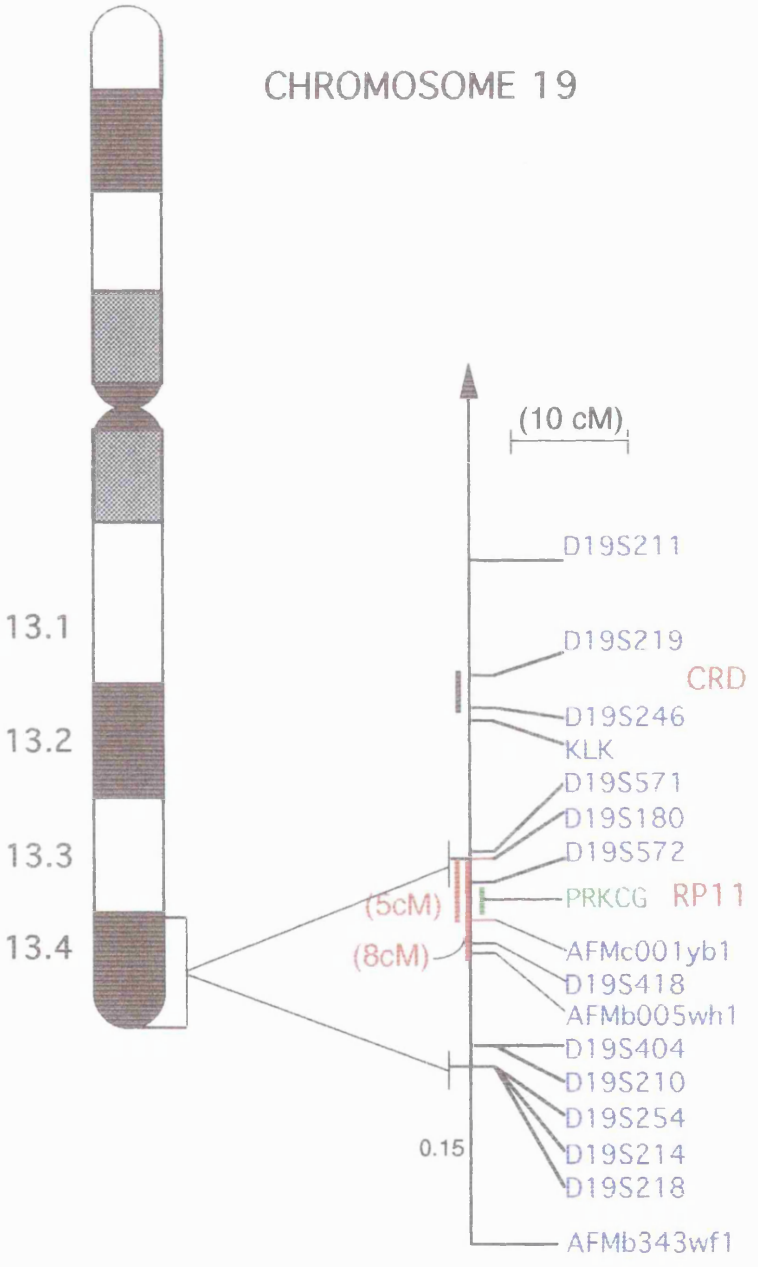

Figure 6.2:
Linkage map of chromosome 19q13.3-q13.4. It shows the localization of the RP11 gene according to haplotype analysis in ADRP5 (8cM), and ADRP29 (5cM). The location of PRKCG gene within the RP11 interval is also shown. Figure also shows the localization of the CRD locus relative to RP11.

CHAPTER VII

A PRELIMINARY MUTATION SCREEN OF A CANDIDATE GENE FOR RP11

7.1 INTRODUCTION:

The candidate gene approach has been successfully used in the identification of many disease genes in general, and most of the retinal disease genes (e.g. rhodopsin and peripherin) in particular. In contrast to positional cloning this approach offers a short cut to the process of disease gene identification. Screening of a suitable candidate gene can lead to the identification of the disease causing mutation or exclusion of such a gene from disease causation. In addtion to being simply in the right place or genetic interval (positional candidate), candidate genes for retinal diseases can be genes which are involved in the visual transduction pathway or structural proteins involved in the formation or function of the retina. Alternatively they could be members of a gene family another member of which is known to cause a related phenotype. Other candidates could be genes which when mutated cause similar phenotype in animal models of human disease (eg. peripherin/RDS and PDEB), or genes which are known to cause phenotypes that could be allelic to the disease under study. The term "candidate" is also used to describe candidate loci identified by linkage analysis, and where genes are not yet identified. Candidate loci can be excluded by linkage analysis in test families of markers which originally showed linkage to related disease phenotypes. The last concept of candidate loci does not apply to the subject of this chapter.

7.2 A CANDIDATE GENE FOR RP11: PRKCG

The RP11 locus has been mapped to chromosome 19q13.4 (chapter 5). The disease interval has been estimated as 5cM between D19S180 and AFMc001yb1 (fig 6.2). This is a relatively large genetic interval, for which physical mapping could be a lengthy process. The candidate gene approach is preferable in such cases if a suitable candidate can be identified. Chromosome 19 is particularly gene rich (Craig and Bickmore 1994). Searching the genome data base for genes in that region identified a number of genes most of which code for proteins whose functions would appear to be unrelated to any mechanism that could result in visual impairment or RP.

However, the gene encoding the isoenzyme protein kinase C gamma (PRKCG) has been previously mapped to chromosome 19q13.2-q13.4 (Coussens *et al.*, 1986, Johnson *et al.*, 1988) and could be considered as a candidate gene (see below).

7.3 What is PRKCG:

Protein kinase C (PKC) is a multifunctional family of closely related serine/threonine protein kinases that are activated by diacylglycerol (DAG) (Hug and Sarre, 1993; Nishizuka, 1992). PKCs function in a wide variety of cellular processes, such as membrane receptor signal transduction, control of gene expression and control of cell division and differentiation (Hug and Sarre, 1993; Nishizuka, 1988). PKC isoenzymes are ubiquitously distributed, but they are expressed in a tissue-specific manner (Ohno *et al.*, 1987; Brandt *et al.*, 1987; Westel *et al.*, 1992)

Initially three related members of this gene family, termed α, β, and γ, were cloned from bovine brain cDNA libraries and homologoes were obtained by screening a human cDNA library with the unique portions of the bovine clones (Coussens *et al.*, 1986). The three human genes were assigned to different autosomes on the basis of segregation in human-rodent hybrid panels and by in situ hybridization. The α gene was assigned to chromosome 17, the β gene to chromosome 16, and the γ gene to chromosome 19 (region 19q13.2-q13.4). These members of the PKC gene family were found to be closely related at both the amino acid and the nucleotide levels. Later cDNAs were cloned from many other PKC isoforms, mostly from brain cDNA libraries (reviewed by Hug and Sarre, 1993). Southern hybridization analysis suggested that an even larger number of PKC genes may exist, and the diversity within this family of proteins may be further increased by alternative splicing in at least some of these genes (for example βI and βII isoenzymes; Hug and Sarre, 1993).

PKCs were divided into two main groups: the Ca^{+2}-dependent or conventional PKCs (cPKCs) and the Ca^{+2}-independent or novel PKCs (nPKCs) (Hug and Sarre, 1993). The earlier isolated PKC isoforms α, βI, βII and γ belong to the Ca^{+2}-dependent group, and the newly identified isoforms δ, ϵ, ζ, η, and θ, to the Ca^{+2}-independent group. The primary amino acid structure of PKCs deduced from the cDNA sequences, can be divided into conserved (presumably functional) domains termed C1-C4, which are separated by variable regions termed V1-V5, the function of which is not yet known (Coussens *et al.*, 1986; fig 7.1). All PKC isoforms contain these constant and variable regions in a single subunit protein. The C-terminal

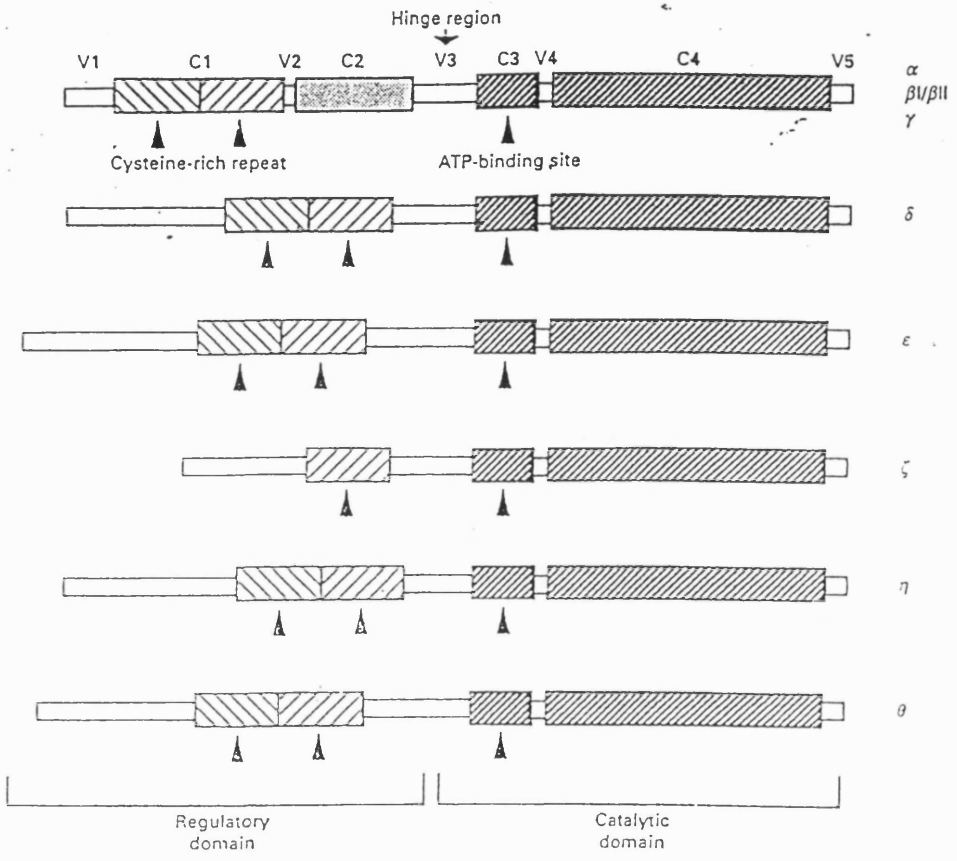

Figure 7.1:

(Figure and legend are from Hug and Sarre, 1993).

Domain structure of PKC isoenzymes. All PKC isoenzymes consists of constant (C) and variable (V) regions. The cys-rich repeats in the C1 region and the ATP binding site in the C3 region are indicated by arrow heads. The arrow points to the hinge region in the V3 domain which separates the regulatory from the catalytic domain.

regions C3-V5 have been defined in all PKC isoenzymes as the catalytic domain, which is separated by the V3 region from the N-terminal regulatory domain. In addition to Ca^{+2} dependence, the two groups of PKC vary in their regulatory domain (fig 7.1). The nPKCs lack the C2 domain. This domain was thought to contain the Ca^{+2} binding site of the cPKCs, but no sequence motif that represents a known Ca^{+2}-binding site, such as the classical E-F hand binding motif, were identified (Hug and Sarre, 1993).

7.4 WHY PRKCG IS A GOOD CANDIDATE GENE FOR RP11:

The following three sections outline the reasons for considering PRKCG as a candidate for RP11.

7.4.1 It maps in the right genetic interval:

The gene for PKCγ isoenzyme was mapped to 19q13.4 region (Coussens *et al.*, 1986; Johnson *et al.*, 1988; this study). Haplotype analysis of the Msp1 polymorphism detected by this gene showed that PRKCG is localized between D19S572 and AFMc001yb1 (see section 5.2.6). This is the interval which was found to segregate with the RP11 phenotype in ADRP5. This colocalization of the two loci (RP11 and PRKCG) suggests that PRKCG could be a candidate gene for RP11.

7.4.2 PKC phosphorylates rhodopsin in the ROS:

The function of PKCγ is not yet clearly defined. However PKCs, in general, have been shown to be expressed widely in the retina and particularly in the outer segments of photoreceptors (Newton and Williams, 1993). Phosphorylation by protein kinase C results in the desensitization of a large number of receptors, suggesting an important function of this group of isoenzymes in the adaptation of cells to extracellullar information (Newton and Williams, 1993). Examples of membrane receptors whose function is modulated by PKC include EGF (epidermal growth factor) and G-protein linked receptors such as the β-adrenergic receptor (Kelleher *et al.*, 1984; Fearn and King, 1985). The observation by Newton and Williams (1991, 1993) that protein kinase C phosphorylates rhodopsin in a light-dependent manner suggests the involvement of PKC in desensitizing rhodopsin. While RK (rhodopsin kinase) activity (see section 1.4.6) predominates at higher light levels, PKC activity was suggested to predominate at low levels. PKC catalyzes the phosphorylation of rhodopsin on a carboxyl terminal domain that does not involve the primary phosphorylation sites of RK. *In vitro* studies reveal that this

phosphorylation is independent of the activation state of rhodopsin (Newton *et al.*, 1994). This PKC-catalyzed phosphorylation of rhodopsin has been shown to uncouple the receptor from transducin *in vitro* (Kelleher and Johnson, 1986), suggesting that the phosphorylation deactivates the rhodopsin molecule. In another study, PKC immunoreactivities were detected in cone photoreceptors of the rat retina, where PKC was suggested to phosphorylate cone visual pigments (Ohki *et al.*, 1994).

7.4.3 PKC mediates a retinal degeneration in Drosophila:

7.4.3.1 Visual transduction in drosophila:

The invertebrate visual cascade, like that in vertebrates, begins with the light activation of rhodopsin molecules and subsequent activation of a G-protein (Smith *et al.*, 1991a). The effector molecule that mediates the vertebrate visual cascade is a G protein-activated cGMP-PDE (see section 1.5), which lowers cGMP concentration in response to light. This leads to the closure of channels and a drop in calcium concentration. In drosophila, a G protein-coupled phospholipase C (PLC) functions as an effector. PLC catalyzes hydrolysis of phosphatidylinositol bisphosphate (PIP_2) into the second messengers inositol trisphosphate (IP_3) and diacylglycerol (DAG). IP3 appears to be a mediator of photoreceptor cell activation (Fein, 1986). This activation leads to the opening of channels and an increase in the cytosolic calcium concentration. In contrast to vertebrates the end result of this activation is the depolarization rather than the hyperpolarization of the photoreceptor cell (fig 7.2). DAG was suggested to function in the feedback regulation through the activation of eye-PKC of drosophila, see below (Nishizuka, 1992).

7.4.3.2 Drosophila retinal degeneration mediated by eye-PKC:

A *Drosophila* melanogaster PKC gene known as eye-PKC was isolated and characterized (Schaeffer *et al.*, 1989). This gene was found to map to position 53E on the second chromosome, within 50kb of another previously reported *Drosophila* PKC gene (Rosenthal *et al.*, 1987). It was found to be exclusively expressed in photoreceptor cells and was related to the cPKC genes (Schaeffer *et al.*, 1989).

The visual systems of both vertebrates and invertebrates are able to modulate their sensitivity to light in a process known as light adaptation (see section 1.4.1). This adaptation appears to be mediated through the changes in the calcium concentration within the photoreceptor cells (Nakatani and Yau, 1988; Matthews *et al.*, 1988; Payne *et al.*, 1986).

Figure 7.2:

(Figure and legend are from Smith et al., 1991b)

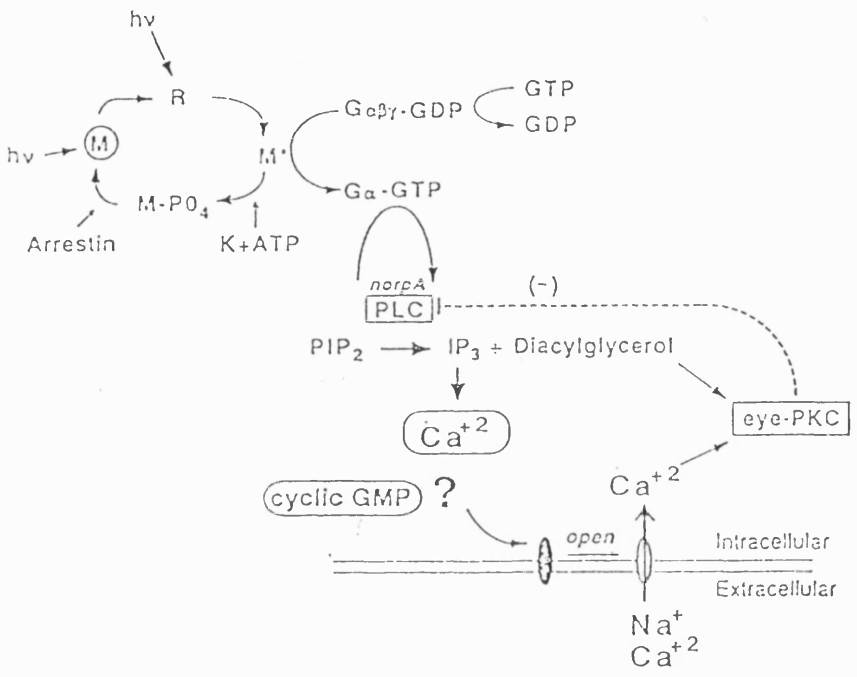

Model of eye-PKC function. Absorption of a photon of light causes a conformational change in the rhodopsin molecule (R) and activates its catalytic properties. Active metarhodopsin (M*) catalyzes G protein activation. The G protein exchanges GDP for GTP and releases the inhibitory βγ subunits. Active G protein catalyzes the activation of the *norpA*-encoded PLC, and PLC hydrolyzes PIP_2 into IP_3 and DAG. The IP_3 is released from the membrane and diffuses to receptors located on the subrhabdomeric cisternae (SRC). This binding is thought to release intracellular calcium from SRC, which appears to be involved in excitation. Cyclic GMP has also been implicated as a possible intracellular messenger mediating excitation (*58, 59*). Extracellular sodium and calcium then enter the cell through the light-activated conductance. The large influx of extracellular calcium activates eye-PKC, which then negatively regulates the phototransduction cascade, perhaps through phosphorylation of PLC. The function of DAG in *Drosophila* phototransduction is not known, but it could modulate basal levels of eye-PKC activity or facilitate calcium activation of eye-PKC. K+ATP, rhodopsin kinase and ATP; $M-PO_4$, phosphorylated metarhodopsin; and filled and open ovals, closed and open light-activated cation channels, respectively. This signaling cascade has been described in detail (*8*).

During excitation of the phototransduction cascade, extracellular calcium ions flow into *Drosophila* photoreceptors through the light activated conductance (see previous section). The calcium is required for triggering deactivation (recovery) and rapid desensitization. This process is specifically defective in the *inaC* drosophila mutant that exhibits photoreceptor deactivation and retinal degeneration (Rangathan *et al.*, 1991). The inaC locus was found to be the eye-PKC gene, the product of which is required for normal calcium-dependent photoreceptor cell deactivation and rapid desensitization (Smith *et al.*, 1991). This suggests that retinal degenerations in humans could result from mutations in a homologous gene to the eye-PKC, and therefore suggests PRKCG as a candidate for RP11.

7.5 THE cDNA SEQUENCE OF HUMAN PRKCG:

Using bovine PKCγ cDNA, a human partial cDNA clone was isolated from a fetal brain library. This clone contains part of the 5' untranslated region (195 bp) and the first 951 nucleotides of the coding region (Coussens *et al.*, 1986; fig 7.3). Another 1.8 kb 3'partial cDNA clone which overlaps with the 5' partial clone was also sequenced and submitted to the genome data base by Hug (1993; accession: Z15114). This clone may contain a potential stop codon in frame with the sequence from the 5' clone, and therefore may contain part of the 3' untranslated region. In addition, the 5' promotor region, 1146 bp upstream from the ATG translation initiation site, has been sequenced and characterized (Mahajna *et al*, 1995; fig 7.3).

7.6 RESULTS:

7.6.1 Haplotype analysis of PRKCG in ADRP5:

An Msp1 polymorphism that is detected by a PRKCG cDNA probe was found to segregate with the adRP phenotype in ADRP5 (see section 5.2.6; fig 5.4). It confirms the previous localization of PRKCG gene to 19q13.2-q13.4 (Coussens *et al.*, 1986; Johnson *et al.*, 1988) and further refines its localization to a 3 cM interval between D19S572 and AFMc001yb1. This interval is part of the region between D19S180 and AFMc001y1 which contains the RP11 locus.

7.6.2 Designing primers from the cDNA sequence:

So far the *Drosophila* PKC was the only PKC gene for which the genomic structure with intron exon boundaries was defined (Rosenthal *et al.*, 1987). The splice junctions separating exons 1,2 and 3 of this Drosophila PKC are exactly conserved in human PKCB (Mahajna *et al.*, 1995). On the assumption that intron position in the PRKCG gene might be similarly conserved,

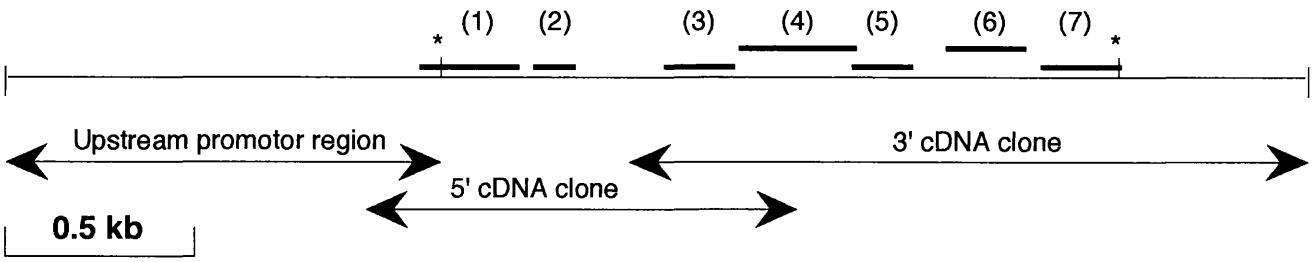

Figure 7.3

A diagram of the PKC cDNA sequence showing the three partial cDNA clones of PRKCG gene as described in the text. * denotes the positions of both the ATG translation initiation site and the stop codon. The PCR fragments that were designed using cDNA primers are numbered from 1-7.

the amino acid sequences of the drosophila and human genes were aligned approximately by eye, and primers were selected to amplify exon sequences which, on this basis, would not be interupted by introns. By the alignment of PKCB and PRKCG sequences, it was also taken into consideration that the selected primers also contain the maximum number of PRKCG specific nucleotides.

7.6.3 Mutation screening of PRKCG:

Seven such primer sets were designed, defining fragments 1-7 in figure 7.3. Primer pairs 1, 2, 3, and 5 gave the expected fragment size of the amplified cDNA fragment. Fragments 6 and 7 gave larger sizes than expected from the cDNA sequence, indicating that introns may have been incorporated within the amplified fragment. Fragment 4 did not amplify, suggesting that the cDNA sequence may be interrupted by a large intron(s), or that the primer sequence itself was interrupted by an intron.

The four fragments (1, 2, 3, and 5) which gave the expected sizes were amplified from 2 affected individuals from each of 14 adRP families, including ADRP5 and ADRP29 (described in chapters 5 and 6), and from 5 normal controls. PCR products were screened for mutations using the heteroduplex analysis method described in chapter 3. All four fragments gave banding patterns inconsistent with homoduplex PCR products in all adRP and control samples. This is probably due to nonspecific amplification of other PKC genes which are conserved and therefore homologous across the amplified region (fig 7.4).

To detect mutations that include large rearrangements (few kilobases), Southern blots of DNA digested with BamHI, MspI, TaqI, and HaeIII were prepared from the 14 adRP families, each of which was represented by one affected and one normal member. These blots were hybridized with PRKCG cDNA probe, and no significant rearrangements were detected. (For the sake of urgency this work was done by another member of the laboratory).

7.7 DISSCUSSION:

The aim of the preliminary screening was to rapidly detect a mutation in the PRKCG gene in ADRP5 or other adRP families. No mutation was detected either by Southern blotting or by heteroduplex analysis. This could be due to a genuine absence of mutations in PRKCG. However, the screen was flawed in several ways. PKC is a gene family, members of which are

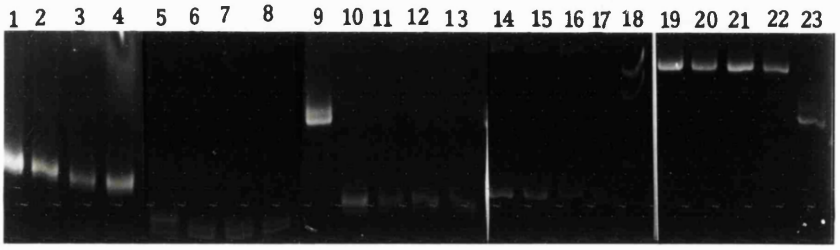

Figure 7.4:

MDE gel photograph of PCR products of PRKCG fragments 1 (lanes 1-4), 2 (lanes 5-8), 3 (lanes 10-13), 5 (lanes 14-17), and 6 (lanes 19-22) described in figure 7.3. Lanes 9 and 23 are positive controls from the rhodopsin gene. Lane 18 contains a size marker with fragment sizes shown from top to bottom 310, 271/281, 234, 194, 118, and 72bp.

highly homologous at both the amino acid and the nucleotide levels (Hug and Sarre, 1993). In such a case, the highest homology would be detected in the coding regions (exonic sequences). This could explain the multiple bands seen in all adRP and control individuals using exonic primers, as these primers could have amplified sequences from several genes from the PKC gene family. Only sequencing the whole gene and identification of intron-exon boundaries, will allow specific amplification from the the PRKCG gene using intronic primers. This will maximize the chances for mutation detection by the available methods. However, only sequencing the whole gene in patients from ADRP5 and other adRP families will ensure its exclusion from the causation of RP11. This work is now being done and some of the introns have already been sequenced.

Despite the fact that PKC appears to be a good candidate gene, further review of the literature has revealed evidence that it is a less likely candidate than had initially been thought. Immunocytochemical studies have failed to localize any of the known PKC isoenzymes to the ROS (Usada *et al.*, 1991; Osborne *et al.*, 1992; Ghalayini *et al.*, 1994; Osborne *et al.*, 1994). However one can argue that the antisera used to detect the expression pattern of PKC isoenzymes in most of these studies were directed against the carboxyl terminal of the protein (Ghalayini *et al.*, 1994; Osborne *et al.*, 1994). Assuming that the PRKCG expressed in the ROSs has an alternative 5' splice site, it might not have been detected using such antisera. Differential splicing of a single gene has already been found to contribute to the diversity seen in PKC isoenzymes (Ono *et al.*, 1987). Furthermore, alternative splicing was suggested in PRKCG itself as two mRNA species, a major species of 3.1 kb and a minor of 2.4 kb, were isolated from bovine cerebellum (Coussens *et al.*, 1986).

Another line of evidence specifically against the involvement of PRKCG in retinal degeneration is that PKCγ mutant mice, produced by gene knockout, were shown to exhibit mild deficits in spatial and contextual learning, but with no visual difficiencies. If PRKCG is to be involved in RP11 disease causation, this observation could be explained by several hypothesis. These mice could have some sort of visual problems which were not tested for, and indeed the learning deficits could be due, in part, to these problems. For example, peripherin/RDS mutations in humans are known to cause a relatively severe form of dominant retinal degenerations, while heterozygous mutations in the mouse homologue of this gene (*rds*) were found to cause a mild phenotype which was only detected by histological and electroretinographic examinations. Alternatively, a gene mutation may have no phenotypic

consequence in one species relative to another e.g. the *mdx* mouse harboring a mutation in the dystrophin gene is very similar in phenotype to normal litter mates. Another hypothesis would be that the RP11 phenotype is characterized by bimodal expression form of incomplete penetrance where obligate carriers remain normal for their entire life (see section 6.3.3) and that this particular mouse model of PRKCG gene knockout represents the nonpenetrant form of the disease. Therefore, although these lines of evidence suggest that the PRKCG is a less likely candidate gene, they do not exclude it from the causation of RP11 phenotype.

Finally, this study resulted in a fine localization of PRKCG to within a 3 cM interval between D19S572 and AFMc001yb1, in the 19q13.4 band and supports the previous *in situ* localization to 19q13.2-q13.4 (Coussens *et al.*, 1986; Johnson *et al.*, 1988). The finer localization will help in relating the two genome maps produced by Genethon and NIH/CEPH (see section 4.4) since PRKCG was used as an anchor marker on both maps.

CHAPTER VIII

GENERAL DISCUSSION AND FUTURE PROSPECTS

8.1 ADVANCES IN MOLECULAR BIOLOGY TECHNIQUES AND THEIR IMPLICATIONS FOR THE STUDY OF RETINAL DEGENERATION:

In the last few years, many of the recent developments in DNA technologies in general and human molecular genetics in particular have been applied successfully in the study of RP. They have led to a greater understanding of the underlying mechanisms of pathogenesis in this group of retinal degenerations, and to the localization and further characterisation of many of the underlying genetic loci (Bird, 1995; Rosenfeld *et al.*, 1994).

Family linkage analysis is one of the most powerful methods for mapping disease genes in humans. Recent studies of the human genome have been revolutionized with the discovery of simple sequence repeat polymorphisms, particularly $(CA)_n$ repeats, and construction of high resolution genome maps. The development of statistical methods and the utilization of computer programs have accelerated the construction of such maps. The NIH/CEPH (1992) map has put together the data of many independent genome mapping groups. The Genethon (Weissenbach *et al.*, 1992; Gyapay *et al.*, 1994) map came after the NIH/CEPH map and introduced a highly informative and completely new set of $(CA)_n$ microsatellites which covered more than 90% of the human genome; it contains more than 2000 markers at an average density of one every 2 cM. These advances in genome maps and linkage analysis made it possible to have a comprehensive view of the human genome. Such a view is crucial for designing efficient strategies for screening the human genome in search of loci implicated in human diseases, and has provided speed and accuracy in mapping such disease genes. In fact since the construction of such genome maps a large number of human disease genes in general and visual disease genes in particular have been localized to specific chromosomal regions (Bird, 1995; Humphries *et al.*, 1992; Rosenfeld *et al.*, 1994).

In addition to dinucleotide repeats, efforts are now being made to establish a tri- and tetranucleotide microsatellite genome map (Businga *et al.*, 1994). These microsatellites are

easier to score as they do not have what is believed to be the replication slippage products of dinucleotide repeats (see section 4.7.4). This will assist in the increased automation of the linkage analysis process. Additionally, the involvement of trinucleotide repeat expansions in several human disorders (e.g. Huntington disease and fragile X syndrome) make them of special interest as more of them may be associated with other human diseases of unknown aetiology.

In addition to the YAC (yeast artificial chromosome) and cosmid contigs of various chromosomes undertaken by several groups (e.g. Trask *et al.*, 1993), the first Genethon physical map of the human genome has already been established (Cohen *et al.*, 1993). It contains YAC clones representative of most of the genome and can be used whenever genetically defined regions of interest need to be isolated for gene identification purposes. Moreover, efforts are now being made to constuct genome maps of tissue specific expressed sequence tags (ESTs). In the near future, a genome directory containing the latest catalogue of ESTs and refined versions of the physical map of the human genome is on its way for puplication (Maddox, 1995). This directory will contain more than 55,000 ESTs corresponding to genes in the human genome from more than 30 different tissues. Relating these genes to Cohen's physical map will create an invaluable resource for identification of human disease genes. With the increasingly detailed genetic and physical maps, the positional candidate approach (Collins, 1995) will soon replace the lengthy process of positional cloning. Positional candidate approach relies on genetically localizing a disease gene to a chromosomal subregion by linkage analysis, assembling a physical contig across the region from the available physical maps, and searching databases for suitable candidate genes (ESTs) within that contig, and testing those candidate genes for disease causing mutations. The availability of such resources in the near future should speed up the process of disease gene identification to a rate that should match the rate of disease gene mapping by linkage analysis.

8.1.1 Heterogeneity in retinal degenerations revealed by such advances:

In the last few years the number of mapped disease genes in general and ophthalmic disease genes in particular have greatly increased. In total, 16 genetic loci are now known to be involved in the pathogenesis of RP as medelian single gene inheritance or digenic inheritance (see section 1.7.1). The large number of mapped loci for syndromic forms of RP suggests even greater genetic heterogeneity. Further complexity within these retinal degenerations exists as a

result of allelic heterogeneity. In addition to causing 20% of adRP, the gene for rhodopsin has been found to cause arRP and dominant CSNB. The peripherin/RDS gene, which is expressed in both rods and cones, has been found to cause both peripheral and central visual impairement resulting in adRP and several types of macular degenerations (Bird, 1995; Rosenfeld *et al.*, 1994). Together with ROM1, this gene has been found to cause digenic RP. In addition to causing arRP, the gene for PDEB has been involved in a dominant form of CSNB (Gal *et al.*, 1994). Recently a rare recessive form of CSNB, known as Oguchi disease, has been found to be caused by mutations in the gene encoding arrestin (Fuchs *et al*, 1995; see section 1.4.7). Furthermore, the two X-linked CSNB loci were mapped to regions of RP2 and RP3, suggesting possible allelic heterogeneity at these loci too. This extensive heterogeneity is still increasing with the mapping of new retinal disease genes. The rate of mapping such genes is only limited by the availability of families in which such mapping is to be performed. However problematic, (see section 8.5), this heterogeniety in retinal degenerations will lead to the characterization of many retinally expressed genes, of which a proportion may be retinal specific, and therefore improve our understanding of the normal development and physiology of the retina as well as visual function. This should also contribute to our understanding of more complex retinal degenerations such as ARMD (see section 1.7.2.1) and simplex RP.

8.2 LINKAGE STUDIES OF RECESSIVE AND COMPLEX TRAITS: IMPLICATIONS FOR RP RESEARCH:

Disease gene mapping of recessive traits by conventional linkage analysis is seriously limited by the family size. About 23% of RP families in the United Kingdom inherit the disease in a recessive form (Bundy and Crews, 1984). Most of these are two generation families (parents and children) which are, in most instances, not sufficient to give satisfactory linkage results. To overcome this problem in RP and other recessively inherited diseases, an effecient strategy has been devised to map such traits without the requirement of large families. This method relies on the homozygosity by descent, due to inbreeding, of the region containing a particular recessive trait. Searching for such regions would be expected to provide a powerful method for mapping such genes in inbred families needing only a single affected individual from each family (Lander and Botstein, 1987). Homozygosity mapping in larger families has been greatly facilitated by the use of a DNA pooling strategy (Preising *et al.*, 1994). This involves pooling the DNA from all affected individuals within a family in one reaction tube (test DNA) and the DNA from normal individuals in another (control DNA), and the subsequent use of such

pooled DNAs as templates for PCR analysis of highly polymorphic microsatellite markers. If a marker is closely linked to a disease gene where no recombination is expected to take place between the two loci, a single band corresponding to the linked allele will be amplified in the test DNA. The control DNAs should show a wide range of bands corresponding to the range of alleles that the marker exhibits in the normal population. This approach has been efficiently used to map a number of human recessive diseases such as Bardet-Biedl syndrome (Sheffield *et al.*, 1994) and a locus for human obesity syndrome on chromosome 15 (Carmi *et al.*, 1995).

It is anticipated that with the current advances in gene mapping strategies, all the loci for single gene disorders will soon be identified. However, the majority of human diseases in general and RP cases in particular are of complex aetiology (simplex RP) which might involve a combination of a number of genetic and environmental factors (multifactorial disorders). Several methods have been developed for mapping such traits. These methods are necessarily similar in principle, and involve the search for a genomic region which has been transmitted through one or several generations to related individuals having the same disorder or phenotype. Affected sib-pair analysis is one such method that has been used to map various multifactorial susceptibility loci such as those for insulin dependent diabetes mellitus (IDDM; Davies *et al.*, 1994) and a locus for sexual orientation (Hamer *et al.*, 1993). Genomic mismatch scanning (Nelson *et al.*, 1993) is another method that can be used to scan the whole genome for regions of identity by descent between related individuals separated by several generations and have the same phenotype (e.g. grandparents and grandchildren). This method could be used to map both single gene disorders and multifactorial susceptibility loci. These methods should allow the mapping and identification of the genes involved in recessive, multigenic, and simplex RP cases. Since these are thought to constitute the majority of RP cases, such approaches are expected to contribute to mapping the majority of RP genes. Identification of such genes could have an immense effect on the basic understanding of eye function and pathogenesis of eye diseases and could contribute to the prevention and treatment of many retinal degeneration disorders.

8.3 PATHOGENESIS OF RP AND MECHANISMS OF RETINAL DEGENERATION:

So far mutations in several genes have been found to cause RP. Speculation have been made to how such mutations could disrupt the function of the photoreceptor at the molecular level and therefore give rise to an RP phenotype. A mutation which give rise to a null allele of the rhodopsin gene (Rosenfeld *et al.*, 1992) has been found to cause arRP. The product of one

normal copy of rhodopsin gene might therefore be enough for phototransduction in heterozygote individuals. However, homozygotes for the null allele would be expected to have an early and severe form of the disease, which is consistent with the autosomal recessive inheritance seen in the family with this rhodopsin mutation. On the other hand, mutations in this gene that result in the accumulation of 50% of rhodopsin in an abnormal form within the photoreceptor cell could have a drastic effect on its function, which might give rise to the dominant form of RP seen with most rhodopsin mutations. This suggests that in most rhodopsin RP, the presence of the abnormal rhodopsin molecules rather than the absence of a proportion of the normal molecules actually causes the RP phenotype. Rhodopsin mutations that affect the salt bridge formation between Lys296 and Glu113 result in severe desensitization of the rod cell (see section 3.5.4) which give rise to CSNB.

Peripherin/RDS gene, a structural protein of both rod and cone photoreceptors, is involved in outer segment morphogenesis and stabilization of the rod discs and cone lamelli (see section 1.6.1). ROM1, a rod specific protein with homology to perirherin/RDS, was found to play a critical role in the biogenesis of the discs and in maintaining the structure of the ROS (see section 1.6.2). Noncovalent interaction between Peripherin/RDS and ROM1 is also involved in the stabilitiy of the ROS. A mutation in the mouse *rds* gene was found to have a semidominant effect where homozygotes have a severe form of retinal dystrophy and fail to form outer segments, while heterozygotes form a rudimentary type of outer segments and have a milder phenotype. Mutations in both peripherin/RDS and ROM1 genes in humans were also found to cause retinal degeneration, probably by compromising the structural integrity of the outer segments of photorecptors.

Mutations in the PDEB, PDEA, and cGMP-gated channel genes cause human arRP. Genes, which code for enzymes or proteins involved in cellular function can be classical examples of autosomal recessive inheritance since the presence of half dose should be sufficient for normal functioning of the cell. The complete absence of cGMP-PDE activity in homozygous individuals for mutations in either the PDEB or PDEA, or the absence of the functional channel protein in the membrane are expected to impair phototransduction, the consequence of which could result in photoreceptor cell degeneration.

The biochemical basis for incomplete penetrance in some forms of retinitis pigmentosa is unknown. Modifier genes are genes capable of modifying the manifestations of a mutant gene

without having an obvious effect on a normal individual (Gruneberg, 1963). Such genes constitute the "genetic background" in which the mutant gene finds itself (Romeo and McKusick, 1994). In humans, modifier genes can not be easily identified, although their action is often suspected. A polymorphism can modify both qualitatively and quantitatively the phenotypic expression of a pathogenic mutation. This phenomenon may yield clues to understanding the molecular basis of incomplete penetrance and/or variable expressivity seen in a proportion of RP families. The bimodal expression in RP11 (chromosome 19 linked) families suggest the involvement of modifier genes that give rise to the "all or none" expression of the disease phenotype. The digenic form of RP caused by ROM1-peripherin/RDS mutations represent a simple form of such interaction. Digenic inheritance could also be involved in a proportion of two generation families (normal parents who have multiple affected children) that are often classified as having autosomal recessive transmission. Tri, tetra or multigenic inheritance could also be involved in these families or in the large fraction of simplex RP cases. Biochemically it has been suggested that the products of such genes should be functionally related. Although environmental factors do not appear to play a significant role in RP pathogenesis (Heckenlively, 1988), their contribution to the variable expression or incomplete penetrance seen in RP can not be excluded.

In summary the mechanism by which mutations in various RP genes result in disruption of the phototransduction process, or compromise the structural integrity of the photoreceptors are largely speculative. Also the mechanism by which these mutations trigger the degenerative process in photoreceptor cells is still unknown. However, recently apoptosis has been proposed as a possible mechanism by which photoreceptors degeneration may occur.

8.3.1 Apoptosis: a common mechanism of photoreceptor cell death ?

One characteristic common to the phenotypes of three extinsively studied mouse models of retinal degeneration (*rd*, *rds*, and rhodopsin Pro347-Ser transgenic mice) is the lack of an inflammatory response despite the large number of degenerated photoreceptors. This observation is consistent with a form of cell death known as apoptosis (Kerr and Harmon, 1991). Programmed cell death (PCD) refers to the stereotypic loss of individual cells at specific times during development (Ellis *et al.*, 1991) and is also termed histogenetic cell death. Apoptosis is a kind of PCD with certain characteristics that include membrane blebbing, chromatin condensation and DNA fragmentation (Wyllie *et al.*, 1984; Kerr and Harmon, 1991). DNA fragmentation in apoptosis occurs in a specific pattern containing 180-200 bp multiples. The

minimal 180-200 bp fragment represents the length of DNA that wraps around a histone octamer in a single nucleosome (Stryer, 1988). The fragments are formed by cleavage of DNA that links multiple nucleosomes. The presence of the 180-200 bp ladder in agarose gels is considered diagnostic for cell death by apoptosis. This is distinct from cell death by necrosis or accidental cell death which form a spectrum of DNA fragment sizes without evidence of a nucleosomal ladder (Kerr and Harmon, 1991). Such a mechanism is normally used by retinal cells during development to fine tune the number of cells in the retina and their interconnections (Young, 1984).

Although the initial mechanisms of pathogenesis in the three studied mouse models are different, it appears that a final common pathway of apoptosis mediates their photoreceptor cell death (Wong, 1993). However the mechanism by which each mutation triggers apoptosis of photoreceptors is still largly unknown. Internucleosomal DNA fragmentation is thought to be mediated by a nuclear endonuclease that can be triggered by a rise in Ca^{+2} ions (Li *et al.*, 1994). A number of genes have been implicated or found to play an important role in apoptosis (Wong *et al.*, 1994). More understanding of the genetic and biochemical basis of apoptosis could lead to the design of new strategies for the prevention of such cell death which include both normal and abnormal photoreceptors.

8.4 IMPLICATIONS FOR RP SUFFERERS:

With the large extent of both clinical and genetic heterogeneity seen in retinal degenerations, diagnosis and counselling of RP patients and their families have become more complicated. In more than 50% of RP with family history, the mode of inheritance can help in classifying the disease. However a great deal of heterogeneity still exists within each group. Genetic counselling in such cases would be unreliable unless the disease locus within a particular family is mapped, or the mutation in the family is identified. However, in many cases an individual family will not be large enough to test by linkage analysis, while allelic heterogeniety complicates mutation search in known genes. In rhodopsin, for example, most of the 87 mutations identified (table 3.1) are family specific. Therefore it may not be practical to apply routine family screening and diagnostic methods to identify possible novel mutations in each RP family or simplex patients.

The ultimate goal in dealing with retinal degeneration patients is the ability to offer them

treatment. There is no environmental, dietary, or drug therapy for the primary RP process in all the forms of classical RP so far studied. Gene therapy is therefore an option which is being examined. This will involve gene replacement in recessively inherited forms of RP and the anti-sense gene therapy which aims to correct dominantly inherited forms of RP. However, given the large number of genes and mutations within each gene that cause RP, strategies of gene therapy aimed at correcting each individual mutation may be an overwhelming task. In contrast, strategies aimed at introducing a gene that would interfere with the cells ability to carry out apoptosis may be a more practical approach as it would be applicable to multiple mutations and genetic types.

8.5 FUTURE WORK RELATED TO THIS PROJECT:

Subsequent to the mapping of the new RP11 locus to chromosome 19, and refinement of the locus to a 5 cM region, the next step will be to identify the disease gene within this interval. The candidate gene approach could offer a short cut to this aim. Therefore, future work will include sequencing and characterization of the genomic structure of the PRKCG gene which is in the right genetic interval for RP11, and mutation screening of this gene in RP11 linked families and other recessive and simplex RP cases (see chapter 7). Only when this gene is excluded, further efforts should be undertaken to genetically reduce the region to a smaller interval. This could be done by mapping more families to the RP11 locus. After further refinement of the genetic interval, a physical map of the region will be constructed by identification of overlapping YAC and/or cosmid clones with markers and STSs flanking and within the disease interval. This should allow the testing of other genes mapping in the region and searching for new expressed sequences. cDNA selection, exon trapping, and direct sequencing may be used in such search. Identification of CpG islands might also help in defining gene containing regions within the interval. New candidate genes will be characterized and screened for mutations in RP11 families. The fact that chromosome 19 is gene rich might complicate this approach. However the telomeric location of the RP11 interval may suggest that it is physically much smaller than it appears genetically. Since several adRP families were mapped to the RP11 locus, this may increase the chances of finding a mutation in a particular candidate gene. Once the mutation is identified, the gene will be fully characterized including upstream and promotor regions. Further work will include characterization of the mutated protein and the possible mechanisms by which it leads to photoreceptor cell degeneration. Construction of transgenic mice model of such a gene might further unravel the genotype-

phenotype relationship, and further our understanding of the normal function of such gene in the context of the whole eye. It would also provide an animal model for therapeutic trials including gene therapy.

REFERENCES:

Al-Maghtheh M., Gregory C., Inglehearn C., Hardcastle A. & Bhattacharya S. (1993). Rhodopsin mutations in autosomal dominant retinitis pigmentosa. Hum. Mutation 2: 249-255.

Al-Maghtheh M., Kim R.Y., Hardcastle A., Inglehearn C. & Bhattacharya S.S. (1993). A 150bp insertion in the rhodopsin gene of an autosomal dominant retinitis pigmentosa family. Hum. Mol. Genet. 3: 205-206.

Al-Maghtheh M., Inglehearn C., Lunt P., Jay M., Bird A. & Bhattacharya S. (1994). Two new rhodopsin transversion mutations (L40R; M216K) in families with autosomal dominant retinitis pigmentosa. Hum. Mutation 3: 409-410.

Al-Maghtheh M., Inglehearn C.F., Keen T.J., Evans K., Moore A.T., Jay M., Bird A.C. & Bhattacharya S.S. (1994). Identification of a sixth locus for autosomal dominant retinitis pigmentosa on chromosome 19. Hum. Mol. Genet. 3: 351-354

Anderson D.H. & Fisher S.K. (1976). The photoreceptors of diurnal squirrels: outer segment disc shedding and protein renewal. J. Ultrastruct. Res. 55: 119. (Bok paper 35)

Andreasson S., Ehinger B., Abrahamson M. & Fex G. (1992). A six generation family with autosomal dominant retinitis pigmentosa and a rhodopsin gene mutation (arginine-135-leucine). Ophthalmol. Paed. Genet. 13: 145-153.

Antinolo G., Sanchez B., Borrego S., Rueda T., Chaparro P. & Cabeza J. (1994). Identification of a new mutation at codon 171 of rhodopsin gene causing autosomal dominant retinitis pigmentosa. Hum. Mol. Genet. 8: 1421.

Apfelstedt-Sylla E., Kunisch M., Horn M., Ruther K., Gal A. & Zrenner E. (1992). Diffuse loss of rod function in autosomal dominant retinitis pigmentosa with Pro-347-Leu mutation of rhodopsin. German J. Ophthalmol. 1: 319-327.

Apte S.S., Mattei M.G., & Olsen B.R. (1994). Cloning of the cDNA encoding human tissue inhibitor of matalloproteinases-3 (TIMP-3) and mapping of the TIMP-3 gene to chromosome 22. Genomics 19: 86-90.

Arikawa K., Molday L.L., Molday R.S. & Williams D.S. (1992). Localization of peripherin/rds in the disc membranes of cone and rod photoreceptors: relationship to disc membrane morphogenesis and retinal degeneration. J. Cell Biol. 116: 659-667.

Artlich A., Horn M., Lorenz B., Bhattacharya S. & Gal A. (1992). Recurrent 3-bp deletion at codon 255/256 of the rhodopsin gene in aGerman pedigree with autosomal dominant retinitis pigmentosa. Am. J. Hum. Genet. 50: 876-878.

Attwood J. & Bryant S. (1988). A computer programe to make analysis with LIPED and LINKAGE easier to perform and less prone to input errors. Ann. Hum. Genet. 52: 259.

Baehr W., Devlin M.J. & Applebury M.L. (1979). Isolation and characterization of cGMP phosphodiesterase from bovine rod outer segments. J. Biol. Chem. 245: 11669-11677.

Baehr W., Morita E.A., Swanson R.J. & Applebury M.L. (1982). Characterization of bovine rod outer segment G-protein. J. Biol. Chem. 257: 6452-6460.

Baird P.A., Anderson T.W., Newcombe H.B. & Lowry R.B. (1988). Genetic disorders in children and young adults: a population study. Am. J. Hum. Genet. 42: 677-93.

Baldwin J.M. (1993). The probable arrangement of the helices in G protein-coupled receptors. EMBO J. 12: 1693-1703.

Bardien S., Ebenezer N., Greenberg J., Inglehearn C.F., Bartmann L., Goliath R., Beighton P., Ramesar R. & Bhattacharya S. (1995). An eighth locus for autosomal dominant retinitis pigmentosa is linked to chromosome 17q. Hum. Mol. Genet. 4: 1459-1462.

Bascom R.A., Manara S., Collins L., Molday R.S., Kalnins V.I. & McInnes R.R. (1992). Cloning of the cDNA for a novel photoreceptor membrane protein (rom-1) identifies a disk rim protein family implicated in human retinopathies. Neuron 8: 1171-1184.

Bashir R., Inglehearn C.F., Keen T.J., Lindsay J., Atif U., Carter S.A., Stevenson A.M., Jackson A., Jay M., Bird A.C., Papiha S.S. & Bhattacharya S.S. (1992). Exclusion of chromosome 6 and 8 in nonrhodopsin autosomal dominant retinitis pigmentosa families: further locus heterogeneity in adRP. Genomics **14**: 191-193.

Basinger S., Bok D. & Hall H. (1976). Rhodopsin in the rod outer segment plasma membrane. J. Cell Biol. 69: 29-42.

Bauer P.H., Muller S., Puzicha M., Pippig S., Obermaier B., Helmreich E.J. & Lohse M.J. (1992). Phosducin is a protein kinase A-regulated G-Protein regulator. Nature 358: 73-76.

Beckmann J.S. & Weber J.L. (1992). Survey of human and rats microsatellites. Genomics 12: 627-631.

Begy C. & Bridges C.D. (1990). Nucleotide and predicted protein sequence of rat retinal degeneration slow (rds). Nucl. Acids Res. 18: 3058.

Bell C., Converse C.A., Collins M.F., Esakowits L., Kelly K.F. & Haites N.E. (1992). Autosomal dominant retinitis pigmentosa (ADRP) - A rhodopsin mutation in aScottish family. J. Med. Genet. 29: 667-668.

Berman E.R. (1991). Biochemistry of the Eye. Ed. C. Blakemore. Plenum Press, New York.

Berson E.L. & Howard J. (1971). Temporal aspects of the electroretinogram in sector retinitis pigmentosa. Arch. Ophthalmol. 86: 653-365.

Berson E.L. & Simonoff E.A. (1979). Dominant retinitis pigmentosa with reduced penetrance. Further studies of the electroretinogram. Arch. Ophthalmol. 97: 1286-91.

Berson E.L., Rosner B., Sandberg M.A. & Dryja T.P. (1991). Ocular findings in patients with autosomal dominant retinitis pigmentosa and a rhodopsin gene defect (Pro-23-His). Arch. Ophthalmol. 109: 92-101.

Berson E.L. (1992). Electrical phenomena in the retina. In: *Adlers's Physiology of the Eye.* p641-707. Ed. William.M. Hart. Mosby-Year Book,Inc.

Best F.Z. (1905). Uber eine Hereditare Maculaaffektion: Beitrage zur Vererbungslehre. Augenheilkd. 13: 199-212.

Bhattacharya S.S., Wright A.F., Clayton J.F., Price W.H., Phillips C.L., McKeown C.M., Bird C.M., Pearson R.L., Southern E.M. & Evans H.J. (1984). Close genetic linkage between X-linked retinitis pigmentosa and a restriction fragment length polymorphism identified by recombinant DNA probe L1.28. Nature 309: 253-255.

Bhattacharya S.S., Inglehearn C.F., Keen J., Lester D., Bashir R., Jay M. & Bird A.C. (1991). Identification of novel rhodopsin mutations in patients with autosomal dominant retinitis pigmentosa. Invest. Ophthalmol. Vis. Sci. 32 (suppl.) 890.

Bird A.C. (1975). X-linked retinitis pigmentosa. Br. J. Ophthalmol. 59: 177-199.

Bird A.C. (1988). Clinical investigation of retinitis pigmentosa. Aus. and N.Z. J. Ophthalmol. 16: 189-198.

Bird A.C. (1995). Retinal photoreceptor dystrophies. Am. J. Ophthalmol. 119: 543-562.

Blanton S.H., Heckenlively J.R., Cottingham A.W., Freidman J., Sadler L.A., Wagner M., Freidman L.H. & Daiger S.P. (1991). Linkage mapping of autosomal dominant retinitis pigmentosa (RP1) to the pericentric region of human chromosome 8. Genomics 11: 857-869.

Bok D. (1985). Retinal photoreceptor-pigment epithelium interactions. Invest. Ophthalmol. Vis. Sci. 26: 1659-1694.

Bokhoven H.V., Genderen C.V., Molloy C.M., van de Pol D.J.R., Cremers C.W.R.J., Aarem A.V., Schwarts M., Rosenberg T., Geurts-Kessel A.H.M., Ropers H. & Cremers F.P.M. (1994). Mapping of the choroideremia-like (CHML) gene at 1q42-qter and mutation analysis in patients with Usher syndrome type II. Genomics 19: 385-387.

Bonneau D., Raymond F., Kremer C., Klossek J.M., Kaplan J. & Patte F. (1993). Usher syndrome type 1associated with bronchiectasis and immotile nasal cilia in two brothers. J. Med. Genet. 30: 253-254.

Botstein D., White R.L., Skolnick M. & Davis R.W. (1980). Construction of a genetic linkage map using restriction fragment length polymorphisms. Am. J. Hum. Genet. 32: 314-331.

Boughman J.A., Confally P.M. & Nance W.E. (1980). Population genetic studies of retinitis pigmentosa. Am. J. Hum. Genet. 32: 223-235.

Bourne H.R., Sanders D.A. & McCormick F. (1990). The GTPase superfamily: a conserved switch for diverse cell function. Nature 348: 125-132.

Bourne H.R., Sanders D.A. & McCormick F. (1991). The GTPase super family: conserved structure and molecular mechanisms. Nature 349: 117-127.

Bowes C., Li T., Danciger M., Baxter L.C., Applebury M.L. & Farber D.B. (1990). Retinal degeneration in the *rd* mouse is caused by a defect in the β subunit of rod cGMP-phosphodiesterase. Nature 347: 677-680.

Brandt S.J., Niedel J.E., Bell R.M. & Scott-Young W. (1987). Distinct patterns of expression of different protein kinase mRNAs in rat tissue. Cell 49: 57-63.

Brown S.D.M. & Steel K.P. (1994). Genetic deafness- progress with mouse models. Hum. Mol. Genet. 3: 1453-1456.

Bundy S. & Crews S.J. (1984). A study of retinitis pigmentosa in the city of Birmingham. II. Clinical and genetic heterogeneity. J. Med. Genet. 21: 421-428.

Bunge S., Wedemann H., David D., Terwilliger D.J., Van Den Born L.I., Aulehla-Schols C., Samanns C., Horn M., Ott J., Schwinger E., Schinzel A., Denton M.J. & Gal A. (1993). Molecular analysis and genetic mapping of the rhodopsin gene in families with autosomal dominant retinitis pigmentosa. Genomics 17: 230-233.

Bunker C.H., Berson E.L., Bromley W.C., Hayes R.P. & Roderick T.H. (1984). Prevalence of retinitis pigmentosa in Maine. Am. J. Ophthalmol. 97: 357-365.

Businga T., Beck J.S., Sunden S.L.F., Duyk G.M., Murray J.C., Weber J.L., Buetow K.H. & Sheffield V.C. (1994). Assignment of 1000 tri and tetranucleotide repeats to chromosomes by somatic cell hybrid analysis. Am. J. Hum. Genet. 55 (suppl.): A182 (abstract no. 1053).

Carmi R., Rokhlina T., Kwitek-Black A., Elbedour K., Nishimora D., Stone E. & Sheffield V. (1995). Use of a DNA pooling strategy to identify a human obesity syndrome locus on chromosome 15. Human Mol. Genet. 4: 9-13.

Cech T.R. (1986). The generality of self-splicing RNA: relationship to nuclear mRNA splicing. Cell 44: 207-210.

Chen C.-K. & Hurley J.B. (1994). Calcium-dependent recoverin/rhodopsin kinase interaction. Invest. Ophthalmol. Vis. Sci. 35 (suppl.): 1485 (abs. no. 1067).

Chen T.-Y., Peng Y.-W., Dhallan R.S., Ahamed B., Reed R.R. & Yau K.-W. (1993). A new subunit of the cyclic nucleotide-gated cation channel in retinal rods. Nature 362: 764-767.

Clark J.M. (1988). Novel non-templated nucleotide addition reactions catalysed by procaryotic and eukaryotic DNA polymerases. Nucleic Acids Res. 16: 9677-9686.

Cohen A.I., (1983). Some cytological and initial biochemical observations on photoreceptors in retinas of rds mice. Invest. Ophthalmol. Vis. Sci. 24, 832-843.

Cohen D., Chumakov I. & Weissenbach J. (1993). A first-generation physical map of the human genome. Nature 366: 698-701.

Collins F.S. (1995). Positional cloning moves from perditional to traditional. Nature Genet. 9: 347-350.

Conneally P.M., Edwards J.H., Kdd K.K., LalouelJ.-M., Morton N.E., Ott J. & White R. (1985). Reports of the committee on methods of linkage analysis and reporting. Cytogenet. Cell Genet. 40: 356-359.

Connell G.J. & Molday R.S. (1990). Molecular cloning, primary structure, and orientation of the vertebrate photoreceptor cell protein peripherin in the rod outer segment disc membrane. Biochem. 29:4691-4698.

Connell G., Bascom R., Molday L., Reid D., McInnes R.R. & Molday R.S. (1991). Photoreceptor peripherin is the normal product of the gene responsible for retinal degeneration in the rds mouse. Proc. Natl. Acad. Sci. USA 88: 723-726.

Cook N.J., Hanke W. & Kaupp U.B. (1987). Identification, purification, and functional reconstitution of the cGMP-dependent channel from rod photoreceptors. Proc. Natl. Acad. Sci. USA 84: 585-589.

Cook N.J., Molday L.L., Reid D., Kaupp U.B. & Molday R.S. (1989). The cGMP-gated channel of bovine rod photoreceptors is localized exclusively in the plasma membrane. J. Biol. Chem. 264: 6996-6999.

Copeland N.G., Jenkins N.A., Gilbert D.J., Eppig J.T., Maltais L.J., Miller J.C., Dietrich W.F., Weaver A., Lincoln S.E., Steen R.G., Stein L.D., Nadeau J.H. & Lander E.S. (1993). A genetic linkage map of the mouse: Current applications and future prospects. Science 262: 57-82.

Cotton R.G.H. (1993). Current methods of mutation detection. Mutation Res. 285: 125-144.

Couloumbre A.J. (1969). The eye. Organogenesis Ed: De. Haan and Ursprung. pp: 219-251.

Coussens L., Parker P.J., Rhee L., Yang-Feng T.L., Chen E., Waterfield M.D., Francke U. & Ultrich A. (1986). Multiple distinct forms of bovine and human protein kinase C suggest diversity in cellular signaling pathways. Science 233: 859-866.

Craft C.M. & Lolley R.N. (1994). Expression of phosducin-like proteins in adult human retinas. Invest. Ophthalmol. Vis. Sci. 35: 1577 (no.1492).

Craig J.M. & Bickmore W.A. (1994). The distribution of CpG islands in mammalian chromosomes. Nature Genet. 7: 376-382.

Crawford J.S. & Morin J.D. (1983). *The eye in childhood*; Normal and abnormal developement of the eye. pp1-17. New York: Grune & Stratton, Inc.

Cremers F.P.L., van de Pol D.J.R., van Kerkhoff L.P.M., Wieringa B. & Ropers H.H. (1990). Cloning of a gene that is rearranged in patients with choroideremia. Nature 347: 674-677.

Cremers F.P.L., Molloy C.M., van de Pol D.J.R., van den Hurk J.A.J.M., Bach I., Geurts van Kessel A.H.M. & Ropers H.H. (1992). An autosomal homologue of the choroideremia gene colocalizes with the Usher syndrome II locus on the distal part of chromosome 1q. Hum. Mol. Genet. 1: 71-75.

Curtis D. & Gurling HMD (1993). A procedure for combining two-point lod scores into a summary multipoint map. Hum. Hered. 43: 173-185.

Daiger S.P., Humphries M.M., Sharp E.M., McWilliams P., Farrar G.J., Bradley D.G., McConnel D.J., Kenna P., Sparkes R.S., Spence M.A., Heckenlively J.R. & Humphries P.H. (1989). Linkage analysis of human chromosome 4: Exclusion of autosomal dominant retinitis pigmentosa (ADRP) and detection of new linkage groups. Cytogenet. Cell Genet. 50: 181-187.

Danciger M., Bowes C., Kozak C., LaVail M.M. & Farber D.B. (1990). Fine mapping of a putative *rd* cDNA and its co-segregation with *rd* expression. Invest. Ophthalmol. Vis. Sci. 31: 1427-1432.

Dausset J., Cann H., Cohen D., Lathrop M., Lalouel J.M. & White R. (1990). Program description-Centre d'Etude-Du-Polymorphisme-Humain (CEPH)-Collaborative Genetic-mapping of the human genome. Genomics 6: 575-577.

Davies J.L., Kawaguchi Y., Bennett S.T., Copeman J.B., Cordell H.J., Pritchard L.E., Reed P.W., Gough S.C.L., Jenkins S.C., Palmer S.M., Balfour K.M., Rowe B.R., Farral M., Barnett A.H., Bain S.C. & Todd J.A. (1994). A genome-wide search for human type 1 diabetes susceptibility genes. Nature 371: 130-136.

Denton M.J., Chen J.D., Serraville S., Colley P., Halliday F.B. & Donald J. (1988). Analysis of linkage relationships of X-linked retinitis pigmentosa with the following Xp loci: L1.28, OTC, 754, XJ-1.1, pERT87 and C7. Hum. Genet. 78: 60-64.

DeRouck A., de Bie S., Kayembe D. (1986). Statistical evaluation of visual functions in dominant and recessive autosomal pigmentary retinopathy. Doc. Ophthalmol. 62: 265-280.

DeStefano J.D., Berson E.L. & Dryja T.P. (1994). Evaluation of the arrestin gene in patients with retinitis pigmentosa or an allied disease. Am. J. Hum. Genet. 55 (suppl.): A357 (abstract no. 2097).

Deterre P., Bigay J., Forquet F., Robert M. & Chabre M. (1988). cGMP phosphodiesterase of retinal rods is regulated by two inhibitory subunits. Proc. Natl. Acad. Sci. USA 85: 2424-2428.

Ding C., Li X., Griffin C.A., Jabs E.W., Hawkins A.L. & Levine M.A. (1993). The gene for human phosducin (PDC), a soluble protein that binds G-protein $\beta\gamma$ dimers, maps to 1q25-q31.1. Genomics 18: 457-459.

Dizhoor A.M., Ray S., Kumar S., Niemi G., Spencer M., Brolley D., Walsh K.A., Philipov P.P., Hurley J.B. & Stryer L. (1991). Recoverin: a calcium sensitive activator of retinal rod guanylate cyclase. Science 251: 915-918.

Doi T., Molday R.S. & Khorana H.G. (1990). Role of the intradiscal domain in rhodopsin assembly and function. Proc. Nat. Acad. Sci. USA 87: 4991-4995.

Dolph P.J., Ranganathan R., Colley N.J., Hardy R.W., Socolich M. & Zuker C.S. (1993). Arrestin function in inactivation of G protein-coupled receptor rhodopsin in vivo. Science 260: 1910-1916.

Donders F.C. (1855). Beitrage zur pathologischen anatomie des auges. v. Grafe's Arch. Ophthalmol. 1(2): 106.

Donis-Keller H., Green P., Helms C., Cartinhour S., Weiffenbach B., Stephens K., Keith T.P., Bowden D.W., Smith D.R., Lander E.S., Botstein D., Akots G., Rediker K.S., Gravus T., Brown V.A., Rising M.B., Parker C., Powers J.A., Watt D.E., Kauffman E.R., Bricker A., Phipps P., Muller-Kahle H., Fulton T.R., Ng S., Schumm J.W., Braman J.C., Knowlton R.G., Barker D.F., Crooks S.M., Lincoln S.E., Daly M.J. & Abrahamson J. (1987). A genetic linkage map of the human genome. Cell 51: 319-337.

Dowling J.E. (1987). The retina, an approachable part of the brain. Belknap press/Harvard University Press, Cambridge.

Dratz E.A., Miljanich G.P., Nemes P.P., Gaw J.E. & Schwartz S. (1979). The structure of rhodopsin and its disposition in the rod outer segment disk membrane. Photochem. Photobiol. 29: 661-670.

Dryja T.P., McGee T.L., Reichel E., Hahn L.B., Cowley G.S., Yandell D.W., Sandberg M.A. & Berson E.L. (1990a). A point mutation of rhodopsin gene in one form of retinitis pigmentosa. Nature 343: 364-366.

Dryja T.P., McGee T.L., Hahn L.B., Cowley G.S., Ollsen J.E., Reichel E., Sandberg M.A. & Berson E.L. (1990b). Mutations within the rhodopsin gene in patients with autosomal dominant retinitis pigmentosa. N. Engl. J. Med. 323: 1302-1307.

Dryja T.P., Hahn L.B., Cowley G.S., McGee T.L. & Berson E.L. (1991). Mutation spectrum of the rhodopsin gene among patients with autosomal dominant retinitis pigmentosa. Proc. Natl. Acad. Sci. USA. 88: 9370-9374.

Dryja T.P. (1992). Rhodopsin and autosomal dominant retinitis pigmentosa. Eye 6: 1-10.

Dryja T.P., Berson E.L., Rao V.R. & Oprian D.D. (1993). Heterozygous missense mutation in the rhodopsin gene as a cause of congenital stationary night blindness. Nature Genet. 4: 280-283.

Ellis R.E., Yuan J. & Horvitz H.R. (1991). Mechanisms and functions of cell death. Ann. Rev. Cell. Biol. 7: 663-698.

Ernst W., Kemp C.M., Arden G.B., Moore A.T. & Bryan S. (1986). Functional heterogeneity in retinitis pigmentosa. In: Retinal signals systems degenerations and Transplants. p 207-222. Eds: E. Agardho & B. Ehinger. Elsevier, Amsterdam.

Evans K., Fryer A., Inglehearn C., Duvall-Young J., Whittaker J., Gregory C.Y., Ebenezer N., Hunt D. & Bhattacharya S.S. (1994). Genetic linkage of cone-rod retinal dystrophy to chromosome 19q and evidence for segregation distortion. Nature Genet. 6: 210-213.

Evans K., Al-Maghtheh M., Fitzke F.W., Moore A.T., Jay M., Inglehearn C.F., Arden G.B. & Bird A.C. (1995). Bimodal expressivity in dominant retinitis pigmentosa genetically linked to chromosome 19q. Br. J. Ophthalmol. 79: 841-846.

Farber D.B. (1995). From mice to men: the cyclic GMP phosphodiesterase gene in vision and disease. Invest. Ophthalmol. Vis. Sci. 36: 263-275.

Farrar G.J., Kenna P., Redmond R., McWilliam P., Bradley D.J., Humphries M.M., Sharp E.M., Inglehearn C.F., Bashir R., Jay M., Watty A., Ludwig M., Schinzel A., Sammans C., Gal A., Bhattacharya S. & Humphries P. (1990). Autosomal dominant retinitis pigmentosa: absence of the rhodopsin proline- histidine substitution (codon 23) in pedigrees from Europe. Am. J. Hum. Genet. 47: 941-945.

Farrar G.J., Kenna P., Jordan S.A., Kumar-Singh R., Humphries M.M., Sharp E.M., Shiels D.M. & Humphries P. (1991a). A three base-pair deletion in the peripherin-RDS gene in one form of retinitis pigmentosa. Nature 354: 478-480.

Farrar G.J., Kenna P., Redmond R., Sheils D., McWilliam P., Humphries M.M., Sharp E.M., Jordan S., Kumar-Singh R. & Humphries P. (1991b). Autosomal dominant retinitis pigmentosa - a mutation in codon 178 of the rhodopsin gene in two families of Celtic origin. Genomics 11: 1170-1171.

Farrar G.J., Findlay J.B.C., Kumar-Singh R., Kenna P., Humphries M.M., Sharpe E. & Humphries P. (1992). Autosomal dominant retinitis pigmentosa: a novel mutation in the rhodopsin gene in the original 3q linked family. Hum. Mol. Genet. 1: 769-771.

Fearn J.C. & King A.C. (1985). EGF receptor affinity is regulated by intracellular calcium and protein kinase C. Cell 40: 991-1000.

Fein A. (1986). Excitation and adaptation of Limulus photoreceptors by light and inositol 1,4,5-trisphosphate. Trends Neurosci. 9: 110-114.

Fesenko E.E., Kolesnikov S.S. & Lyubarsky A.L. (1985). Induction by cGMP of cationic conductance in plasma membrane of retinal rod outer segment. Nature 313:310-313.

Fisher R.A. (1922). The systematic location of genes by means of crossover observations. Am. Naturelist 56: 406-411.

Fishman G.A. (1978). Retinitis pigmentosa: Visual loss. Arch. Ophthalmol. 96: 1185-1188.

Fishman G.A., Alexander K.R. & Anderson R.J. (1985). Autosomal dominant retinitis pigmentosa. A method of classification. Arch. Ophthalmol. 103: 366-374.

Fishman G.A., Vendenburg K., Stone E.M., Gilbert L.D., Alexander K.R. & Sheffield V.C. (1992). Ocular findings associated with rhodopsin gene codon 267 and 190 mutations in dominant retinitis pigmentosa. Arch. Ophthalmol. 110: 1582-1588.

Fitzgibbon J., Appukuttan B., Gayther S., Wells D., Delhanty J. & Hunt D.M. (1994). Localization of the human blue cone pigment gene to chromosome band 7q31.3-32. Hum. Genet. 93: 79-80.

Fitzke F.W., Owens S., Moore A.T., Jay M., Inglehearn C.F., Bhattacharya S. & Bird A.C. (1991). Comparison of functional characteristics of autosomal dominant retinitis pigmentosa with

different amino acid changes in rhodopsin molecule. Invest. Ophthalmol. Vis. Sci. 32: (suppl.) (no.1200) p912.

Franke U., Ochs H.D., Martinville de B., Giacalone L., Lindgren V., Disteche C., Pagon R.A., Hofker M.H., van Ommen G.-J., Pearson P.L. & Wedgwood R.J. (1985). Minor Xp21 deletion in a male associated with expression of Duchenne muscular dystrophy, chronic granulomatous disease, retinitis pigmentosa and McLeod syndrome. Am. J. Hum. Genet. 37: 250-267.

Franke R.R., Sakmar T.P., Graham R.M., Khorana H.G. (1992). Structure and function in rhodopsin: Studies of the interaction between the rhodopsin in cytoplasmic domain and transducin. J. Biol. Chem. 267: 14767-14774.

Fuchs S., Nakazawa M., Maw M., Tamai M., Oguchi Y. & Gal A. (1995). A homozygous 1-base pair deletion in the arrestin gene is a frequent cause of Oguchi disease in Japanese.

Fujiki K., Hotta Y., Hayakawa M., Sakuma H., Shiono T., Noro M., Sakuma T., Tamai M., Hikiji K., Kawaguchi R., Hoshi A., Nakajima A. & Kanai A. (1992). Point mutations of rhodopsin gene found in Japanese families with autosomal dominant retinitis pigmentosa (adRP). Jpn. J. Hum. Genet. 37: 125-132.

Fujiki K., Hotta Y., Murakami A., Yoshii M., Hayakawa M., Nicolas M.G., Takeda M., Yano H.,, Kishishita H., Yokoyama T. & Kanai A. (1995). Heterozygous Asn-15-Ser and Gly-174-Ser mutations in rhodopsin gene found in Japanese retinitis pigmentosa. Invest. Ophthalmol. Vis. Sci. 36 (suppl.): S890 (abstract no. 4086).

Fung B.K.-K., Hurley J.B. & Stryer L. (1981). Flow of information in the light-triggered cyclic nucleotide cascade of vision. Proc. Natl. Acad. Sci. U.S.A. 78: 152-156.

Fung B.K.-K. (1987). Transducin: Structure, function and role in phototransduction. Prog. Retnal Res. 6: 151-177.

Fung B.K.-K., Young J.F., Yamane H.K. & Griswol-Prenner I. (1990). Subunit stoichiometry of retinal rod cGMP phosphodiesterase. Biochemistry 29: 2657-2664.

Gal A., Artlich A., Ludwig M., Niemeyer G., Olek K., Schwinger I. & Schinzel A. (1991). Pro-347-Arg of the rhodopsin gene in autosomal dominant retinitis pigmentosa. Genomics 11: 468-470.

Gal A., Orth U., Baehr W., Schwinger E. & Rosenberg T. (1994). Heterozygous missense mutation in the rod cGMP phosphodiesterase B-subunit gene in autosomal dominant stationary night blindness. Nature genet. 7: 64-67.

Ghalayini A.J., Koutz C.A., Wetsel W.C., Hannun Y.A. & Anderson R.E. (1994). Immunolocalization of PKCζ in rat photoreptor inner segments. Curr. Eye Res. 13: 145-150.

Gibson F., Walsh J., Mburu P., Varela A., Brown K.A., Antonio M., Beisel K.W., Steel K.P. & Brown S.D.M. (1995). A type VII myosin encoded by themouse deafness gene *shaker-1*. Nature 374: 62-64.

Gorczyca W.A., Gray-Keller M.P., Detwiler P.B. & Palczewski K. (1994). Purification and physiological evaluation of a guanylate cyclase activating protein from retinal rods. Proc.Natl. Acad. Sci. 91: 4014-4018.

Gray-Keller M.P., Polans A.S., Palczewski K., Detwiler P.B. (1993). The effect of recoverin-like calcium-binding proteins on the photoresponse of retinal rods. Neuron 10: 523-531.

Greenberg J., Goliath R., Beighton P. & Ramesar R. (1994). A new locus for autosomal dominant retinitis pigmentosa on the short arm of chromosome 17. Hum. Mol. Genet. 3: 915-918.

Grompe M. (1993). The rapid detection of unknown mutations in nucleic acids. Nature Genet. 5: 111-117.

Gruneberg H. (1963). The pathology of development. 5-Blackwell Scientific, Oxford.

Gyapay G., Morissette J., Vignal A., Dib C., Fizames C., Millasseau P., Marc S., Bernardi G., Lathrop M. & Weissenbach J. (1994). The 1993-94 Genethon human genetic linkage map. Nature Genet. 7:246-339.

Haldane J.B.S. (1919). The combination of linkage values and the calculation of distances between the loci of linked factors. J. Genet. 8: 299-309.

Hamer D.H., Hu S., Magnuson V.L., Hu N. & Pattatucci A.M.L. (1993). A linkage between DNA markers on the X chromosome and male sexual orientation. Science 261: 321-327.

Hamm H.E. & Bownds M.D. (1986). Protein complement of rod outer segments of frog retina. Biochemistry 25: 4512-4523.

Hargrave P.A., Fong S.-L., McDowell J.H., Mas M.T., Curtis D.R., Wang J.K., Juszczak E. & Smith D.P. (1980). The partial primary structure of bovine rhodopsin and its topography in the retinal rod cell disc membrane. Neurochem. Int. 1: 231-244.

Hargrave P.A. & McDowell J.H. (1992). Rhodopsin and phototransduction: a model system for G protein-linked receptors. FASEB J. 6: 2323-2331.

Hawkins R.K., Jansen H.G. & Sanyal S. (1985). Developement and degeneration of retina in *rds* mutant mice: photoreceptor abnormalities in the heterozygotes. Exp. Eye Res. 41, 701-720.

Hearne C.M., Ghosh S. & Todd J. (1992). Microsatellites for linkage analysis of genetic traits. Trends in Genet. 8: 288-294.

Heckenlively J.R. (1988). "Retinitis Pigmentosa". (Lippincott, Philadelphia, PA).

Heckenlively J.R., Rodriguez J.A. & daiger S.P. (1991). Autosomal dominant sectorial retinitis pigmentosa: Two families with transversion mutation in codon 23 of rhodopsin. Arch. Ophthalmol. 109: 84-91.

Hildebrandt J.D., Codina J., Rosenthal W., Birnbaumer L., Neer E.J., Yamazaki A. & Bitensky M.W. (1985). Characterization by two-dimentional peptide mapping of the γ subunit

of N_s and N_i, the regulatory proteins of adenylyl cyclase, and of transducin, the guanine nucleotide-binding protein of rod outer segments of the eye. J. Biol. Chem. 260: 14867-14872.

Hogan M.J., Wood I. & Steinberg R.H. (1974). Phagocytosis by pigment epithelium of human retinal cones. Nature 252: 305.

Horn M., Humphries P., Kunisch M., Marchese C., Apfelstedt-Sylla E., Fugi L., Zrenner E., Kenna P., Gal A. & Farrar J. (1992). Deletions in exon five of the human rhodopsin gene causing a shift in reading frame and autosomal dominant retinitis pigmentosa. Hum. Genet. 90: 255-257.

Hsu Y.-T. & Molday R. (1993). Modulation of the cGMP-gated channel of rod photoreceptor cells by calmodulin. Nature 361: 76-79.

Huang S.H., Huang X., Pittler S.J., Oliveira L., Berson E.L.& Dryja T.P. (1995). A mutation in the gene encoding the à-subunit of rod cGMP phosphodiesterase (PDEA) in retinitis pigmentosa. Invest. Ophthalmol. Vis. Sci. 36(suppl.): S825 (abstract no. 3815).

Hug H. & Sarre T.F. (1993). Protein kinase C isoenzymes: divergence in signal transduction. Biochem. J. 291: 329-343.

Hug H.P. (1993). (Data submission to the genome data base).

Humphries P., Kenna P. & Farrar G.J. (1992). On the molecular genetics of retinitis pigmentosa. Science 256: 804-808.

Hurley J.B., Dizhoor A.M., Ray S., Stryer L. (1993). Recoverin's role: Conclusion withdrawn. Science 260: 740.

Illing M., Colville C.A., Williams A.J. & Molday R.S. (1994). Sequencing cloning and characterization of a third subunit of the cyclic nucleotide-gated channel complex of rod outer segments. Invest. Ophthalmol. Vis. Sci. 35: 1474 (no.1022).

Inglehearn C.F., Keen T.J., Bashir R., Jay M., Fitzke F., Bird A.C. & Bhattacharya S.S. (1992). A complete screen for mutations of the rhodopsin gene in a panel of patients with autosomal dominant retinitis pigmentosa. Hum. Mol. Genet. 1: 41-45.

Inglehearn C.F., Carter S.A., Keen T.J., Lindsay J. Stephenson A.M., Bashir R., Al-Maghtheh M., Moore A.T., Jay M., Bird A.C. & Bhattacharya S.S. (1993). A new locus for autosomal dominant retinitis pigmentosa on chromosome 7p. Nature Genet. 4: 51-53.

Inglehearn C.F., Keen T.J., Al-Maghtheh M., Gregory C.Y., Jay M.R., Moore A.T., Bird A.C. & Bhattacharya S.S. (1994). Further refinement of the location for autosomal dominant retinitis pigmentosa on chromosome 7p (RP9). Am. J. Hum. Genet. 54: 675-680.

Inglehearn C.F., Keen T.J., Tarttelin E.E., Al-Maghtheh M., Evans K.E., Peacock R.E., Patel R.J., Jay M., Bird A.C. & Bhattacharya S.S. (1995). Genetic refinement and a YAC contig across the chromosome 7p autosomal dominant retinitis pigmentosa locus (RP9) and an estimation of the frequency of this and other forms of dominant RP in the UK. Invest. Ophthalmol. Vis. Sci. 36 (suppl.):1044 (abstract no. 4827).

Jacobson S.G., Kemp C.M., Cideciyan A.V., Macke J.P., Sung C-H. & Nathans J. (1994). Phenotypes of stop codon and splice site rhodopsin mutations causing retinitis pigmentosa. Invest. Ophthalmol. 35: 2521-2534.

Jansen H.G. & Sanyal S. (1984). Developement and degeneration of retina in *rds* mutant mice: electron microscopy. J. Comp. Neurol. 224, 71-84.

Jay B. (1972). Hereditary aspects of pigmentary retinopathy. Trans. Ophthalmol. Soc. UK. 92:173-178

Jay M. (1982a). On the heredity of retinitis pigmentosa. Br.J. Ophthal. 66: 405-416.

Jay M. (1982b). Figures and fantacies: the frequencies of the different genetic forms of retinitis pigmentosa. Birth Defects Original Article Series 18: 167-173.

Jeffreys A.J., Wilson V. & Thein S.L. (1985). Hypervariable 'minisatellite' regions in human DNA. Nature 314: 67-73.

Johnson K.J., Jones P.J., Spurr N., Nimmo E., Davies J., Creed H., Weiss M. & Williamson R. (1988). Linkage relationships of the protein kinase C gamma gene which exclude it as a candidate for myotonic dystrophy. Cytogenet. Cell Genet. 48: 13-15.

Jordan S.A., Farrar G.J., Kenna P. & Humphries P. (1992a). Polymorphic variation within 'conserved' sequences at the 3'end of the human RDS gene which results in amino acid substitution. Hum. Mutation 1: 240-247.

Jordan S.A., Farrar G.J., Kumar-Singh R., Kenna P., Humphries M.M., Allamand V., Sharp E.M. & Humphries P. (1992b). Autosomal dominant retinitis pigmentosa (adRP; RP6): Cosegregation of RP6 and the peripherin-RDS locus in a late-onset family of Irish origin. Am. J. Hum. Genet. 50: 634-639.

Jordan S.A., Farrar G.J., Kenna P., Humphries M.M., Sheils D., Kumar-Singh R., Sharp E.M., Benitez J., Carmen A. & Humphries P. (1993). Localisation of an autosomal dominant retinitis pigmentosa gene to 7q. Nature Genet. 4: 54-58.

Kajiwara K., Hahn L.B., Mukai S.,Travis G.H., Berson E.L. & Dryja T.P. (1991). Mutations in the human retinal degeneration slow gene in autosomal dominant retinitis pigmentosa. Nature 354: 480-483.

Kajiwara K., Sandgerg M.A., Berson E.L., & Dryja T.P. (1993). A null mutation in the human peripherin/rds gene in a family with autosomal dominant retinitis punctata albescens. Nature genet. 3: 208-212.

Kajiwara K., Berson E.L. & Dryja T.P. (1994). Digenic retinitis pigmentosa due to mutations at the unlinked peripherin/RDS and ROM1 loci. Science 264: 1604-1608.

Kaplan J., Bonneau D., Frezal J., Munnich A. & Dufier J-L. (1990). Clinical and genetic heterogeneity in retinitis pigmentosa. Hum. Genet. 85: 635-642.

Kaplan J., Gerber S., Bonneau D., Rozet J.M., Delrieu m.L., Briard M.L., Dollfus H., Ghazi

I., Dufier J.L., Frezal J. & munnich A. (1992). A gene for Usher syndrome type 1 (USH1A) maps to chromosome 14q. Genomics 14: 979-987.

Kaplan J., Gerber S., Larget- Piet D., Rozet J.-M., Dolldus H., Dufier J.-L., Odent S., Postel-Vinay A., Janin N., Briard M.-L., Frezal J. & Munnich A. (1993). A gene for Stargardt's disease (fundus flavimaculatus) maps to the short arm of chromosome 1. Nature Genet. 5: 308-311.

Karnik S.S. & Khorana H.G. (1990). Assembly of functional rhodopsin requires a disulfide bond between cysteine residues 110 and 187. J. Biol. Chem. 265: 17520-17524.

Kaupp U.B., Niidome T., Tanabe T., Terada S., Bonigk W., Stuhmer W., Cook N.J., Kangawa K., Matsuo H., Hirose T., Mayata T. & Numa S. (1989). Primary structure and functional expression from complementary DNA of the rod photoreceptor cyclic GMP-gated channel. Nature 342: 762-766.

Kaushal S. & Khorana H.G. (1994). Structure and function in rhodopsin (7). Point mutations associated with autosomal dominant retinitis pigmentosa. Biochemistry 33: 6121-6128.

Kawamura S. & Murakami M. (1991). Calcium-dependent regulation of cyclic GMP phosphodiesterase by a protein from frog retinal rods. Nature 349: 420-423.

Kawamura S., Takamatsu K. & Kitamura K. (1992). Purification and characterization of S-modulin, a calcium dependent-regulator on cGMP phosphodiesterase in frog rod photoreceptors. Biophys. Res. Commun. 186: 411-417.

Keeler C. (1924). The inheritance of a retinal abnormality in white mice. Proc. Natl. Acad. Sci. USA 10: 329-333.

Keen T.J., Inglehearn C.F., Lester D.H., Bashir R., Jay M., Bird A.C. & Bhattacharya S.S. (1991a). Autosomal dominant retinitis pigmentosa: Four new mutations in rhodopsin, one of them in the retinal attachment site. Genomics 11: 199-205.

Keen J., Lester D., Inglehearn C., Curtis A. & Bhattacharya S.S. (1991b). Rapid detection of single base mismatches as heteroduplexes on Hydrolink gel. Trends Genet. 7:5.

Keen T.J., Inglehearn C.F., Kim R., Bird A.C. & Bhattacharya S. (1994). Retinal pattern dystrophy associated with a 4 bp insertion at codon 140 in the RDS-peripherin gene. Hum. Mol. Genet. 3: 367-368.

Kelleher D.J., Pessin J.E., Ruoho A.E. & Johnson G.L. (1984). Phorbol ester induces desensitization of adenylate cyclase and phosphorylation of the β-adrenergic receptor in turkey erythrocytes. Proc. Natl. Acad. Sci. USA 81: 4316-4320.

Kelleher D.J. & Johnson G.L. (1986). Phosphorylation of rhodopsin by protein kinase c *in vitro*. J.Biol. Chem. 261: 4749-4757.

Kemp C.M., Jacobson S.G., Cideciyan A.V., Kimura A.E., Sheffield V.C. & Stone E.M. (1994). RDS gene mutations causing retinitis pigmentosa or macular degeneration lead to the same abnormality in photoreceptor function. Invest. Ophthalmol. Vis. Sci. 35: 3154-3162.

Kerr J.F.R. & Harmon B.V. (1991). Definition and incidence of apoptosis: an historical perspective. In Apoptosis: The Molecular Biology of Cell Death. Tomei L.D. & Cope F.O., eds. (Cold Spring Harbor, New York: Cold Spring Harbor Press), pp. 5-30.

Khani S.C., Lin D., Magovcevic I., Berson E.L. & Dryja T.P. (1994). Characterization and mapping of the human rhodopsin kinase gene and screening of the gene for mutations in patients with retinitis pigmentosa. Am. J. Hum. Genet. 55 (suppl.): A134 (abstract no. 768).

Khokha R. & Denhardt D.T., Matrix metalloproteinases and tissue inhibitor of metalloproteinases: a review of their role in tumorigenesis and tissue invasion. Invasion Metastasis 9: 391-405.

Kim R.Y., Al-Maghtheh M., Fitzke F.W., Arden G.B., Jay M., Bhattacharya S.S. & Bird A.C. (1993). Dominant retinitis pigmentosa associated with two rhodopsin gene mutations: Leu-40-Arg and an insertion disrupting the 5'-splice junction of exon 5. Arch. Ophthalmol. 111: 1518-1524.

Kim R.Y., Fitzke F.W., Moore A.T., Jay M., Inglehearn C., Arden G.B., Bhattacharya S.S. & Bird A.C. (1995). Autosomal dominant retinitis pigmentosa mapping to chromosome 7p exhibits variable expression. British J. Ophthalmo. 79: 23-27.

Kimberling W.J., Moller C.G., Davenport S., Priluck I.A., Beighton P.H., Greenberg J., Reardon W., Weston M.D., Kenyon J.B., Grunkemeyer J.A., Pieke Dahl S., Overbeck L.D., Blackwood D.J., Brower A.M., Hoover D.M., Rowland P. & Smith R.J.H. (1992). Linkage of Usher syndrome type 1 gene (USH1B) to the long arm of chromosome 11. Genomics 14: 988-994.

Kimberling W.J., Weston M.D., Moller C., Davenport S.L., Shugart Y.Y., Priluck I.A., Martini A., Milani M. & Smith R.J. (1990). Localization of Usher syndrome type II to chromosome 1q. Genomics: 7: 245-249.

Klein R., Klein B.E. & Linton K.L.P. (1992). Prevalence of age-related maculopathy: the Beaver Dam Eye Study. Ophthalmology 99: 933-943.

Knowles J.A., Vieland V.J. & Gilliam T.C. (1992). Perils of gene mapping with microsatellite markers. Am. J. Hum. Genet. 51: 905-909.

Knowles J.A., Shugart Y., Banerjee P., Gilliam T.C., Lewis C.A., Jacobson S.G. & Ott J. (1994). Identification of a locus, distinct from RDS-peripherin, for autosomal recessive retinitis pigmentosa on chromosome 6p. Hum. Mol. Genet. 3: 1401-1403.

Kock K.-W. & Stryer L. (1988). Highly cooperative feedback control of retinal rod guanylate cyclase by calcium ions. Nature 334: 64-66.

Konig B., Arendt A., McDowell J.H., Kahlert M., Hargrave P.A. & Hofmann K.P. (1989). Three cytoplasmic loops of rhodopsin interact with transducin. Proc. Natl. Acad. Sci. USA 86: 6878-6882.

Kornfeld R. & Kornfeld S. (1985). Assembly of asparagine-linked oligosaccharides. Annu. Rev. Biochem. 54: 631-664.

Kosambi D.D. (1994). The estimation of map distances from recombination values. Ann. Eugen. 12: 172-175.

Kumaramanickavel G., Maw M., Denton M.J., John S., Srikumari C.R.S., Orth U., Oehlmann R. & Gal A. (1994). Missense rhodopsin mutation in a family with recessive RP. Nature Genet. 8: 10-11.

Kuhn H. (1974). Light-dependent phosphorylation of rhodopsin in living frogs. Nature 250: 588-590.

Kumar-Singh R., Farrar F.J., Monsergh F., Kenna P., Bhattacharya S.S., Gal A. & Humphries P. (1993). Exclusion of the involvement of all known retinitis pigmentosa loci in the disease present in a family of Irish origin provides evidence for a sixth autosomal locus (RP8). Hum. Mol. Genet. 2: 875-878.

Kunkel T.A. (1993). Slippery DNA and diseases. Nature 365: 207-208.

Kylstra J.A. & Aylsworth A.S. (1993). Cone-rod retinal dystrophy in a patient with neurofibromatosis type 1. Can. J. Ophthalmol. 28: 79-80.

Lambrecht H.-G. & Koch K.-W. (1991). A 26 kDabinding protein from bovine rod outer segments as modulator of photoreceptor guanylate cyclase. EMBO J. 10: 793-798.

Lander E.S. & Botstein D. (1987). Homozygosity mapping: A way to map human recessive traits with the DNA of inbred children. Science 236: 1567-1570.

Lathrop G.M., Lalouel J.M., Julier C. & Ott J. (1984). Strategies for multilocus linkage analysis in humans. Proc. Natl. Acad. Sci. USA 81: 3443-3446.

Lathrop G.M. & Lalouel J.M. (1984). Easy calculations of lod scores and genetic risks on small computers. Am. J. Hum. Genet. 36: 460-465.

Lee R.H., Lieberman B. & Lolley R.N. (1987). A novel complex from bovine visual cells of a 33000-Daltons phosphoprotein with β and γ-transducin: Purification and subunit structure. Biochemistry 26: 3983-3990.

Lee R.H., Lieberman B. & Lolley R.N. (1990). Retinal accumulation of the phosducin/T beta, gamma and transducin complexes in developing normal mice and in mice and dogs with inherited retinal degeneration. Exp. Eye Res. 51: 325-333.

Lee R.H., Ting T.D., Lieberman B.S., Tobias D.T., Lolley R.N. & Ho Y.-K. (1992). Regulation of retinal cGMP cascade by phosducin in bovine rod photoreceptor cells: Interaction of phosducin and transducin. J. Biol. Chem. 267: 25104-25112.

Lerman L.S. & Silverstein K. (1987). Computational simulation of DNA melting and its application to denaturing gel electophoresis. Meth. Enzymol. 155: 482-501.

Lester D.H., Inglehearn C.F., Bashir R., Ackford H., Esakowitz L., Jay M., Bird A.C., Wright A.F., Papiha S.S. & Bhattacharya S.S. (1990). Linkage to D3S47 (C17) in one large autosomal dominant retinitis pigmentosa family and exclusion in another: confirmation of genetic

heterogeneity. Am. J. Hum. Genet. 47: 536-541.

Levitt R.C., Kiser M.B., Dragwa C., Jedlicka A.E., Xu J., Meyers D.A. & Hudson J.R. (1994). Fluorescence-Based resource for semiautomated genomic analyses using microsatellite markers. Genomics 24: 361-365.

Li S.T., Chang C.J., Abler A.S. & Tso M.O.M. (1994). Inhibitory effects of cyclohexamide and Flunarizine on light-induced apoptosis of photoreceptor cells. Invest. Ophthalmol. Vis. Sci. 35 (suppl.): 1518 (abstract no. 1227).

Li T., Franson W.K., Gordon J.W., Berson E.L. & Dryja T.P. (1995). Continuous activation of phototransduction by K296E opsin is not the cause of photoreceptor degeneration. Invest. Ophthalmol. Vis. Sci. 36 (suppl.): S423 (abstract no. 1942).

Litt M., Luty J.A. (1989). A hypervariable microsatellite revealed by *in vitro* amplification of a dinucleotide repeat within the cardiac muscle actin gene. Am. J. Hum. Genet. 44: 397-401.

Lolley R.N., Craft C.M. & Lee R.H. (1992). Photoreceptors of the retina and pinealocytes of the pineal gland share common components of signal transduction. Neurochem. Res. 17: 81-89.

Lyness A.L., Ernst W., Quinlan M.P., Clover G.M., Ardev G.B., Carter R.M., Bird A.C. & Parker J.A. (1985). A clinical, psychophysical and electroretinographic survey of patients with autosomal dominant retinitis pigmentosa. Br. J. Ophthalmol. 69: 326-339.

Lyon M.F. (1988). X-chromosome inactivation and the location and expression of X-linked genes. Am. J. Hum. Genet. 42: 8-16.

Macke J.P., Davenport C.M., Jacobson S.G., Hennessey J.C., Gonzalez-Fernandes F., Conway B.P., Heckenlively J., Palmer R., Maumenee I.H., Sieving P., Gouras P., Good W. & Nathans J. (1993). Identification of novel rhodopsin mutations responsible for retinitis pigmentosa: Implications for the structure and function of rhodopsin. Am. J. Hum. Genet. 53: 80-89.

Maddox J. (1995). Directory to the human genome. Nature 376: 459-460.

Mahajna J., King P., Parker P. & Haley J. (1995). Autoregulation of cloned human protein kinase C β and γ gene promotors in U937 cells. DNA Cell Biol. 14: 213-222.

Mansergh F.C., Kenna P.F., Farrar G.J., Kumar-Singh R., Humphries M.M., Meitinger T., Rudolph G. & Humphries P. (1994). Confirmation of linkage of Best's macular dystrophy to 11q13, and evidence for genetic heterogeneity. Am. J. Hum. Genet. 55 (suppl): abstract no 1130.

Marti T., Otto H., Rosselet S.J., Heyn M.P. & Khorana H.G. (1992). Consequences of amino acid insertions and/or deletions in transmembrane helix C of bacteriorhodopsin. Proc. Natl. Acad. Sci. USA 89: 1219-1223.

Matheke M.L., Fliesler S.J., Basinger S.F. & Holtzman E. (1984). The effects of monensin on transport of membrane components in the frog retinal photoreceptor. I. Light microscopic autoradiography and biochemical analysis. J. Neurosci. 4: 1086-1092.

Matthews R., Murphy R.L.W., Fain G.L. & Lamb T.D. (1988). Photoreceptor light adaptation is mediated by cytoplasmic calcium concentration. Nature 334: 67-69.

Massof R.W. & Finkelstein D. (1981). Two forms of autosomal dominant primary retinitis pigmentosa. Doc. Ophthalmol. 51: 289-346.

McGee T.L., Lin D., Berson E.L. & Dryja T.P. (1994). Defects in the rod cGMP-GATED channel gene in patients with retinitis pigmentosa. Invest. Ophthalmol. Vis. Sci. (suppl.) 35:1716 (no.2154).

McGinnis J.F., Lerious V., Pazik J., Austin B., Elliott R.W., Bateman B., Heinzman C., Klisak I. & Sparkes R.S. (1993). An experimental model for cancer associated retinopathy and its correlation with the human recoverin gene. Invest. Ophthalmol. Vis. Sci. 34 (suppl.): 1148 (abs. no. 2190)

McGinnis J.F., Austin B., Klisak I., Heizman C., Kojis T., Sparkes R.S., Bateman J.B. & Lerious V. (1995). Chromosomal assignment for the human gene for the cancer-associated retinopathy protein (recoverin) to chromosome 17p13.1. J. Neuroscience res. 40: 165-168.

McKusick V.A. (ed.): Mendelian inheritance in man. Baltimore: Johns Hopkins University Press, 1992.

Mclaughlin M.E., Sandberg M.A., Berson E.L. & Dryja T.P. (1993). Recessive mutations in the gene encoding the β-subunit of rod phosphodiesterase in patients with retinitis pigmentosa. Nature Genet. 4: 130-134.

McLaughlin M.E., EhrhartT.L., Sandberg M.A., Berson E.L. & Dryja T.P. (1994). Mutations in the beta subunit of rod phosphodiesterase in patients with autosomal recessive retinitis pigmentosa. Invest. Ophthalmol. Vis. Sci. (suppl) 35: 1718 (no.2162).

McWilliam P., Farrar G.J., Kenna P., Bradly D.G., Humphries M.M., Sharp E.M., McConnel D.J., Lawler M., Sheils D., Ryans C., Stevens K., Daiger S.P. & Humphries P. (1989). Autosomal dominant retinitis pigmentosa (ADRP): Localization of an ADRP gene to the long arm of chromosome 3. Genomics 5: 619-622.

Milani S. et al. (1994). Differential expression of matrix metalloproteinase-1 and -2 genes in normal and fibrotic human liver. Am. J. Pathol. 144: 528-537.

Mishra S.K., Helms C., Dorsey D., Permutt M.A. and Donis-Keller H. (1992). A 2-cM genetic linkage map of human chromosome 7p that includes 47 loci. Genomics 12: 326-334.

Molday L.L., Cook N.J., Kaupp U.B., & Molday R.S. (1990). The cGMP-gated cation channel of bovine rod photoreceptor cells is associated with a 240 KDa protein exhibiting immunochemical cross-reactivity with spectrin. J. Biol. Chem. 265: 18690-18695.

Moller C.G., Kimberling W.J., Davenport S.L.H. et al. (1989). Usher syndrome: An otoneurologic study. Laryngoscope 99: 73-79.

Moore A.T., Fitzke F., Jay M., Arden G.B., Inglehearn C.F., Keen T.J., Bhattacharya S.S. & Bird A.C. (1993). Autosomal dominant retinitis pigmentosa with apparent incomplete

penetrance: a clinical, electrophysiological, psychophysical and molecular genetic study. Br. J. Ophthalmol. 77: 473-479.

Morton N.E. (1955). Sequential tests for the detection of linkage. Am. J.Hum. Genet. 7: 277-318.

Murakami A., Yajima T. & Inana G. (1992). Isolation of human retinal genes: Recoverin cDNA and gene. Biochem. Biophys. Res. Commun. 187: 234-244.

Myers R.M., Maniatis T., & Lerman L.S. (1987). Detection and localization of single base changes by denaturing gradient gel electrophoresis. Meth. Enzymol. 155: 501-527.

Nagao S., Yamazaki A., & Bitenski K.M. (1987). Calmodulin and calmodulin binding proteins in amphibian rod outer segments. Biochemistry 26: 1659-1665.

Nakatani K. & Yau K.-W. (1988). Calcium and light adaptation in retinal rods and cones. Nature 334: 69-71.

Nakazawa M., Xu S., Gal A. & Tamai M. (1995). Phenotypic characteristics of a Japanese family with autosomal dominant retinitis pigmentosa closely linked to chromosome 19q. Invest. Ophthalmol. Vis. Sci. 36(suppl.): S891 (abstract no. 4092).

Nathans J. & Hogness D.S. (1984). Isolation and nucleotide sequence of the gene encoding human rhodopsin. Proc. Natl. Acad. Sci. USA 81: 4851-4855.

Nathans J., Thomas D., & Hogness D.S. (1986a). Molecular genetics of human color vision: the genes encoding blue, green and red pigments. Science 232: 193-202.

Nathans J., Piantanida T.P., Eddy R.L., Shows T.B. & D.S. (1986b). Molecular genetics of inherited variation in human colour vision. Science 232: 203-210.

Nathans J. (1990). Determinants of visual pigment absorbance: identification of the retinyldiene Schiff's base counterion in bovine rhodopsin. Biochemistry 29: 9746-9752.

Nathans J. (1994). In the eye of the beholder: Visual pigments and inherited variation in human vision. Cell 78: 357-360.

Neer E.J. & Clapham D.E. (1988). Roles of G protein subunits in transmembrane signalling. Nature 333: 129-134.

Nelson S.F., McCusker J.H., Sander M.A., Kee Y., Modrich P. & Patrick O.B. (1993). Genomic mismatch scanning: a new approach to genetic linkage mapping. Nature Genet. 4: 11-18.

Newton A.C. & Williams D.S. (1991). Involvement of protein kinase C in the phosphorylation of rhodopsin. J.Biol. Chem. 266: 17725-17728.

Newton A.C. & Williams D.S. (1993). Rhodopsin is the major *in situ* substrate of protein kinase C in rod outer segments of photoreceptors. J. Biol. Chem. 268: 18181-18186.

Newton A.C., Greene N.M. & Williams D.S. (1994). Phosphorylation of rhodopsin by protein kinase C: Biochemical and structural analysis. Invest. Ophthalmol. Vis. Sci. 35 (suppl.): 1473 (abstract no.1018)

Nichols B.E., Sheffield V.C., Vandenburgh K., Drack A.V., Kimura A.E., & Stone E.M. (1993). Butterfly-shaped pigment dystrophy of the fovea caused by a point mutation in codon 167 of the RDS gene. Nature Genet. 3: 202-207.

NIH/CEPH Collaborative Mapping Group (1992). A complete genetic linkage map of the human genome. Science 258: 67-86.

Nishizuka Y. (1988). The molecular heterogeneity of protein kinase C and its implications for cellular regulation. Nature 334: 661-665.

Nishizuka Y. (1992). Intracellular signalling by hydrolysis of phospholipids and activation of protein kinase C. Science 258: 607-614.

Ohki K., Yoshida K., Imaki J., Harada T. & Matsuda H. (1994). The existence of protein kinase C in cone photoreceptors in the rat retina. Curr. Eye Res. 13: 547-550.

Ohno S., Kawasaki H., Imajoh S., Suzuki K., Inagaki M., Yokokura H., Sakoh T. & Hidaka H. (1987). Tissue specific expression of three distinct types of rabbit protein kinase C. Nature 325: 161-166.

Oliveira L., Miniou P., Viegaspequignot E., Rozet J.M. Dollfus H. and Pittler S.J. (1994). Human retinal guanylate-cyclase maps to 17p13.1. Invest. Ophthalmol. Vis. Sci. 35: 1264.

Ono Y., Kikkawa U., Ogita K., Fujii T., Kurokawa T., Asaoka Y., Sekiguchi K., Ase K., Igarashi K. & Nishizuka Y. (1987). Expression and properties of two types of protein kinase C: alternative splicing from a single gene. Science 236: 1116-1120.

Orita M., Suzuki Y., Sekiya T. & Hayashi K. (1989). Rapid and sensitive detection of point mutations and DNA polymorphisms using the polymerase chain reaction. Genomics 5: 874-879.

Osborne N.N., Barnett N.D., Morris N.J. & Huang F.L. (1992). The occurence of three isoenzymes of protein kinase C (α, β, and γ) in retinas of different species. Brain Res. 570: 161-166.

Osborne N.N., Wood J. & Groome N. (1994). The occurence of three calcium-independent protein kinase C subspecies (δ, ϵ, and ζ) in retina of different species. Brain Res. 637: 156-162.

Ott J. (1974). Estimation of the recombination fraction in human pedigrees: efficient computation of the likelihood for human linkage studies. Am. J. Hum. Genet. 26: 588-597.

Ott J.: A short guide to linkage analysis, in Davies K.E. (ed) (1986): *Human Genetic Diseases: A Practical approach.* IRL Press, Washington DC, pp 19-32.

Ott J., Bhattacharya S., Chen S., Denton M.J., Donald J., Dubay C., Farrar G.J., Fishman G.A., Frey D., Gal A., Humphries P., Jay B., Litt M., Machler M., Musarella M.A., Neugebauer M., Nussbaum R.L., Terwilliger J.D., et al. (1990). Localizing multiple X-

chromosome linked retinitis pigmentosa loci using multilocus homogeneity tests. Proc. Natl. Acad. Sci. USA 87: 701-704.

Ott J. (1991). Analysis of human genetic linkage. 2nd ed. Johns Hopkins University Press, Baltimore.

Ott J. (1992). Strategies for characterizing highly polymorphic markers in human gene mapping. Am. J. Hum. Genet. 51: 283-290.

Palczewski K., Subbaraya I., Gorczyca W.A., Helekar B.S., Ruiz C.C., Ohguro H., Huang J., Zhao X., Crabb J.W., Johnson R.S., Walsh K., Gray-Keller M.P., Detwiler P.B. & Baehr W. (1994). Molecular cloning and characterization of retinal photoreceptor guanylyl cyclase-activating protein. Neuron 13: 395-404.

Payne R., Corson D.W., Fein A. & Berridge M.J. (1986). Excitation and adaptation of Limulus ventral photoreceptors by inositol 1,4,5-trisphosphate results from a rise in intracellular calcium. J. Gen. Physiol. 88: 127-142.

Pearson W.R. & Lipman J.D. (1988). Improved tools for biological sequence comparison. Proc. Natl. Acad. Sci. 85: 2444-2448.

Pelletier J.P., Mineau F., Faure M.P., & Martel-Pelletier J. (1990). Imbalance between the mechanisms of activation and inhibition of metalloproteinases in the early lesions of experimental osteoarthritis. Arthritis Rheum. 33: 1466-1476.

Pfeffer B.A., Clark V.M., Flannery J.G. & Bok D. (1986). Membrane receptors for retinol-binding protein in cultured human retinal pigment epithelium. Invest. Ophthalmol. Vis. Sci. 27: 1031-1040.

Pieke Dahl S., Kimberling W.J., Gorin M.B., Weston M.D., Furman J.M., Pikus A. & Moller C. (1993). Genetic heterogeneity of Usher syndrome type II. J. Med. Genet. 30: 843-848.

Pittler S.J. & Baehr W. (1991). Identification of a nonsense mutation in the rod photoreceptor cGMP phosphodiesterase β subunit gene of the *rd* mouse. Procl. Natl. Acad. Sci. 88: 8322-8326.

Pittler S.J., Keeler C.E., Sidman R.L. & Baehr W. (1993). PCR analysis of DNA from 70-year-old sections of rodless retina demonstrates identity with the mouse *rd* defect. Proc. Natl. Acad. Sci. 90: 9616-6919.

Preising M., Muller B. & Pawlowitzki I.H. (1994). Pooled DNA PCR: a new procedure for gene localization studies. Invest. Ophthalmol. Vis. Sci. 35(suppl.): 1312 (abstract no. 273).

Pugh E.N.,Jr., & Cobbs W.H. (1986). Visual transduction in vertebrate rods and cones: a tale of two transmitters, calcium and cGMP. Vision Res. 26: 1613-1643.

Rangathan R., Harris G.L., Stevens C.F. & Zuker C.S. (1991). A drosophila mutant defective in extracellular calcium-dependent photoreceptor deactivation and rapid desensitization. Nature 354: 230-232.

Rao V.R., Cohen G.B., and Oprian D.D. (1994). Rhodopsin mutation G90D and a molecular mechanism for congenital night blindness. Nature 367: 639-642.

Reig C., Llecha N., Antich J., Gaen E., Tejada I., Molina M., Reventos J. & Carballa M. (1994). A missense mutation (^{211}His→Arg) and a silent (^{160}Thr) mutation within the rhodopsin gene in a Spanish autosomal dominant retinitis pigmentosa family. Hum. Mol. Genet. 3: 195-196.

Restango G., Maghtheh M., Bhattacharya S., Ferrone M., Garnerone S., Samuelly R. & Carbonara A. (1993). A large deletion at the 3' end of the rhodopsin gene in an Italian family with a diffuse form of autosomal dominant retinitis pigmentosa. Hum. Mol. Genet. 2: 207-208.

Reuter J.H. & Sanyal S. (1984). Developement and degeneration of the retina in *rds* mutant mice: the electroretinogram. Neurosci. Lett. 46, 231.

Richards J.E., Kuo C.Y., Boehnke M., & Sieving P.A. (1991). Rhodopsin Thr-58-Arg mutation in a family with autosomal dominant retinitis pigmentosa. Ophthalmology 98: 1797-1805.

Richards R.I. & Sutherland G.R. (1994). Simple repeat DNA is not replicated simply. Nature Genet. 6: 114-116.

Ripps H., Brin K.P. & Weale R.A. (1978). Rhodopsin and visual threshold in retinitis pigmentosa. Invest. Ophthalmol. Vis. Sci. 19: 1030-1037.

Robinson P.R., Cohen G.B., Zhukovsky E.A. & Oprian D.D. (1992). Constitutively active mutants of rhodopsin. Neuron 9: 719-725.

Rodriguez J.A., Herrena C.A., Birch D.G. & Daiger S.P. (1993a). A leucine to arginine amino acid substitution at codon 46 of rhodopsin gene is responsible for a severe form of autosomal dominant retinitis pigmentosa. Human Mutation 2: 205-213.

Rodriguez J.A., Herrera C.A., Birch D.G., Heckenlively J.R. & Daiger S.P. (1993b). Rhodopsin mutations in patients with retinitis pigmentosa. Am. J. Hum. Genet. 53: 1224.

Rosenfeld P.J., Cowley G.S., McGee T.L., Sandberg M.A., Berson E.L. & Dryja T.P. (1992). A null mutation in the rhodopsin gene causes rod photoreceptor dysfunction and autosomal recessive retinitis pigmentosa. Nature Genet. 1: 209-213.

Romeo G. & McKusick V.A. (1994). Phenotypic diversity, allelic series and modifier genes. Nature Genet. 7: 451-453.
Rosenfeld P.J., McKusick V.A., Amberger J.S. & Dryja T.P. (1994). Recent advances in the gene map of inherited eye disorders: primary hereditary diseases of the retina, choroid, and vitreous. J. Med. Genet. 31: 903-915.

Rosenfeld P.J. and Dryja T.P. (1995). Molecular genetics of retinitis pigmentosa and related retinal degenerations. In: Molecular genetics of ocular diseases. p 99-126. Ed: J.L. Wiggs. Wiley-Liss puplication.

Rosenthal A., Rhee L., Yadegari R., Paro R., Ullrich A. & Goeddel D.V. (1987). Structure and nucleotide sequence of a drosophila melanogaster protein kinase c gene. EMBO J. 6: 433-

441.

Rozet J.M., Gerber S., Bonneau D., Souied E., Frezal J., Munnich A. & Kaplan J. (1995). Exclusion of the cone-specific alpha-subunit of the transducin gene in Stargardts disease. Invest. Ophthalmol. Vis. Sci. 36 (suppl.): 919 (abstract no. 4226).

Rysavy F.R., Bishop M.J., Gibbs G.P. & Williams G.W. (1992). The UK Genome Mapping Project online computing service. Comput. Appl. Biosci. 8: 149-154.

Saiki R.K., Gelfand D.H., Stoffel S., Scharf S.J., Higuchi R., Horn G.T., Mullis K.B. & Erlich H.A. (1988). Primer directed enzymatic amplification of DNA with a thermostable DNA polymerase. Science 239: 487-491.

Sakmar T.P., Franke R.R. & Khorana H.G. (1989). Glutamic acid-113 serves as the retinyldiene Schiff base counterion in bovine rhodopsin. Proc. Natl. Acad. Sci. 86: 8309-8313.

Sanger F., Nicklen S.T. & Coulsen A.R. (1977). DNA sequencing with chain termination inhibitors. Proc. Natl. Acad. Sci. 74: 5463.

Sankila E.-M., Pakarinen L., Kaariainen H., Aittomaki K., Karjalainen S., Sistonen P.& de la Chapelle A. (1995). Assingment of an Usher syndrome type III (USH3) gene to chromosome 3q. Hum. Mol. Genet. 4: 93-98.

Sanyal S. & Jansen H. (1981). Absence of receptor outer segments in the retina of *rds* mutant mice. Neurosci. Lett. 21, 23-26.

Sanyal S. (1987). Cellular site of expression and genetic interaction of the *rd* and the *rds* loci in the retina of the mouse. In: Degenerative retinal disorders: clinical and laboratory investigations (J.G. Hollyfield, R.E. Anderson, and M.M. LaVail, eds). Alan R. Liss, New York p175-194.

Schaeffer E., Smith D., Mardon G., Quinn, W. & Zuker C. (1989). Isolation and characterization of two new drosophila protein kinase C genes, including one specifically expressed in photoreceptor cells. Cell 57: 403-412.

Scott K., Sieving P.A., Bingham E., Bhagat V.J., Sullivan J., Alpern M. & Richards J.E. (1993). Rhodopsin mutations associated with autosomal dominant retinitis pigmentosa. Am. J. Hum. Genet. 53: 147.

Sheffield V.C., Cox D.R., Lerman L.S. & Myers R.M. (1989). Attachment of a 40-base-pair G+C-rich sequence (GC-clamp) to genomic DNA fragments by the polymerase chain reaction results in improved detection of single-base changes. Proc. Natl. Acad. Sci. USA 86: 232-236.

Sheffield V.C., Fishman G.A., Beck J.S., Kimura A.E. & Stone E.M. (1991). Identification of novel rhodopsin mutations associated with retinitis pigmentosa using GC-clamped denaturing gradient gel electrophoresis. Am. J. Hum. Genet. 49: 699-706.

Sheffield V., Carmi R., Kwitek-Black A., Rokhlina T., Nishimora D., Duyk G., Elbodour K., Sunden S. & Stone E. (1994). Identification of a Bardet-Biedl syndrome locus on chromosome 3 and evaluation of an efficient approach to homozygosity mapping. Human Mol. Genet. 3:

1331-1335.

Shichi H. & Somers R.L. (1978). Light dependent phosphorylation of rhodopsin. Purification and properties of rhodopsin kinase. J. Biol. Chem. 253: 7040-7046.

Shieh B.-H., Stamnes M.A., Seavello S., Harris G.L. & Zuker C.S. (1989). The ninaA gene required for visual transduction in Drosophila encodes a homologue of cyclosporin A-binding protein. Nature 338: 67-70.

Sieving P.A., Richards J.E., Bingham E.L. & Naarendorp F. (1992). Dominant congenital complete nyctalopia and Gly-90-Asp rhodopsin mutation. Invest. Ophthalmol. Vis. Sci. (suppl.) 33: 1397.

Simon M.I., Strathmann M.P. & Gautam N. (1991). Diversity of G proteins in signal transduction. Science 252: 802-808.

Small K.W., Weber J.L., Roses A., Lennon F., Vance J.M. & Pericak-Vance M.A. (1992). North Carolina macular dystrophy is assigned to chromosome 6. Genomics 13; 681-685.

Small K.W., Sanchez A.R., Yelchits S.V., Kelley K.C., Jimenez-Morillas M.E., Mullen L.M., Stalvey M.S., Dickel C.D., Rao N. & Pettenati M.J. (1994). Physical mapping of the MCDR1 (North Carolina macular dystrophy) locus. Invst. Ophthalmol. Vis. Sci. (suppl) 35: 1717 (no. 2158).

Smith D.P., Stamnes M.A. & Zuker C.S. (1991a). Signal transduction in the visual system of drosophila. Annu. Rev. Cell Biol. 7: 161-190.

Smith D.P., Ranganathan R., Hardy R.W., Marx J., Tsuchida T. & Zuker C.S. (1991b). Photoreceptor deactivation and retinal degeneration mediated by a photoreceptor-specific protein kinase C. Science 254: 1478-1484.

Smith R.J.H., Lee E.C., Kimberling W.J., Daiger S.P., Pelias M.Z., Keats B.J.B., Jay M., Bird A., Reardon W., Guest M., Ayyagari R. & Hejtmancik J.F. (1992). Localization of two genes for Usher syndrome type I to chromosome 11. Genomics 14: 995-1002.

Soest S.V., Born L.I., Gal A., Farrar G.J., Bleeker-Wagemakers L.M., Westerveld A., Humphries P., Sandkuijl L.A. & Bergen A.A.B. (1994). Assignment of a gene for autosomal recessive retinitis pigmentosa (RP12) to chromosome 1q31-q32.1 in an inbred and genetically heterogeneous disease population. Genomics 22: 499-504.

Souied E., Gerber S., Rozet J-M., Bonneau D., Dufier J-L., Ghazi I., Philip N., Soubrane G., Coscas G., Munnich A. & Kaplan J. (1994). Five novel missense mutations of the rhodopsin gene in autosomal dominant retinitis pigmentosa. Hum. Mol. Genet. 3: 1433-1434.

Southern E.M. (1975). Detection of specific sequences among DNA fragments separated by gel electrophoresis. J. Mol. Biol. 98: 503-517.

Sparkes R.S., Klisak I., Kaufman D., Mohandas T., Tobin A.J. & McGinnis J.F. (1986). Assignment of rhodopsin gene to human chromosome three, region 3q21-3q24 by in situ hybridization studies. Curr. Eye Res. 5: 797-798.

Sparkes R.S., Lee R.H., Shinohara T., Craft C.M., Kojis T., Klisak I., Heinzmann C. & Bateman B. (1993). Assignment of the phosducin (PDC) gene to human chromosome 1q25-1q32.1 by somatic cell hybridization and in situ hybridization. Genomics 18: 426-428.

Stamnes M.A., Shieh B.-H., Chuman L., Harris G.L. & Zuker C.S. (1991). The cyclophylin homologue, ninaA, is a tissue-specific integral membrane protein required for the proper synthesis of a subset of Drosophila rhodopsins. Cell 65: 219-227.

Stargardt K. (1909). Ueber familiare, progressive degeneration in der makulagegend des auges. Graefe Arch. Klin. Exp. Ophal. 71: 534-549.

Steel K.P. & Harvey P. (1992). Development of auditory and vestibular systems. Vol 2 (ed. Romand R.) 221-242 (Elsevier, Amsterdam).

Steinberg R.H., Fisher S.K. & Anderson D.H. (1980). Disk morphogenesis in vertebrate photoreceptors. J. Comp. Neurol. 190: 501.

St. Jules R.S. & O'Brien P.J. (1986). The acylation of rat rhodopsin in vitro and in vivo. Exp. Eye Res. 43: 929-940.

St. Jules R.S., Wallingford J.C., Smith S.B. & O'Brien P.J. (1989). Addition of the chromophore to rat rhodopsin is an early post translational event. Exp. Eye Res. 48: 653-665.

Stone E.M., Kimura A.E., Nicholas B.E., Khadivi P., Fishman G.A. & Sheffield V.C. (1991). Regional distribution of retinal degeneration in patients with the proline to histidine mutation in codon 23 of the rhodopsin gene. Ophthalmology 98: 1806-1813.

Stone E.M., Nichols B.E., Sterb L.M., Kimura A.E., & Sheffield V.C. (1992). Genetic linkage of vitelliform macular degeneration (Best's disease) to chromosome 11q13. Nature Genet. 1: 246-250.

Stone E.M., Vandenburgh K., Kimura A.E., Lam B.L., Fishman G.A., Heckenlively J.R., Castillo T.A. & Sheffield V.C. (1993). Novel mutations in the peripherin (RDS) and rhodopsin genes associated with autosomal dominant retinitis pigmentosa (ADRP). Invest. Ophthalmol. Vis. Sci. 34: 1149.

Stone E.M., Nichols B.E., Kimura A.E., Weingeist T.A., Drack A. & Sheffied V.C. (1994). Clinical features of a Stargardt-like dominant progressive macular dystrophy with genetic linkage to chromosome 6q. Arch. Ophthalmol. 112: 765-772.

Stryer L. (1986). Cyclic GMP cascade of vision. Annu. Rev. Neurosci. 9: 87-119.

Stryer L. (1988). Biochemistry; third edition. W.H. Freeman and Company, New York.

Stryer L. (1991). Visual exitation and recovery. J. Biol. Chem. 266: 10711-10714.

Suber M.L., Pittler S.J., Qin N., Wright G.C., Holcombe V., Lee R.H., Craft C.M., Lolley R.N., Baehr W. & Hurwitz R.L. (1993). Irishsetter dogs affected with rod/cone dysplasia contain a nonsense mutation in the rod cGMP phosphodiesterase β-subunit gene. Proc. Natl. Acad. Sci. USA 90: 3968-3972.

Sullivan L.J., Makris G.S., Dickinson P., Mulhall L.E.M., Forrest S., Cotton R.G.H. & Loughnan M.S. (1993a). A new codon 15 rhodopsin gene mutation in autosomal dominant retinitis pigmentosa is associated with sectorial disease. Arch. Ophthalmol. 111: 1512-1517.

Sullivan L.J., Scott K.M., Falls B.E., Richards J.E. & Sieving P.A. (1993b). A novel rhodopsin mutation at the retinal binding site (Lys-296-Met) in adRP. Invest. Ophthalmol. Vis. Sci. 34: 1149.

Sung C-H., Davenport C.M., Hannessey J.C., Maumenee I.H., Jacobson S.G., Heckenlively J.R., Nowakowski R., Fishman G., Gouras P. & Nathans J. (1991a). Rhodopsin mutations in autosomal dominant retinitis pigmentosa. Proc. Natl. Acad. Sci. USA 88: 6481-6485.

Sung C-H., Schneider B.G., Agarwal N., Papermaster D.S. & Nathans J. (1991b). Functional heterogeneity of mutant rhodopsins responsible for autosomal dominant retinitis pigmentosa. Proc. Natl. Acad. Sci. USA 88: 8840-8844.

Torre V., Matthews H.R. & Lamb T.D. (1986). Role of calcium in regulating the cyclic GMP cascade of phototransduction in retinal rods. Proc. Natl. Acad. Sci. USA 83: 7109-7113.

Trask B., Fertitta A., Christensen M., Youngblom J., Bergmann A., Copeland A., Jong p., Mohrenweiser H., Olsen A., Carrano A. & Katherine T. (1993). Fluorescence in situ hybridization mapping of human chromosome 19: Cytogenetic band location of 540 cosmids and 70 genes or DNA markers. Genomics 15: 133-145.

Travis G.H., Brennan M.B., Danielson P.E., Kozak C. A. & Sutcliffe J.G. (1989). Identification of a photoreceptor-specific mRNA encoded by the gene responsible for retinal degeneration slow (*rds*). Nature 338: 70-73.

Travis G.H., Sutcliffe J.G. & Bok D. (1991a). The retinal degeneration slow (rds) gene product is a photoreceptor disc membrane-associated glycoprotein. Neuron 6: 61-70.

Travis G.H., Christerson L., Danielson P.E., Klisak I., Sparkes R.S., Hahn L.B., Dryja T.P. & Sutcliffe J.G. (1991b). The human retinal degeneration slow (RDS) gene: chromosome assingment and structure of the mRNA. Genomics 10: 733-739.

Turner D.L., Snyder E.Y. & Cepko C.L. (1990). Lineage-independent determination of cell type in the embryonic mouse retina. Neuron 4: 833-845.

Usada N., Kong Y., Hagiwara M., Uchida C., Terasawa M., Nagata T. & Hidaka H. (1991). Differential isolation of protein kinase C isoenzyme in retinal neurons. J. Cell Biol. 112: 1241-1247.

Vaithinathan R., Berson E.L. & Dryja T.P. (1994). Further screening of the rhodopsin gene in patients with autosomal dominant retinitis pigmentosa. Genomics 21: 461-463.

Van nie R., Ivanyi D. & Demant P. (1978). A new H-2 linked mutation, rds, causing retinal degeneration slow in mouse. Tissue Antigens 12, 106-108.

Vogel F. & Rathenberg R. (1975). Spontaneous mutations in man. Adv. Hum. Genet. 5: 223-318.

Vollarth D., Nathans J. & Davies R.W. (1988). Tandem array of human visual pigment genes at Xq28. Science 240: 1669-1672.

Wald G. (1968). The molecular basis of visual excitation. Nature 219: 800-807.

Warburg M., Sjo O. & Fledelius H.C. (1991). Deletion mapping of a retinal cone-rod dystrophy: assignment to 18q211. Am. J. Med. Genet. 39: 288-293.

Watanabe Y., Kawasaki K., Miki N. & Kuo C.H. (1990). Isolation and analysis of the human MEKA gene encoding a retina-specific protein. Biochem. Biophys. Res. Commun. 170: 951-956.

Weber B.H.F., Walker D., Muller B. & Mar L. (1994a). Best's vitelloform dystrophy (VMD2) maps between D11S903 and PYGM: no evidence for locus heterogeneity. Genomics 20: 267-274.

Weber B.H.F., Vogt G., Wolz W., Ives E.J. & Ewing C.C. (1994b). Sorsby's fundus dystrophy is genetically linked to chromosome 22q13-qter. Nature Genet. 7: 158-161.

Weber B.H.F., Vogt G., PruettR.C., Stohr H. & Felbor U. (1994c). Mutations in the tissue inhibitor of metalloproteinases-3 (TIMP3) in patients with Sorsby's fundus dystrophy. Nature Genet. 8: 352-356.

Weber J.L. & May P.E. (1989). Abundant class of human DNA polymorphisms which can be typed using the polymerase chain reaction. Am. J. Hum. Genet. 44: 388-396.

Weber J.L., Wang Z., Hansen K., Stephenson M., Kappel C., Salzman S., Wilkie P.J., Keats B., Dracopoli N.C., BrandriffB.F. & Olsen A.S. (1993). Evidence for human meiotic recombination interference obtained through construction of a short tandem repeat-polymorphism linkage map of chromosome 19. Am. J. Hum. Genet. 53: 1079-1095.

Wells J., Wroblewski J., Keen J., Inglehearn C., Jupp C., Eckstein A., Jay M., Arden G., Bhattacharya S., Fitzke F. & Bird A. (1993). Mutations in the human retinal degeneration slow (RDS) gene can cause either retinitis pigmentosa or macular dystrophy. Nature Genet. 3: 213-218.

Weil D., Blanchard S., Kaplan J., Guilford P., Gibson F., Walsh J., Mburu P., Varela A., Levilliers J., Weston M.D., Kelley P.M., Kimberling W.J., Wagenaar M., Levi-Acobas F., Larget-Piet D., Munnich A., Steel K.P., Brown S.D.M. & Petit C. (1995). Defective myosin VIIA gene responsible for Usher syndrome type 1B. Nature 374: 60-61.

Weissenbach J., Gyapay G., Dib C., Vignal A., Morissette J., Millasseau P., Vaysseix G. & Lathrop M. (1992). A second-generation linkage map of the human genome. Nature 359: 794-801.

Wetsel W.C., Kahn W.A., Merchenthaler I., Rivera H., Halpern A.E., Phung H.M., Negro-Vilar A. & Hannun Y. (1992). Tissue and cellular distribution of the extended family of protein kinase C isoenzymes. J. Cell Biol. 117: 121-133.

Wetts R. & Fraser S.E. (1988). Multipotent precursors can give rise to all major cell types of

the frog retina. Science 239: 1142-1145.

Wilden U. & Kuhn H. (1982). Light-dependent phosphorylation of rhodopsin: Number of phosphorylation sites. Biochemistry 21: 3014-3022.

Wilden U., Hall S.W. & Kuhn H. (1986). Phosphodiesterase activation by photoexcited rhodopsin is quenched when rhodopsin is phosphorylated and binds the intrinsic 48-kda protein of rod outer segments. Proc. Natl. Acad. Sci. USA 83: 1174-1178.

Wilkie T.M., Gilbert D.J., Olsen A.S., Chen X.N., Amatruda T.T., Korenberg J.R., Trask B.J., de Jong P., Reed R.R. & Simon M.I. (1992). Evolution of the mammalian G protein α subunit multigene family. Nature Genet. 1: 85-91.

Wong F. (1993). How shall research in the treatment of retinitis pigmentosa proceed? Ach. Ophthalmol. 111: 754-756.

Wong P., vanVeen T., Kutty K., Bernstein S., Borst D., Rodriguez I., Pfeffer B., Wiggert B., Tenniswood M. & Chader G. (1994). Molecular characterization of an apoptosis inducible gene, TRPM-2/clusterin, and its expression in the mammalian eye. Invest. Ophthalmol. Vis. Sci. 35 (suppl.): 1820 (abstract no. 2618).

Wright A.F., Bhattacharya S.S., Clayton J.F., et al. (1987). Linkage relationships between X-linked retinitis pigmentosa and nine short arm markers; exclusion of the disease locus from Xp21 and localisation to between DXS7 and DXS14. AM. J. Hum. Genet. 41: 635-644.

Wright A.F. (1990). Towards the identification of genes in X-linked retinitis pigmentosa. Prog. Retina Res. 9: 197-227.

Wyllie A.H., Morris R.G., Smith A.L. & Dunlop D. (1984). Chromatin cleavage in apoptosis: association with condensed chromatin morphology and dependence on macromolecular synthesis. J. Pathol. 142: 67-77.

Yamagata K., Goto K., Kuo C.-H., Kondo H. & Miki N. (1990). Visinin: a novel calcium binding protein expressed in retinal cone cells. Neuron 2: 469-476.

Yamaki K., Tsuda M., Kikuchi T., Chen K.-H., Huang K.-P. & Shinohara T. (1990). Structural organization of the human S-antigen gene. J. Biol. Chem. 265: 20757-20762.

Yatsunami K. & Khorana H.G. (1985). GTPase of bovine rod outer segments: The amino acid sequence of the α subunit as derived from the cDNA sequence. Proc. Natl. Acad. Sci. USA 82: 4316-4320.

Yau K.-W. & Baylor D.A. (1989). Cyclic GMP-activated conductance of retinal photoreceptor cells. Annu. Rev. Neurosci. 12: 289-327.

Young R.W. & Bok D. (1969). Participation of the retinal pigment epithelium in the rod outer segment renewal process. J. Cell Biol. 42: 392-403.

Young R.W. (1984). Cell death during differentiation of the retina in the mouse. J. Comp. Neurol. 229: 362-373.

Zhang K., Bither P.P., Park R., Donoso L.A., Seidman J.G. & Seidman C.E. (1994). A dominant Stargardt's macular dystrophy locus maps to chromosome 13q34. Arch. Ophthalmol. 112: 759-764.

Zhang K., Seidman C.E., Seidman J.G. & Donoso L.A. (1995). Assessing rhodopsin kinase as a candidate gene for dominant Stargardt's macular dystrophy. Invest. Ophthalmol. Vis. Sci. 36 (suppl.): 1064 (abstract no. 4896).

Zhukovsky E.A., Robinson P.R. & Oprian D.D. (1991). Transduction activation by rhodopsin without a covalent bond to the 11-cis retinal chromphore. Science 251: 558-560.

Ziegle J.S., Su Y., Corcoran K.P., Nie L., Mayrand P.E., Hoff L.B., McBride L.J., Kronick M.N. & Diehl S.R. (1992). Application of automated DNA sizing technology for genotyping microsatellite loci. Genomics 14: 1026-1031.

HUMAN MUTATION 2:249–255 (1993)

MUTATION UPDATE

Rhodopsin Mutations in Autosomal Dominant Retinitis Pigmentosa

Mai Al-Maghtheh, Cheryl Gregory, Chris Inglehearn, Alison Hardcastle, and Shomi Bhattacharya*

Department of Molecular Genetics, Institute of Ophthalmology, University of London, Bath Street, London EC1V 9EL, England; Fax: 071-6086-863

Communicated by Thaddeus P. Dryja

Retinitis pigmentosa is an inherited progressive disease which is a major cause of blindness in western communities. It can be inherited as an autosomal dominant, autosomal recessive, or X-linked recessive disorder. In the autosomal dominant form (adRP), which comprises about 25% of total cases, approximately 30% of families have mutations in the gene encoding the rod photoreceptor-specific protein rhodopsin. This is the transmembrane protein which, when photoexcited, initiates the visual transduction cascade. So far, 41 single-base-pair (bp) substitutions, one two-bp substitution, and four deletions ranging from 3 to 42 bp have been identified in this gene. These mutations do not appear to be significantly clustered in a specific part of the protein, but occur in all three major domains, namely the intradiscal, transmembrane, and cytoplasmic regions. Different mutations appear to cause differences in the severity of the disease, though there is considerable variability in severity even within the same family, at least in certain of these mutations. Identification of all the mutations involved in rhodopsin-RP should allow accurate and early detection of affected individuals, informed genetic counselling, as well as furthering our knowledge of the disease process involved.

INTRODUCTION

Retinitis pigmentosa is a group of heterogeneous degenerative retinal disorders which affect one to two in every 5000 births in the western world (Boughman et al., 1980; Bundey and Crews, 1984; Bunker et al., 1984). It primarily involves degeneration of rod photoreceptors of the retina, resulting in night blindness and tunnel vision in the early stages of the disease and progressing in some cases to extensive overall visual loss in the later stages. The disease derives its name from the characteristic pigmentary deposits seen in the retina (which have a bone spicule like configuration) of most patients with this disorder. These may result from abnormal proliferation and/or migration of the retinal pigment epithelial (RPE) cells, or the pigment containing cells may be blood-borne macrophages that incorporate pigment on their way from choriocapillaries to the neural retina.

RP can be inherited as an autosomal dominant (adRP), autosomal recessive (arRP), or X-linked disease (x1RP). A significant proportion of cases is not classified because of lack of family history, while some other RP patients are classified as having autosmal recessive syndromes, the most common of which is Usher's syndrome (RP and deafness). These different modes of inheritance indicate the underlying genetic heterogeneity of the disease. adRP, which accounts for about 25% of total RP cases (Bundy and Crews, 1984; Jay, 1982), can be divided into two distinct types (Massof and Finkelstein, 1981): type I where rods lose function before cones, and type II where there is simultaneous loss of both rod and cone function. This classification system corresponds to another described by Lyness and co-workers (1985) based on psychophysical and fundoscopic examination of the retina. These are D-type which is similar to type I, and R-type which is similar to type II. D-type is characterised by a diffuse pattern of rod photoreceptor functional loss throughout the retina in the presence of relatively normal cone function, while R-type results in regional patches of functional loss of both rods and cones. Generally speaking, type I or D-type is early in onset while type II or R-type has a variable age of onset. Sector

Received December 23, 1992; accepted April 8, 1993.

*To whom reprint requests/correspondence should be addressed.

RP is found considerably less frequently and presents with bone specule pigmentation and visual field loss limited to one or two quadrants of the retina, usually inferior nasal, consistently in all affected members within a family (Berson and Howard, 1971).

In 1989 McWilliam and co-workers reported close genetic linkage between polymorphic DNA marker C17 (D3S47), on the long arm of chromosome 3, and the adRP disease phenotype in a large Irish pedigree. The rhodopsin gene, which is involved in the phototransduction cycle, has been isolated (Nathans and Hogness, 1984), and mapped to chromosome three region 3q21–3q24 (Nathans et al., 1986; Sparkes et al., 1986) and was therefore a candidate for adRP. Dryja and coworkers (1990a) reported a C-to-A transversion in codon 23 of rhodopsin (Pro-to-His), which correlated with the disease phenotype in a family with early onset adRP. Since that time 46 rhodopsin mutations have been reported in adRP families, all of which change the amino acid sequence and cosegregate with the disease phenotype. Rhodopsin mutations have since been shown to account for around one-third of adRP cases in four surveys, one in the UK and three in the United States (Sung et al., 1991a; Dryja et al., 1991; Sheffield et al., 1991; Inglehearn et al., 1992).

MUTATIONS AND POLYMORPHISMS

The mutations so far identified in adRP patients are spread evenly throughout the coding region of the rhodopsin gene. No single mutation has been found to account for a large fraction of the disease cases, perhaps due to natural selection against dominant mutations which would result in expression of disease in the heterozygotes. Forty-one single base-pair substitutions, one two base-pair substitution, and four small deletions have been found in the rhodopsin gene [Table 1a]. DNA sequence variations in rhodopsin which do not correlate with adRP (polymorphisms) have also been reported in the coding (silent third position changes) and the noncoding regions of the gene (Dryja et al., 1990b; Sung et al., 1991a; Tables Ib and II). As with single base substitutions at other loci, transitions greatly outnumber transversions (Vogel and Rathenberg, 1975). A partial explanation for the excess of transitions lies in the tendency for methylated cytidine in the dinucleotide CpG to mutate to T, making CpG a mutational hot spot. This may explain the occurence of the Pro-347-Leu mutation which is due to C-to-T transition in a CpG sequence. This mutation has been seen in several unrelated British families (Inglehearn et al., 1992, and unpublished data) as well as German (Apfelstedt-Sylla et al., 1992), American (Dryja et al., 1990b), and Japanese families (Fujiki et al., 1992). In contrast the Pro-23-His mutation (C-to-A transversion), which has attained a frequency of 12% in the American adRP patients (Dryja et al., 1990a; Sheffield et al., 1991; Sung et al., 1991a), has not been reported anywhere else. Patients who have this mutation were found to share the same rare allele at the CA repeat polymorphism in intron one of the rhodopsin gene, which strongly supports the hypothesis that this mutation arose once in one common ancestor (Dryja et al., 1991). This mutation has been found to be absent in a study of 91 European adRP families (Farrar et al., 1990). Recently a null mutation in codon 249 has been reported as a cause of retinitis pigmentosa in an autosomal recessive family (Rosenfeld et al., 1992). This might give some insight into possible pathogenic mechanisms of the disease (see next section).

BIOLOGICAL RELEVANCE

Rhodopsin is a transmembrane protein found in the outer segment discs of the rod photoreceptor cells. It consists of seven helical hydrophobic domains connected by hydrophylic loops. The hydrophobic domains traverse the lipid bilayer of the disc, with the carboxyl terminus on the cytoplasmic side. The amino terminus, which bears two oligosaccharide attachment sites, is on the intradiscal side of the membrane (Fig. 1). Certain amino acids are known to have essential roles in determining the structure and function of the opsin protein. For example, the cysteines at codons 110 and 187 have been found to form a disulphide bond (Karnik and Khorana, 1990), while lysine at codon 296 is the site for attachment of 11-*cis*-retinal to form the functional photopigment. However, mutations are not confined to conserved amino acids or to those with already defined functions.

Thirteen of the mutations identified were found to fall into two classes on the basis of in vitro functional assays (Sung et al., 1991b). Mutant opsins were expressed in tissue culture, and tested for their yield, ability to bind 11-*cis*-retinal, and subcellular localisation. Class I resembled wild-type rhodopsin in all respects, while class II were expressed at lower levels, regenerated rhodopsin variably or not at all, and were inefficiently transported to the plasma membrane. It has therefore been hypothezised that some mutant proteins fail

TABLE 1a. Mutations in the Rhodopsin Gene That Correlate With Disease Phenotype in adRP Patients[a]

Exon	Codon	Sequence change	Amino acid change	Reference
1	4	ACA-AAA	Thr-Lys	Gal et al., unpublished
1	17	ACG-ATG	Thr-Met	Sung et al., 1991a
1	23	CCC-CAC	Pro-His	Dryja et al., 1990a
1	23	CCC-CTC	Pro-Leu	Dryja et al., 1991
1	28	CAG-CAC	Gln-His	Gal et al., unpublished
1	45	TTT-CTT	Phe-Leu	Sung et al., 1991a
1	46	CTG-CGG	Leu-Arg	Rodriguez et al., 1993
1	51	GGC-GTC	Gly-Val	Dryja et al., 1991
1	51	GGC-CGC	Gly-Arg	Dryja et al., 1992
1	53	CCC-CGC	Pro-Arg	Inglehearn et al., 1992
1	58	ACG-AGG	Thr-Arg	Dryja et al., 1990b
1	68–71	del:CTGCGCACGCCT	del:Leu-Arg-Thr-Pro	Keen et al., 1991a
1	87	GTC-GAC	Val-Asp	Sung et al., 1991a
1	89	GGT-GAT	Gly-Asp	Sung et al., 1991a
1	90	GGC-GAC	Gly-Asp	Sieving et al., 1992
1	106	GGG-TGG	Gly-Trp	Sung et al., 1991a
1	106	GGG-AGG	Gly-Arg	Inglehearn et al., 1992
1	110	TGC-TAC	Cys-Tyr	Dryja et al., 1992
2	125	CTG-CGG	Leu-Arg	Dryja et al., 1991
2	135	CGG-CTT	Arg-Leu	Sung et al., 1991a
2	135	CGG-TGG	Arg-Trp	Sung et al., 1991a
2	135	CGG-GGG	Arg-Gly	Gal et al., unpublished
2	167	TGC-CGC	Cys-Arg	Dryja et al., 1991
2	171	CCA-CTA	Pro-Leu	Dryja et al., 1991
3	178	TAC-TGC	Tyr-Cys	Sung et al., 1991a
3	181	GAG-AAG	Glu-Lys	Dryja et al., 1991
3	182	GGC-AGC	Gly-Ser	Sheffield et al., 1991
3	186	TCG-CCG	Ser-Pro	Dryja et al., 1991
3	188	GGA-AGA	Gly-Arg	Dryja et al., 1991
3	190	GAC-GGC	Asp-Gly	Sung et al., 1991a
3	190	GAC-AAC	Asp-Asn	Keen et al., 1991a
3	190	GAC-TAC	Asp-Tyr	Stone et al., personal communication
3	211	CAC-CCC	His-Pro	Keen et al., 1991a
3	220	TTT-TGT	Phe-Cys	Gal et al., unpublished
3	222	TGC-CGC	Cys-Arg	Gal et al., unpublished
4	249	GAG-TAG	Glu-stop	Rosenfeld et al., 1992
4	255/256	ATC-del	Ile-del	Inglehearn et al., 1991
4	267	CCC-CTC	Pro-Leu	Sheffield et al., 1991
4	296	AAG-GAG	Lys-Glu	Keen et al., 1991a
5	340–348	42bp-del	8 a.a.-del	Restango et al., 1993
5	341–343	8bp-del	2a.a.-del and frameshift	Gal et al., personal communication
5	344	CAG-TAG	Gln-stop	Sung et al., 1991a
5	345	GTG-ATG	Val-Met	Dryja et al., 1991
5	347	CCG-CTG	Pro-Leu	Dryja et al., 1990b
5	347	CCG-TCG	Pro-Ser	Dryja et al., 1990b
5	347	CCG-CGG	Pro-Arg	Gal et al., 1991

[a]del, deletion; a.a., amino acid.

TABLE 1b. Polymorphisms in Coding Region

Exon	Codon	Sequence change	Amino acid change	Reference
1	120	GGC-GGT	Gly-Gly	Dryja et al., 1991
2	160	ACC-ACA	Thr-Thr	Sung et al., 1991a
2	173	GCC-GCT	Ala-Ala	Dryja et al., 1991
4	248	AAG-AAA	Lys-Lys	Sung et al., 1991a

to fold properly and accumulate in the endoplasmic reticulum, disrupting the normal cell function, while others are produced and exported to rod outer segments (ROS) normally, and cause disease by a different mechanism. Mutations in codons 106, 178, and 190 surrounding Cys-110 and Cys-187 have been classified as class II (Sung et al., 1991b). These mutations may prevent formation

TABLE 2. Polymorphisms Including Restriction Fragment Length Polymorphism in Noncoding Region

Position	Sequence (change)	Restriction enzyme	Reference
5′ untranslated region	A→G	*Sac*II	Dryja et al., 1991
Intron 1	(CA)n	—	Weber and May, 1989
Intron 3	C→T	*Rsa*I	Dryja et al., 1991
Intron 4	G→A	—	Sung et al., 1991a
3′ untranslated region	C→A	—	Dryja et al., 1990b

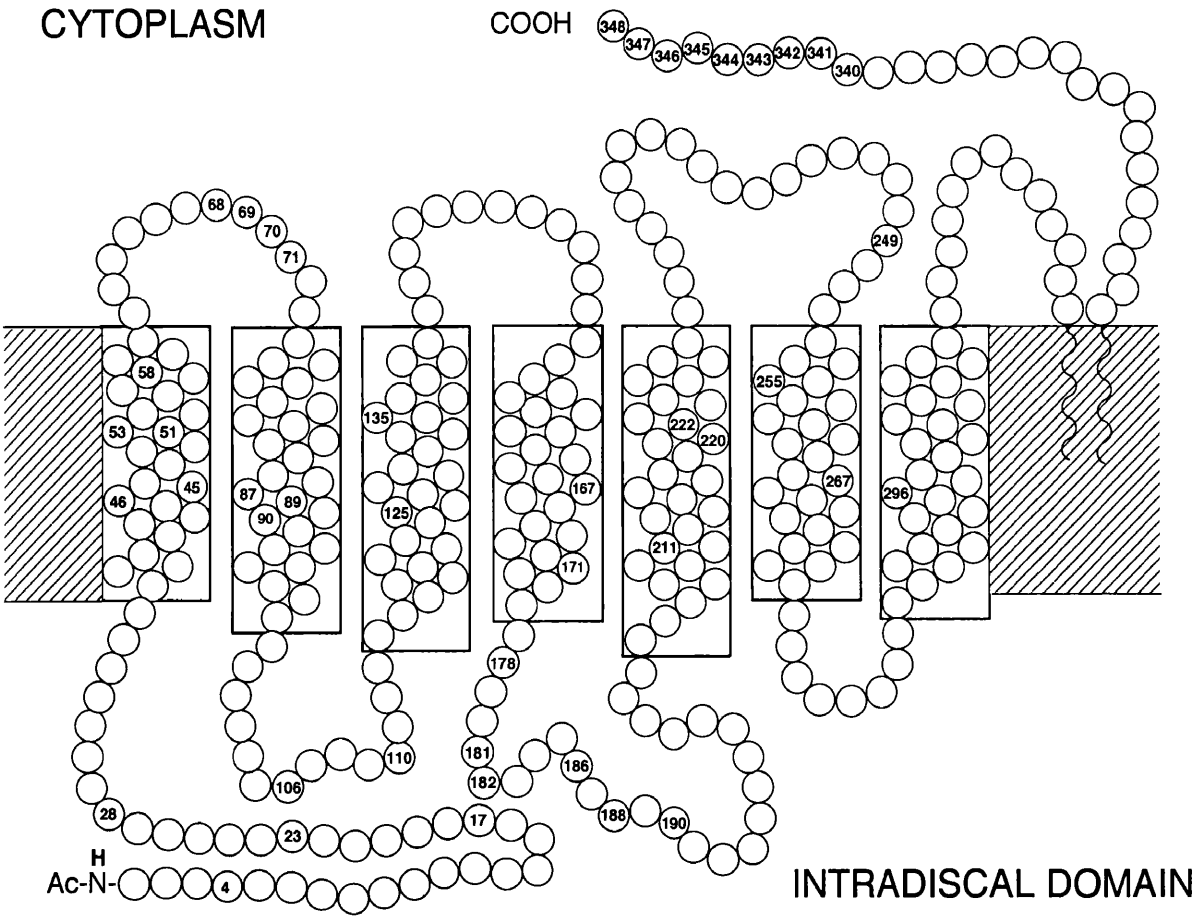

FIGURE 1. Graphic representation of the rhodopsin molecule. Numbers on the sequence correspond to amino acid changes which result from rhodospin gene mutations.

of a disulphide bond between the two cysteine residues, therefore disturbing the protein structure. Mutations in codons 181, 186, and 188 might have similar effects, though they have not been classified in this way. Similarly the class II mutants Pro-23-His and Val-87-Asp (Sung et al., 1991b) that change nonpolar hydrophobic residues to charged residues in the intradiscal and transmembrane domains, respectively, might prevent the mutant protein from properly spanning the disc membrane. On this basis it is possible to speculate that the Lys-296-Glu mutation is probably a class II mutation though again it has not been classified in this way to date. Conserved lysine 296 functions as a retinal attachment site. Substitution of lysine with glutamic acid, which lacks the amino group to which retinal normally binds, constitutively activates rhodopsin, suggesting that degeneration of the photoreceptor cells in individuals with this mutation may result from persistent stimulation of the phototransduction pathway (Robinson et al., 1992). Without retinal newly synthesised opsin has been shown to accumulate in the rough endoplasmic reticulum of isolated rat retina (St. Jules and O'Brien, 1986).

Rhodopsin accounts for 80% of protein in a nor-

mal rod outer segment (Basinger et al., 1976), and therefore the presence of large quantities of structurally altered mutant protein may lead to photoreceptor cell degeneration. This hypothesis is supported by the finding of a null mutation in an autosomal recessive RP family (Rosenfeld et al., 1992). This shows that the photoreceptor cell remains relatively healthy with only 50% of normal rhodopsin present in heterozygote carriers of the null mutation. In other words total absence of the mutated product in the presence of 50% of the normal is not harmful to the cell as illustrated by this example, but in all other cases it can be postulated that in some way it is the presence of the mutant product which causes the disease by simply being there.

CLINICAL RELEVANCE

Most of rhodopsin mutations correspond to type I/D, and sectorial RP. The remaining rhodopsin unlinked families mainly have type II/R phenotype and are believed to have mutations somewhere else in the genome. However, different mutations within the rhodopsin gene result in different clinical parameters which correspond to variation in severity of the disease (Fitzke et al., 1991). All sectorial RP cases studied in this laboratory have mutations in exon one (either in codon 58 or codon 106). Other studies also reported the sector phenotype with a codon 23 mutation (Heckenlively et al., 1991; Stone et al., 1991), however, the same mutation causes variable phenotypes according to another study (Berson et al., 1991). Fishman and co-workers also described sector RP with codon 190 mutation in a family with autosomal dominant retinitis pigmentosa (Fishman et al., 1992), therefore it would appear that sector RP is not confined to exon one mutations. The mutation in codon 296, which is the retinal attachment site, leads to a severe phenotype (Keen et al., 1991a), while a mutation in codon 90 was found to be associated with congenital complete nightblindness (Sieving et al., 1992).

DIAGNOSTIC RELEVANCE

The fact that different mutations in the rhodopsin gene result in different phenotypes in some families may help in the identification of possible mutations. However, the relatively large number of rhodopsin mutations and the substantial phenotypic overlap between these mutations make predictive diagnosis difficult. The existence of phenotypic variation within families carrying the same mutation also further complicates this approach. However, once the specific mutation in a given family has been established, further screening of affected and unaffected family members will become relatively simple. A significant proportion of these mutations alters a restriction enzyme site and therefore PCR (polymerase chain reaction) amplification of the target DNA followed by restriction enzyme digestion may prove to be a quick and easy test to perform for the detection of such mutations. Simple methods have also been developed for the identification of single base mismatches or small rearrangements (Orita et al., 1990; Keen et al., 1991b) which should allow for rapid screening of the whole rhodopsin gene to localise the mutation to a specific exon. This can then be followed by direct sequencing of that exon to identify the mutation. This should ultimately lead to informed counselling for all rhodopsin RP sufferers.

FUTURE PROSPECTS

As stated earlier, 30% of adRP cases are caused by rhodopsin mutations. Peripherin/rds mutations account for another 2–4% of adRP (Kajiwara et al., 1991; Wells et al., 1993). Genetic linkage studies have localized further new loci for adRP to the pericentromeric region of chromosome 8 (Blanton et al., 1991), chromosome 7 short arm (Inglehearn et al., 1993), and long arm (Jordan et al., 1993). These studies were based on single large families. It remains to be seen what proportion of adRP results from mutations in either chromosome 7p/7q or chromosome 8 genes. It has also been established in this laboratory (unpublished data) that in at least one other family, the gene defect does not map to any of the known loci on chromosomes 3, 6, 7p, 7q, or 8, therefore confirming further genetic heterogeneity. In the near future, further research will lead to the mapping of new gene(s) causing adRP as well as other forms of retinal degenerations. This research should give a clearer understanding of the relation between genotype and phenotype, which in turn will facilitate diagnosis and counselling. It would also give further insight into pathological mechanisms responsible for photoreceptor cell degeneration and will therefore lead to a greater understanding of the normal development and functions of the eye and the visual transduction pathway. In the longer term it may lead to possible treatment of RP and other degenerative retinopathies.

ACKNOWLEDGMENTS

We gratefully acknowledge the Wellcome Foundation (Grant number 035535/Z/92/Z/REH), the RP Foundation Fighting Blindness USA, The George Gund Foundation, and the British Retinitis Pigmentosa Society for funding our research.

REFERENCES

Apfelstedt-Sylla E, Kunisch M, Horn M, Ruther K, Gal A, Zrenner E (1992) Diffuse loss of rod function in autosomal dominant retinitis pigmentosa with Pro-347-Leu mutation of rhodopsin. German J Ophthalmol (in press).

Basinger S, Bok D, Hall H (1976) Rhodopsin in the rod outer segment plasma membrane. J Cell Biol 69:29–42.

Berson EL, Howard J (1971) Temporal aspects of the electroretinogram in sector retinitis pigmentosa. Arch Ophthalmol 86: 653–365.

Berson EL, Rosner B, Sandberg MA, Dryja TP (1991) Ocular findings in patients with autosomal dominant retinitis pigmentosa and a rhodopsin gene defect (Pro-23-His). Arch Ophthalmol 109:92–101.

Bunker CH, Berson EL (1984) Prevalence of retinitis pigmentosa in Maine. Am J Ophthalmol 97:357–365.

Blanton SH, Heckenlively JR, Cottingham AW, Freidman J, Sadler LA, Wagner M, Freidman LH, Daiger SP (1991) Linkage mapping of autosomal dominant Retinitis Pigmentosa (RP1) to the pericentric region of human chromosome 8. Genomics 11: 857–869.

Boughman JA, Confally PM, Nance WE (1980) Population genetic studies of retinitis pigmentosa. Am J Hum Genet 32: 223–235.

Bundey S, Crews SJ (1984) A study of retinitis pigmentosa in the city of Birmingham. II. Clinical and genetic heterogeneity. J Med Genet 21:421–428.

Dryja TP (1992) Rhodopsin and autosomal dominant retinitis pigmentosa. Eye 6:1–10.

Dryja TP, McGee TL, Reichel E, Hahn LB, Cowley GS, Yandell DW, Sandberg MA, Berson EL (1990a) A point mutation of rhodospin gene in one form of retinitis pigmentosa. Nature (London) 343:364–366.

Dryja TP, McGee TL, Hahn LB, Cowley GS, Ollsen JE, Reichel E, Sandberg MA, Berson EL (1990b) Mutations within the rhodopsin gene in patients with autosomal dominant retinitis pigmentosa. N Engl J Med 323:1302–1307.

Dryja TP, Hahn LB, Cowley GS, McGee TL, Berson EL (1991) Mutation spectrum of the rhodopsin gene among patients with autosomal dominant retinitis pigmentosa. Proc Natl Acad Sci USA 88:9370–9374.

Farrar GJ, Kenna P, Redmond R, McWilliam P, Bradley DJ, Humphries MM, Sharp EM, Inglehearn CF, Bashir R, Jay M, Watty A, Ludwig M, Schinzel A, Sammans C, Gal A, Bhattacharya S, Humphries P (1990) Autosomal dominant retinitis pigmentosa: absence of the rhodopsin proline/histidine substitution (codon 23) in pedigrees from Europe. Am J Hum Genet 47:941–945.

Fishman GA, Vendenburgh K, Stone EM, Gilbert LD, Alexander KR, Sheffield VC (1992) Ocular findings associated with rhodopsin gene codon 267 and codon 190 mutations in dominant retinitis pigmentosa. Arch Ophthalmol 110:1582–1588.

Fitzke FW, Owens S, Moore AT, Jay M, Inglehearn CF, Bhattacharya S, Bird AC (1991) Comparison of functional characteristics of autosomal dominant retinitis pigmentosa with different amino acid changes in the rhodopsin molecule. Invest Ophthalmol Vis Sci (suppl.) 32:1200.

Fujiki K, Hotta Y, Hayakawa M, Sakuma H, Shiono T, Noro M, Sakuma T, Tamai M, Hikiji K, Kawaguchi R, Hoshi A, Nakajima A, Kanai A (1992) Point mutations of rhodopsin gene found in Japanese families with autosomal dominant retinitis pigmentosa (adRP). Jpn J Hum Genet 37:125–132.

Gal A, Artlich A, Ludwig M, Niemeyer G, Olek K, Schwinger I, Schinzel A (1991) Pro-347-Arg of the rhodopsin gene in autosomal dominant retinitis pigmentosa. Genomics 11:468–470.

Heckenlively JR, Rodriguez JA, Daiger SP (1991) Autosomal dominant sectorial retinitis pigmentosa: Two families with transversion mutation in codon 23 of rhodopsin. Arch Ophthalmol 109:84–91.

Inglehearn CF, Keen TJ, Bashir R, Jay M, Fitzke F, Bird AC, Bhattacharya SS (1992) A complete screen for mutations of the rhodopsin gene in a panel of patients with autosomal dominant retinitis pigmentosa. Hum Mol Genet 1:41–45.

Inglehearn CF, Carter SA, Keen TJ, Lindsay J, Stephenson AM, Bashir R, Al-Maghtheh M, Moore AT, Jay M, Bird AC, Bhattacharya SS (1993) A new locus for autosomal dominant retinitis pigmentosa on chromosome 7p. Nature Genet 4:51–53.

Jay M (1982) Figures and fantasies: the frequencies of the different genetic forms of retinitis pigmentosa. Birth Defects Original Article Series 18:167–73.

Jordan SA, Farrar GJ, Kenna P, Humphries MM, Sheils D, Kumar-Singh R, Sharp EM, Benitez J, Carmen A, Humphries P (1993) Localisation of an autosomal dominant retinitis pigmentosa gene to 7q. Nature Genet 4:54–58.

Kajiwara K, Hahn LB, Mukai S, Travis GH, Berson EL, Dryja TP (1991) Mutations in the human retinal degeneration slow gene in autosomal dominant retinitis pigmentosa. Nature (London) 354:480–483.

Karnik SS, Khorana HG (1990) Assembly of functional rhodopsin requires a disulfide bond between cysteine residues 110 and 187. J Biol Chem 265:17520–17524.

Keen TJ, Inglehearn CF, Lester DH, Bashir R, Jay M, Bird AC, Bhattacharya SS (1991a) Autosomal dominant retinitis pigmentosa: Four new mutations in rhodopsin, one of them in the retinal attachment site. Genomics 11:199–205.

Keen J, Lester D, Inglehearn C, Curtis A, Bhattacharya SS (1991b) Rapid detection of single base mismatches as heteroduplexes on hydrolink gel. Trends Genet 7:5.

Lyness AL, Ernst W, Quinlan MP, Clover GM, Arden GB, Carter RM, Bird AC, Parker JA (1985) A clinical, psychophysical and electroretinographic survey of patients with autosomal dominant retinitis pigmentosa. Br J Ophthalmol 69:326–339.

Massof RW, Finkelstein D (1981) Two forms of autosomal dominant primary retinitis pigmentosa. Doc Ophthalmol 51:289–346.

McWilliam P, Farrar GJ, Kenna P, Bradly DG, Humphries MM, Sharp EM, McConnel DJ, Lawler M, Sheils D, Ryans C, Stevens K, Daiger SP, Humphries P (1989) Autosomal dominant retinitis pigmentosa (ADRP): Localization of an ADRP gene to the long arm of chromosome 3. Genomics 5:619–622.

Nathans J, Hogness DS (1984) Isolation and nucleotide sequence of the gene encoding human rhodopsin. Proc Natl Acad Sci USA 81:4851–4855.

Nathans J, Piantanida TP, Eddy RL, Shows TB, Hogness DS (1986) Molecular genetics of inherited variation in human colour vision. Science 232:203–210.

Orita M, Suzuki Y, Sekiya T, Hayashi K (1989) Rapid and sensitive detection of point mutations and DNA polymorphisms using the polymerase chain reaction. Genomics 5:874–879.

Restagno G, Maghtheh M, Bhattacharya S, Ferrone M, Garnerone S, Samuelly R, Carbonara A (1993) A large deletion at

the 3′ end of the rhodopsin gene in an Italian family with a diffuse form of autosomal dominant retinitis pigmentosa. Hum Mol Genet 2:207–208.

Robinson PR, Cohen GB, Zhukovsky EA, Oprian DD (1992) Constitutively active mutants of rhodopsin. Neuron 9:719–725.

Rodriguez JA, Herrena CA, Birch DG, Daiger SP (1993) A leucine to arginine amino acid substitution at codon 46 of rhodopsin gene is responsible for a severe form of autosomal dominant retinitis pigmentosa. Hum Mut 2:205–213.

Rosenfeld PJ, Cowley GS, McGee TL, Sandberg MA, Berson EL, Dryja TP (1992) A null mutation in the rhodopsin gene causes rod photoreceptor dysfunction and autosomal recessive retinitis pigmentosa. Nature Genet 1:209–213.

Sheffield VC, Fishman GA, Beck JS, Kimura AE, Stone EM (1991) Identification of novel rhodopsin mutations associated with retinitis pigmentosa using GC-clamped denaturing gradient gel electrophoresis. Am J Hum Genet 49:699–706.

Sieving PA, Richards JE, Bingham EL, Naarendorp F (1992) Dominant congenital complete nyctalopia and Gly-90-Asp rhodopsin mutation. Invest Ophthalmol Vis Sci (suppl.) 33: 1397.

Sparkes RS, Klisak I, Kaufman D, Mohandas T, Tobin AJ, McGinnis JF (1986) Assignment of the rhodopsin gene to human chromosome three, region 3q21-3q24 by in situ hybridization studies. Curr Eye Res 5:797–798.

St. Jules RS, O'Brien PJ (1986) The acylation of rat rhodopsin in vitro and in vivo. Exp Eye Res 43:929–940.

Stone EM, Kimura AE, Nicholas BE, Khadivi P, Fishman GA, Sheffield VC (1991) Regional distribution of retinal degeneration in patients with the proline to histidine mutation in codon 23 of the rhodopsin gene. Ophthalmology 98:1806–1813.

Sung C-H, Davenport CM, Hennessey JC, Maumenee IH, Jacobson SG, Heckenlively JR, Nowakowski R, Fishman G, Gouras P, Nathans J (1991a) Rhodopsin mutations in autosomal dominant retinitis pigmentosa. Proc Natl Acad Sci USA 88:6481–6485.

Sung CH, Schneider BG, Agarwal N, Papermaster DS, Nathans J (1991b) Functional heterogeneity of mutant rhodopsins responsible for autosomal dominant retinitis pigmentosa. Proc Natl Acad Sci USA 88:8840–8844.

Vogel F, Rathenberg R (1975) Spontaneous mutations in man. Adv Hum Genet 5:223–318.

Weber JL, May PE (1989) Abundant class of human DNA polymorphisms which can be typed using the polymerase chain reaction. Am J Hum Genet 44:388–396.

Wells J, Wroblewski J, Keen J, Inglehearn C, Jubb C, Eckstein A, Jay M, Arden G, Bhattacharya S, Fitzke F, and Bird A (1993) Mutations in the human retinal degeneration slow (RDS) gene can cause either retinitis pigmentosa or macular dystrophy. Nature Genet 3:213–218.

Human Molecular Genetics, 1994, Vol. 3, No. 1 205–206

A 150 bp insertion in the rhodopsin gene of an autosomal dominant retinitis pigmentosa family

M.Al-Maghtheh*, R.Y.Kim, A.Hardcastle, C.Inglehearn and S.S.Bhattacharya

Department of Molecular Genetics, Institute of Ophthalmology, Bath Street, London EC1V 9EL, UK

Received September 27, 1993; Revised and Accepted November 3, 1993

Retinitis pigmentosa is a group of heterogeneous inherited retinal degenerations, that affects one to two in every 5000 births in the western world (1). It results in night blindness and tunnel vision in early stages of the disease and may progress to complete blindness at later stages. The pattern of inheritance can be autosomal dominant (adRP), autosomal recessive (arRP) or X-linked (xlRP). Within the adRP category there is further genetic heterogeneity (2). Rhodopsin, on chromosome 3q21, is one of the genes which was found to be mutated in adRP families and accounts for around 30% of total adRP cases (3). Most of the mutations reported in the rhodopsin gene are single base substitutions. However, one two base pair substitution, and four relatively small deletions (3–42 bp) have also been reported (3).

We report here, for the first time, a relatively large insertion in the 3′ end of the rhodopsin gene which cosegregates with the disease phenotype in an adRP family (Figure 1). This mutation was not seen in 150 normal controls. This insertion was detected by PCR amplification of genomic DNA and electrophoresis of the product on a 2.8% agarose gel. Two bands were visualized, the smaller one corresponding to the normal fragment and the other to the insertion. The larger fragment was excised after separation on a 2% NuSieve agarose gel, and PCR amplified again using nested primers. The reamplified product was cloned using a TA cloning kit (Invitrogen Corporation), and then used for sequencing (4).

Sequence analysis reveals an insertion of 150 bp (Figure 2) which replaces 30 bp of normal sequence from nucleotide position 5145 in intron 4 to nucleotide position 5174 at the 5′ end of exon 5. The sense strand sequence of the insert is almost entirely composed of A_nG_n repeats, accounting for 88% of the residues. The sequence was analysed for homology using the FASTA algorithm (5) against standard databases. The highest homologies scored were 73% identity over 126 bp with rat N-myc (GenBank), and 69% identity over 93 bp with mouse T-cell receptor (GenBank). These homologies, along with others scored from different databases, were to GA-rich non-coding regions and appear to have no biological significance.

The deleted sequence includes the conserved 3′ splice junction of intron 4 and the first 7 nucleotides of exon 5. It may be speculated that the resultant nuclear pre-mRNA would have any of 3 alternative splicing patterns. Firstly a search for a consensus 3′ splice junction (6) in the insertion sequence identified only one possible site after nucleotide position 17. The resultant truncated protein would only code for four amino acids as exon 5, namely Lys-Lys-Lys-Arg-Stop, the DNA sequence of which is underlined in Figure 2. Secondly, if splicing were not to take place within the insert, the next AG sequence ends at position 5206 within exon 5. The sequence at that region is compatible with a potential splice site. The resultant truncated protein would be deleted for the first 13 codons of exon 5, but in-frame for the remainder of the exon. The third possibility is that neither of the two potential splicing events described above occur, resulting in the continuation of protein synthesis after exon 4 into intron 4 up to position 4776, where a stop codon would terminate translation. The resultant protein would be 111 residues larger

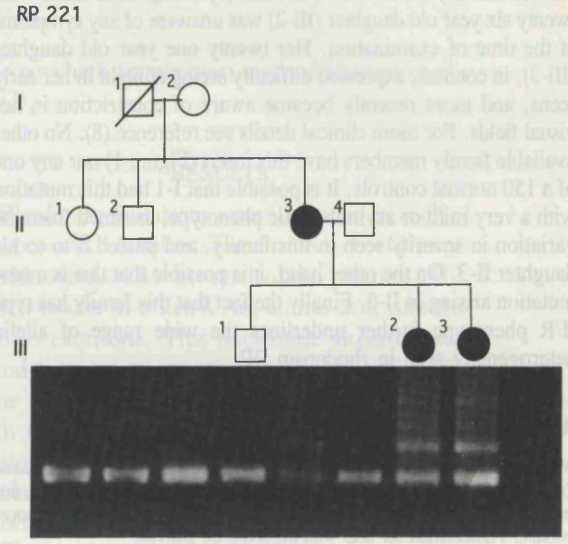

Figure 1. Pedigree and agarose gel photograph of rhodopsin exon 5 PCR products. It shows segregation of the insert with affected individuals of the family. Smaller fragment seen in all individuals corresponds to the normal PCR products of exon 5.

```
     5144-t acatattaca ttataagaaa aaaaaaaggt agaggaaggg*
          a tgtataatgt aatattcttt ttttttcca tctccttccc

aggaagggaa ggggagggag gaagtggaga tgtggagacg cgagaggaag
tccttccctt cccctccctc cttcacctct acacctctgc gctctccttc

agagagaggc agagggagag ggaaaggtgg ggagagagga gggggcagag
tctctctccg tctccctctc cctttcctcc cctctctcct ccccgtctc

agagaggtgg A-5175
tctctccacc T
```

Figure 2. Insert sequence (150 bp) including one normal flanking nucleotide from both sides of the insertion point, and its position within the normal genomic sequence of the rhodopsin gene. *3′ splice junction and stop codon (both double underlined), and in between sequence of exon 5 (underlined) as described in the text.

* To whom correspondence should be addressed

than the normal rhodopsin protein. It is therefore not possible to deduce exactly what would be the amino acid sequence of the protein coded by the altered rhodopsin gene. Functional assays such as those reported by Nathans and coworkers (7) would be necessary to elucidate the role of this protein in pathogenesis of retinal degeneration in this family, and to classify it as either class I or class II as described in the above reference.

Interestingly, the phenotype in this family is characterized by regional distribution of photoreceptor cell degeneration of both rods and cones in the same region of the retina together with variation in the age of onset and severity of symptoms (8). This phenotype corresponds to type II/R by the clinical criteria of Lyness and coworkers (9), which is unlike the previously described phenotype in most rhodopsin RP families (3). Patient II-3 had first experienced mild difficulty seeing at night in her early teens. Subsequent ophthalmic evaluation lead to the diagnosis of her as having retinitis pigmentosa (8). Neither her parents nor any relatives had any history of night blindness. Her twenty six year old daughter (III-2) was unaware of any symptoms at the time of examination. Her twenty one year old daughter (III-3), in contrast, expressed difficulty seeing at night in her early teens, and more recently became aware of constriction in her visual fields. For more clinical details see reference (8). No other available family members have this insert (Figure 1) nor any one of a 150 normal controls. It is possible that I-1 had this mutation with a very mild or asymptomatic phenotype, assumed from the variation in severity seen in this family, and passed it to to his daughter II-3. On the other hand, it is possible that this is a new mutation arising in II-3. Finally the fact that this family has type II/R phenotype further underlines the wide range of allelic heterogeneity seen in rhodopsin RP.

ACKNOWLEDGMENTS

We gratefully acknowledge the British Retinitis Pigmentosa Society, the Wellcome Trust and the American Retinitis Pigmentosa Foundation for supporting this research. We would like to thank Dr. Devjani Chatterjee (Jefferson Cancer Institute, Philadelphia) for help with the sequence analysis.

REFERENCES

1. Boughman,J.A., Conneally,P.M. and Nance,W.E. (1980) *Am. J. Hum. Genet.et al.* **32**, 223–235.
2. Lindsay,S., Inglehearn,C.F., Curtis,A. and Bhattacharya,S.S. (1992) *Curr. Opin. Genet. Dev.* **2**, 459–466.
3. Al-Maghtheh,M., Gregory,C., Inglehearn,C. and Bhattacharya,S. (1993) *Hum. Mut.* **2**, 249–255.
4. Sanger,F., Nicklen,S. and Coulson,A.R. (1977) *Proc. Natl. Acad. Sci. USA* **74**, 5463–5467.
5. Pearson,W.R. and Lipman,J.D. (1988) *Proc. Natl. Acad. Sci. USA* **85**, 2444–2448.
6. Cech,T.R. (1986) *Cell* **44**, 207–210.
7. Sung,C.H., Schneider,B.G., Agarwal,N., Papermaster,D.S. and Nathans,J. (1991) *Proc. Natl Acad. Sci. USA* **88**, 8840–8844.
8. Kim,R.Y., Al-Maghtheh,M., Fitzke,F.W., Arden,G.B., Jay,M., Bhattacharya,S.S. and Bird,A. (1993) *Arch. Ophthalmol.* (in press).
9. Lyness,A.L., Ernst,W., Quinlan,M.P., Clover,G.M., Arden,G.B., Carter,R.M., Bird,A.C. and Parker,J.A. (1985) *Brit. J. Ophthalmol.* **69**, 326–339.

HUMAN MUTATION 3:409–410 (1994)

MUTATION IN BRIEF

Two New Rhodopsin Transversion Mutations (L40R; M216K) in Families With Autosomal Dominant Retinitis Pigmentosa

Mai Al-Maghtheh*, Chris Inglehearn, Peter Lunt, Marcelle Jay, Alan Bird, and Shomi Bhattacharya

Department of Molecular Genetics, Institute of Ophthalmology, London EC1V 9EL (M.A.-M., C.I., S.B.); Department of Clinical Ophthalmology, Moorfields Eye Hospital, London EC1V 9EL (M.J., A.B.); Clinical Genetics Service, Institute of Child Health, Bristol Royal Hospital for Sick Children, Bristol BS2 8BJ (P.L.), England

Communicated by Peter Humphries

INTRODUCTION

Retinitis pigmentosa (RP) is the term used to describe a heterogeneous group of inherited retinal degenerations primarily affecting rod photoreceptor cells. In the initial stages of the disease, patients experience night blindness and peripheral loss of visual fields, while at the later stages this may progress to complete blindness. RP can be inherited in an autosomal dominant, autosomal recessive or X-linked manner. Autosomal dominant RP (adRP) is genetically heterogeneous and can be caused by mutations in at least six genes (Kumar-Singh et al., 1993) localized to different parts of the genome. The gene for rhodopsin was the first to be implicated in adRP causation and accounts for almost 30% of families with adRP (Sung et al., 1991a). More than 50 mutations spanning the entire coding region have so far been identified (reviewed by Al-Maghtheh et al., 1993). Here we report the identification of two new rhodopsin mutations, Leu40Arg (L40R), and Met216Lys (M216K), in families with adRP.

MATERIALS AND METHODS

Blood samples were taken from patients with adRP and their relatives in the two families described. DNA was extracted from peripheral blood lymphocytes. Polymerase chain reaction (PCR) amplification was carried out for the coding region of the rhodopsin gene using primers flanking all five exons, as previously described by Keen et al. (1991a). The PCR products were electrophoretically separated on Hydrolink gels for mutation detection, using the heteroduplex method (Keen et al., 1991b). Specific exons showing heteroduplex formation were then directly sequenced using the dideoxy chain termination method (Sanger et al., 1977).

RESULTS

Rhodopsin mutations were identified in each of the two adRP families. The first is a T→G transversion (Fig. 1A) at nucleotide position 413, which results in a Leu40Arg amino acid substitution in exon one. This nucleotide alteration was found to create a new site for the restriction enzyme Sau 96.1. Cosegregation of the mutation with the disease phenotype was confirmed by digestion of the PCR products with Sau 96.1 in all available individuals from the family (data not shown).

The second mutation is a T-to-A transversion (Fig. 1b) at nucleotide position 3929, resulting in a Met216Lys substitution in the third exon of the rhodopsin gene. This mutation was found to disrupt a restriction site for the enzyme Nla III. All affected individuals in this family showed the nucleotide substitution on sequence analysis. Both sequence changes were absent from 50 normal controls screened in this laboratory.

DISCUSSION

So far all of the 50 or more rhodopsin mutations described in adRP families have segregated with the disease. This laboratory has previously screened 37 control population samples for rho-

Received November 17, 1993; accepted January 14, 1994.

*To whom reprint requests correspondence should be addressed.

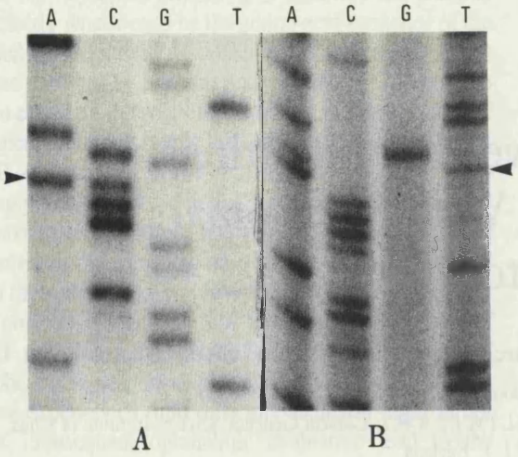

FIGURE 1. **Sequencing gel photograph showing rhodopsin nucleotide substitution. A: Exon 1 A→C on the reverse strand, which corresponds to T→G on the forward strand. B: Exon 3 T→A substitution in the forward strand.**

dopsin mutations, and laboratories in the United States have looked at a further 235. These screens together with adRP family screening have revealed four nucleotide polymorphisms, but no neutral amino acid polymorphisms. An amino acid change has been described in carriers with no clinical RP symptoms, by Rosenfeld and co-workers (1992), which causes recessive RP. However since both of the above mutations segregate with adRP and result in conservative amino acid substitutions, it is likely that they are causative of the adRP phenotype in these families.

Clinically, the codon 40 (L40R) mutation was associated with the early onset of night-blindness in the first decade. By the fourth decade, severe retinal functional loss was evident on dark adapted static threshold perimetry and electroretinographic (ERG) responses were absent or barely detectable (Kim et al., 1993). The clinical phenotype in the family with Met216Lys mutation is typical of RP, with abnormal ERG responses and defective dark adaptation. Affected individuals displayed variable age of onset of night blindness.

Rhodopsin is a transmembrane protein which is synthesized in the rod inner segment and then exported to the outer segment (ROS), where it is incorporated into the disc membrane. It consists of an opsin molecule bound to the ligand 11-*cis*-retinal. Structurally the opsin molecule has seven hydrophobic transmembrane domains connected by hydrophilic loops. The seven transmembrane helices are believed to form the binding pocket for 11-*cis*-retinal (Hargrave and McDowell, 1992).

Codons 40 and 216 lie in the first and fourth transmembrane domains of the opsin molecule, respectively. The change of nonpolar hydrophobic to positively charged residues in each mutation could disrupt the three-dimensional structure of the protein and could interfere with its proper folding. Such alterations could prevent appropriate binding of 11-*cis*-retinal to form a functional chromophore. It is therefore possible to speculate that, like the biochemical class II mutations described by Sung and co-workers (1991b), the altered protein remains in the endoplasmic reticulum, where it accumulates and results in the eventual degeneration of the rod cell.

Furthermore, the mutations described in this paper can be detected by the appropriate restriction enzyme digestion of PCR products which will simplify adRP diagnosis in respective families and in mutation screening in general.

ACKNOWLEDGMENT

We gratefully acknowledge the support provided by the British Retinitis Pigmentosa Society and by the Wellcome Trust (grant 035535/Z/92/Z/REH/SMD) for this research.

REFERENCES

Al-Maghtheh M, Gregory C, Inglehearn C, Hardcastle A, Bhattacharya S (1993) Rhodopsin mutations in autosomal dominant retinitis pigmentosa. Hum Mutat 2:249–255.

Hargrave PA, McDowell JH (1992) Rhodopsin and phototransduction: A model system for G protein-linked receptors. FASEB J 6:2323–2331.

Keen TJ, Inglehearn CF, Lester DH, Bashir R, Jay M, Bird AC, Bhattacharya SS (1991a) Autosomal dominant retinitis pigmentosa: Four new mutations in rhodopsin, one of them in the retinal attachment site. Genomics 11:199–205.

Keen J, Lester D, Inglehearn C, Curtis A, Bhattacharya SS (1991b) Rapid detection of single base mismatches as heteroduplexes on hydrolink gels. Trends Genet 7:5.

Kim RY, Al-Maghtheh M, Fitzke FW, Arden GB, Jay M, Bhattacharya SS, Bird AC (1993) Dominant retinitis pigmentosa associated with two rhodopsin gene mutations: Leu-40-Arg and an insertion disrupting the 5′-splice junction of exon 5. Arch Ophthalmol 111:1518–1524.

Kumar-Singh R, Farrar FJ, Monsergh F, Kenna P, Bhattacharya SS, Gal A, Humphries P (1993) Exclusion of the involvement of all known retinitis pigmentosa loci in the disease present in a family of Irish origin provides evidence for a sixth autosomal locus (RP8). Hum Mol Genet 2:875–878.

Rosenfeld PJ, Cowley GS, McGee TL, Sandberg MA, Berson EL, Dryja TP (1992) A null mutation in the rhodopsin gene causes rod photoreceptor dysfunction and autosomal recessive retinitis pigmentosa. Nature Genet 1:209–213.

Sanger F, Nicklen S, Coulson AR (1977) DNA sequencing with chain-terminating inhibitors. Proc Natl Acad Sci USA 74: 5463–5467.

Sung C-H, Davenport CM, Hennessey JC, Maumenee IH, Jacobson SG, Heckenlively JR, Nowakowski R, Fishman G, Gouras P, Nathans J (1991a) Rhodopsin mutations in autosomal dominant retinitis pigmentosa. Proc Natl Acad Sci USA 88:6481–6485.

Sung C-H, Schneider BG, Agarwal N, Papermaster DS, Nathans J (1991b) Functional heterogeneity of mutant rhodopsins responsible for autosomal dominant retinitis pigmentosa. Proc Natl Acad Sci USA 88:8840–8844.

Human Molecular Genetics, 1994, Vol. 3, No. 2 351–354

Identification of a sixth locus for autosomal dominant retinitis pigmentosa on chromosome 19

Mai Al-Maghtheh, Chris F.inglehearn, T.Jeffrey Keen, Kevin Evans, Anthony T.Moore, Marcelle Jay, Alan C.Bird and Shomi S.Bhattacharya*

Departments of Molecular Genetics and Clinical Ophthalmology, Institute of Ophthalmology, Bath Street, London EC1V 9EL, UK

Received November 17, 1993; Revised and Accepted December 20, 1993

We report the mapping of a sixth locus for autosomal dominant retinitis pigmentosa (adRP) to 19q13.4. After a total genome linkage search using over 300 markers in a single large pedigree, marker loci on the long arm of chromosome 19 showed significant linkage with the disease locus. Since the mapping information for the marker loci used in this study was derived from two different genome maps, we established genetic distances between relevant marker loci so that linkage information could be combined from both maps. A conventional three point analysis between the adRP phenotype and markers D19S180 and D19S214 gave a maximum lod score of 4.87. Combining data from these and other markers, we used the recently described multiple two point programme FASTMAP to simulate a multipoint analysis of the full data set. This gave a lod score of 5.34 in the interval between markers D19S180 and D19S214. Recently this laboratory has also reported the linkage of another form of retinal degeneration known as cone-rod dystrophy (CRD) to a genetically different set of markers from 19q. Linkage data presented here clearly supports the existence of two separate retinal genes in this part of the genome.

INTRODUCTION

Retinitis pigmentosa (RP) is an inherited progressive retinal degeneration for which five autosomal dominant loci have been described previously.. These are the rhodopsin (1) and RDS/peripherin (2,3) genes and as yet unidentified genes on chromosomes 8cen (4), 7p (5) and 7q (6). In addition to adRP, loci have been identified for other forms of retinal degeneration. These include a locus for cone-rod dystrophy (CRD) on chromosome 19q reported recently by this laboratory (7). Now we can also report linkage of a sixth adRP locus to 19q in a single large family, but to markers more distal to CRD, in the region 19q13.4.

The family used in this study, known as ADRP5 (pedigree shown in Figure 1), has been described in greater clinical detail elsewhere (family 4 in reference 8). The majority of patients experience night blindness in the first or second decade, with progressive visual field loss in later life. However some individuals have no clinical evidence of the disease, though they have both an affected parent and an affected child. Genetic studies in this family have excluded all of the previously known retinal dystrophy loci (reference 9 and unpublished data). In total, 259 microsatellites and 44 VNTR/RFLP loci were excluded from linkage with the disease, corresponding to approximately 80% of the genome, before linkage was detected.

RESULTS

Significant lod scores of 3.20 and 3.95 were obtained between the disease phenotype and the microsatellite markers D19S214 and D19S180 respectively. Other poly-CA markers from the region also gave positive lod scores (Table 1). The marker D19S180 is at the distal end of chromosome 19q on the CEPH consortium genome map (10), while D19S214 is on 19qter on the poly-CA genome map of Weissenbach and co-workers (11). From the position of the anchor marker PRKCG on both maps, it is evident that D19S214 is distal to D19S180. Also the position of anchor marker D19S178 allows the placement of marker D19S211 from the poly-CA map, proximal to KLK and close to APOC2 on the CEPH map. In order to combine the information from both maps, a panel of families available in this laboratory were used to calculate the distance between markers D19S180 from the CEPH map and D19S214 from the poly-CA map. The inter marker distance obtained, using the Kosambi mapping function, was 22 centimorgans (cM) with a peak lod score of 7.26. This made it possible to combine information from both maps, as shown in Figure 2.

Multipoint analysis with all of the marker loci was not possible due to the large family size and the complexity of the marker systems used. However three point analysis was performed using only D19S180 and D19S214, with the programme LINKMAP (12). This gave a maximum lod score of 4.87 at a position 4 cM distal to D19S180. We then used the programme FASTMAP (13) to simulate a multipoint analysis with the complete data set. The output from FASTMAP performed with the data shown in Table 1, is plotted in Figure 3. This analysis gave a maximum lod score of 5.34, again at 4 cM distal to D19S180. Both from this data and from haplotype analysis, a locus for adRP between markers D19S180 and D19S214 is clearly indicated.

The cone-rod dystrophy locus recently described by this laboratory has been excluded in family ADRP5. Two point linkage analyses in ADRP5 with markers D19S225, D19S49 and D19S47, which are closely linked to the CRD locus, show no evidence of linkage (Table 2). Also marker D19S214, which is tightly linked to the disease phenotype in ADRP5, shows no evidence of linkage to cone-rod dystrophy (7). It is therefore very unlikely that these families have allelic mutations in the same gene.

*To whom correspondence should be addressed

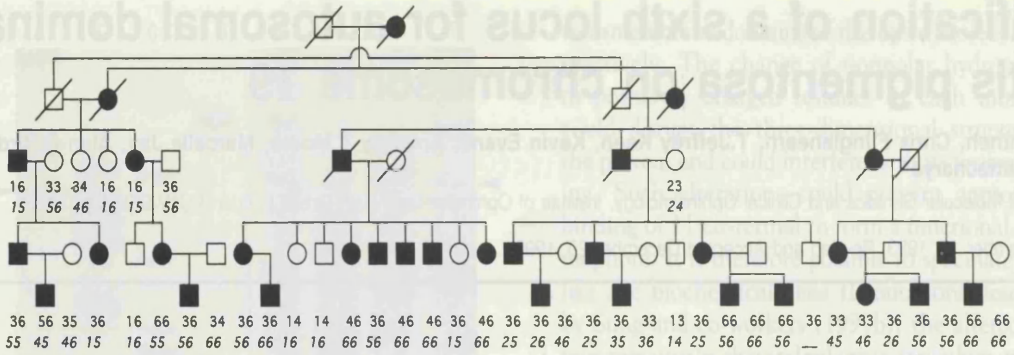

Figure 1. Pedigree showing members of ADRP5 used in the linkage study. Below each symbol are the genotypes for D19S180 and D19S214 (*italics*). Affected individuals and obligate disease gene carriers are marked with filled in symbols.

DISCUSSION

The data presented clearly demonstrate the presence of a new adRP locus close to the telomere of chromosome 19q. Furthermore, to support this finding, we now have preliminary data suggesting linkage in another adRP family with a phenotype indistinguishable from that of ADRP5 (family 3 in reference 8). This shows a lod score of 1.9 with no recombination between marker D19S180 and adRP. Of the five adRP loci described prior to this report, only rhodopsin accounts for an appreciable proportion of adRP (14). In addition, a family has been described in the literature for which all of these loci have been excluded (15). It is therefore possible that the 19qter adRP locus is more common as a cause of adRP than those located on 7p, 7q and 8cen, since all of these localisations were based on single families. Further experiments will be required to determine whether this is indeed the case or whether other adRP loci remain to be discovered.

It is interesting to note that the mapping of this locus proved an exceedingly lengthy process, which might in part be due to its telomeric location. Telomeres are thought to be regions of map expansion in which genetic mapping is more difficult. Genetic markers are relatively sparse in this particular region on both the CEPH and poly-CA genome maps (11,12). We have presented data which allow the combination of these two maps for 19qter, providing more comprehensive representation of this region. However, initially it will be necessary to obtain a better genetic localisation of the disease gene prior to a physical mapping and cloning exercise.

The new adRP locus and the recently described 19q CRD locus lie in a region of the genome where so far no retina specific genes have been described. The syntenic region on mouse chromosome 7 also has no obvious candidate genes (16). It therefore seems likely that these are the loci for as yet undiscovered genes with important roles in retinal function or development. Identification and cloning of such genes will not only provide more insight into the pathogenic mechanisms that result in these two different diseases but may also facilitate a greater understanding of normal retinal physiology.

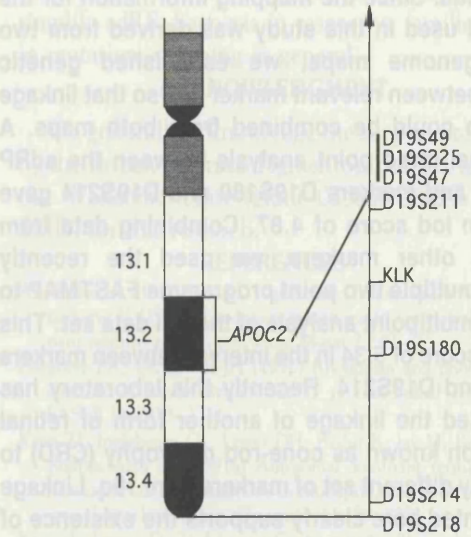

Figure 2. Diagram of the chromosome 19q region showing the position of markers linked to ADRP5 and to cone rod dystrophy from both genome maps (10,11). Estimated genetic distances between markers linked to ADRP5 locus are described in the legend to Figure 3.

MATERIALS AND METHODS

A whole genome linkage search was carried out in a panel of affected members of ADRP5. DNA was prepared from peripheral blood lymphocytes. VNTR and RFLP markers were typed by Southern blotting onto Hybond-N and N+ membranes using conditions and protocols recommended by the manufacturer (Amersham). Microsatellite markers were typed by polymerase chain reaction (PCR) using one radioactively end labelled primer. Multiplex PCR reactions of two markers were used. The end labelling reaction was performed in 30 μl containing 80 picomoles of each primer (sufficient for 40 PCR reactions), 3 μl of One-Phor-All buffer (Pharmacia), 30 μCi of γ-^{32}P-ATP (specific activity 3000 Ci/mmol), and 9 units of polynucleotide kinase. This was incubated at 37°C for 30 minutes. PCR reactions were performed in a 12.5 μl volume containing 150 ng DNA, 2 picomoles of each primer, 0.2 mM each of dATP, dCTP, dGTP and dTTP, 0.2 units of Taq polymerase, 10 mM Tris−HCl, 50 mM KCl, 1.5 mM $MgCl_2$ and 0.1% non-ionic detergent. Amplification was carried out at 94°C for 1 minute, 55°C (or as specified) for 1 minute and 72°C for 1 minute, with 30 cycles, on an Omnigene thermal cycler (Hybaid). PCR products were then separated on 6% polyacrylamide denaturing gels which were subsequently dried and autoradiographed.

Two point and multipoint lod scores were computed using the Linkage package version 5.1 (12), from data prepared by the LINKSYS data management package (17). FASTMAP takes as its input the two point lod scores between the disease locus and a number of markers, allele frequencies for each marker and the inter marker distances. It then implements an algorithm to provide an approximate multipoint lod score for the disease against the marker loci used.

To address the problem of incomplete penetrance in this family, only a few unaffected siblings were used in the analysis. These were either a) over 60 years old; b) over 40 with two or more normal children; or c) over 40 and recently

Table 1. Lod scores from two point linkage analysis between the disease phenotype in ADRP5 and markers from chromosome 19q13.4. Two point linkage analysis was performed using MLINK from the LINKAGE package (13)

DNA marker	Theta value 0.00	0.01	0.05	0.10	0.20	0.30	0.40	θ_{max}	Z_{max}
D19S211	−8.26	−4.69	−1.62	−0.36	0.52	0.60	0.33	0.27	**0.62**
KLK	−1.73	0.14	0.69	0.81	0.72	0.47	0.19	0.11	**0.81**
D19S180	1.49	3.63	3.95	3.75	2.92	1.82	0.56	0.04	**3.95**
D19S214	−8.79	0.34	2.62	3.16	2.94	2.09	0.93	0.12	**3.28**
D19S218	−0.77	1.24	1.67	1.63	1.24	0.79	0.37	0.07	**1.68**

Table 2. Lod scores from two point linkage analysis between the disease phenotype in ADRP5 and markers linked to the 19q cone-rod dystrophy locus

DNA marker	Theta value 0.00	0.01	0.05	0.10	0.20	0.30	0.40	Exclusion* to θ
D19S225	−8.95	−5.25	−3.08	−1.79	−0.62	−0.14	0.00	0.09
D19S49	−5.52	−4.38	−2.49	−1.62	−0.79	−0.30	−0.06	0.07
D19S47	−5.47	−3.75	−2.30	−1.40	−0.58	−0.22	−0.08	0.06

*Exclusion indicates a lod score of −2.

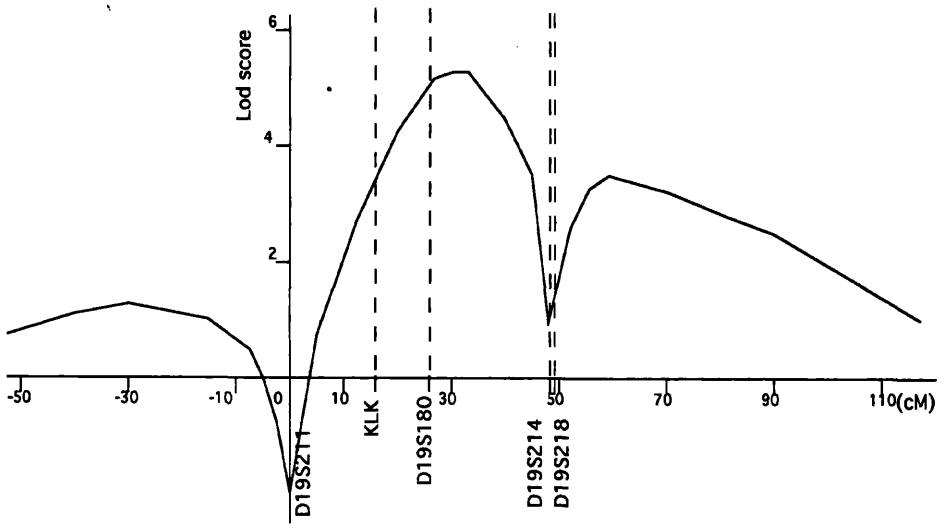

Figure 3. Simulated multipoint graph of the lod score between the disease locus in ADRP5 and markers on chromosome 19q using the multiple two point programme FASTMAP. Distances between the linked markers are derived from three different sources. The interval between markers D19S218 and D19S214 (1cM) is given in reference 11. Interval D19S214 to D19S180 (22cM) was calculated from our own data. Interval D19S180 to KLK (10 cM) is given in rference 10. Placement of marker D19S211 relative to KLK (16 cM) is based on the position of anchor marker D19S178 on both the CEPH and poly-CA genome maps, and is therefore only approximate. Distances were calculated using the Kosambi mapping function.

examined by an ophthalmologist. Even with these stringent criteria, the penetrance was set at 0.7 for linkage analysis, since three of the ten known gene carriers (people with affected children) had no symptoms.

ACKNOWLEDGMENTS

We gratefully acknowledge the British Retinitis Pigmentosa Society, the American Retinitis Pigmentosa Foundation, the George Gund Foundation and the Wellcome Trust (grant number 035535/Z/92/Z) for funding this research.

REFERENCES

1. Dryja,T.P., McGee,T.L., Reichel,E., Hahn,L.B., Cowley,G.S., Yandell,D.W., Sandberg,M.A. and Berson,E.L. (1990) *Nature* **343**: 364−366.
2. Kajiwara,K., Hahn,L.B., Mukai,S.,Travis,G.H., Berson,E.L. and Dryja,T.P. (1991) *Nature* **354**: 480−483.
3. Farrar,G.J., Kenna,P., Jordan,S.A., Kumar-Singh,R., Humphries,M.M., Sharp,E.M., Shiels,D.M. and Humphries,P. (1991) *Nature* **354**: 478−480.
4. Blanton,S.H., Heckenlively,J.R., Cottingham,A.W., Freidman,J., Sadler,L.A., Wagner,M., Freidman,L.H., Daiger,S.P. (1991) *Genomics* **11**: 857−869.
5. Inglehearn,C.F., Carter,S.A., Keen,T.J., Lindsay,J. Stephenson,A.M., Bashir,R., Al-Maghtheh,M., Moore,A.T., Jay,M., Bird,A.C. and Bhattacharya,S.S. (1993) *Nature Genet.* **4**: 51−53.
6. Jordan,S.A., Farrar,G.J., Kenna,P., Humphries,M.M., Sheils,D.M., Kumar-Singh,R., Sharp,E.M., Soriano,N., Ayuso,C., Benitez,J. and Humphries,P. (1993) *Nature Genet.* **4**: 54−57.
7. Evans,K., Fryer,A., Inglehearn,C., Duvall-Young,J., Whittaker,J., Gregory,C.Y., Ebenezer,N., Hunt,D. and Bhattacharya,S.S. (1994) *Nature Genet.* in press.

8. Moore,A.T., Fitzke,F., Jay,M., Arden,G.B., Inglehearn,C.F., Keen,T.J., Bhattacharya,S.S. and Bird,A.C. (1993) *Brit. J. Ophthalmol.* **77**: in press.
9. Bashir,R., Inglehearn,C.F., Keen,T.J., Lindsay,J., Atif,U., Carter,S.A., Stevenson,A.M., Jackson,A., Jay,M., Bird,A.C., Papiha,S.S. and Bhattacharya,S.S. (1992) *Genomics* **14**: 191–193.
10. NIH/CEPH Collaborative Mapping Group (1992) *Science* **258**: 67–86.
11. Weissenbach,J., Gyapay,G., Dib,C., Vignal,A., Morissette,J., Millasseau,G., Vaysseix,G. and Lathrop,M. (1992) *Nature* **359**: 794–801.
12. Lathrop,G.M., Lalouel,J.M., Julier,C. and Ott,J. (1984) *Proc. Natl. Acad. Sci. USA* **81**: 3443–3446.
13. Curtis,D. and Gurling,H. (1993) *Hum. Hered.* **43**: 173–185.
14. Al-Maghtheh,M., Gregory,C., Inglehearn,C., Hardcastle,A. and Bhattacharya,S. (1993) *Human Mutation* **2**: 249–255.
15. Kumar-Singh,R., Farrar,G.J., Mansergh,F., Kenna,P., Bhattacharya,S., Gal,A. and Humphries,P. (1993) *Hum. Mol. Genet.* **2**: 875–878.
16. Copeland,N.G., Jenkins,N.A., Gilbert,D.J., Eppig,J.T., Maltais,L.J., Miller,J.C., Dietrich,W.F., Weaver,A., Lincoln,S.E., Steen,R.G., Stein,L.D., Nadeau,J.H. and Lander,E.S. (1993) *Science* **262**: 57–82.
17. Attwood,J. and Bryant,S. (1988) *Ann. Hum. Genet.* **52**: 259.

Reprinted from the Archives of Ophthalmology
November 1993, Volume 111

CLINICAL SCIENCES

Dominant Retinitis Pigmentosa Associated With Two Rhodopsin Gene Mutations

Leu-40-Arg and an Insertion Disrupting the 5′-Splice Junction of Exon 5

Robert Y. Kim, MD; Mai Al-Maghtheh; Fred W. Fitzke, PhD; Geoffrey B. Arden, PhD; Marcelle Jay, PhD; Shomi S. Bhattacharya, PhD; Alan C. Bird, MD

Objective: To determine the phenotypes of two families in which retinitis pigmentosa cosegregates with a rhodopsin (*RHO*) gene mutation: a leucine-to-arginine change at codon 40 (Leu-40-Arg) in one family, and a 150–base pair insertion that disrupts the *RHO* 5′-splice junction of exon 5 in another.

Patients: Three affected members of each family.

Results: The Leu-40-Arg mutation was associated with the onset of night blindness in the first decade of life. By the fourth decade, severe retinal functional loss was evident on dark-adapted static threshold perimetry, and electroretinographic responses were absent or barely detectable. In contrast, the *RHO* 150–base pair insertion was associated with the later onset of mild night vision difficulties; in two individuals, mild night vision difficulties were first noticed in the second decade while a third, a 25-year-old woman, was asymptomatic. Dark-adapted static threshold perimetry of this latter individual revealed a "regional" or class 2 pattern of retinal functional loss associated with equal loss of rod and cone electroretinographic responses.

Conclusion: The *RHO* Leu-40-Arg mutation causes symptomatic retinal dysfunction by the end of the first decade while the insertion disrupting the 5′-splice junction of *RHO* exon 5 causes later onset "regional" or class 2 retinal dysfunction.

(Arch Ophthalmol. 1993;111:1518-1524)

RETINITIS PIGMENTOSA (RP) constitutes a heterogeneous group of inherited disorders characterized by progressive photoreceptor degeneration.[1] Symptoms typically consist of night blindness and reduced peripheral vision, with central vision preserved relatively long. Occurring in about one in 5000 individuals, RP is inherited in an autosomal dominant manner in 10% to 24% of cases.[2-8]

A breakthrough in the understanding of autosomal dominant RP occurred with the finding of mutations in the gene encoding the rod photoreceptor-specific protein rhodopsin (*RHO*).[9,10] Over 50 different mutations affecting the *RHO* gene have since been identified,[11] accounting for at least 30% of autosomal dominant RP.

Retinitis pigmentosa phenotypes associated with several *RHO* gene mutations have been described.[12-22] To date, the disorders have shown either a class 1 or "diffuse" pattern of disease with early onset of symptoms, or altitudinal distribution of visual loss with or without slow dark adaptation. Here we describe the phenotypes associated with two new *RHO* gene mutations (M.A.-M., unpublished data, 1993; M.A.-M., R.Y.K., Anita Hardcastle, Chris Ingleheam, PhD, S.S.B, unpublished data, 1993): a substitution of arginine for leucine at codon 40 (Leu-40-Arg) and a 150–base pair (bp) insertion in the fourth intron that disrupts the 5′-splice junction of exon 5.

From the Departments of Clinical Ophthalmology (Drs Kim, Jay, and Bird), Molecular Genetics (Ms Al-Maghtheh and Dr Bhattacharya), Visual Sciences (Dr Fitzke), and Electrophysiology and Psychophysics (Dr Arden), Institute of Ophthalmology and Moorfields Eye Hospital, London, England.

RESULTS

RHO LEU-40-ARG MUTATION (FAMILY 1)

All three individuals III-1, III-4, and IV-4 exhibited only central islands of measurable threshold sensitivities with field loss

See Patients and Methods on next page

Accepted for publication
24 April 1995

reported between different families. Differences between members of the same family, variable

detailed general medical history and a brief physical examination were undertaken.

PATIENTS AND METHODS

FAMILY 1: *RHO* LEU-40-ARG MUTATION

Patient III-1 was a 54-year-old man who noted loss of night vision and peripheral vision by age 12 years (**Figure 1**, left). At the time of examination, his visual acuity was 6/24 OD and 6/18 OS. The lenses were clear. Fundus examination revealed bilateral waxy disc pallor, retinal vascular narrowing, and midperipheral bone-spicule changes. The left eye was studied further.

Patient III-4 was a 34-year-old man who could not recall ever being able to see in the dark. He noticed reduced side vision by age 10 years. At the time of examination, his visual acuity was 6/18 OD and 6/36 OS. Mild posterior subcapsular lens changes were noted in each eye. In the fundi, the optic discs were pale and the retinal blood vessels narrow, and midperipheral bone-spicule changes were prominent (**Figure 2**, top left). The left eye was studied further.

Patient IV-4 was a 33-year-old woman who had poor night vision as long as she could remember but who denied having reduced peripheral vision. At the time of examination, her visual acuity was 6/12 OD and 6/9 OS. Her visual fields were markedly constricted. The lenses were clear in both eyes. The optic discs were pale and the retinal vessels attenuated, and there were midperipheral retinal bone-spicule changes (Figure 2, top right). The left eye was studied further.

FAMILY 2: 150-bp *RHO* INSERTION

Patient III-4 was a 52-year-old woman who first experienced mild difficulty seeing at night in her teenage years and reduced peripheral vision in her mid-20s (Figure 1, right). Neither her parents nor antecedent relatives had nyctalopia. Her visual acuity was 6/9 OD and 6/6 OS. The anterior segment was normal. Fundus examination revealed pallor of the optic discs, narrowing of retinal vessels, and midperipheral intraretinal bone-spicule pigmentation (Figure 2, bottom left). The left eye was studied further.

Patient IV-7 was the 26-year older daughter of patient III-4. She was asymptomatic with visual acuity of 6/6 OU; her anterior segments and fundi appeared normal. She considered herself to be unaffected until she was found to carry a mutant *RHO* allele. Her left eye was subsequently studied further.

Patient IV-8 (Figure 1) was the 21-year younger daughter of patient III-4. In contrast to her older sister, patient IV-8 first noticed difficulty seeing in the dark in her teenage years. In the previous year she became aware of mild constriction of her peripheral vision. As a child, she had an esotropia resulting in mild amblyopia of the left eye. Her visual acuity was 6/5 OD and 6/9 OS. The anterior segment was normal in each eye. Changes in the fundi were limited to an irregular appearance of the retinal pigment epithelium in the midperiphery (Figure 2, bottom right). The right eye was studied further.

GENOMIC ANALYSIS

Ten milliliters of whole blood was collected in sodium-ethylenedinitraminetetraacetic acid and stored at −70°C until DNA was isolated for genomic analysis as described previously.[23] Details of molecular genetic findings will be reported elsewhere (M.A.-M., unpublished data, 1993). Briefly, direct genomic sequencing of *RHO* exon 1 in affected members of family 1 showed a codon 40 *CTG* to *CGG* change, resulting in a Leu-to-Arg amino acid change in rhodopsin. In family 2, affected individuals possessed a 150-bp insertion that disrupts the 5′-splice junction of exon 5. Unaffected members of each family did not have mutant *RHO* alleles.

PSYCHOPHYSICAL TESTING

Dark-adapted static threshold perimetry and dark adaptometry were performed using a modified Humphrey automated perimeter (Allergan Humphrey, San Leandro, Calif) as described previously.[24-27] Briefly, following dilation of pupils with 1% cyclopentolate and 2.5% phenylephrine hydrochloride, patients were dark-adapted for 40 minutes before being studied. Dark-adapted perimetry was performed with the background illumination turned off using a standard Humphrey 30-2 program and size 5 red and blue stimuli to test cone and rod sensitivities, respectively. When dark adaptometry was performed, prebleach thresholds at selected positions were obtained immediately afterward. Following a 2-minute exposure to bright white light sufficient to bleach 95% of rhodopsin, the recovery of sensitivity was followed for both size 3 and size 5 blue stimuli in a modified Humphrey perimeter.[27] Central color vision testing was performed using a computer graphics system.[28]

ELECTROPHYSIOLOGIC TESTING

Traces were obtained from dark-adapted rods (blue stimulus), dark-adapted cones (red stimulus), maximal dark-adapted responses (white stimulus), oscillatory potentials, and flicker responses to a 30-Hz flickering white light stimulus using a protocol[29] that accords with the International Standard for Clinical Electroretinography.[30]

too extensive to permit dark adaptometry (**Figure 3**). The only electrophysiologic response detected in individual III-1 was a barely detectable (<1 μV) delayed response to a 30-Hz flicker stimulus. No electroretinographic responses were detected in either individual III-4 or IV-4. Color vision along the protan-deutan axis was normal, with a slight tendency toward tritanopia.

RHO INSERTION DISRUPTING THE 5′-SPLICE JUNCTION OF EXON 5 (FAMILY 2)

All three affected individuals were studied with dark-adapted static threshold perimetry (Figure 3). Twenty-five-year old patient IV-7, the most mildly affected family member, was the most informative (**Figure 4**, top). Thresholds for both

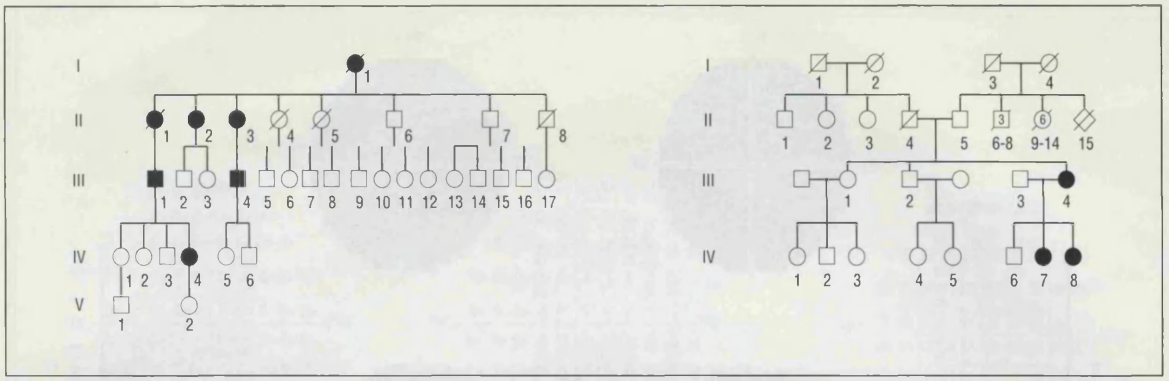

Figure 1. *Pedigree of families with retinitis pigmentosa. Left, Family 1 in which rhodopsin (*RHO*) Leu-40-Arg cosegregates with retinitis pigmentosa. Right, Family 2 in which an insertion disrupting the 5'-splice junction of* RHO *exon 5 cosegregates with retinitis pigmentosa.*

Figure 2. *Fundus photographs of affected individuals. Top left, Left eye of affected family 1 member III-4. Top right, Left eye of affected family 1 member IV-4. Bottom left, Left eye of affected family 2 member III-4. Bottom right, Right eye of family 2 affected member IV-8.*

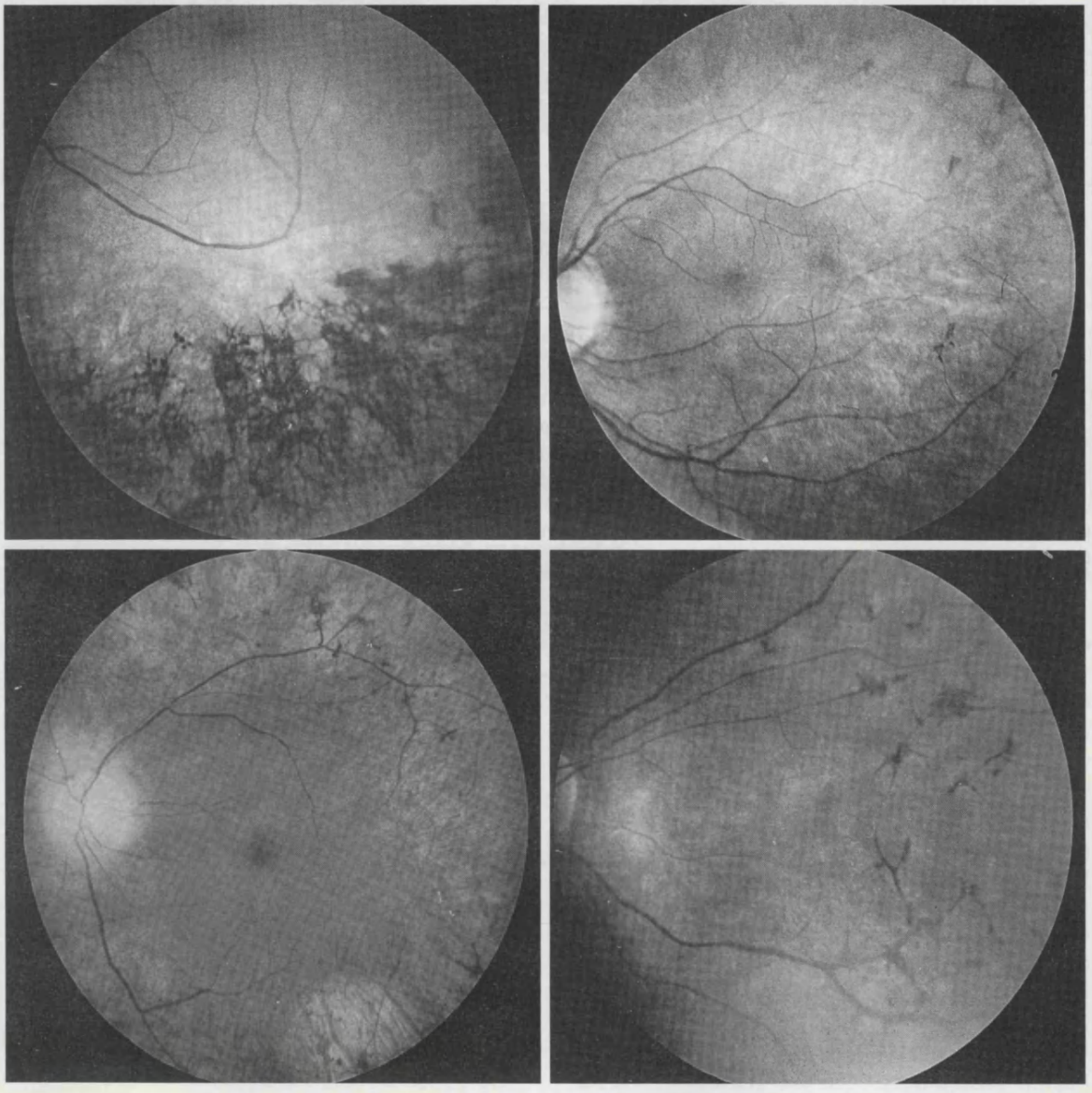

Accepted for publication
24 April 1995

reported between different families. Differences between members of the same family, variable detailed general medical history and a brief physical examination were undertaken.

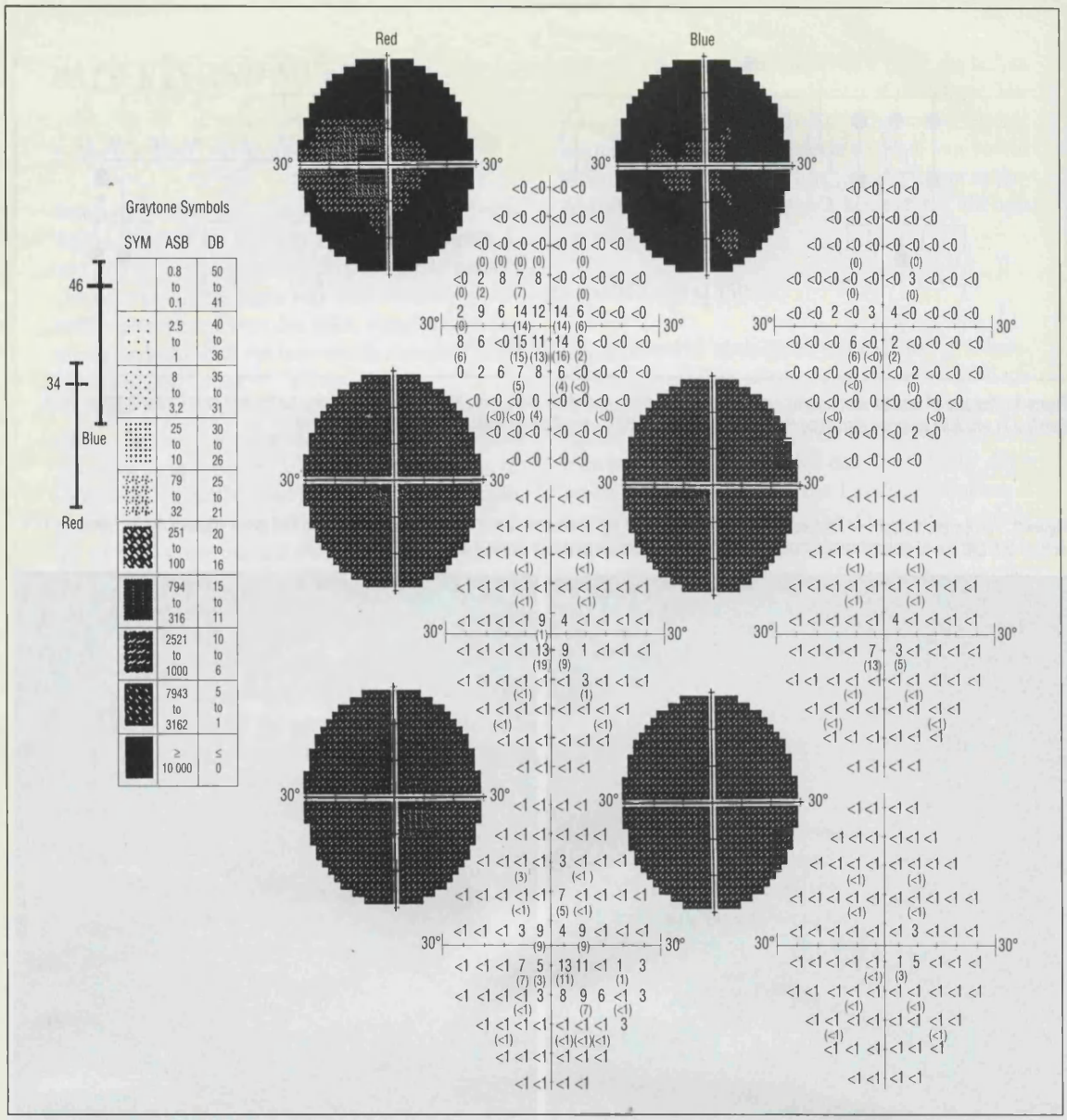

Figure 3. *Dark-adapted static threshold perimetry of affected individuals in family 1 (rhodopsin [RHO] Leu-40-Arg). Family 1 members III-1 (top), III-4 (center) and IV-4 (bottom) were dark-adapted for 40 minutes and then tested with red (left) and blue (right) stimuli on a dark background. Graytone images are accompanied by corresponding numerical sensitivities (decibels [dB]). Average sensitivities (ASBs) (with bars indicating range) for normal individuals are indicated on the grayscale at the left.*

red and blue stimuli (corresponding to cones and rods, respectively) were elevated by about 1 log unit, except in the superonasal field where thresholds were elevated by 1.5 log units. Dark adaptometry revealed a normal rate of dark adaptation with final thresholds elevated by 1 to 1.5 log units (**Figure 5**, top). Dark-adapted rod and cone b-wave responses were present but delayed and reduced in amplitude (**Figure 6**). Oscillatory potentials were attenuated. Responses to a 30-Hz flickering stimulus were delayed and reduced in amplitude. Patient IV-8 (her younger sister), in contrast, was more severely affected with extensive regions of more than 3–log unit threshold elevation to both red and blue stimuli (Figure 4, center). Her rate of dark adaptation was normal, reaching baseline values within 30 minutes (Figure 5, bottom). The only electroretinographic response detected was a low-amplitude, delayed-flicker response (Figure 6). Patient III-4 had only a central island of sensitivity (Figure 4, bottom) and an undetectable electroretinogram (Figure 6). Central color contrast sensitivity for patients III-4 and IV-3 were normal.

COMMENT

A variety of *RHO* gene mutations have been described,[11] many of which have been found only in single families. To our knowledge, the *RHO* gene mutations that we studied have not been observed in any other families to date. The number of individuals available to us for study was limited. With other *RHO* gene mutations, considerable intrafamilial and interfamilial variability can occur.[13]

Autosomal dominant inheritance requires that 50% of offspring carry the mutant gene over at least three gen-

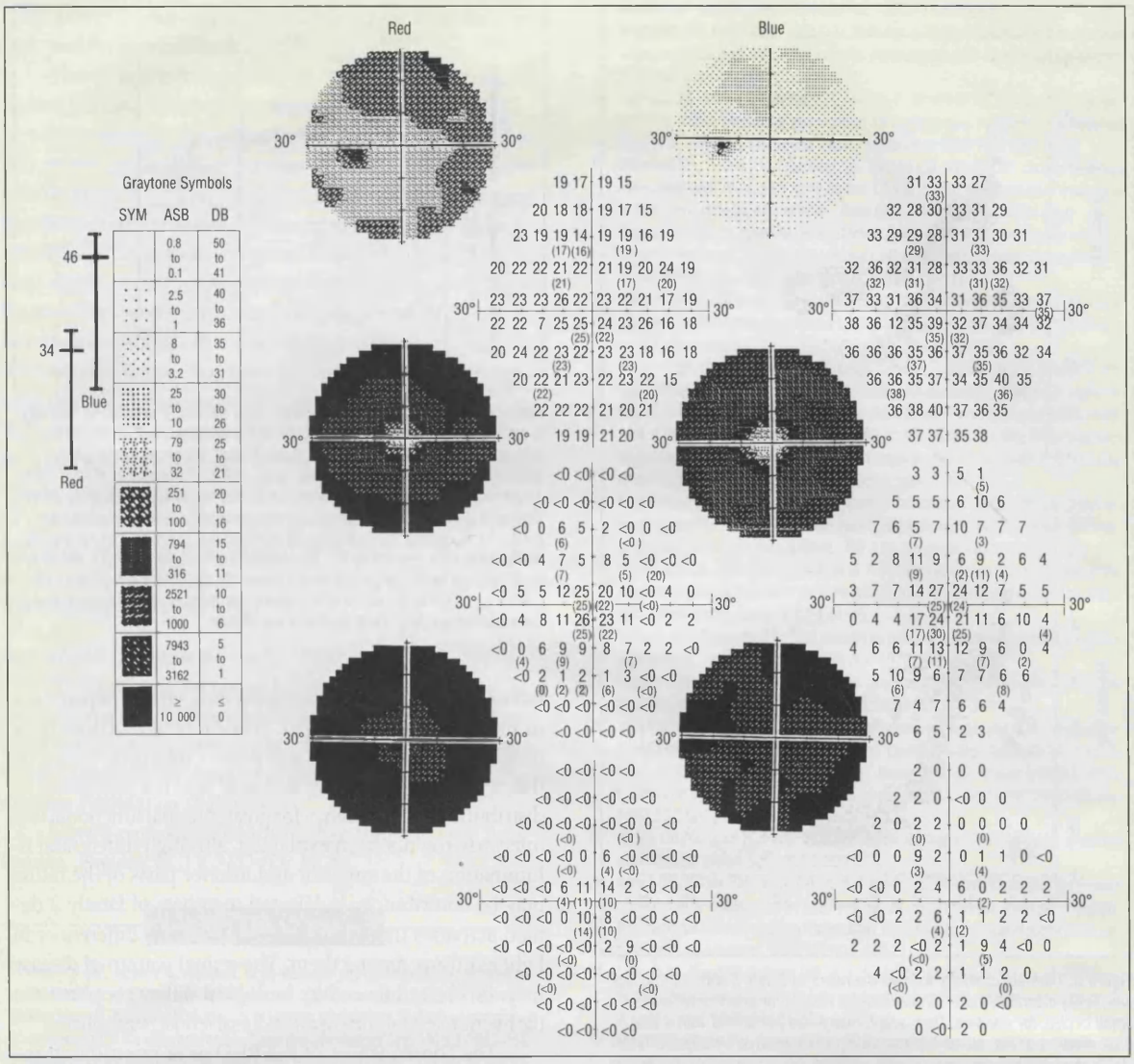

Figure 4. *Dark-adapted static threshold perimetry of affected individuals in family 2 (rhodopsin [RHO] insertion). Family 2 members IV-7 (top), IV-8 (center), and III-4 (bottom) were dark-adapted for 40 minutes and then tested with red (left) and blue (right) stimuli on a dark, unlit background. Graytone images are accompanied by corresponding numerical sensitivities (decibels [dB]). Average sensitivities (ASBs) for normal individuals (with bars indicating range) are indicated on the grayscale at the left.*

erations, with equal involvement of male and female family members and evidence of male-to-male transmission. While neither family in this report satisfies all of these criteria, it is difficult to invoke any other mode of inheritance. The source of the *RHO* insertion in generation II of family 2 is unclear (Figure 1, top). The phenotype of IV-7 is mild. Consequently, although deceased individual II-4 never reported visual difficulties, we cannot exclude the possibility that he was asymptomatic but had the *RHO* gene insertion. (His siblings II-1, II-2, and II-3 were not available for study.) Alternatively, a new germ-line mutation may have occurred in II-4 or II-5.

The *RHO* Leu-40-Arg mutation changes affect the first transmembrane domain of rhodopsin. While leucine has a nonpolar side chain, arginine is a basic amino acid with a larger, polar side chain, which would predictably perturb the first transmembrane α-helix and destabilize the normal conformation of rhodopsin. The Leu-40-Arg mutation is associated with the onset of symptomatic night blindness in the first decade in all three affected individuals studied. By the fourth decade, retinal functional loss is too great to permit classification of the pattern of functional loss.[25,31] The Leu-40-Arg mutation leads to more severe retinal dysfunction than another mutation affecting the first transmembrane domain of rhodopsin, threonine to arginine at codon 58, which leads to inferior altitudinal retinal dysfunction and delayed dark adaptation.[15,16,32] With this latter mutation, although the side chain of arginine is larger than that of threonine and is of opposite charge, the polar nature at residue 58 is conserved. The presence of a polar residue at position 58 may be important for the normal structure of rhodopsin and may help explain why the Thr-58-

Accepted for publication
24 April 1995

reported between different families. Differences between members of the same family, variable

detailed general medical history and a brief physical examination were undertaken.

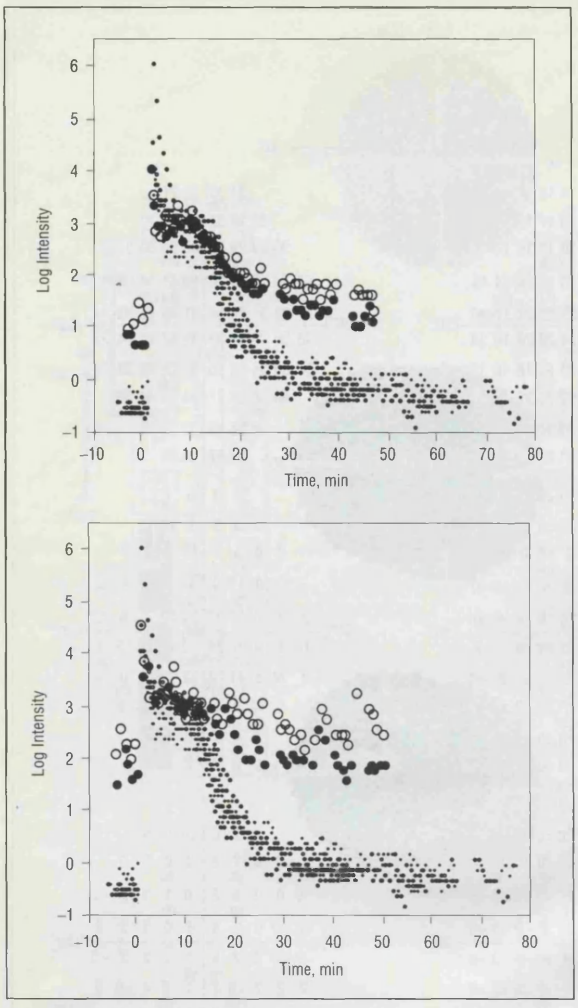

Figure 5. *Dark adaptometry for two members of family 2 with the rhodopsin (RHO) insertion. Large circles indicate results for affected patients; small circles, for normals. Dark adaptometry was performed with a size 5 blue stimulus at two points corresponding to more severely affected retina (large open circles) and less severely affected retina (large solid circles) as determined in Figure 4. Prebleach measurements were made before time 0. Top, Patient IV-7 was studied at positions +9°, −9° (large open circles) and −9°, +9° (large solid circles) corresponding to Figure 4, top. Bottom, Patient IV-8 was studied at positions +3°, −3° (large open circles) and +3°, +3°) (large solid circles) corresponding to Figure 4, center.*

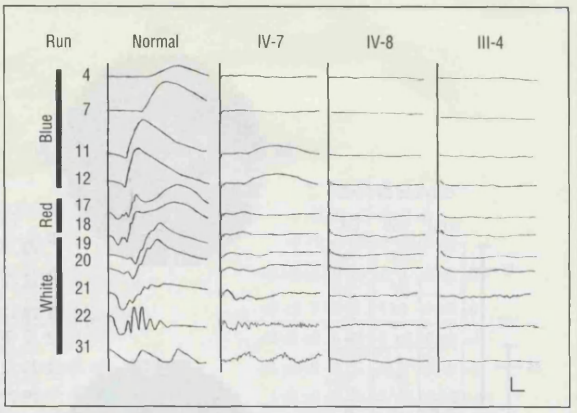

Figure 6. *Electroretinographic findings. Blue flashes of increasing intensity in runs 4 to 12 generate preferentially rod responses. Red flashes of increasing intensity in runs 17 and 18 elicit cone responses (early peak) separated from rod responses (late peak). White flashes used in runs 19 to 31 generate, respectively, mixed rod and cone responses, oscillatory potentials, and 30-Hz flicker responses. At the lower right is a calibration standard. The horizontal bar indicates 20 milliseconds for runs 4 to 18 and 10 milliseconds for runs 19 to 31. The vertical bar indicates 100 μV for runs 4 to 12 and 19 to 21, 50 μV for runs 17 and 18, 10 μV for run 22, and 25 μV for run 31. Electroretinoraphic waveforms from a normal individual and from individuals IV-7, IV-8, and III-4 are shown.*

Arg mutation causes less severe disease than Leu-40-Arg. The *RHO* insertion disrupting the 5′-splice junction of exon 5 is associated with a more variable phenotype than Leu-40-Arg. Two members (III-4 and IV-8) in family 2 first noticed night vision difficulties in the second decade while the third (patient IV-7) was asymptomatic. Interestingly, asymptomatic individual IV-7 is 4 years older than her more severely affected younger sister IV-8. Dark-adapted static threshold perimetry of individual IV-7 demonstrated regional[31] or class 2[25] retinal functional loss, in contrast to diffuse[31] or class 1[25] functional loss; individuals III-4 and IV-8 (as well as members of family 1 with the *RHO* Leu-40-Arg mutation) were too severely affected to make this distinction.

Regional functional loss has been observed with a number of other *RHO* gene mutations,[12,15-17,19,22,32,33] with the inferior part of the retina demonstrating greater impairment in an altitudinal distribution. While retinal functional loss in family 2 member IV-7 was greater inferiorly (affecting the superior visual field), it clearly was not altitudinal in distribution. The tendency for greater retinal functional loss inferiorly has not been explained, although differential illumination of the superior and inferior parts of the retina may be contributory.[12] Affected members of family 2 denied activities that would have resulted in differences in light exposure among them. The retinal pattern of disease may also be influenced by biological differences between the inferior/ventral and superior/dorsal retinal hemispheres.[34-38]

The consequences of the *RHO* gene insertion on the structure of rhodopsin are difficult to predict. As the insertion disrupts the 5′-splice junction of exon 5, splicing of *RHO* messenger RNA transcripts is almost certainly affected, with the likely generation of an abnormal reading frame downstream of exon 4–codon 312. If mutant transcripts are transported from the nucleus to the cytoplasm, the translated mutant protein may be shorter or longer than the normal protein at its cytoplasmic carboxy terminus, depending on the position of the first stop codon in the new reading frame of the aberrantly spliced transcript. Carboxy-terminal amino acid residues 312 to 348 that are likely to be altered include two cysteines believed to be palmitoylated and anchored in the disc membrane as well as three serines and five threonine residues that can be phosphorylated.[39]

An *RHO* splice junction mutation was previously reported in an individual heterozygous for a base substitution in the donor splice site of intron 4.[40] The phenotype of this clinically normal individual was remarkable only for subtle electrophysiologic abnormalities suggesting that this "loss-of-function" allele represents a *null* mutation. In

contrast, the splice junction mutation affecting our family 2 represents a "gain-of-function" allele, suggesting that mutant protein is translated.

The clinical phenotypes of several other mutations affecting the cytoplasmic C-terminus of rhodopsin vary. The best documented is the proline-to-leucine mutation at codon 347, which causes diffuse[31] or class 1[25] functional loss of variable severity.[14,18,21] The phenotype of the glutamine to stop mutation at codon 344 is characterized by minimal rod sensitivity loss throughout the visual field without evidence of cone dysfunction in early disease.[15] Two small deletions (8 bp and 1 bp) in the terminal coding region of *RHO* exon 5 have been reported, with brief clinical descriptions suggestive of mild disease that have not been described in sufficient detail for comparison with our data.[41] Similarly, a 42-bp deletion in exon 5 associated with diffuse/type 1 retinal dysfunction has been reported but the associated clinical phenotype has not been described in detail.[42]

The two families in this report further illustrate the heterogeneity of retinal degeneration with respect to the severity and qualitative attributes of disease consequent on mutations in the *RHO* gene.

Accepted for publication July 1, 1993.

This study was supported by grants from the British Retinitis Pigmentosa Society and the National Retinitis Pigmentosa Foundation (Baltimore, Md). Dr Kim is a recipient of a Career Development Award from the National Retinitis Pigmentosa Foundation (Baltimore).

Reprint requests to Moorfields Eye Hospital, City Road, London, England EC1V 2PD (Dr Bird).

REFERENCES

1. Marmor MF, Aguirre G, Arden G, et al. Retinitis pigmentosa: a symposium on terminology and methods of examination. *Ophthalmology.* 1983;90:126-131.
2. Pearlman JT. Mathematical models of retinitis pigmentosa: a study of the rate of progression in the different forms. *Trans Am Ophthalmol Soc.* 1979;77:643-656.
3. Boughman JA, Conneally PM, Nance WE. Population genetic studies of retinitis pigmentosa. *Am J Hum Genet.* 1980;32:223-235.
4. Hu D. Genetic aspects of retinitis pigmentosa in China. *Am J Hum Genet.* 1982; 12:51-56.
5. Jay M. On the heredity of retinitis pigmentosa. *Br J Ophthalmol.* 1982;66:405-416.
6. Boughman JA, Fishman GA. A genetic analysis of retinitis pigmentosa. *Br J Ophthalmol.* 1983;67:449-454.
7. Bunker CH, Berson EL. Prevalence of retinitis pigmentosa in Maine. *Am J Ophthalmol.* 1984;97:357-365.
8. Heckenlively JR, Boughman JA, Friedman LH. Diagnosis and classification of retinitis pigmentosa: pedigree analysis. In: Heckenlively JR. *Retinitis Pigmentosa.* Philadelphia, Pa: JB Lippincott; 1988:14-24.
9. Dryja TP, McGee TL, Reichel E, et al. A point mutation of the rhodopsin gene in one form of retinitis pigmentosa. *Nature.* 1990;343:364-366.
10. Inglehearn CF, Bashir R, Lester DH, May M, Bird AC, Bhattacharya SS. A 3-bp deletion in the rhodopsin gene in a family with autosomal dominant retinitis pigmentosa. *Am J Hum Genet.* 1991;48:26-30.
11. Al-Maghtheh M, Gregory C, Inglehearn C, Bhattacharya S. Rhodopsin mutations in autosomal dominant retinitis pigmentosa. *Hum Mutation.* In press.
12. Heckenlively JR, Rodriguez JA, Daiger SP. Autosomal dominant sectoral retinitis pigmentosa: two families with transversion mutation in codon 23 of rhodopsin. *Arch Ophthalmol.* 1991;109:84-91.
13. Berson EL, Rosner B, Sandberg MA, Dryja TP. Ocular findings in patients with autosomal dominant retinitis pigmentosa and a rhodopsin gene defect (Pro-23-His). *Arch Ophthalmol.* 1991;109:92-101.
14. Berson EL, Rosner B, Sandberg MA, Weigel-DiFranco C, Dryja TP. Ocular findings in patients with autosomal dominant retinitis pigmentosa and rhodopsin, proline-347-leucine. *Am J Ophthalmol.* 1991;111:614-623.
15. Jacobson SG, Kemp CM, Sung C-H, Nathans J. Retinal function and rhodopsin levels in autosomal dominant retinitis pigmentosa with rhodopsin mutations. *Am J Ophthalmol.* 1991;112:256-271.
16. Fishman GF, Stone EM, Gilbert LD, Kenna P, Sheffield VC. Ocular findings associated with a rhodopsin gene codon 58 transversion mutation in autosomal dominant retinitis pigmentosa. *Arch Ophthalmol.* 1991;109:1387-1393.
17. Fishman GA, Stone EM, Sheffield VC, Gilbert LD, Kimura AE. Ocular findings associated with rhodopsin gene codon 17 and codon 182 transition mutations in dominant retinitis pigmentosa. *Arch Ophthalmol.* 1992;110:54-62.
18. Shiono T, Hotta Y, Noro M, et al. Clinical features of Japanese family with autosomal dominant retinitis pigmentosa caused by point mutation in codon 347 of rhodopsin gene. *Jpn J Ophthalmol.* 1992;36:69-75.
19. Kemp CM, Jacobson SG, Roman AJ, Sung C-H, Nathans J. Abnormal rod dark adaptation in autosomal dominant retinitis pigmentosa with proline-23-histidine rhodopsin mutation. *Am J Ophthalmol.* 1992;113:165-174.
20. Fishman GA, Vandenburgh K, Stone EM, Gilbert LD, Alexander KR, Sheffield VC. Ocular findings associated with rhodopsin gene codon 267 and codon 190 mutations in dominant retinitis pigmentosa. *Arch Ophthalmol.* 1992;110:1582-1588.
21. Apfelstedt-Sylla E, Kunisch M, Horn M, Ruther K, Gal A, Zrenner E. Diffuse loss of rod function in autosomal dominant retinitis pigmentosa with Pro-347-Leu mutation of rhodopsin. *Ger J Ophthalmol.* 1992;1:319-327.
22. Hayakawa M, Hotta Y, Imai Y, et al. Clinical features of autosomal dominant retinitis pigmentosa with rhodopsin gene codon 17 mutation and retinal neovascularization in a Japanese patient. *Am J Ophthalmol.* 1993;115:168-173.
23. Inglehearn CF, Keen TJ, Bashir R, et al. A completed screen for mutations of the rhodopsin gene in a panel of patients with autosomal dominant retinitis pigmentosa. *Hum Molec Genet.* 1992;1:41-45.
24. Massof RW, Finkelstein D. Rod sensitivity relative to cone sensitivity in retinitis pigmentosa. *Invest Ophthalmol Vis Sci.* 1979;18:263-272.
25. Massof RW, Finkelstein D. Two forms of autosomal dominant primary retinitis pigmentosa. *Doc Ophthalmol.* 1979;51:289-346.
26. Jacobson SG, Voigt WJ, Parel J-M, et al. Automated light- and dark-adapted perimetry for evaluating retinitis pigmentosa. *Ophthalmology.* 1986;93:1604-1611.
27. Chen J, Fitzke F, Pauliekhoff D, Bird AC. Functional loss in age-related Bruch's membrane change with choroidal perfusion defect. *Invest Ophthalmol Vis Sci.* 1992;33:334-340.
28. Arden GB, Gunduz K, Perry S. Color vision testing with a computer graphics system. *Clin Vision Sci.* 1988;2:303-320.
29. Arden GB, Carter RM, Hogg CR, et al. A modified ERG technique and the results obtained in X-linked retinitis pigmentosa. *Br J Ophthalmol.* 1981;67:419-430.
30. International Standardization Committee. Standard for clinical electroretinography. *Arch Ophthalmol.* 1989;107:816-819.
31. Lyness AL, Ernst W, Quinlan MP, et al. A clinical, psychophysical, and electroretinographic survey of patients with autosomal dominant retinitis pigmentosa. *Br J Ophthalmol.* 1985;69:326-339.
32. Moore AT, Fitzke FW, Kemp CM, et al. Abnormal dark adaptation kinetics in autosomal dominant sector retinitis pigmentosa due to rod opsin mutation. *Br J Ophthalmol.* 1992;76:465-469.
33. Fishman GA, Stone EM, Gilbert LD, Sheffield VC. Ocular findings associated with a rhodopsin gene codon 106 mutation. *Arch Ophthalmol.* 1992;110:646-653.
34. McCaffery P, Neve RL, Drager UC. A dorso-ventral asymmetry in the embryonic retina defined by protein conformation. *Proc Natl Acad Sci U S A.* 1990;87:8570-8574.
35. McCaffery P, Tempst P, Lara G, Drager UC. Aldehyde dehydrogenase is a positional marker in the retina. *Development.* 1991;112:693-702.
36. Zack DJ, Bennett J, Wang Y, et al. Unusual topography of bovine rhodopsin promoter-lac Z fusion gene expression in transgenic mouse retinas. *Neuron.* 1991;6:187-199.
37. Szel A, Rohlich P, Caffe AR, Juliusson B, Aguirre G, Van Veen T. Unique topographic separation of two spectral classes of cones in the mouse retina. *J Comp Neurol.* 1992;325:327-342.
38. McCaffery P, Lee M-O, Wagner MA, Sladek NE, Drager UC. Asymmetric retinoic acid synthesis in the dorsoventral axis of the retina. *Development.* 1992;115:371-382.
39. Khorana HG. Minireview: rhodopsin, photoreceptor of the rod cell. *J Biol Chem.* 1992;267:1-4.
40. Rosenfeld PJ, Cowley GS, McGee TL, Sandberg MA, Berson EL, Dryja TP. A null mutation in the rhodopsin gene causes rod photoreceptor dysfunction and autosomal dominant retinitis pigmentosa. *Nature Genet.* 1992;1:209-213.
41. Horn M, Humphries P, Kunisch M, et al. Deletions in exon 5 of the human rhodopsin gene causing a shift in the reading frame and autosomal dominant retinitis pigmentosa. *Hum Genet.* 1992;90:255-257.
42. Restagno G, Maghtheh M, Bhattacharya S, et al. A large deletion at the 3' end of the rhodopsin gene in an Italian family with a diffuse form of autosomal dominant retinitis pigmentosa. *Hum Molec Genet.* 1993;2:207-208.

Printed and Published in the United States of America

Accepted for publication
24 April 1995

reported between different families. Differences between members of the same family, variable detailed general medical history and a brief physical examination were undertaken.

Bimodal expressivity in dominant retinitis pigmentosa genetically linked to chromosome 19q

K Evans, M Al-Maghtheh, F W Fitzke, A T Moore, M Jay, C F Inglehearn, G B Arden, A C Bird

Abstract

A clinical, psychophysical, and electrophysiologic study was undertaken of two autosomal dominant retinitis pigmentosa pedigrees with a genetic mutation assigned to chromosome 19q by linkage analysis. Members with the abnormal haplotype were either symptomatic with adolescent onset nyctalopia, restricted visual fields, and non-detectable electroretinographic responses by 30 years of age, or asymptomatic with normal fundus appearance and minimal or no psychophysical or electroretinographic abnormalities. There was no correlation in the severity in parents and their offspring. Pedigree analysis suggested that although the offspring of parents with the genetic mutation were at 50% risk of having the genetic defect, the risk of being symptomatic during a working lifetime was only 31%. Such bimodal phenotypic expressivity in these particular pedigrees may be explained by a second, allelic genetic influence and may be a phenomenon unique to this genetic locus. Genetic counselling in families expressing this phenotype can only be based on haplotype analysis since clinical investigations, even in the most elderly, would not preclude the presence of the mutant gene.

(*Br J Ophthalmol* 1995; 79: 841–846)

Epidemiological studies of retinitis pigmentosa consistently report a frequency of one in 5000 of the general population suggesting that there are approximately 100 000 retinitis pigmentosa sufferers in Europe and a similar number in the USA.[1] A family history of retinitis pigmentosa can be demonstrated in approximately 50% of new cases, and all three mendelian inheritance patterns occur. Autosomal dominant inheritance accounts for approximately 17–25% of all cases[1-3] and the condition has been found to be genetically heterogeneous. Over 60 different mutations in the rhodopsin gene on chromosome 3q[4] and 18 peripherin/RDS gene mutations[5] have been found in different autosomal dominant retinitis pigmentosa pedigrees. Five other loci for dominant retinitis pigmentosa genes have been identified on chromosomes 7p,[6] 7q,[7] 8cen,[8] 17p,[9] and 19q[10] by genetic linkage analysis.

In addition to the genetic diversity seen in autosomal dominant retinitis pigmentosa, phenotypic variability is also well established. Differences in clinical presentation have been reported between different families. Differences between members of the same family, variable expressivity, is also a common characteristic of autosomal dominant disease.[11] Here we report an extended clinical, psychophysical, and electrophysiological study of two families expressing a retinitis pigmentosa phenotype genetically linked to chromosome 19q.[10] Haplotype data have now allowed sound genetic diagnosis, making it possible to compare accurately the severity of disease in patients with that in their offspring. This has led to the identification of a large number of asymptomatic individuals carrying the disease gene suggesting an unusual polarity of phenotype in that those with the disease gene seem either to be severely afflicted or are asymptomatic with little psychophysical or electroretinographic abnormality, a phenotype unlike that reported in other retinitis pigmentosa genotypes.

Patients and methods

Some clinical details on these unrelated families have been reported previously (family 3 and 4 respectively).[12] The former originates in south Wales and the latter from northeast England. Further clinical studies and linkage analysis have allowed the identification of eight symptomatic and eight disease haplotype carriers not included in the previous report. Autosomal dominant inheritance is evident with symptomatic individuals in each generation and male to male transmission. Asymptomatic patients were assigned as having the causative genetic mutation if they had the same haplotype as symptomatic individuals within a 20 centimorgan region of chromosome 19q. Family members with this haplotype have a >98% probability of carrying the disease mutation.[10] Thirty individuals were identified as having the abnormal gene and enrolled into the study. In family '3' this included five symptomatic individuals and four asymptomatic individuals with the disease haplotype. One of these asymptomatic patients, an obligate carrier, had a symptomatic child. In family '4', 13 symptomatic patients and eight asymptomatic individuals with the disease haplotype were examined (including three obligate carriers).

An extensive ophthalmic history was recorded including details of visual acuity loss and age of onset of nyctalopia. Full ophthalmic examination was undertaken which included assessment of visual acuity, examination of the anterior segment and fundus. To assess whether or not a systemic abnormality might segregate with ocular disease, a detailed general medical history and a brief physical examination were undertaken.

Department of Clinical Ophthalmology and Electrodiagnostics, Moorfields Eye Hospital
K Evans
M Jay
G B Arden
A T Moore
A C Bird

Departments of Visual Sciences and Molecular Genetics, Institute of Ophthalmology, London
F W Fitzke
C F Inglehearn
M Al-Maghtheh

Correspondence to:
K Evans, Department of Clinical Ophthalmology, Moorfields Eye Hospital, City Road, London EC1V 2PD.

Accepted for publication 24 April 1995

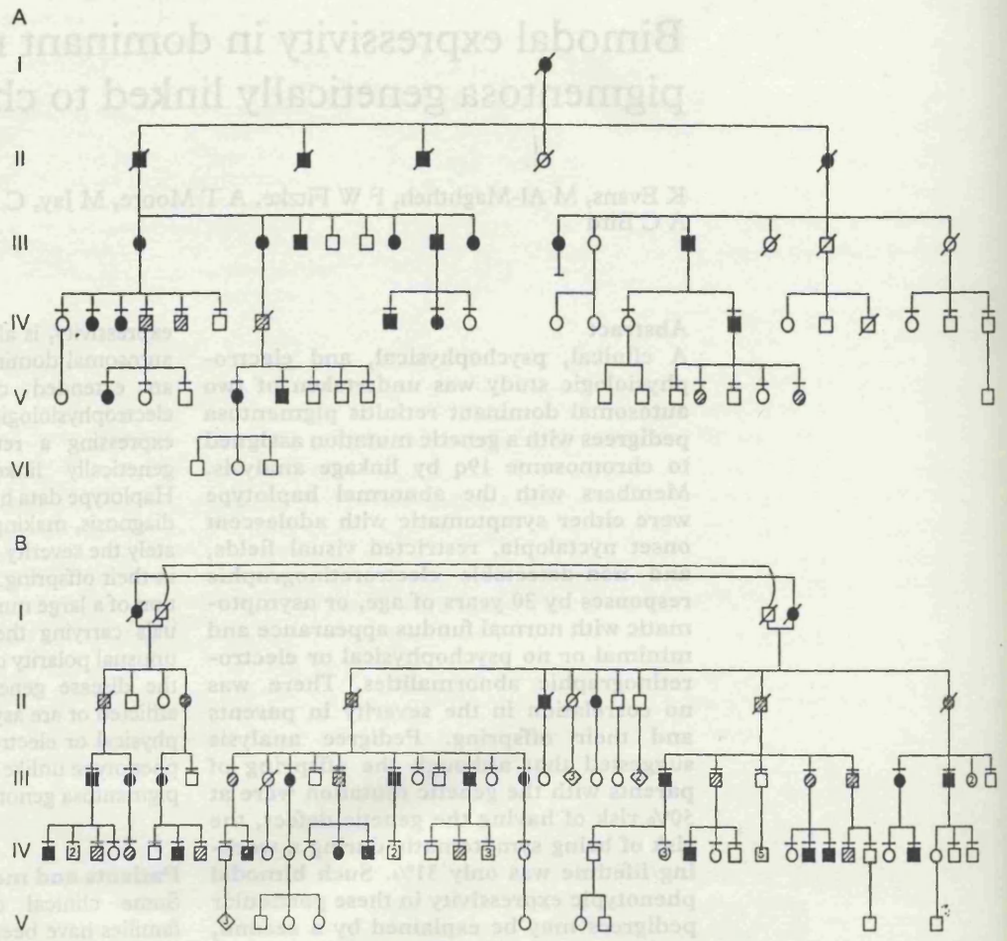

Figure 1 Pedigrees for families 3 (A) and 4 (B). ■ Symptomatic male, ○ unaffected female, ◍ disease-haplotype carrier. Bar above symbol identifies patients who underwent DNA examination.

For psychophysical studies pupils were dilated with 1% cyclopentolate hydrochloride and 2·5% phenylephrine hydrochloride, and subjects dark adapted for 40 minutes. Dark adapted static perimetry was undertaken using a modified Humphrey automated perimeter (Allergan Humphrey, San Leandro, CA, USA).[13–15] Cone and rod sensitivities were assessed using a standard Humphrey 30-2 program with the background illumination turned off. Size 5 red and blue test stimuli were used. In each case the eye with the better visual acuity was tested. For dark adaptometry, prebleach thresholds were then determined at selected positions. Patients were exposed to bright white light for 2 minutes sufficient to bleach 95% of rhodopsin (7·5 log scotopic Tröland-second delivered over 45 seconds). Recovery of sensitivity with time was assessed with size 5 blue test stimuli.[16–18]

Selected subjects underwent electrophysiological investigation using a 'short-protocol' adapted from that recommended by the International Standard for Clinical Ophthalmology.[19 20] Dark adapted electroretinography including blue flash ('run 7' to elicit rod isolated responses), red flash ('run 18', cone dominated responses), white flash ('run 20', mixed photoreceptor responses) and 30 Hz flicker ('run 31' cone isolated) responses were recorded. Electro-oculography was performed as previously described.[21]

The study was approved by the local ethics committee and informed consent was obtained from each subject enrolled into the study.

Results

Revised pedigrees are presented in Figures 1A and 1B. Linkage studies in both families identified seven individuals as recombinant over the entire 19q linked region. This prompted a reappraisal of their clinical status which had previously been based on ophthalmic history only. These examinations resulted in redesignation of disease status of two subjects in pedigree 3 (3-III-14 and 3-IV-20 as phenotypically normal) and five in pedigree 4 (4-III-7, 4-IV-1, and 4-IV-15 as phenotypically abnormal, 4-IV-25 and 4-IV-46 as normal). This and the identification of nine extra asymptomatic disease haplotype carriers accounts for differences from previously published family trees, more accurately reflecting segregation of the disease.[12] Because information was based on historical data in some generations, segregation of disease status was examined in generations III–V only in pedigree 3 and II–IV only in pedigree 4. This identified 57 symptomatic plus disease haplotype carriers and 63 unaffected individuals born to symptomatic or disease haplotype carrier parents. Approximately half (48%) of at risk individuals had inherited the disease

Table 1 Clinical details of 30 symptomatic and disease haplotype carrier patients

Patient	Age (years)	Genetic status	Nyctalopia age at onset (years)	Visual acuity Right	Visual acuity Left	Lens opacities	Fundal examination
3-IV-2	62	s	6	6/60	6/60	PSC	MA, PEA, BS 360°
3-IV-15	61	s	10	6/36	6/36	PSC	MA, PEA, BS 360°
3-V-2	24	s	11	6/9	6/9	None	PEA, BS, BS 360°
3-V-5	57	s	15	6/9	6/12	PSC	PEA, BS 360°
3-V-6	52	s	9	6/24	6/36	None	PEA, BS 360°
4-III-1	61	s	8	6/60	6/60	PSC, CO	PEA, BS 360°
4-III-2	50	s	9	6/18	6/12	PSC	PEA, BS 360°
4-III-3	54	s	18	6/18	6/9	PSC	MO, PEA, BS 360°
4-III-13	60	s	10	6/60	6/60	PSC	MO, PEA, BS 360°
4-III-15	52	s	5	6/9	6/9	PSC	PEA, BS 360°
4-III-29	48	s	4	<3/60	<3/60	PSC	MA, PEA, BS 360°
4-IV-1	26	s	No	<3/60*	6/6	None	ONH, PEA, BS 360°
4-IV-8	25	s	5	6/12	6/12	PSC	MO, BS 360°
4-IV-11	45	s	5	6/18	6/9	PSC	PEA, BS 360°
4-IV-29	25	s	8	6/6	6/6	None	PEA, BS 360°
4-IV-38	33	s	13	6/12	6/9	None	MO, PEA, BS 360°
4-IV-39	30	s	10	6/9	6/9	None	PEA, BS 360°
4-IV-43	28	s	15	6/9	6/5	None	MO, BS 360°
3-IV-5	57	d	No	6/6	6/9	None	Normal
3-IV-6	55	d	No	6/6	6/6	None	Normal
3-V-13	33	d	No	6/6	6/6	None	Normal
3-V-16	24	d	No	6/5	6/5	None	Normal
4-III-5	75	d	No	6/9	6/9	CO	Normal
4-III-25	49	d	No	6/5	6/6	None	Normal
4-III-27	57	d	No	6/6	6/6	None	Normal
4-III-28	55	d	No	6/9	6/9	CO	Normal
4-IV-6	28	d	No	6/6	6/6	None	Normal
4-IV-9	26	d	No	6/9	6/6	None	Normal
4-IV-20	30	d	No	6/6	6/6	None	Normal
4-IV-40	26	d	No	6/6	6/6	None	Normal

3=Pedigree fig 1A, 4=pedigree Fig 1B. s=Symptomatic, d=disease haplotype carrier. PSC=posterior subcapsular lens opacities, CO=cortical lens opacities, PEA=retinal pigment epithelial atrophy, BS=bone spicule retinal pigmentation, MO=macular oedema, MA=macular atrophy, *=reduced acuity owing to optic nerve head hypoplasia (ONH) urelated to retinitis pigmentosa.

haplotype but only 37 (31%) were symptomatic.

Seventeen symptomatic patients had eight (47%) symptomatic and nine (53%) disease haplotype carrier children. This compared with 12 asymptomatic disease haplotype carrier patients who had 19 (76%) symptomatic and six (24%) disease haplotype carrier children. The difference between the percentages of symptomatic children born to symptomatic and asymptomatic disease haplotype carrier parents was not statistically significant ($\chi^2=3{\cdot}7$, $p=0{\cdot}05$). Of the 27 symptomatic individuals whose parents were also included in generations III–V of pedigree 3 and II–IV of pedigree 4, 17 had a male parent carrying the disease gene and 10 a female parent. Of 15 asymptomatic disease haplotype carriers with parents included in these generations 10 had a male parent carrying the disease gene and five a female parent. Therefore the sex of the parent carrying the disease gene did not seem to influence the likelihood that a child with the disease gene would be symptomatic.

Table 2 Dark adapted static sensitivities. Loss relative to lower normal limit

Patient	Genetic status	Dark adapted sensitivity loss (dB) Blue stimulus 3°	Blue stimulus 9°	Blue stimulus 27°	Red stimulus 3°	Red stimulus 9°	Red stimulus 27°
3-IV-15	s	28	31	31	22	26	26
3-V-2	s	6	31	31	7	26	26
3-V-5	s	27	31	31	15	26	26
3-V-6	s	28	31	31	26	26	26
4-III-15	s	31	31	31	16	26	26
4-IV-11	s	15	31	31	4	22	26
4-IV-29	s	4	10	31	6	22	26
4-IV-38	s	23	31	31	13	26	26
3-IV-5	d	2	1	0	0	0	0
3-IV-6	d	0	0	0	0	0	0
3-V-13	d	0	0	0	0	0	0
3-V-16	d	0	0	0	0	0	0
4-III-5	d	2	1	2	0	0	0
4-III-25	d	2	1	1	0	0	0
4-III-27	d	6	5	2	2	0	1
4-III-28	d	0	0	0	0	0	0
4-IV-40	d	2	0	0	0	0	0

Normal sensitivity ranges, blue=31–50 dB, red=26–37 dB.
s=Symptomatic, d=disease-haplotype carrier.

The results of clinical examinations are presented in Table 1. No individual identified as a disease haplotype carrier reported nightblindness in contrast with all symptomatic individuals, who reported nyctalopia by their mid teens. Typical fundus features of extensive peripheral retinal degeneration were seen in even the youngest examined symptomatic patient (24 years) with macular atrophy, oedema, and secondary cataract formation in older symptomatic individuals. Normal visual acuities and fundus examinations were recorded for even the oldest asymptomatic disease haplotype carrier (75 years). No systemic abnormality was identified as segregating with eye disease.

All symptomatic individuals assessed (24–61 years of age) had elevated dark adapted threshold sensitivities for the whole 30° field tested with matching areas of rod and cone functional deficit (Table 2). Relative preservation of a central island of vision was evident in younger symptomatic individuals extending to approximately 9° around fixation. In middle age this island was <3°. In contrast, minimal threshold elevations were detected in the central 30° of asymptomatic disease haplotype carriers (within 7 dB of the normal limit). Abnormal dark adaptometry results were obtained from all symptomatic patients tested with elevation of prebleach thresholds and elevated final thresholds (Table 3). Prebleach threshold elevation above 50 dB precluded dark adaptometry in symptomatic individuals over 52 years of age. All symptomless disease haplotype carrier individuals gave responses within 5 dB of normal mean values.

Electroretinographic responses were not detectable (that is, <5 mV) in symptomatic individuals over 30 years of age. Significantly reduced electro-oculographic responses and ERG changes indicative of a severe rod-cone type photoreceptor deficit were seen in all younger symptomatic individuals (Table 4). Minor abnormalities in scotopic responses (within 34 mV of the lower normal limit with normal implicit times) were also evident in two asymptomatic disease haplotype carrier patients (4-V-16, 24 years and 4-IV-5, 57 years). Dramatic differences were therefore seen in the results of field analysis and electrical responses of the youngest symptomatic patients in comparison with those from even the oldest disease haplotype carriers. These differences were not attributable to age.

Discussion

Matching areas of both rod and cone functional loss classify the phenotype seen in these families as R type (regional, type II), which contrasts with the widespread reduction in rod sensitivity with relative sparing of cone function seen in D type (diffuse, type I) disease.[22 23] Some rhodopsin mutations appear to cause D type

Table 3 Dark adaptometry

Patient		Genetic status	Dark adapted rod prebleach threshold, elevation (dB)	Time to cone/rod break (minutes)	Time to prebleach threshold (minutes)	Dark adaption curve profile
Normal			0	9–11	30–45	
3-V-2	x	s	20	7	>45	Elevated final threshold
	y		30	12	>45	relative to prebleach value
4-IV-29	x	s	22	6	>45	Elevated final threshold
	y		40	13	>45	relative to prebleach value
4-III-25	x	d	8	9	35	Normal
	y		9	9	35	
4-III-5	x	d	10	12	40	Normal
	y		10	12	40	
4-III-27	x	d	10	6	42	Normal
	y		15	6	42	
4-III-28	x	d	9	9	37	Normal
	y		9	9	37	

s=Symptomatic, d=disease-haplotype carrier, x=visual field locus (3,3), y=visual field locus (9,9).

functional loss,[24–26] and others an R type loss associated with an altitudinal distribution of visual field deficit unlike that seen here.[18 27–34] Regional functional loss has also been described with peripherin/RDS mutations although severity was consistently related to age.[35] Detailed phenotype descriptions for pedigrees linked to 7q, 8cen, and 17p are as yet unpublished. A phenotype with variable expression and an R type pattern of deficit has been described for the dominant retinitis pigmentosa pedigree linked to chromosome 7p.[12] However, a graded disease severity has been reported with mild, moderate, and severely affected individuals. By extending the clinical study on the two families, the present study has identified a large number of haplotype carriers who on clinical examination and intensive investigation are essentially normal. This establishes the phenotype, R type functional deficit with bimodal expressivity, as a real phenomenon in two large families that may be a unique feature of the 19q locus, and allows analysis of segregation of disease in the pedigrees.

To explain this unusual phenotypic expression, another influence in addition to the underlying causative mutation mapping to 19q is most probably operating. This is unlikely to be environmental since such an effect would be expected to be dose dependent, and produce a graded rather than the 'all or nothing' phenotype seen here. In addition, despite extensive research, environmental factors such as ambient lighting have not been proved to have a large influence on disease severity in retinitis pigmentosa.[3 36] A number of genetic mechanisms have been associated with variable expression of disease phenotype. Anticipation describes disease severity related to increasing trinucleotide repeat expansion as seen in fragile X syndrome[37] and myotonic dystrophy.[38] Imprinting is often the basis for a phenotype influenced by sex of the carrier parent.[39] Incomplete penetrance in certain retinoblastoma pedigrees has been attributed to mutations in gene promoter sequence[40] or 'mild' germline mutations which reduce but do not eliminate tumour suppression protein function.[41] Anticipation, with severity related to position in a pedigree was not seen in this study, and the sex of the disease gene carrying parent did not influence the likelihood of a disease gene carrier being symptomatic. Also, the mechanism seen in retinoblastoma would not explain the bimodal expressivity seen in this study since incomplete penetrance of the retinoblastoma phenotype is usually associated with a relatively severe 'second hit' null mutation in somatic cells.[41] Such somatic cell mutations could not explain the panretinal disease seen in retinitis pigmentosa.

Digenic inheritance describes the association of germline mutations in different genes that result together in phenotype expression but cause minimal or no function deficit when inherited individually.[42] In retinitis pigmentosa cases associated with digenic inheritance, the gene products (peripherin/RDS and ROM1) are structural proteins known to interrelate functionally at a cellular level. Such a mechanism may imply that disease status in a particular individual linked to gene mutation at the 19q locus would be determined by the presence of a second gene expressing a functionally related protein. This suggests that the 19q mutation and another modulating gene may encode related structural proteins, ion transport channel subunits, or related membrane bound proteins. The protein products of these two mutations may also possibly be enzyme subunits. Mutations of enzyme coding genes conventionally result in recessive

Table 4 Electrodiagnostic results

			Electroretinography									
			Run 7 b wave		Run 18 b wave		Run 20 a wave		Run 20 b wave		Run 31	
Patient	Age (years)	EOG %	amp	imp	amp	imp	amp	imp	amp	imp	amp	imp
3-V-2 (s)	24		0	–	15	50	30	30	20	50	10	40
4-IV-1 (s)	26	100/110	0	–	30	50	30	30	30	50	5	42
4-IV-29 (s)	25	137/135	0	–	10	46	7	30	18	50	10	47
4-IV-43 (s)	28	100/100	0	–	16	42	6	20	18	48	10	32
3-IV-5 (d)	57	195/210	45	120	60	50	50	30	220	50	35	31
3-V-13 (d)	33		120	100	60	42	120	15	280	45	30	30
3-V-16 (d)	24	141/161	55	95	60	48	41	25	220	51	25	35
4-III-25 (d)	25	370/335	140	90	120	46	80	23	270	45	25	30
4-III-27 (d)	57	200/218	160	100	200	44	60	22	260	44	35	30
4-IV-9 (d)	26		80	106	40	20	41	25	200	40	20	32
Normal mean			199	100	153	47	132	22	384	45	43	29
Normal limits		160 to 400	79	126	59	57	41	25	208	49	10	32

EOG=electro-oculogram. Electroretinogram run 7 (rod isolated), run 18 (cone dominant), run 20 (mixed photoreceptor), and run 31 (cone photoreceptor) correspond to a 'short protocol' regimen.[19] amp=Wave amplitude, imp=implicit time. Normal limits for electroretinographic responses refer to the normal mean −2 SD for wave amplitudes and the normal mean +2 SD for implicit times. s=Symptomatic, d=disease haplotype carrier.

disease, but this well established dogma is not incontrovertible since a mutation in the β subunit of the enzyme phosphodiesterase has been associated with a dominant congenital stationary nightblindness.[43] The large number of symptomatic individuals from symptomless disease haplotype carriers would suggest that the second proposed mutation, derived from the unrelated spouse, may be common in the general population. Since in itself this second mutation is not associated with disease it could be described as a gene polymorphism. However, it would be expected that if digenic inheritance explained the disease segregation in this study, then symptomatic individuals would be significantly more likely to have symptomatic children than disease haplotype carriers. This was not the case in these families since only 50% of children carrying the disease gene derived from symptomatic individuals were themselves symptomatic compared with 76% of children with the disease gene derived from a disease haplotype carrier parent. This finding may be explained if the second genetic influence in these families was in fact allelic to the 19q mutation. Such allelic mutations, modifying disease expression have been identified in *Drosophila* where the phenomenon is termed intragenic complementation.[44] Also, an allelic, symptomless polymorphism of the spectrin gene, common in the population, has been implicated as modulating the severity of symptoms in humans with a primary spectrin mutation causing hereditary haemolytic anaemia.[45] This hypothesis will easily be testable once the 19q mutant gene is isolated.

Despite intensive work on cDNA libraries in many laboratories, to date no research worker has identified a retina specific gene on chromosome 19. However, techniques used to generate tissue specific libraries usually identify genes that give rise to larger amounts of protein. the 19q gene product, although important to cell function, may not be a large contributor to the protein content of retinal cells.[46] Alternatively, the gene of interest may not be retina specific. Although no systemic disease was identified, the function of the defective gene may be compensated for in other tissues in a way not possible in the retina.

In the past genetic counselling of such families has been difficult since clinical examination and extensive investigation would not exclude the presence of the abnormal gene even in late life. Although, as expected, roughly 50% of at risk individuals had the disease haplotype the overall risk of being significantly visually handicapped during a working lifetime was only 31%. In addition, 'minimal' disease in a parent did not imply an increased likelihood of 'minimal' disease in offspring. In these families accurate counselling is therefore dependent upon molecular genetic haplotype analysis.

1 Heckenlively JR. *Retinitis pigmentosa.* Philadelphia: JB Lippincott, 1988.
2 Bundey S, Crews SJ. A study of retinitis pigmentosa in the city of Birmingham. II. Clinical and genetic heterogeneity. *J Med Genet* 1984; 21: 421–8.
3 Jay M. On the heredity of retinitis pigmentosa. *Br J Ophthalmol* 1982; 66: 405–16.
4 Al-Maghtheh M, Gregory CY, Inglehearn CF, Hardcastle A, Bhattacharya SS. Rhodopsin mutations in autosomal dominant retinitis pigmentosa. *Hum Mutat* 1993; 2: 249–55.
5 Farrar GJ, Jordan SA, Kumar-Singh R, Inglehearn CF, Gal A, Gregory CY, *et al.* Extensive genetic heterogeneity in autosomal dominant retinitis pigmentosa. In: Hollyfield JG, Anderson RE, LaVail MM, ed. *Retinal degeneration. Clinical and laboratory applications.* New York: Plenum, 1994: 63–77.
6 Inglehearn CF, Carter SA, Keen TJ, Lindsey J, Stephenson AM, Bashir R, *et al.* A new locus for autosomal dominant retinitis pigmentosa on chromosome 7p. *Nature Genet* 1993; 4: 51–3.
7 Jordan SA, Farrar GJ, Kenna P, Humphries MM, Sheils DM, Kumar Singh R, *et al.* Localization of an autosomal dominant retinitis pigmentosa gene to chromosome 7q. *Nature Genet* 1993; 4: 54–8.
8 Blanton SH, Heckenlively JR, Cottingham AW, Friedman J, Sadler LA, Wagner M, *et al.* Linkage mapping of autosomal dominant retinitis pigmentosa (RP1) to the pericentric region of human chromosome 8. *Genomics* 1991; 11: 857–69.
9 Greenberg J, Goliath R, Beighton P, Ramesar R. A new locus for autosomal dominant retinitis pigmentosa on the short arm of chromosome 17. *Hum Mol Genet* 1994; 3: 915–8.
10 Al-Maghtheh M, Inglehearn CF, Keen TJ, Evans K, Moore AT, Jay M, *et al.* Identification of a sixth locus for autosomal dominant retinitis pigmentosa on chromosome 19. *Hum Mol Genet* 1994; 3: 351–4.
11 Weleber RG, Carr RE, Murphey WH, Sheffield VC, Stone EM. Phenotypic variation including retinitis pigmentosa, pattern dystrophy, and fundus flavimaculatus in a single family with a deletion of codon 153 or 154 of the peripherin/RDS gene. *Arch Ophthalmol* 1993; 111: 1531–42.
12 Moore AT, Fitzke F, Jay M, Arden GB, Inglehearn CF, Keen TJ, *et al.* Autosomal dominant retinitis pigmentosa with apparent incomplete penetrance: a clinical, electrophysiological, psychophysical and molecular genetic study. *Br J Ophthalmol* 1993; 77: 473–79.
13 Massof RW, Finklestein D. Rod sensitivity relative to cone sensitivity in retinitis pigmentosa. *Invest Ophthalmol Vis Sci* 1979; 18: 263–72.
14 Jacobson SG, Voigt WJ, Parel JM, Apathy PP, Nghiem Phu L, Myers SW, *et al.* Automated light- and dark-adapted perimetry for evaluating retinitis pigmentosa. *Ophthalmology* 1986; 93: 1604–11.
15 Chen JC, Fitzke FW, Pauleikhoff D, Bird AC. Functional loss in age-related Bruch's membrane change with choroidal perfusion defect. *Invest Ophthalmol Vis Sci* 1992; 33: 334–40.
16 Ernst W, Faulkner DJ, Hogg CR, Powell DJ, Arden GB. An automated static perimeter/adaptometer using light emitting diodes. *Br J Ophthalmol* 1983; 67: 431–42.
17 Steinmetz RL, Polkinghorne PC, Fitzke FW, Kemp CM, Bird AC. Abnormal dark adaptation and rhodopsin kinetics in Sorsby's fundus dystrophy. *Invest Ophthalmol Vis Sci* 1992; 33: 1633–6.
18 Moore AT, Fitzke FW, Kemp CM, Arden GB, Keen TJ, Inglehearn CF, *et al.* Abnormal dark adaption kinetics in autosomal dominant sector retinitis pigmentosa due to rod opsin mutation. *Br J Ophthalmol* 1992; 76: 465–9.
19 Arden GB, Carter RM, Hogg CR, Powell DJ, Ernst WJK, Clover GM, *et al.* A modified ERG technique and the results obtained in X-linked retinitis pigmentosa. *Br J Ophthalmol* 1981; 67: 419–30.
20 International Standardisation Committee. Standard for clinical electroretinography. *Arch Ophthalmol* 1989; 107: 816–9.
21 Arden GB, Barrada A, Kelsey JH. New clinical test of retinal function based upon the standing potential of the eye. *Br J Ophthalmol* 1962; 46: 449–67.
22 Massof RW, Finkelstein D. Two forms of autosomal dominant primary retinitis pigmentosa. *Doc Ophthalmol* 1979; 51: 289–346.
23 Lyness AL, Ernst WJK, Quinlan MP, Clover GM, Arden GB, Carter RM, *et al.* A clinical, psychophysical and electroretinographic survey of patients with autosomal dominant retinitis pigmentosa. *Br J Ophthalmol* 1985; 69: 326–39.
24 Berson EL, Rosner B, Sandberg MA, Weigel-DiFranco C, Dryja TP. Ocular findings in patients with autosomal dominant retinitis pigmentosa and rhodopsin, proline-347-leucine. *Am J Ophthalmol* 1991; 111: 614–23.
25 Jacobson SG, Kemp CM, Sung CH, Nathans J. Retinal function and rhodopsin levels in autosomal dominant retinitis pigmentosa with rhodopsin mutations. *Am J Ophthalmol* 1991; 112: 256–71.
26 Restagno G, Maghtheh M, Bhattacharya S, Ferrone M, Garnerone S, Samuelly R, *et al.* A large deletion at the 3' end of the rhodopsin gene in an Italian family with a diffuse form of autosomal dominant retinitis pigmentosa. *Hum Mol Genet* 1993; 2: 207–8.
27 Kemp CM, Jacobson SG, Roman AJ, Sung CH, Nathans J. Abnormal rod dark adaption in autosomal dominant retinitis pigmentosa with proline-23-histidine rhodopsin mutation. *Am J Ophthalmol* 1992; 113: 165–74.
28 Fishman GA, Stone EM, Gilbert LD, Sheffield VC. Ocular findings associated with a rhodopsin gene codon 106 mutation. *Arch Ophthalmol* 1992; 110: 646–53.
29 Fishman GA, Vandenburgh K, Stone EM, Gilbert LD, Alexander KR, Sheffield VC. Ocular findings associated with rhodopsin gene codon 267 and codon 190 mutations

in dominant retinitis pigmentosa. *Arch Ophthalmol* 1992; **110**: 1582–8.
30 Fishman GA, Stone EM, Sheffield VC, Gilbert LD, Kimura AE. Ocular findings associated with rhodopsin gene codon 17 and codon 182 transition mutation in dominant retinitis pigmentosa. *Arch Ophthalmol* 1992; **110**: 54–62.
31 Hayakawa M, Hotta Y, Imai Y, Fujiki K, Nakamura A, Yanashima K, *et al.* Clinical features of autosomal dominant retinitis pigmentosa with rhodopsin gene codon 17 mutation and retinal neovascularization in a Japanese patient. *Am J Ophthalmol* 1993; **115**: 168–73.
32 Kranich H, Bartkowski S, Denton MJ, Krey S, Dickinson P, Duvigneau C, *et al.* Autosomal dominant 'sector' retinitis pigmentosa due to a point mutation predicting an Asn-15-Ser substitution of rhodopsin. *Hum Mol Genet* 1993; **2**: 813–4.
33 Sullivan LJ, Makris GS, Dickenson P, Mulhall LEM, Forrest S, Cotton RGH, *et al.* A new codon 15 rhodopsin gene mutation in autosomal dominant retinitis pigmentosais associated with sectoral disease. *Arch Ophthalmol* 1993; **111**: 1512–7.
34 Kim RY, Al-Maghtheh M, Fitzke FW, Arden GB, Jay M, Bhattacharya SS, *et al.* Dominant retinitis pigmentosa associated with two rhodopsin gene mutations. *Arch Ophthalmol* 1993; **111**: 1518–24.
35 Wells J, Wroblewski J, Keen J, Inglehearn C, Jubb C, Eckstein A, *et al.* Mutations in the human retinal degeneration slow (RDS) gene can cause either retinitis pigmentosa or macular dystrophy. *Nature Genet* 1993; **3**: 213–8.
36 Berson EL. Light deprivation and retinitis pigmentosa. *Vision Res* 1980; **20**: 1179–84.
37 Richards RI, Holman K, Friend K, Kremer E, Hillen D, Staples A, *et al.* Evidence of founder chromosomes fragile X syndrome. *Nature Genet* 1992; **1**: 257–60.
38 Tsilfidis C, MacKenzie AE, Mettler G, Barcelo J, Korneluk RG. Correlation between CTG trinucleotide repe length and frequency of severe congenital myotonic d trophy. *Nature Genet* 1992; **1**: 192–5.
39 Magenis RE, Toth-Fejel S, Allen LJ, Black M, Brown MG, Budden S, *et al.* Comparison of the 15q deletions in Prader-Willi and Angelman syndromes: specific regions, extent of deletions, parental origin, and clinical consequences. *Am J Med Genet* 1990; **35**: 333–49.
40 Sakai T, Ohtani N, McGee L, Robbins PD, Dryja TP. Oncogenic germ-line mutations in SP1 and ATF sites in the human retinoblastoma gene. *Nature* 1991; **353**: 83–6.
41 Dryja TP, Rapaport J, McGee TL, Nork TM, Schwartz TL. Molecular etiology of flow penetrance retinoblastoma in two pedigrees. *Am J Hum Genet* 1993; **52**: 1122–8.
42 Kajiwara K, Berson EL, Dryja TP. Digenic retinitis pigmentosa due to mutations at the unlinked peripherin/RDS and ROM1 loci. *Science* 1994; **264**: 1604–8.
43 Gal A, Orth U, Baehr W, Schwinger E, Rosenberg T Heterozygous missense mutation in the rod cGMP phodiesterase b-subunit gene in autosomal domina stationary night blindness. *Nature Genet* 1994; **7**: 64–8.
44 Suzuki DT, Griffiths AJF, Lewontin RC. *An introduction to genetic analysis.* San Francisco: WH Freeman, 1981.
45 Gratzer W. Silence speaks in spectrin. *Nature* 1994; **372**: 620–1.
46 Bowes-Rickman C, Rapaport A, Danciger M, Cavallo C Kozak C, Farber DB. Cloning and characterization of novel photoreceptor-specific cDNAs. *Invest Ophthalmol Vis Sci* 1994; **35** (suppl): 1833.